

# **Trafficking and Signalling of Oncogenic Met**

**Carine JOFFRE**

This thesis is submitted for the degree of Doctor of Philosophy  
University of London

2010

Institute of Cancer & CR-UK Clinical Centre  
Centre for Tumour Biology, Spatial Signalling Group  
Barts and The London School of Medicine and Dentistry  
Charterhouse Square, London EC1M 6BQ

## **DECLARATION OF AUTHORSHIP**

I confirm that the work presented in this thesis is my own and the work of other persons has been properly cited and acknowledged.

## ABSTRACT

The Receptor Tyrosine Kinase (RTK) Met influences behaviour of several cancers by controlling growth, survival and metastasis. Recently, compartmentalisation of signals generated by RTKs, due to their endocytosis / trafficking, has emerged as a major determinant of various cell functions. The aim of my project was to study oncogenic Met signalling in relation to endosomal trafficking and to determine the consequences of such spatial changes on tumour cell growth and migration *in vitro* and *in vivo*.

The model studied was NIH3T3 cells stably transfected with Wild type (Wt) Met or with three distinct mutants reported in human cancers. I found that two activating mutations in the kinase domain are highly tumorigenic *in vivo*. Using functional assays and tumour growth experiments, I demonstrated that one mutant is highly sensitive to Met specific tyrosine kinase inhibitors (TKI) while another is resistant. Such results suggested that therapeutical approaches to these mutants should be different.

Furthermore, I demonstrated a direct link between endocytosis and tumorigenicity, suggesting a major role for Met endosomal signalling in cancer progression. Using confocal microscopy and quantitative biochemical assays, I demonstrated that Met mutants displayed an increased endocytosis and recycling and a decreased degradation profile. This led to an accumulation of phosphorylated Met on endosomes that induced activation of the GTPase Rac1, loss of stress fibres and increased cell migration. Blocking endocytosis by pharmacological and genetic

means inhibited mutants' anchorage independent growth and, strikingly, tumorigenesis and experimental metastasis. Interestingly, the mutant resistant to TKI inhibition was sensitive to endocytosis inhibition. Taken together, these results suggest that Met localisation constitutes a major determinant in neoplastic development, while Met activation alone is insufficient to effect this change.

# TABLE OF CONTENTS

<b>DECLARATION OF AUTHORSHIP.....</b>	<b>2</b>
<b>ABSTRACT.....</b>	<b>3</b>
<b>TABLE OF CONTENTS.....</b>	<b>5</b>
<b>LIST OF ABBREVIATIONS.....</b>	<b>12</b>
<b>LIST OF FIGURES.....</b>	<b>16</b>
<b>INTRODUCTION.....</b>	<b>17</b>
<b>1. The Met Receptor Tyrosine Kinase.....</b>	<b>19</b>
<b>2. Met ligand: Hepatocyte Growth Factor.....</b>	<b>22</b>
<b>3. Met/HGF signalling.....</b>	<b>24</b>
3.1. Met activation.....	24
3.2. Kinase activity of Met is tightly regulated.....	25
3.3. Met signalling.....	26
3.3.1. Met adaptors.....	26
3.3.2. Main signalling partners.....	26
3.3.3. The Rho GTPase Rac1 and cell migration.....	27
3.3.4. A pathway for several functions and several pathways for one function.....	31
<b>4. Met trafficking.....</b>	<b>32</b>
4.1. RTK endocytosis <i>via</i> the clathrin pathway.....	33
4.1.1. Ubiquitination.....	33
4.1.2. Clathrin-coated-vesicle formation.....	33
4.1.3. Vesicle sorting.....	37
4.1.4. RTK degradation and recycling.....	38

4.1.5. Role of endocytosis in signalling: “endosomal signalling” .....	41
4.2. Met endocytosis / trafficking.....	44
4.2.1. Met endocytosis.....	44
4.2.2. Met trafficking .....	45
4.2.3. Met degradation.....	47
4.2.4. Met endosomal signalling .....	48
<b>5. Biological effects of Met/HGF .....</b>	<b>49</b>
5.1. Implications of Met/HGF signalling at development stages.....	50
5.2. Implications of Met/HGF signalling into post-natal life .....	51
<b>6. Met/HGF and cancer .....</b>	<b>52</b>
6.1. Met/HGF overexpression.....	53
6.2. Identification of Met mutations and experimental evidence of their role in tumorigenesis.....	55
6.3. Mechanisms of Met activating mutations in cell transformation .....	56
6.3.1. Met activation.....	56
6.3.2. Downstream signalling.....	59
<b>7. RTKs mutations and cancer .....</b>	<b>61</b>
7.1. Mutations and trafficking modifications.....	62
7.1.1. Impaired down-regulation: EGFR.....	62
7.1.2. Incorrect maturation leading to intracellular accumulation.....	63
<b>8. Targeting Met in cancer .....</b>	<b>64</b>
8.1 Main approaches .....	65
8.1.1. Antagonism of ligand/receptor interaction.....	65
8.1.2. Inhibition of the tyrosine kinase catalytic activity.....	70
8.1.3. Interference with the recruitment of downstream molecules .....	76
8.2. Limitations.....	77
8.2.1. Ligand stimulated only .....	77
8.2.2. Resistance due to mutations.....	78

<b>AIM OF THE PROJECT</b> .....	<b>81</b>
<b>MATERIALS AND METHODS</b> .....	<b>83</b>
<b>1. Cell culture</b> .....	<b>83</b>
<b>2. Reagents</b> .....	<b>84</b>
2.1. Antibodies for immunofluorescence.....	84
2.2. Antibodies for Western blotting .....	84
2.3. Antibodies for flow cytometry .....	85
2.4. Growth factors, inhibitors and drugs .....	85
2.5. Plasmids .....	86
2.6. RNAi, and short hairpin RNA .....	86
<b>3. Cell Transfection</b> .....	<b>87</b>
3.1. Transfection using Lipofectamine™ 2000 and Plus reagent™ .....	87
3.2. Transfection with Amaxa® Nucleofector® technology.....	88
3.3. Lentiviral transduction .....	89
<b>4. Western Blotting</b> .....	<b>89</b>
4.1. Cell lysis.....	89
4.2. Western blot analysis.....	90
4.3. Densitometry.....	90
<b>5. Immunoprecipitation</b> .....	<b>91</b>
5.1. Standard protocol .....	91
5.2. Protein A sepharose-antibody coupling .....	91
<b>6. Ubiquitination assay</b> .....	<b>93</b>
6.1. Boiling SDS-lysis method.....	93
6.2. Nickel-NTA-agarose purification .....	93
<b>7. Immunofluorescence</b> .....	<b>94</b>
7.1. Confocal microscopy analysis.....	95
7.2. Transferrin uptake.....	95
7.3. Labelling of HGF with Alexa-555 .....	95

7.4.	HGF-Alexa-555 uptake .....	95
7.4.	Co-localisation measurement and statistic analysis.....	95
<b>8.</b>	<b>Biochemical quantification of Met basal distribution .....</b>	<b>96</b>
	Biotinylation surface removal	
<b>9.</b>	<b>Met internalisation and recycling assays .....</b>	<b>97</b>
9.1.	Biotinylation internalisation assay .....	97
9.2.	Biotinylation recycling assay .....	98
<b>10.</b>	<b>Biochemical quantification of Met degradation .....</b>	<b>99</b>
10.1.	Total Met degradation.....	99
10.2.	Biotinylation degradation assay .....	99
<b>11.</b>	<b>Rac1 activation assay .....</b>	<b>100</b>
<b>12.</b>	<b>Cell morphology assay.....</b>	<b>101</b>
<b>13.</b>	<b>Transwell chemotactic migration assay .....</b>	<b>101</b>
<b>14.</b>	<b>Survival assay (protection against anoikis) .....</b>	<b>102</b>
<b>15.</b>	<b>Soft agar assay .....</b>	<b>103</b>
<b>16.</b>	<b><i>In vivo</i> tumorigenicity assays.....</b>	<b>103</b>
16.1	Tumour growth assay .....	103
16.2	Lung colonisation assay .....	104
<b>17.</b>	<b>Statistical analysis.....</b>	<b>104</b>

## **RESULTS - PART I**

<b>Small Molecule Inhibitors Differentially Affect Distinct Oncogenic Met Mutants .....</b>	<b>105</b>
---	------------

<b>1. Met mutants are highly phosphorylated and tumorigenic ....</b>	<b>106</b>
--	------------

2.	The three Met inhibitors tested inhibit the basal activation of the M1268T mutant efficiently but have little or no effect on D1246N .....	110
3.	The three Met inhibitors revert transformed morphology, migration and survival of cells expressing the M1268T Met mutant, but not the D1246N Met mutant .....	116
4.	Topical application of PHA-665752 and PF-2341066 inhibited tumour growth of cells expressing the M1268T Met mutant, but not the D1246N Met mutant .....	122
5.	Oral administration of PF-2341066 inhibited growth of M1268T Met mutant tumours but not of D1246N Met mutant expressing cells .....	126

## **DISCUSSION - PART I .....**

**Activation of Met mutants .....**

**No requirement for HGF binding for alteration of various cell functions.....**

**Different mutants, different TKIs, and the importance of characterising the sensitivity of each mutation: typing cancer patients to optimise therapies .....**

**Distinct Met mutations sensitivity to the same TKIs .....**

**Drugs dose efficiency .....**

**Met specific TKIs and angiogenesis .....**

**New perspectives .....**

**TKIs with a new binding mode.....**

**Multitargeting drugs .....**

**HSP90 inhibitors .....**

A new way for drug administration.....	141
Preventing endosomal signalling .....	142

## **RESULTS - PART II**

### **A Direct Role For Met Endocytosis In Tumorigenesis ..... 144**

1. The active D1246N and M1268T Met mutants accumulate in intracellular compartments.....	144
2. The D1246N and M1268T Met mutants shuttle between the plasma membrane and endosomes .....	148
3. Endocytosis of the D1246N and M1268T Met mutants is clathrin, dynamin and Grb2 dependent but independent of high activation status.....	154
4. The D1246N and M1268T Met Mutants present an impaired degradation due to HSP90 activity .....	162
5. The D1246N and M1268T Met mutants require the endocytosis machinery to stimulate cell migration.....	168
6. The D1246N and M1268T Met Mutants induce Rac1 activation, which is dependent on endocytosis .....	177
7. Blocking endocytosis reduces tumour transformation, stimulated by the D1246N and M1268T Met Mutants, both <i>in vitro</i> and <i>in vivo</i> .....	186

### **DISCUSSION - PART II ..... 196**

Enhanced intracellular localisation of the M1268T and D1246N Met mutants.....	196
Intracellular and plasma membrane localisation .....	196
Increased endocytosis .....	198
Decreased degradation .....	199

<b>Endosomal signalling: specificity of pathways and of cellular outcome.....</b>	<b>203</b>
<b>Endocytosis and cancer.....</b>	<b>204</b>
<b>Constitutive endocytosis / recycling and defect in degradation: signal specificity and persistence lead to transformation.....</b>	<b>206</b>
<b>Signalling on the endosome positively influence tumorigenesis .....</b>	<b>208</b>
<b>Interfering with endocytic trafficking or endosomal signalling as an anti-tumour strategy?.....</b>	<b>210</b>
<b>CONCLUDING REMARKS .....</b>	<b>212</b>
<b>REFERENCES.....</b>	<b>215</b>
<b>ACKNOWLEDGEMENTS .....</b>	<b>244</b>

## LIST OF ABBREVIATIONS

AMSH	Associated Molecule with the SH3 domain of STAM
ATP	Adenosine 5' TriPhosphate
BSA	Bovine Serum Albumin
CLASP	Clathrin-Associated Sorting Protein
CCV	Clathrin-Coated Vesicle
CHC	Clathrin Heavy Chain
Cy	Cyanine
DCS	Donor Calf Serum
DMP	DiMethylpimelimidate
DMSO	DiMethyl SulphOxide
DNA	Deoxyribo Nucleic Acid
ECL	Enhanced ChemiLuminescence
EDTA	EthyleneDiamineTetraacetic Acid
EEA1	Early Endosome Antigen 1
EGF	Epidermal Growth Factor
EGFR	Epidermal Growth Factor Receptor
ER	Endoplasmic Reticulum
ERC	Endocytic Recycling Compartments
ERK	Extracellular signal-Related Kinase
ESCRT	Endosomal Sorting Complexes Required for Transport
FACS	Fluorescence Activated Cell Sorting
FAK	Focal Adhesion Kinase
FGF	Fibroblast Growth Factor

FGFR3	Fibroblast Growth Factor Receptor 3
FLT-3	FMS-Like Tyrosine kinase 3
FYVE	Fab1/YOTB/Vac1/EEA1
HCC	HepatoCellular Carcinoma
HGF	Hepatocyte Growth Factor
HNSCC	Head and Neck Squamous Cell Carcinoma
Hrs	HGF-Regulated tyrosine kinase Substrate
HOS	Human Osteogenic Sarcoma
HPRC	Hereditary Papillary Renal Carcinoma
HSC-70	Heat Shock Cognate protein 70
Gab1	Grb2-Associated Binder 1
GAP	GTPase Activating Protein
GDI	Guanine nucleotide Dissociation Inhibitor
GDP	Guanosine DiPhosphate
GEF	Guanine nucleotide Exchange Factor
Grb2	Growth-factor-Receptor-Bound protein 2
GST	Glutathione S-Transferase
GTP	Guanosine TriPhosphate
GTPase	Guanosine Triphosphatase
IgG	Immunoglobulin G
IAA	IodoAcetAmide
LRIG1	Leucine Rich Repeats and ImmunoGlobulin-like domain1
MSP	Macrophage Stimulating Protein
MEK	MAPK or ERK Kinase
MAPK	Mitogen-Activated Protein Kinase

MesNa	Mercaptoethanesulphonate
MMP	Matrix MetalloProteinase
MP1	MEK Partner 1
MVB	MultiVesicular Body
NGF	Nerve Growth Factor
NSCLC	Non-Small Cell Lung Cancer
PBS	Phosphate Buffered Saline
PDGFR	Platelet-Derived Growth Factor Receptor
PI	Propidium Iodide
PI3-K	Phosphatidylinositol 3-kinase
PLC	PhosphoLipase C
PKC	Protein Kinase C
PTB	PhosphoTyrosine Binding
PIP2	Phosphatidylinositol 4,5 bisphosphate
PIP3	Phosphatidylinositol 3, 4, 5-trisphosphate
RON	Receptor d"Origine Nantaise"
RTK	Receptor Tyrosine Kinase
SARA	SMAD Anchor for Receptor Activation
SCLC	Small Cell Lung Carcinoma
SDS-PAGE	Sodium Dodecyl Sulphate-PolyAcrylamide Gel electrophoresis
SF	Scatter Factor
SH2	Src-Homology-2
SH3	Src-Homology-3
Shc	SH2-domain-containing
Ship1	SH2-domain-containing Inositol-5-Phosphatase

Shp2	SH2-containing protein tyrosine Phosphatase 2
SNARE	Sensitive N-ethylmaleimide factor Attachment protein Receptor
Sos	Son Of Sevenless
SPH	Serine Proteinase Homologue
STAM	Signal-Transducing Adaptor Molecule
TBS	Tris Buffered Saline
TPR	Translocated Promoter Region
UBPY	UB-specific Protease Y
UIM	Ubiquitin Interacting Motif.
uPA	Urokinase Plasminogen Activator
VEGFR	Vascular Endothelial Growth Factor Receptor

## LIST OF FIGURES

<b>Figure 1</b>	Main Receptor Tyrosine Kinases .....	18
<b>Figure 2</b>	The Met Receptor Tyrosine Kinase .....	21
<b>Figure 3</b>	Schematic representation of HGF/SF .....	23
<b>Figure 4</b>	Met signalosome .....	28
<b>Figure 5</b>	Clathrin-coated-vesicle formation .....	35
<b>Figure 6</b>	RTK internalisation via clathrin-coated pathway .....	39
<b>Figure 7</b>	PKC controls Met trafficking .....	46
<b>Figure 8</b>	Missense mutations of Met identified in human cancers .....	57
<b>Figure 9</b>	Different strategies to inhibit Met-dependent signalling .....	66
<b>Figure 10</b>	Structures of three small-molecule Met inhibitors .....	74
<b>Table 1</b>	Summary of results obtained on Met mutations D1246N, M1268T and Y1248C localised in the kinase domain .....	58
<b>Table 2</b>	HGF/Met inhibitors other than kinase inhibitors .....	69
<b>Table 3</b>	Met-specific kinase inhibitors .....	71
<b>Table 4</b>	Broad spectrum kinase inhibitors .....	138

## INTRODUCTION

Receptor tyrosine kinases (RTKs) form a large family of enzymes, more than fifty, that control fundamental cellular processes including the cell cycle, proliferation/differentiation, cell migration, survival and cellular metabolism<sup>1</sup>. As these receptors catalyse the transfer of a phosphate to tyrosine residues on their substrates, using Adenosine Tri-Phosphate (ATP) as a phosphate donor, they are identified as protein tyrosine kinases<sup>2</sup>. RTKs are cell surface receptors for the majority of growth factors.

RTKs share structural characteristics and can be subdivided schematically into five functional domains: an extracellular ligand binding region usually glycosylated, a single transmembrane segment, a juxtamembrane domain, a catalytic domain and a C-terminal tail<sup>3</sup>. Twenty RTK subfamilies have been identified on the basis of their extra-cellular domains. Most of them are formed with a single polypeptide chain, as is the case for the EGF receptor (Epidermal Growth Factor), which belongs to the largest subfamily of RTKs. However, the insulin receptor and Met subfamilies are composed of a dimer consisting of two polypeptide chains (**Fig. 1**).

RTKs are activated by their dimerisation. Ligand binding induces this dimeric state that leads to autophosphorylation of the receptor that, in turn, results in trans-autophosphorylation of tyrosines located in their C-terminal tail. The phosphorylation of these tyrosines permits the recruitment and then the activation of a wide variety of signalling molecules<sup>1</sup>.

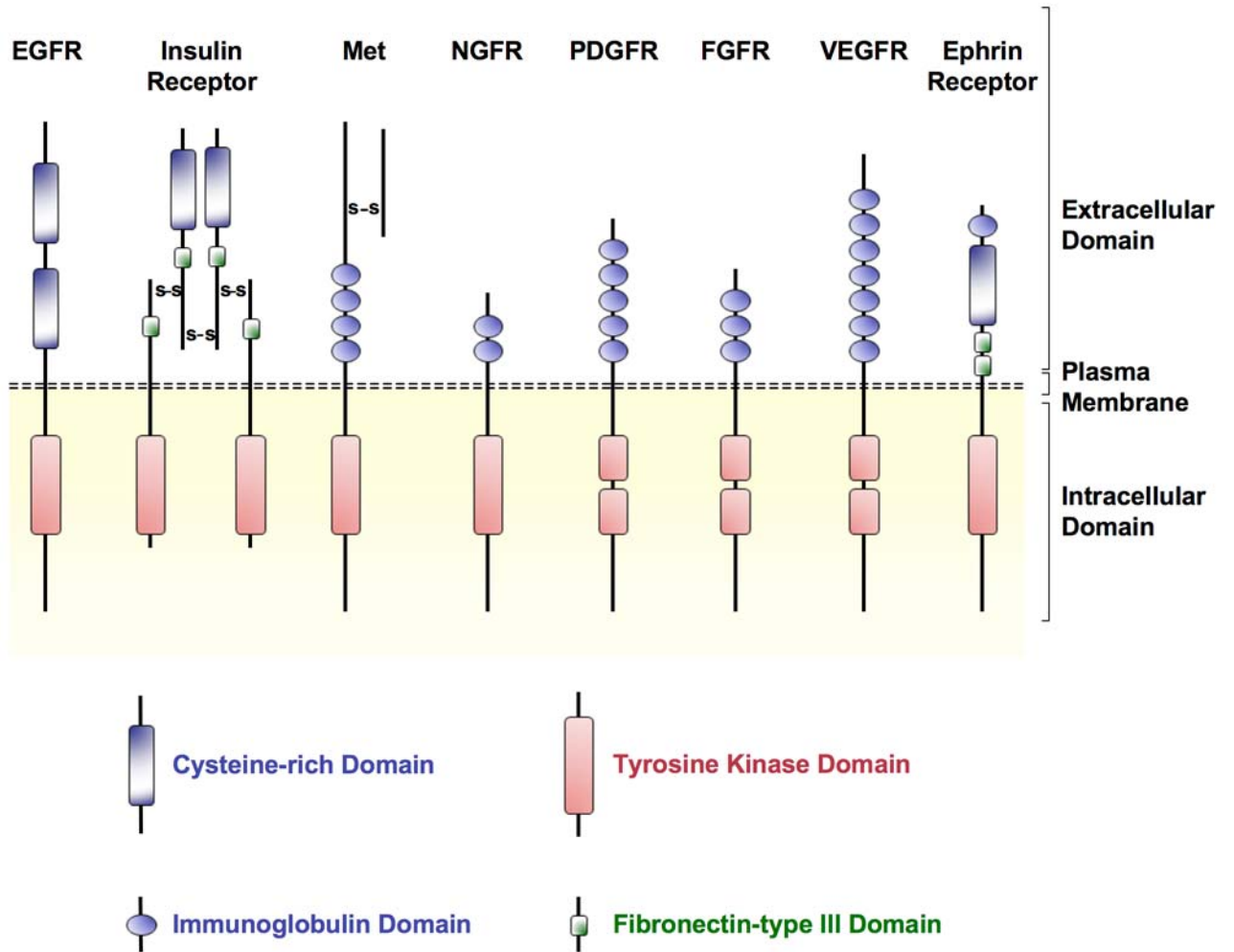


Figure 1. Main Receptor Tyrosine Kinases

The Met family includes only three members: RON (Receptor d"Origine Nantaise")<sup>4</sup>, the avian oncogene Sea<sup>5</sup> and, the prototype of the family, Met. A family of related proteins serve as ligands for these receptors.

### **1. The Met Receptor Tyrosine Kinase**

Met originally was identified in 1984 by Cooper *et al*<sup>6</sup> as an activated oncogene corresponding to a fusion protein, "TPR/Met", resulting from chromosomal translocation in a human osteogenic sarcoma (HOS) cell line treated with the chemical carcinogen N-Methyl-N-nitro-N-nitrosoguanidine<sup>6</sup>. Met's name derived from this chemical treatment. The Met proto-oncogene, located on the long arm of chromosome 7 (q11.2-q21.1)<sup>7</sup>, was involved in a translocation that placed the TPR locus (Translocated Promoter Region) on chromosome 1 just upstream of a portion of the Met gene. TPR/Met was shown to be constitutively active<sup>8</sup>. A couple of years after its discovery, Met was found to belong to the family of RTKs<sup>9</sup> but its ligand still was unknown.

The Met gene spans more than 120 kb in length and consists of 21 exons separated by 20 introns<sup>10</sup>. Met was first found expressed as a 9.0-kb RNA in epithelial cells<sup>8,9,11</sup>. At least three Met mRNA variants, generated by alternative splicing, have been reported. The most abundant form of Met, present in a large variety of tissue and cell lines, differs from the first published<sup>11</sup> by the absence of 54 bp predicted to encode 18 amino acids<sup>12</sup>. Lee and Yamada also reported a Met variant, termed Met<sub>sm</sub> for small, that presents with a deletion of 47 amino acids in the juxtamembrane domain<sup>13</sup>.

Based on sequence similarity and structural characteristics, the Met family can be classified as a new subfamily within the RTK family. Indeed, Met is a disulphide-linked heterodimer, which results from cleavage by furin of a 170 KDa glycosylated precursor. This mature Met, with an apparent molecular weight of 190 kDa, comprises an N-terminal  $\alpha$  chain (45kDa) located outside the membrane and a C-terminal  $\beta$  chain that contains an extracellular part, a single membrane spanning segment and a cytoplasmic part (145kDa) (**Fig. 2**). The  $\alpha$  chain and the first 212 amino acids of the  $\beta$  chain are responsible for ligand binding and these two Met regions are both homologous to the sema-domain (domain identified in the semaphorin protein). The remainder of the Met  $\beta$  chain ectodomain contains a PSI domain - also found in the plexins, semaphorins and integrins, hence its name, including 4 disulphide bonds followed by 4 IPT domains related to immunoglobulin-like domains named after their presence in plexins and transcription factors<sup>14,15</sup> (**Fig. 2**). The intracellular region of Met includes three domains: (1) juxta-membrane, (2) tyrosine kinase and (3) a C-terminal region that contains an unique multifunctional-docking site, essential for the recruitment of adaptors and several transducers<sup>15</sup> (**Fig. 2**).

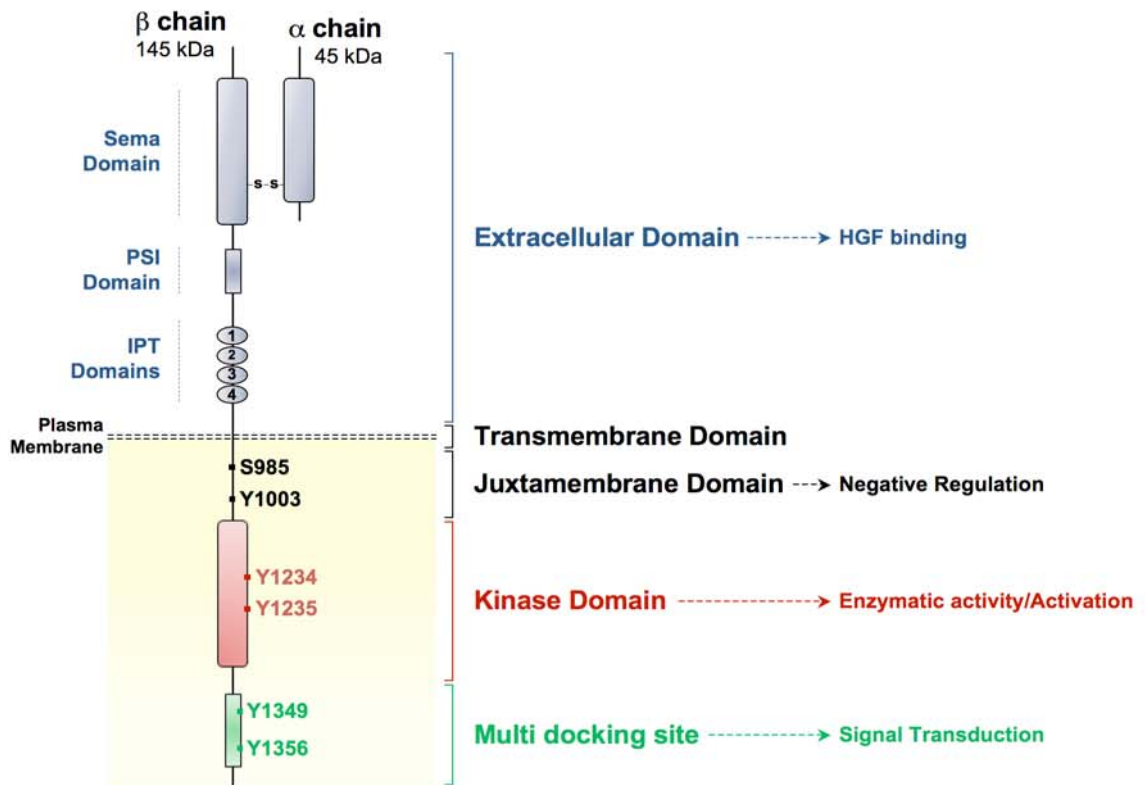


**Figure 2. Schematic structure of Met**

Met is constituted by 2 chains associated by a disulphide bond. The  $\alpha$  chain is a short extracellular subunit of 45 kDa constituted mainly by a Sema domain and involved in HGF/SF binding. The  $\beta$  chain is a transmembrane molecule of 145 kDa divided from the amino-terminal part to the carboxy-terminal end into 3 functional regions:

- (1) an extracellular domain involved in HGF/SF binding and constituted by a sema domain, a Plexin/Semaphorin/Integrin (PSI) domain and 4 Immunoglobulin-like fold, Plexins, Transcription factors (IPT) domains.
- (2) a transmembrane/juxtamembrane region negatively regulating the activity of the receptor.
- (3) an intracellular region subdivided into a kinase domain and a multi docking site both involved in signal transduction.

*Adapted from Comoglio PM et al, Nat. Drug. Disc, 2008*

## 2. Met ligand: Hepatocyte Growth Factor

Two soluble factors were discovered independently in 1987: a motility factor, called Scatter Factor, (SF)<sup>16</sup>, which induced the scattering and the motility of epithelial cells through a paracrine mode since its production and release were found to be limited to mouse and human fibroblast cells; and a mitogenic factor, first purified from rat platelets, named Hepatocyte Growth Factor (HGF)<sup>17</sup> since it was a potent mitogen for rat hepatocytes. It was only a couple of years later, after the cloning of the human HGF<sup>18</sup>, that it became apparent that these two factors were the same molecule and were established as the natural Met ligand<sup>19-22</sup>.

HGF/SF is a large multidomain protein, similar to plasminogen. It consists of six domains: amino-terminal hairpin loop (N), four kringle domains, K1-K4, (80 amino-acids defined by three conserved disulphide bridges), and a Serine Proteinase Homology (SPH) domain with no enzymatic activity<sup>14,15</sup> (**Fig. 3**). HGF/SF is synthesised and secreted as a single chain precursor (pro-HGF) of 92 kDa missing biological activity until it is proteolytically cleaved in the extracellular environment into a two-chain, active heterodimer<sup>23</sup>. The conversion of pro-HGF to the mature form is done by several extracellular serine proteases, which cleave the bond between Arg494 and Val495. They include the urokinase plasminogen activator (uPA), tissue-type plasminogen activator and coagulation factors X, XI and XII<sup>23,24</sup>. This cleavage process generates a factor composed of an  $\alpha$ -chain of 69 kDa and a  $\beta$ -chain of 34 kDa, linked by disulphide bonds.

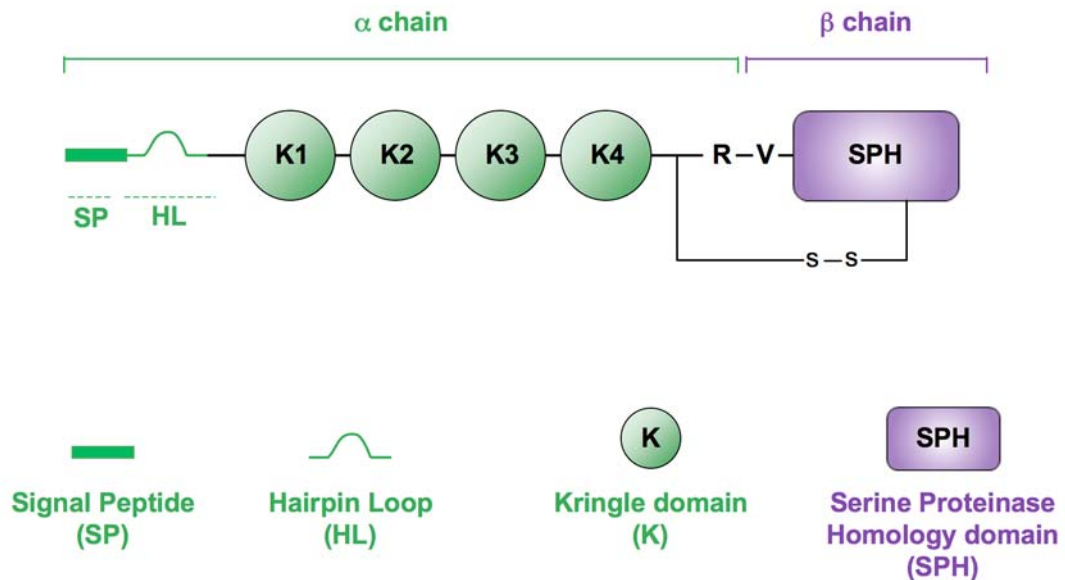


**Figure 3. Schematic representation of pro-Hepatocyte Growth Factor (HGF) / Scatter Factor (SF)**

The inactive form of HGF (pro-HGF/SF) is secreted as a single chain constituted, from the amino-terminal region to the carboxy-terminal end, by a signal peptide (SP), a hairpin loop (HL), 4 kringle domains (K) and a Serine Proteinase Homology (SPH) domain. The maturation of this precursor relies on the enzymatic activity of extracellular proteases which cleave the bond between Arginine 494 and Valine 495. The bioactive HGF/SF is a heterodimer formed by an  $\alpha$  and a  $\beta$  chain linked together by a disulphide bond.

*Adapted from  
Comoglio PM et al, Nat. Drug. Disc, 2008  
Birchmeier et al, Nature Reviews, 2003*

This unique Met ligand binds also to heparan-sulphate proteoglycans with high affinity. However this interaction is not essential for receptor activation. HGF is homologous to Macrophage Stimulating Protein (MSP), which is the ligand of the highly Met homologous, RON receptor.

### **3. Met/HGF signalling**

#### **3.1. Met activation**

Met is activated through binding of HGF/SF. How HGF and Met interact is still not well understood. HGF is a bivalent molecule that contains 2 Met binding sites with distinct receptor affinities. The low-affinity binding site, located in the  $\beta$  chain of HGF and accessible only when the HGF is active, interacts with the Sema domain of Met. The high affinity site was only identified recently<sup>25</sup>. It was found in the  $\alpha$  chain of HGF and binds with the IPT domains 3 and 4 of Met independently of the activation status of HGF<sup>25</sup>.

Using cryo-electron microscopy and small-angle-x-ray scattering, Gherardi *et al*<sup>26</sup> have proposed a model for the active HGF-Met complex, in which a 2:2 ligand-receptor complex is stabilised through dimerisation of the 'N' and 'K1' domains of HGF (see **Fig. 3**).

HGF binding induces Met dimerisation. This step results in the stabilisation of the receptor in an active conformation that leads to its trans-autophosphorylation on a doublet of tyrosines ( $Y^{1234}$ - $Y^{1235}$ ) located in the kinase domain, followed by the phosphorylation on two other tyrosines ( $Y^{1349}$ - $Y^{1356}$ ) in its C-terminal part. These two tyrosine residues, with their surrounding amino-acids, constitute a unique C-terminal multisubstrate-

docking site, well conserved among Met family members. This short sequence (Y<sup>1349</sup>VHVNATY<sup>1356</sup>VNV) alone is responsible for mediating high affinity interactions with a wide range of transducers and is responsible for the concomitant activation of several signalling pathways<sup>27</sup>. This multi-docking site is specific for Met, as most RTKs have several tyrosines distributed along the intracellular domain and each tyrosine binds specific signalling molecules.

### **3.2. Kinase activity of Met is tightly regulated**

In parallel to the activation of signalling pathways, Met activation also leads to negative feed-back in order to modulate, and eventually switch off, its activity.

One negative regulation is the result of the phosphorylation of the Serine<sup>985</sup> located in the juxtamembrane domain<sup>5,28,29</sup>. Once phosphorylated, Serine<sup>985</sup> causes Met inhibition by reducing tyrosine phosphorylation. This Serine<sup>985</sup> is embedded in a sequence for phosphorylation by Protein Kinase-C (PKC) and by Calcium ion (Ca<sup>2+</sup>)-dependent kinases. These kinases become active when the intracellular Ca<sup>2+</sup> concentration is increased. Met activates PhosphoLipase-C $\gamma$  (PLC $\gamma$ ) leading to the generation of diacyl-glycerol, a powerful activator of PKC. PKC then generates inositol-3-phosphate, which increases the intracellular concentration of Ca<sup>2+</sup><sup>28,29</sup>. This Ser<sup>985</sup> is found at a position similar to that of the regulatory Threonine<sup>654</sup> of EGFR<sup>30</sup>.

Another negative regulation operates *via* the phosphorylation of the Tyrosine<sup>1003</sup> within the juxtamembrane domain. The E3 ubiquitin ligase c-

Cbl binds to phosphorylated Tyrosine<sup>1003</sup> and induces Met down regulation. This mechanism will be examined in more detail later (see section 4. “Met trafficking”).

### **3.3. Met signalling**

When the multidocking site, or “supersite”, becomes phosphorylated, Met interacts with multiple adaptors and signal transducers.

#### **3.3.1. Met adaptors**

The two major Met adaptors are Grb2 (Growth-factor-receptor-Bound protein 2) and Gab1 (Grb2-Associated Binder 1). Among other RTKs, Gab1 has particular relationships with Met. Indeed, Gab1 contains a specific binding site of thirteen amino-acids, called the “Met binding site”, that mediates direct interaction with Met<sup>31</sup>. Such strong interaction mediates prolonged Gab1 phosphorylation upon HGF/SF binding compared with other RTKs. Moreover, this direct interaction is possible on both tyrosines present in the docking site, Y<sup>1349</sup> and Y<sup>1356</sup><sup>32</sup> (but mostly Y<sup>1349</sup>). Moreover, Gab1 can bind Met indirectly via its interaction with another Met adaptor, Grb2<sup>33,34</sup>, meaning that two molecules of Gab1 can interact, directly and indirectly, with the same Met dimer. Unlike Gab1, Grb2 can only bind Met on one tyrosine, the Y<sup>1356</sup><sup>35</sup>.

#### **3.3.2. Main signalling partners**

Several signalling partners can bind Met directly on tyrosines in the docking site and/or, indirectly *via* binding to phosphorylated Gab1 or Grb2.

Most of them contain an SH2 domain (Src-homology-2) or have a PhosphoTyrosine-Binding (PTB) domain, allowing recognition and binding to tyrosine-phosphorylated sequences<sup>36</sup> (**Fig. 4**). These interacting proteins<sup>15</sup> include Phosphatidylinositol 3-Kinase (PI3-K), SH2-containing protein tyrosine Phosphatase 2 (Shp2), PhosphoLipase C (PLC), Crk<sup>37</sup>, Src, SH2-domain-containing (Shc), SH2-domain-containing Inositol-5-Phosphatase (Ship1), the small GTPase Ras and the transcription factor Stat3<sup>38</sup>. Met activation, through the complex Grb2/Sos (Son Of Sevenless), leads to the activation of the Mitogen-Activated Protein Kinase (MAPK) signalling pathway. Sos is a Guanine Exchange Factor (GEF) that promotes the shift of Ras protein from the inactive form (GDP-bound) to the active form (GTP-form)<sup>39</sup>. Ras, once activated, can then trigger the activation of the Raf/MAPK cascade. In addition, Ras can, as well, stimulate PI-3K that in turn *via* production of the lipid phosphatidylinositol (3,4,5) triphosphate (PIP3), will elicit GEF activation<sup>40</sup>.

### 3.3.3. The Rho GTPase Rac1 and cell migration

The Rho GTPase Rac1 was shown to be activated by Met<sup>41,42</sup> for the control of cell migration. HGF through activating Met, induces the motility and the scattering of several types of cells including MDCK cells<sup>43</sup>. In these cells, Rac was shown to be activated by Met and to be necessary to promote actin reorganisation and subsequent cell scattering<sup>44,45</sup>.

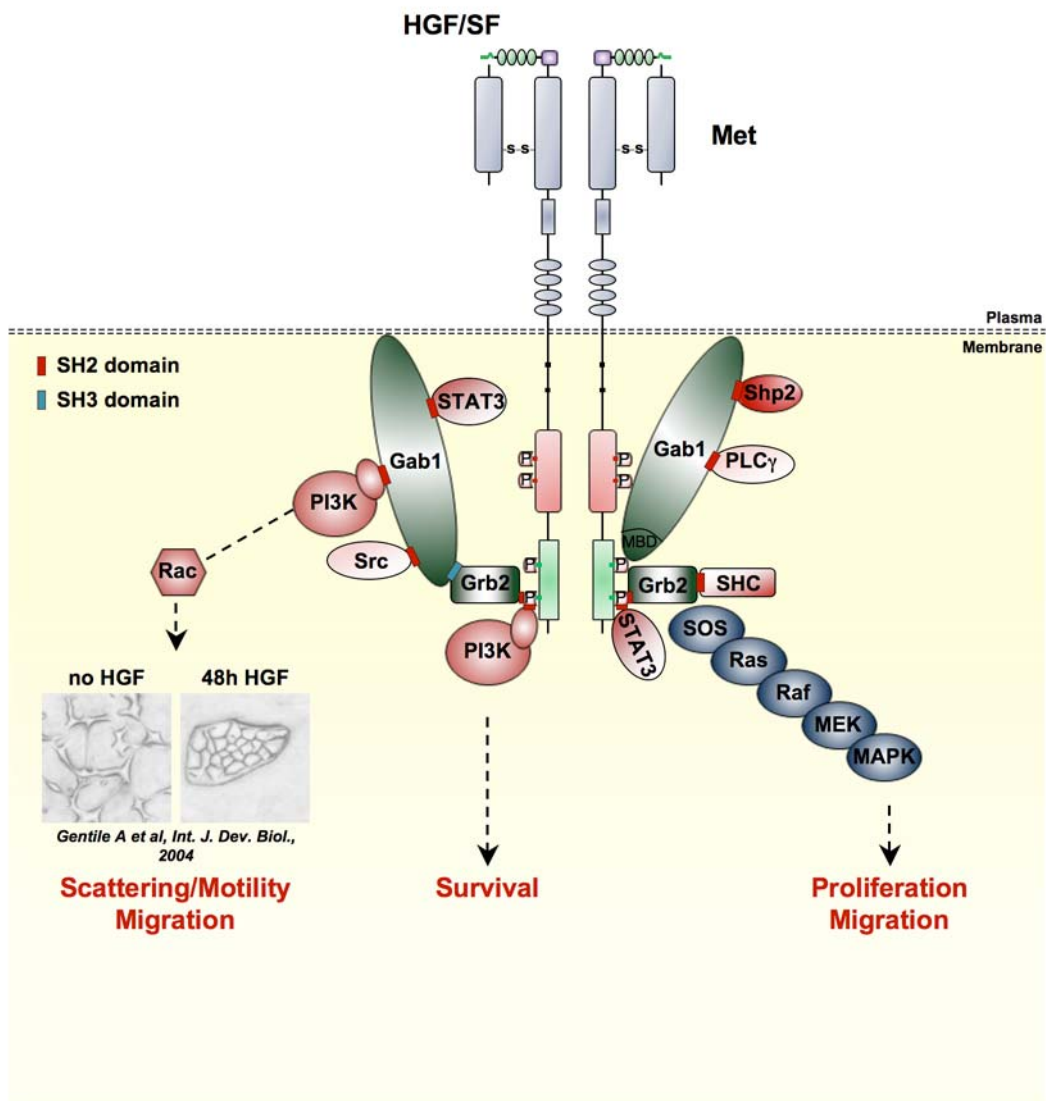


Figure 4. Met Signalosome

Rac1 is a member of the Rho Guanosine TriPhosphatases (GTPases), within the Ras superfamily of small GTPases (21kDa), which constitutes a family of 30 members<sup>46,47</sup>. All these molecules cycle between two conformational states, inactivated GDP-bound and active GTP-bound.

The switch between these two states is highly regulated. There are three different types of molecules that control their activation status<sup>47,48</sup>.

One set of molecule called GEFs (Guanine nucleotide Exchange Factor) increased their activity<sup>49</sup>. They promote GDP dissociation and then the binding to GTP. Conversely, two other set of molecules, GAPs (GTPase Activating Proteins) and GDIs (Guanine nucleotide Dissociation Inhibitor), participate in the inactivation of the Rho GTPases. GAPs enhance the intrinsic GTPase activity of the Rho GTPases and then promote the hydrolysis of the GTP into GDP<sup>50</sup>. GDIs sequester the Rho GTPases in the cytoplasm by preventing their binding to the membranes<sup>51</sup>. Usually GDIs bind to the C-terminal prenyl groups of Rho GTPases when they are GDP-loaded. This lipid group allows the interaction of the Rho GTPases with the membrane, thus the binding of the GDI on the top of this group avoids interaction between the Rho GTPases and the membrane. GDIs prevent as well the binding between the Rho proteins and their effectors.

Once activated, Rho proteins bind to their effectors and control many biological functions through the regulation of the actin cytoskeleton<sup>52,53</sup> including cell division, cell adhesion, cell polarity, vesicular trafficking<sup>54,55</sup> and cellular motility/migration<sup>56</sup>.

The three most studied and best characterised Rho GTPases are Rac1, RhoA, and Cdc42.

Rac1, through promoting actin polymerisation, triggers the assembly of actin-rich surface protrusions at the plasma membrane, called lamellipodia<sup>57,58</sup>. Lamellipodia and membrane ruffle extension occurs at the front of migrating cells, where they contribute to push forward the leading edge of the membrane. This represents the first steps of an orientated migration. The three following step in migration are: formation of new adhesions, cell body contraction and tail detachment<sup>56,59</sup>. Rac proteins are also implicated in the formation and control of cell adhesions but the two final steps are more regulated by Rho proteins<sup>56</sup>.

Conversely to Rac, RhoA leads to stress fibre formation that usually causes a decrease in cell motility<sup>44,47,60</sup>.

Cdc42, also through promoting actin polymerisation, induces the formation of filipodia, which are actin-rich finger-like protrusions from the cell surface<sup>61</sup>.

How does Met activate Rac and how does Met induce cell movement through Rac? The activation of Rho GTPases by RTKs appears to be mediated by GEFs, which can be activated directly or indirectly by the RTKs<sup>62</sup>. In MDCK cells, the Met-dependent Rac activation, lamellipodia formation and cell dissociation was shown to require the activity of PI3-K<sup>45</sup>, suggesting in this case an indirect activation between Met and the Rac-GEF. The PI3-K, which produces the lipid PIP3, was shown to be able to activate Rac upon HGF stimulation<sup>42</sup>. This may occur via the activation of a Rac-GEF, since PIP3 was shown to bind and activate several GEFs<sup>40,62,63</sup>. Once activated, Rac coordinates lamellipodium

extension at the leading edge of the cells to promote directional cell movement.

Activated Rac is localised preferentially at the front of migrating cells<sup>64</sup> and the classical model is that it gets activated at the plasma membrane<sup>59</sup>. Interestingly, a recent study reported that Rac activation may not only happen at the plasma membrane. Indeed, upon HGF stimulation (or Rab5 expression), Rac1 was found to be present on endosomes and to be activated from there by a Rac-GEF, Tiam1, located or recruited in these compartments<sup>41,65</sup>. How can the Rac GTP-bound form reach the leading edge of the cells from the endosomal compartment? The GTPase Arf6, implicated in membrane trafficking, including recycling, was shown to be implicated in the transport, possibly along the microtubules, of vesicles-containing activated Rac1 from the endosomes to the zone of the membrane ruffling<sup>65,66</sup>. These new findings are in favour of the “endosomal signalling” concept.

#### 3.3.4. A pathway for several functions and several pathways for one function

Since HGF can trigger several cell responses, including proliferation, motility and morphogenesis (see section entitled “Biological Effects”), many studies have aimed to identify which individual downstream effectors of Met lead to specific cellular responses. For example, PI3-K was found to control cell survival upon HGF/Met activation<sup>67,68</sup> and the MAPK pathway was found to be essential for the early step of cell migration<sup>69</sup>. However, Met signalling is actually more complex than initially thought and

different pathways are interconnected. Moreover, one pathway can trigger several functions while several pathways that act in synergy or compete usually are required to trigger one function. In addition, several signalling molecules are shared between different pathways.

Therefore, an unresolved, but major, question is how signalling pathways of Met are spatially and temporally integrated in the cell to generate the appropriate cell functions? This is the concept of spatio-temporal signalling which underpins much of the work I have been doing. The emerging concept of endosomal signalling may constitute an element of response. Indeed, it has been discovered recently that Met endocytic trafficking plays a role in its signalling<sup>70,71</sup>. Based on these concepts it seems likely that receptor location, the signalling pathways, their intensity and their duration, all could be different in their activity according to their sub-cellular distribution and therefore could influence cell function in different fashions.

#### **4. Met trafficking**

Initially, RTKs were thought to remain at the plasma membrane where they would make the link between the extracellular environment and the inside of the cell. EGFR was the first RTK described as being internalised after ligand binding and shown to be sorted to early and late endosomes<sup>72</sup>. Nowadays we know that this observation is true for all the RTKs<sup>73</sup>. Internalisation was first described as a desensitisation mechanism but now it also is emerging as a positive signalling regulator prior to desensitisation.

#### **4.1. RTK endocytosis via the clathrin pathway**

Endocytosis can occur by four mechanisms: macropinocytosis, the caveolin-mediated pathway, the clathrin-mediated pathway and the clathrin-and caveolin-independent pathway<sup>74</sup>. As the major route for RTK endocytosis in most cells, and the best understood, is the clathrin-coated pathway and so far the only pathway described for Met endocytosis, I will focus on this pathway.

##### **4.1.1. Ubiquitination**

Ubiquitination plays a key role in RTK endosomal trafficking. Ubiquitin consists of 76 amino-acids that attach to Lysine (Lys) residues on target proteins. There are three different modes of ubiquitination: **mon**ubiquitination (1 molecule of ubiquitin on 1 Lys residue), **multi**ubiquitination (1 ubiquitin on several Lys residues) and **poly**ubiquitination (several ubiquitin molecules on 1 Lys residue).

Degradation of RTKs seems to be driven mainly by monoubiquitination<sup>75</sup>. Molecules of ubiquitin are added onto RTKs by an E3 ubiquitin- ligase, c-Cbl, that binds phosphorylated receptors<sup>76</sup>.

##### **4.1.2. Clathrin-coated-vesicle formation (Fig. 5)**

RTKs can move laterally along the membrane. When the ligand-receptor interaction occurs, the complex accumulates in specific membrane regions called clathrin coated pits. Clathrin accumulates around the pits, drives its invagination and helps to stabilise the nascent vesicle. The clathrin-coated vesicle (CCV) is then formed and gets pinched off the membrane.

However, endocytosis is a complex mechanism still not fully understood. Despite extensive research, for more than two decades, the understanding of the molecular interactions leading to the recruitment of activated RTKs into coated pits and receptor internalisation is limited. Clathrin does not act alone and many clathrin endocytic adaptors and scaffold proteins are necessary to promote clathrin recruitment, polymerisation at the plasma membrane and formation of clathrin-coated vesicles as well as the subsequent trafficking<sup>77</sup>.

- Endocytic adaptors are usually defined by the fact that they can bind: i) clathrin, ii) Phosphatidylinositol bisphosphate PIP2 enriched in the cytoplasmic leaflet of the plasma membrane and iii) sorting signals present on the receptor. They are grouped in two classes: the multimeric Adaptor Protein complex AP-2, and the monomeric adaptor proteins Clathrin-Associated Sorting Protein (CLASP). AP180, Eps15, and epsin are the most important CLASPs for RTK internalisation<sup>77</sup>.

The endocytic process is thought to be initiated by the recruitment of these endocytic adaptors at the plasma membrane where they bind PIP2. In addition, adaptors recognise and bind the receptor to sorting signals that are present in the cytosolic tail of the receptor. The sorting signals include, but are not limited to, phosphorylation and/or ubiquitination of the RTK. Then, adaptors recruit clathrin to the plasma membrane.

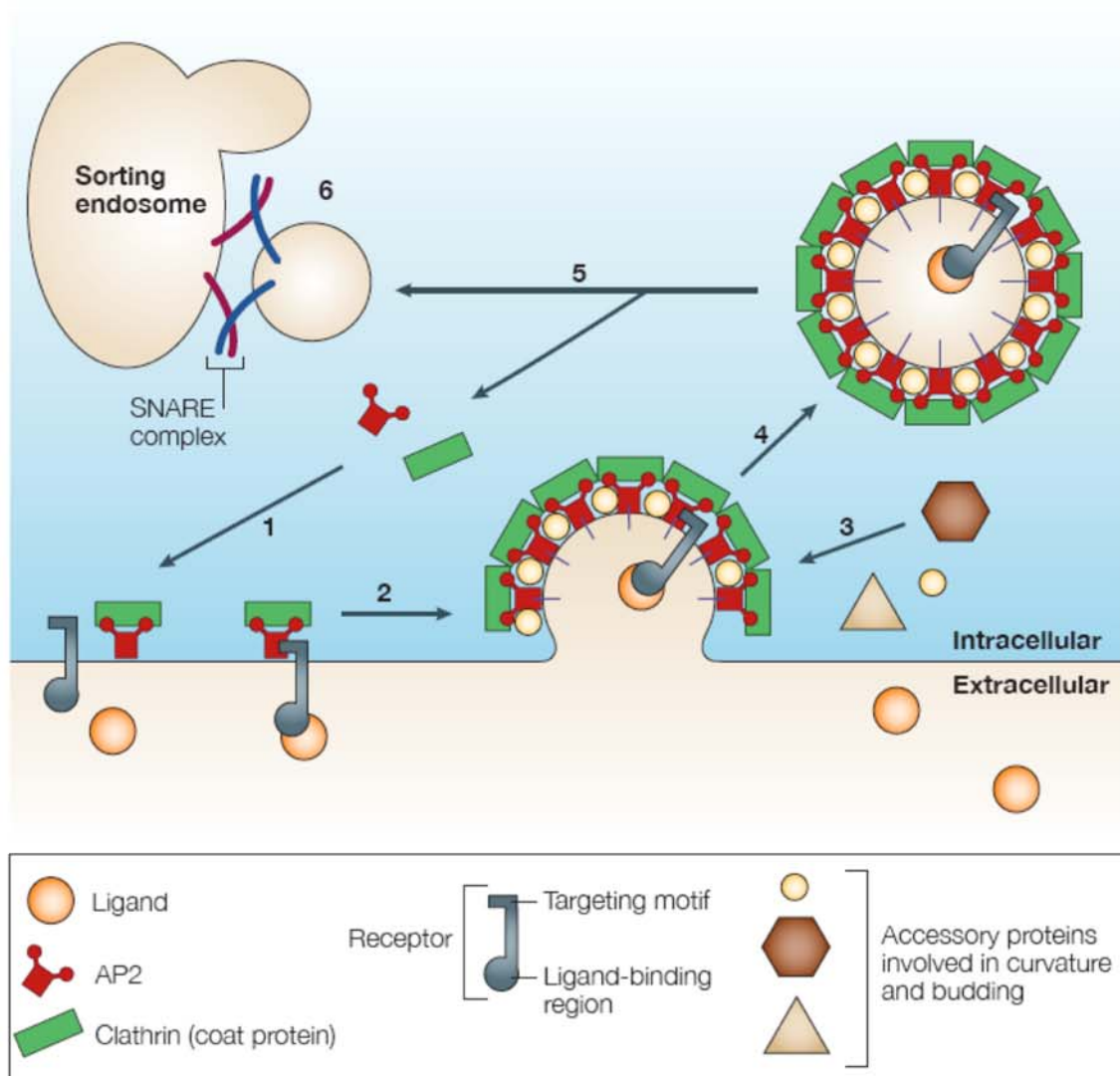


**Figure 5. Clathrin-coated-vesicle formation**

1. Recruitment of endocytic adaptor to the plasma membrane. 2. Adaptor protein binds to specialised motifs in the cytoplasmic domain of receptors and to clathrin. 3. Recruitment of accessory proteins 4. Pinching off the clathrin-coated vesicle. 5. Clathrin removal. 6. Newly formed endosomes fuse with pre-existing sorting endosome.

*From Maxfield and McGrow, Mol Cell Biol, 2004*

- Recruitment of scaffold proteins synchronises and organises all these interactions, such as those involving Esp15, that act within the forming vesicle structure.
- The combined action of the clathrin coats and the curvature driving molecules such as epsin, amphiphysin and endophilin, allow membrane curving to form a vesicle.
- c-Cbl, a molecule mostly known for its E3 ubiquitin ligase activity, has been shown to play a role in the curvature step through linking the receptor to endophilin via binding to the adaptor CIN85 (c-Cbl INTERacting protein of 85kDa)<sup>78</sup>.
- Modification of RTKs by ubiquitination initially was widely believed to be the mechanism responsible for endocytosis. Indeed ubiquitination is required for internalisation of several receptors, such as nerve growth factor or  $\beta$ 2-adrenergic receptor<sup>79</sup>. However, controversial data exist in the literature. EGFR mutants for ubiquitination (lysine mutants)<sup>80</sup> or for direct binding to the ubiquitin ligase c-Cbl (Y1045F)<sup>81</sup> can still be internalised. Moreover, it has been suggested that EGFR normally is internalised by clathrin-coated pits by using a tyrosine kinase-, Grb2-, and c-Cbl-dependent mechanism. Even if an ubiquitination event is involved in this pathway, the ubiquitination of the receptor is not necessary for its internalisation. This suggest that ubiquitination of an unidentified protein by c-Cbl is required to mediate EGFR endocytosis. Moreover if kinase activity is partially inhibited, ubiquitination of the receptor can mediate its internalisation<sup>80</sup>. Thus, EGFR internalisation, and probably that of other RTKs, can be mediated by multiple mechanisms. Such robustness of this

step of RTKs trafficking and the redundancy of the internalisation mechanisms can explain why these mechanisms are so difficult to elucidate.

- The last step is the scission of the new vesicles from the plasma membrane, with the help of late acting components such as the GTPase Dynamin<sup>74,77</sup>.

#### 4.1.3. Vesicle sorting

After the pinching off from the plasma membrane, clathrin is removed and the newly formed vesicles will fuse with one another and with pre-existing early endosomes and, more precisely, with sorting endosomes. This fusion process mainly is regulated by the small GTPase Rab5, EEA1 (Early Endosome Antigen 1) and SNAREs (Sensitive N-ethylmaleimide factor Attachment protein Receptor) proteins (**Fig. 5**). EEA1 contain a membrane lipid targeting domain, FYVE (Fab1/YOTB/Vac1/EEA1), that selectively recognises Phosphatidylinositol-3-Phosphate (PtdIns(3)P). PtdIns(3)P has a specific endosomal localisation, which strongly suggests that FYVE-containing proteins have a role in vesicular trafficking<sup>82</sup>. Actually, early endosomes correspond to two distinct endosomal organelles: sorting endosomes and Endocytic Recycling Compartments (ERC). The role of sorting endosomes is to target the receptors to their correct destinations. Three destinations are possible: the plasma membrane, the ERC or the late endosome (**Fig. 6**). In sorting endosomes, since the pH is around 6, the ligand can dissociate from the receptor allowing the recycling of the receptor back to the plasma membrane,

where it will be free to be re-stimulated by the ligand<sup>83</sup>. From ERC, receptors are recycled back to the plasma membrane, a process regulated by the small GTPase Rab11, or are directed to the trans-Golgi network or to late endosomes/ MVB (MultiVesicular Body).

#### 4.1.4. RTK degradation and recycling

When proteins are targeted to late endosomes, RTKs can be internalised into intraluminal vesicles of MVB. At this step the cytoplasmic tail of the receptor is no longer exposed, leading to the end of the signal and preventing the RTKs from recycling to the cell surface. MVB subsequently fuse with lysosomes and the receptor is then degraded. The first step in targeting a receptor to late endosomes often is the ubiquitination of its cytoplasmic domain.

The ubiquitinated receptors are recognised by multiple proteins of the endocytic pathway that contain an Ubiquitin Interacting Motif (UIM). The first recruited, in regions of the endosomes containing a specialised bilayered clathrin coat, is Hrs (HGF-Regulated tyrosine kinase Substrate). This interaction might be important for retaining the receptor in maturing endosomes, leading to its delivery to late endosomes<sup>83</sup>. Hrs seems also to be implicated in receptor degradation by recruiting the ESCRT complex (Endosomal Sorting Complexes Required for Transport) that helps sort ubiquitinated receptors from early endosomes to lysosomes via MVB<sup>84</sup>.

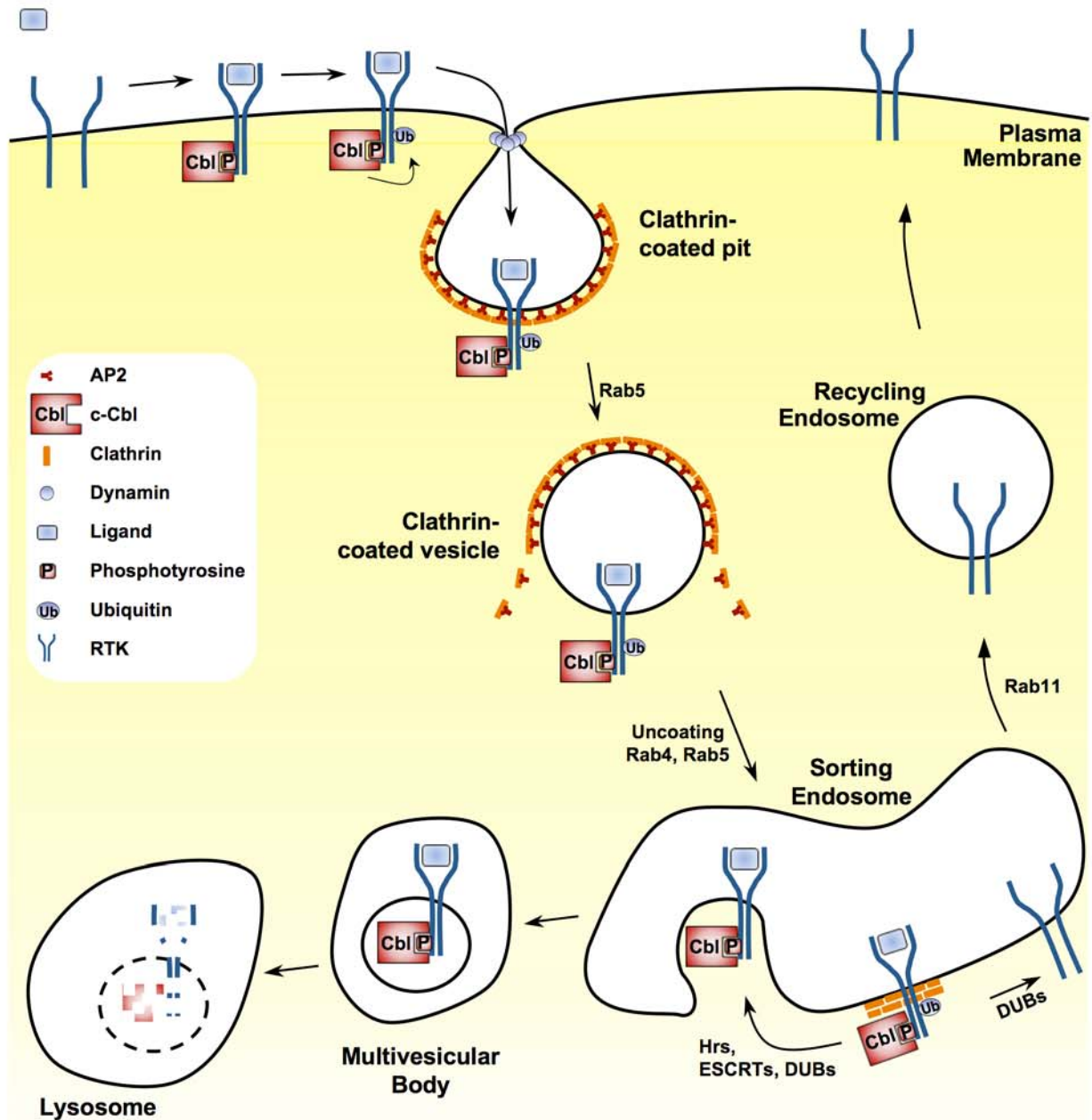


**Figure 6. RTK internalisation via clathrin-coated pathway**

After RTK activation, c-Cbl is recruited and induces receptor ubiquitination. The vesicle is then formed and fuses with sorting endosomes. Ubiquitinated RTKs are then enriched in an endosomal microdomain characterised by a bilayered clathrin coat. Receptors are subsequently internalised in inner vesicles. This process involves multiple proteins that contain ubiquitin-interacting motifs (Hrs, ESCRT complexes). Fusion of MVB with lysosomes leads to RTK degradation. RTKs that are not ubiquitinated, or that have been deubiquitinated, are not sequestered in the bilayered clathrin coat and recycle to the cell surface.

*Adapted from Peschard et al, Cancer Cell, 2003  
and Gould et al, Nat. Rev. Mol. Cell Biol., 2009*

Instead of being translocated into internal vesicles of the MVB, and thence being degraded, another fate for the RTK could be possible. Indeed, endosomal DeUBiquitinating proteases (DUBs) can deubiquitinate the RTKs, leading to the escape of the receptor from the MVB; the RTKs are no longer targeted to degradation and can be recycled back to the plasma membrane<sup>85</sup>. This was described recently for EGFR by the DUB called AMSH (Associate Molecule with the SH3 domain of STAM (Signal Transducing Adaptor Molecule))<sup>86</sup>.

It seems that the balance between degradation and recycling could be determined by the pathway of RTK internalisation: clathrin-dependent or independent. Sigismund et al reported that the EGFR internalisation pathway varies upon the doses of EGF: a low dose would promote a clathrin dependent internalisation while a high dose would preferentially trigger non-clathrin dependent internalisation<sup>87</sup>. When it is endocytosed via clathrin-independent mechanisms, EGFR would predominantly be targeted to degradation. In contrast, when its internalisation is mediated mainly via a clathrin pathway, EGFR would rather be recycled back to the cell surface<sup>87</sup>.

Traditionally, the goal of endocytosis was thought to be only the degradation of the receptor in order to switch off the signal, at least when recycling does not occur. Recently, it has become evident that receptor trafficking after internalisation participates considerably in modulating receptor signalling.

#### 4.1.5. Role of endocytosis in signalling: “endosomal signalling”

In the early 1990's, studies started to demonstrate that RTKs remain active after their internalisation within the endosomes and thus could signal from intracellular compartments before their degradation. In 1994, EGFR was the first RTK to be found associated with signalling partners in early endosomes, suggesting a persisting signalling in this compartment<sup>88</sup>. Two years later, the Nerve Growth Factor (NGF) receptor was also found to be activated and bound to its ligand, in endocytic compartments; a discovery leading to the concept of “Endosomal Signalling”<sup>89</sup>. Since then, several studies, mainly done on EGFR, have confirmed this concept<sup>73,90,91</sup>. By Fluorescence Resonance Energy Transfert (FRET), interaction between EGFR and Grb2 was observed on endosomes, showing for the first time in a living cell, interaction on endosomes between an activated RTK and an adaptor molecule<sup>92</sup>.

The detection of signalling proteins in the endosomal compartment raised the question as to whether signal transduction actually can occur from the endocytic membrane. Wang et al reported that endosomal localisation of EGFR<sup>93,94</sup> and PDGFR<sup>95</sup> is sufficient to activate signal transduction. PDGFR was shown to be associated with several proteins (Grb2, SHC and the p85 subunit of PI3-K) in the endosomes<sup>95</sup> while the TGF- $\beta$  receptor, a serine/threonine kinase receptor, was also found recruited on endosomes *via* the association with the compartment-specific adaptor protein, SARA (SMAD Anchor for Receptor Activation), a FYVE domain protein<sup>96</sup>. Further studies demonstrated the importance of endosomal

localisation in TGF- $\beta$  signalling to generate specific signals from this compartment<sup>97</sup>.

It was further suggested that trafficking of activated RTKs could therefore have an impact on their signalling. Studies aiming at interfering with receptor trafficking have been pioneered by Viera *et al*<sup>98</sup>. By overexpressing a dynamin dominant-negative construct in Hela cells, to impair EGFR internalisation, it was shown that some signalling molecules were hypophosphorylated (such as ERK) but others were hyperphosphorylated (such as PLC- $\gamma$ ), showing evidence of the need for correct receptor trafficking in establishing specific signalling pathways. Endosomal signalling was also shown to be pathway selective for the insulin receptor<sup>99</sup>. But some proteins appear to be found activated in the endosome and at the plasma membrane. It is the case for Ras GTPase<sup>100,101</sup>. ERK has been found activated at the plasma membrane, in focal adhesion complexes or in endosomes<sup>101</sup>.

Signalling from the endosome appears to require specific scaffolds that “anchor” the signalling complexes to the endosome in response to growth factor stimulation. Indeed, ERK was reported to be localised and activated on late endosomes through association with the scaffold protein MP1 (MEK1-binding Partner), itself bound to the adaptor p14, attached to the cytoplasmic face of endosomes<sup>102,103</sup>. Recently, p18, a novel lipid raft adaptor anchored to late endosomes, was shown to directly bind the p14-MP1 complex, thus assembling the p14-MP1-MEK-ERK complex on late endosomes<sup>104</sup>. Moreover, this endosomal localisation, thanks to the

association with MP1/P14, was necessary for full ERK activation upon EGF stimulation<sup>103</sup>.

More recently, Akt and its substrate GSK-3 $\beta$  have been found recruited by the Rab5 effector Appl1 on newly identified endosomes bearing Rab5 and Appl proteins<sup>41</sup>, thus called “Appl endosomes”<sup>105</sup>. In addition, Appl1 was also required to recruit, directly or indirectly with its ligand the NGF, activated TrkA on endosomes, hence allowing ERK and AKT activation<sup>106</sup>. Different receptor locations could mean different activated pathways leading to different cellular responses<sup>107</sup>. Recent studies support the hypothesis that “endosomal signalling” is an important mechanism to control RTK-generated cell responses such as cell migration<sup>70,71,108,109</sup> and cell survival<sup>41,94,95</sup>. Endosomal signalling was also shown to influence cell proliferation, although this could be both positively<sup>95,110</sup>, or negatively<sup>98</sup>. Further investigations are required for a better understanding of how these two diametrically opposed actions are evoked. One of the strongest pieces of evidence supporting the concept of “signalling endosomes” was probably made by Schenck et al<sup>41</sup>. They demonstrated, for the first time, the importance of “endosomal signalling” *in vivo*. They showed that specific signals were generated from the endosomal compartment, and moreover were required for AKT-dependent survival in zebrafish development<sup>41</sup>.

Together, these findings have identified RTK endosomal signalling as requiring more than just ligand-receptor interactions at the cell surface. Signalling can occur at the plasma membrane and could be continued on endosomes thus modifying signal intensity, or signalling can require

endocytosis to generate endosome-specific signals, thus contributing to signal diversification and specificity<sup>111,112</sup>. How is it that endosomes could generate specific signals? Endosomal membranes are composed of particular lipids, only present on endosomes, such as PtdIns(3)P. This induces the recruitment of specific adaptor proteins, such as EEA1 or p18 on late endosomes<sup>104</sup>. In addition, this lipid composition evolves during endosome maturation leading to the recruitment of other/new partners. For example, Appls are present on early stages of early endosomes and then will be replaced by proteins such as EEA1 as endosomal maturation occurs<sup>113</sup>.

Moreover, the pH of endosomes is acidic and that can be required for the activity of diverse enzymes<sup>114</sup>. Endosomes define restricted compartments in which activated receptors and signals are in close juxtaposition and then act by providing protection against phosphatases<sup>115</sup>.

Thus, the current concept is that endosomes represent a platform, which integrates signalling pathways temporally, and spatially to determine response specificity that has important biological and pathological consequences<sup>111,116,117</sup>.

## **4.2. Met endocytosis / trafficking**

### 4.2.1. Met endocytosis

Studies on Met endocytosis and trafficking have only started relatively recently. After ligand binding, and therefore activation, Met is internalised via a typical clathrin-mediated process<sup>118-120</sup>. Indeed Met endocytosis is impaired when clathrin-mediated endocytosis is blocked by dynamin

mutant expression<sup>70,118</sup> or by overexpression of the COOH part of the endocytic adaptor, AP180<sup>119</sup> or by knock-down of clathrin<sup>70</sup>. Met endocytosis is fast, the totality of Met present at the cell surface being internalised within a few minutes upon HGF stimulation<sup>119</sup>.

So far, the mechanisms found to regulate Met endocytosis are similar to the ones described for EGFR (detailed above). They include c-Cbl-CIN85-endophilin complex formation<sup>121</sup> and c-Cbl indirect binding to Met via Grb2 associated to c-Cbl ubiquitin ligase activity<sup>122</sup>. Indeed, when the indirect interaction of c-Cbl to Met via Grb2 is abrogated, the step of endocytosis is impaired. However, a c-Cbl mutant able to bind Grb2 but lacking its ubiquitin ligase activity failed to promote Met internalisation; thus, as for EGFR, the ubiquitin ligase activity of c-Cbl is required for Met endocytosis<sup>122</sup>. Accordingly a dual role for c-Cbl, as an ubiquitin ligase and as an endocytic adaptor, is involved in Met endocytosis.

#### 4.2.2. Met trafficking

After internalisation, following 15 min of HGF stimulation, Met shows a good co-localisation with the early endosomal compartment marker, EEA1. This co-localisation is lost at later time points (120 min) as Met has trafficked from early endosomes to a perinuclear compartment<sup>118,119</sup>. This perinuclear compartment, in part, includes the Golgi<sup>119</sup> and has also been reported to correspond to late endosomes<sup>118</sup>. This traffic is an active regulated process as it is microtubule-dependent and regulated by PKC activity<sup>119</sup> (**Fig. 7**).

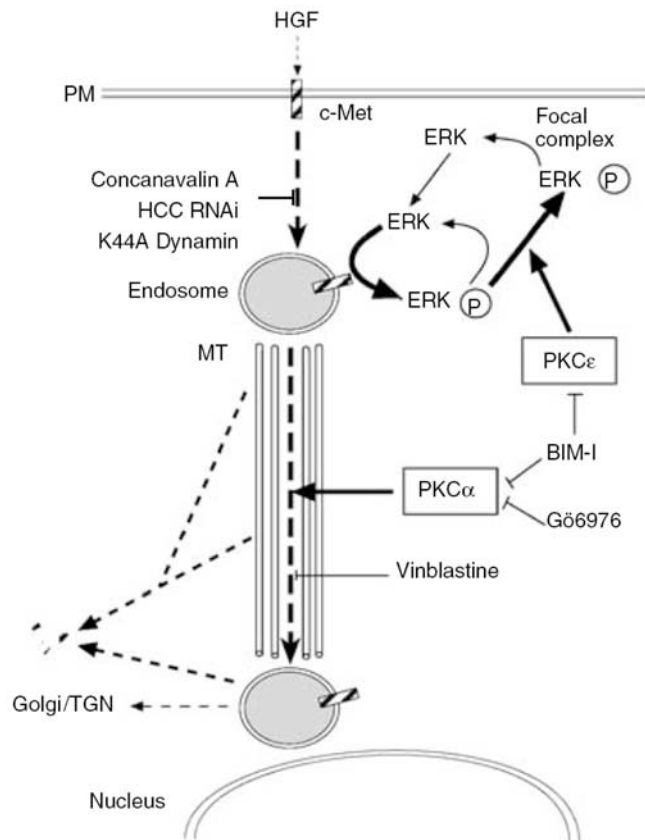


**Figure 7. PKC controls Met trafficking**

Met is internalised via the clathrin-coated pathway. Met's trafficking from peripheral endosomes to a perinuclear compartments is an active process as it is microtubule-dependent and regulated by the Protein Kinase-C activity.

*From Kermorgant et al, Embo J, 2004*

#### 4.2.3. Met degradation

Endocytosed Met upon HGF stimulation gets further degraded such that 50% of the molecule is degraded after 120 minutes of stimulation<sup>119</sup>.

As it is for EGFR, the requirement of Met ubiquitination by c-Cbl for it to be degraded has clearly been established. The recruitment of c-Cbl to Met leads to its ubiquitination<sup>123</sup> and c-Cbl can directly bind Met on its phosphorylated Tyr<sup>1003</sup><sup>123,124</sup>. Again like for EGFR<sup>81</sup>, when the direct interaction between Met and c-Cbl is impaired by mutation of the Tyr<sup>1003</sup>, Met degradation is delayed (but the internalisation is intact)<sup>124</sup>. The Y1003F mutant fails to interact with Hrs, suggesting that Met needs to go in endosomes, to interact and phosphorylate Hrs, in order to be degraded<sup>124,125</sup>.

The nature of the degradative pathway for Met remains controversial in the literature. After ligand binding, Met was reported to be polyubiquitinated<sup>118,126</sup> but also multimono-ubiquitinated<sup>125</sup>. In addition, Met has been characterised as being degraded not only via the lysosomal pathway<sup>118,125</sup>, which represents a classical pathway for membrane receptors, but also via the proteasomal pathway<sup>119</sup>. Perhaps, several mechanisms are implicated in Met degradation and it is a question of the balance between the various pathways that changes depending on the cell environmental conditions. It also is possible that the proteasome pathway is only implicated indirectly (maybe the proteasomal degradation of a molecule is needed to allow the degradation of Met via the lysosome). In addition, lysosomal sorting of EGFR has been shown to be influenced by proteasome inhibition<sup>127</sup>.

Interestingly, Met degradation does not require the trafficking to the perinuclear location and could be generated from peripheral endosomal compartments<sup>119</sup>.

Finally, a novel transmembrane protein, LRIG1 recently was identified and reported to induce Met degradation in a ligand-c-Cbl independent manner via the lysosome pathway<sup>128</sup>.

Met degradation can be regulated by the chaperone protein HSP90 (Heat Shock Protein 90) activity. Webb et al developed a cell-based assay in MDCK cells in which HGF stimulation induced the high activation of plasmin protease activity<sup>129</sup>. Over 1000 compounds were tested and geldanamycin, an Hsp90 inhibitor, was identified as a potent inhibitor of plasmin activation<sup>129</sup>. These authors proved that HSP90 inhibitors hampered Met induced pathways. In addition this study, and others, demonstrated that geldanamycin treatment induced Met down regulation suggesting, at least in part, that HSP90 is involved in Met protection against degradation<sup>130,131</sup>.

In contrast with EGFR, no recycling of Met, with or without ligand stimulation, has so far been described.

#### 4.2.4. Met endosomal signalling

As for other RTKs, Kermorgant *et al* showed that Met undergoes an “Endosomal signalling”<sup>70,71,119</sup>. Endosomal Met was shown to be associated with a phosphotyrosine signal, indicating it is still active in these vesicular compartments<sup>70</sup>. In the same study, Kermorgant *et al* demonstrated that Met dependent ERK1/2 phosphorylation requires

endocytosis<sup>70</sup>. The sustained ERK1/2 phosphorylation was not due to a persistent signal from the plasma membrane but rather was due to endosomal signalling. It was concluded that the spatial control of Met signalling events might be critical in determining cellular responses<sup>70,132</sup>. Moreover, a recent paper from Kermorgant et al has confirmed the importance of Met endosomal signalling in Stat3 activation and nuclear translocation. In this study, it was reported that, not only is endocytosis required for Met dependent Stat3 activation but that Met trafficking to a perinuclear endosome was necessary to induce a robust Stat3 phosphorylation and consequent nuclear accumulation of phosphorylated Stat3<sup>71,133,134</sup>.

## **5. Biological effects of Met/HGF**

HGF/SF is produced by tumour stroma and acts in a paracrine manner to stimulate epithelial cells that express Met. By the activation of multiple pathways Met triggers a wide range of biological activities, that comprise proliferation, protection from apoptosis, cell dissociation (scattering), motility, migration, cell polarisation and invasion of the surrounding matrix<sup>15,135</sup>. The coordination of all these biological responses under physiological conditions results in the establishment of the so-called “branching morphogenesis”<sup>15</sup> or “invasive growth program”<sup>136,137</sup> which takes place during embryonic development or when Met/HGF signalling is deregulated during tumour progression.

### **5.1. Implications of Met/HGF signalling at development stages**

Knock out (KO) for Met or HGF/SF are both lethal and the mice die *in utero*, showing the crucial role of Met/HGF in development<sup>138,139</sup>. Two side-by-side papers, and another published the same year in Nature, in 1995 showed that HGF/SF knock out and Met knock out mice respectively die between 13 and 16.5 days of embryogenesis (E13-E19.5) with a slight reduction in body size. The three groups found that the most marked phenotype was a strong reduction in the size of the liver<sup>139,140</sup>. A defect in placenta formation, with a reduced number of trophoblast cells, also was observed. This could explain the embryonic lethality suggesting it occurred by a defect in nutrient transport from the mother.

A complete absence of muscle in the limbs, shoulders and diaphragm was observed, due to an absence of migrative myogenic progenitors. In contrast, the muscles that do not originate from migrative precursors, such as axial muscles, were normal. Indeed, HGF/SF is expressed in a sequential manner that drives Met progenitor muscle cells to their final destination to constitute new muscles<sup>138</sup>. This observation established the important role of Met/HGF signalling in control of migration during embryogenesis. Both Met and HGF/SF are expressed in the developing nervous system. A similar role for Met/HGF signalling could be attributed in neuronal development and, more precisely, in the development of the projection of spinal motor axons to target muscle cells<sup>141</sup>. In fact, explanted mouse limb bud mesenchyme attracts axons from motor neurons in a collagen matrix<sup>142</sup>. As they are for the muscle development, HGF/SF and Met are expressed in patterns that are consistent with a

chemoattractant guidance role: Met is expressed by motor neurons and HGF/SF by the limb bud mesenchyme<sup>142</sup>. HGF/Met interactions were also shown to be implicated in human embryonic gut development; a dynamic expression and localisation pattern of HGF and Met that followed the morphogenesis of the gut, according to time of development, was identified<sup>143</sup>.

### **5.2. Implications of Met/HGF signalling into post-natal life**

Met/HGF interactions also play a major role throughout adult life. Indeed, the expression of both Met and HGF/SF was found to be increased after various injuries<sup>144,145</sup>. Increased HGF expression levels could be a defensive reaction of the injured organ in order to protect or heal itself.

After hepatectomy in the rat, a huge increase in HGF/SF plasma levels was detected, leading hepatocytes to synthesise DNA and thus proliferate<sup>144</sup>. This result confirmed older studies conferring upon HGF a mitogenic capacity for hepatocytes<sup>17</sup>. In a rat model of ischaemia/reperfusion injury, plasma HGF levels and Met mRNA levels in the ischaemic myocardium were found to be increased considerably<sup>145</sup>. HGF has also been shown to be cardioprotective *in vivo*<sup>145</sup>.

In 2007, the group of Walter Birchmeier demonstrated that Met signalling is necessary in skin wound healing<sup>146</sup>. They generated conditional mice, where Met was knocked out only in keratinocytes, and found that such animals were unable to induce *in vivo* skin wound healing and that no compensatory systems appeared to exist.

HGF/SF is also known as an angiogenic factor. *In vitro* studies showed that HGF can act directly on endothelial cells, shown to express Met, by inducing their proliferation and their migration/motility<sup>147,148</sup>. A study conducted on rabbit corneas showed that HGF promotes formation of new capillaries without inducing an inflammatory reaction<sup>147</sup>.

All these data prove that Met/HGF interactions play a key role in several postnatal processes and these actions are necessary for maintaining homeostasis. Deregulation of these normal interactions could lead to human malignancies.

## **6. Met/HGF and cancer**

A large amount of evidence suggests that RTKs are implicated in the development of human cancers either through receptor gain of function mutations or through ligand/receptor overexpression. Indeed, half of the members of the RTK family have been associated with human malignancies<sup>2</sup>. Met is one of them. Historically, as described in the section “The Met receptor tyrosine kinase”, Met was identified as a proto-oncogene corresponding to a fusion protein “TPR/Met” in a cell line treated with a chemical carcinogen. In 1991, this translocation was reported to occur spontaneously in gastric carcinomas, suggesting a role for oncogenic Met in cancer progression<sup>149</sup>. Met is also able to induce cell transformation when it is transfected into fibroblasts (that do not express endogenous Met)<sup>150</sup>. These cells are able to grow in an anchorage independent manner (soft agar assay), to generate a tumour when grafted into mouse models<sup>150</sup>, and to generate metastases<sup>151</sup>. The cells originating

from the parental tumour explants have an enhanced tumorigenic potential correlating with an increase in total Met expression<sup>151</sup>. In conclusion, in mesenchymal cells, Met signalling by itself appears to promote tumorigenesis.

Additionally *in vitro* studies showed that HGF/Met signalling could enhance the migration and the invasiveness of many cancer cell lines. Invasion through Matrigel was shown to be facilitated by the stimulation, by HGF, of the production/activity of several Metalloproteinases (MMP), including MMP-1 and -2<sup>152</sup>. An autocrine loop was described in a gastric cancer cell line that promotes migration, suggesting the possible involvement of HGF/Met autocrine signalling in the progression of stomach cancer<sup>153</sup>.

Moreover, Met/HGF signalling has been reported to be deregulated in a large variety of human cancers<sup>14,154</sup>. Met-dependent signalling could, for example, be increased through overexpression of the receptor due to gene amplification, enhanced transcription or post-transcriptional modifications<sup>155</sup>, by ligand binding (autocrine and paracrine) or because of activating mutations<sup>156</sup>. In addition, Met could be activated in an aberrant way by other cell surface receptors, such as CD44, integrin or other RTKs as has been shown to occur for EGFR or RON<sup>154,157,158</sup>.

### **6.1. Met/HGF overexpression**

Met and/or HGF/SF have been found to be expressed or overexpressed in several human carcinomas and in other types of cancers, and also in their metastases<sup>14,15</sup>. Moreover, their levels of (over)expression could serve as indicators of prognosis.

- Met overexpression has been linked to tumour progression of several cancers, including breast, colon, liver and kidney<sup>159-161</sup>. For example, based on micro-array analysis, Met overexpression in hepatocellular carcinomas has been associated with expression of a pattern of Met regulated genes which composed the signature of an aggressive cancer which carried an increased probability of death<sup>162</sup>.

Met gene amplification, leading to overexpression, was reported in several human cancers<sup>14</sup> including 8% of oesophageal carcinomas<sup>163</sup>, 23 % of gastric carcinomas<sup>164</sup>, metastases of oesophageal carcinomas in the lymph node<sup>163</sup> and of colorectal carcinomas in the liver<sup>165</sup>. More recently, a quantitative PCR study reported that more than 78% of HNSCC tested had a higher Met gene copy number as compared to normal tissue<sup>166</sup>.

Finally, trisomy of chromosome 7, the chromosome bearing Met, was identified in 95% of sporadic Papillary Renal Carcinomas (PRC) and in 100% of Hereditary Papillary Renal Carcinomas (HPRC)<sup>167-169</sup>.

- HGF/SF has also been found to be overexpressed in tumours of the breast with a correlation with poor prognosis<sup>170</sup>. In this study, these investigators established that the intra-tumoral quantity of HGF correlated with the disease free interval and the patient's survival. A high amount of HGF was linked with a shorter disease free time and with a reduction in overall survival<sup>170</sup>.

## **6.2. Identification of Met mutations and experimental evidence of their role in tumorigenesis**

A possible direct link between Met and cancer was the identification, in 1997 by Schmidt *et al*, of Met mutations in HPRC and sporadic PRC<sup>168</sup>. Nine missense mutations were found in the tyrosine kinase region of Met (exon 17,18,19) including five germline and four somatic mutations. Germline mutations were detected in 4/7 HPRC tested families and somatic mutations in 3/60 patients with sporadic HPRC. At this time nothing had proved that these mutations lead directly to tumorigenesis but this was suggested. Six of these identified mutations correspond to a change in amino-acid class, implying an impact on protein function. Commonly, these tumours present a trisomy of chromosome 7, as mentioned above, and further studies showed that it was particularly the chromosome with the mutated allele of Met that was duplicated, suggesting its involvement in tumorigenesis<sup>171</sup>. Moreover, these mutations are located in codons homologous to codons that are the target of disease-producing mutations in other receptor tyrosine kinases, such as RET and Kit<sup>172,173</sup>.

In order to know whether these mutations could play a role in cancer development/progression, Jeffers *et al* introduced them in mouse Met cDNA and transfected constructs containing such altered cDNA into NIH3T3 fibroblast cells<sup>156</sup>. They demonstrated that these cells were more transformed *in vitro* than cells expressing Wild type (Wt) Met and this occurred without the need for HGF binding. Indeed, they had lost contact inhibition and acquired the capacity to form foci. Interestingly, the mutated

receptor exhibited an increased level of tyrosine phosphorylation when compared to Wt Met. Moreover, these cells were more tumorigenic than Wt Met expressing cells when grafted into nude mice<sup>156</sup> and induced metastasis *in vivo*<sup>174</sup>. Similar results were obtained with NIH3T3 expressing a chimeric Met composed of the extracellular domain of NGF fused with the intracellular domain of Met with or without the different mutations. Conclusions from these studies were that mutationally activated Met forms reside in a partially activated state (without ligand binding) that can be enhanced further through ligand stimulation and that these biochemical changes might play a crucial role in HPRC.

Since 1997, these missense Met mutations, and others, have been identified in several human cancers (**Fig. 8, Table 1**). They are localised either in the tyrosine kinase domain<sup>166,167,175-178</sup>, the juxtamembrane region<sup>166,179-182</sup>, or in the semaphorin domain<sup>166,179,183,184</sup>. In 2006, a somatic intronic mutation, leading to the deletion of exon 14, which encodes for the juxtamembrane domain, was identified in non-small cell lung cancer<sup>185</sup>.

### ***6.3. Mechanisms of Met activating mutations in cell transformation***

#### **6.3.1. Met activation**

The question now is to understand how these oncogenic Met mutations confer upon the cell a transforming potential. So far, investigations have been mainly performed on the mutations found in the kinase domain.

Computational studies reported that the M1268T and D1246N mutations would contribute to the stabilisation of Met in an active conformation<sup>186</sup>.

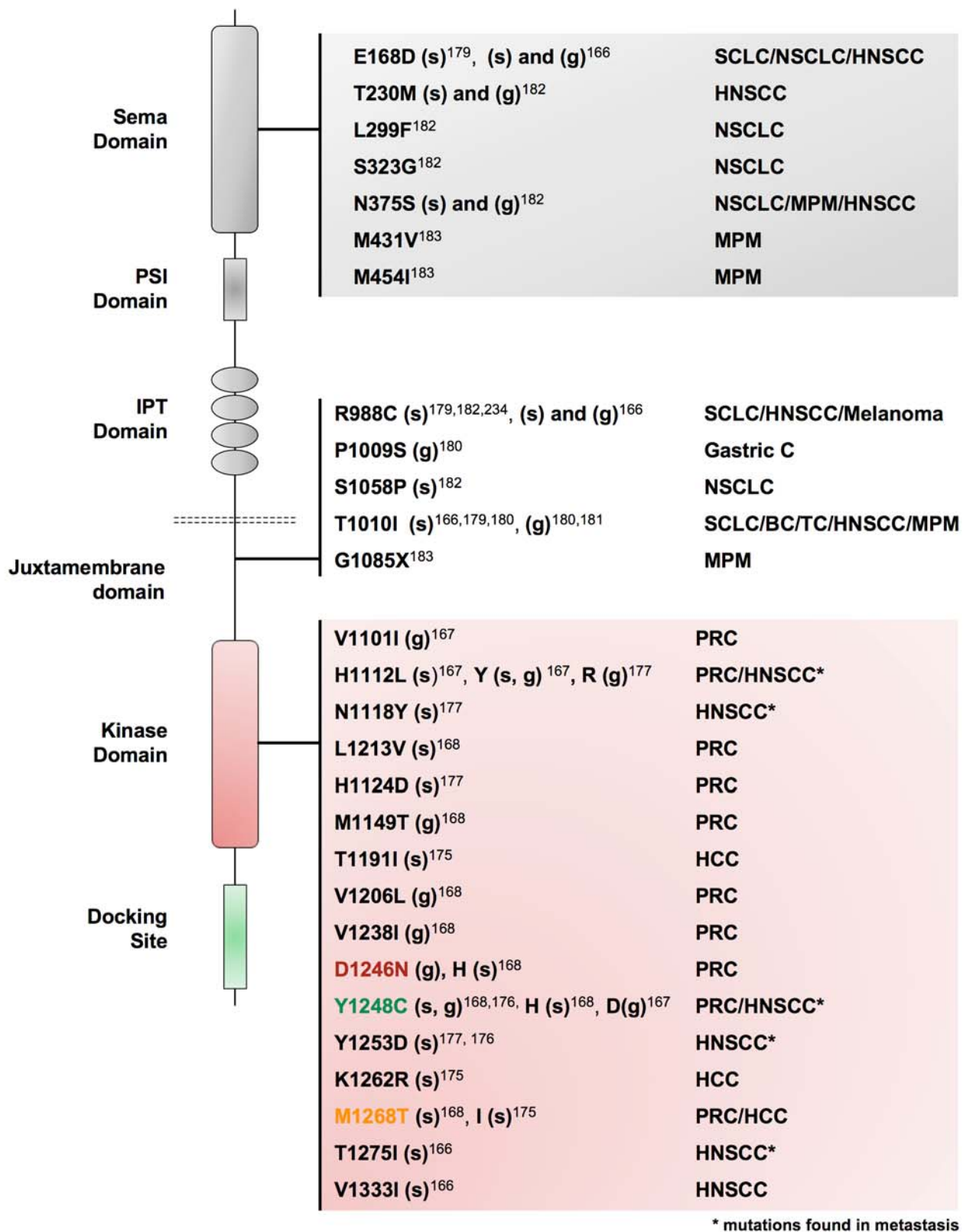


**Figure 8. Missense mutations of Met identified in human cancers**

The known missense mutations of Met found are summarised in this diagram. Semaphorin (SM); Immunoglobulin (Ig); Juxtamembrane (JM); Somatic (s); Germline (g); Breast Cancer (BC); Small Cell Lung Cancer (SCLC); Non Small Cell Lung Cancer (NSCLC); Malignant Pleural Mesothelioma (MPM); Papillary Renal Carcinoma (PRC); Head and Neck Squamous Cell Carcinoma (HNSCC); HepatoCellular Carcinomas (HCC); Thyroid Carcinoma (TC).

			Transforming potential		
			basal activation	Tumorigenicity <sup>156,174</sup>	
Type of cancer				<i>In vitro</i> (Foci formation)	<i>In vivo</i> (Tumour size)
<b>D1246N</b>	germline	HPRC <sup>168</sup>	++	++	++
<b>M1268T</b>	somatic	HPRC <sup>168</sup> HCC <sup>175</sup>	+++	+++	+++
<b>Y1248C</b>	germline	HPRC <sup>168</sup> HNSCC (metastasis) <sup>176</sup>	+(+)	+	+(+)

**Table 1. Summary of results obtained on Met mutations D1246N, M1268T and Y1248C, localised in the kinase domain**

HPRC: Hereditary Papillary Renal Carcinoma; HNSCC: Head and Neck Squamous Cell Carcinoma; HCC: HepatoCellular Carcinoma

The tyrosines identified to be essential in Met/HGF signalling<sup>27,187</sup>, Y<sup>1349</sup> and Y<sup>1356</sup>, are indispensable to the mutants for inducing transforming ability<sup>188-190</sup>. Indeed, when these tyrosines were converted into phenylalanines, such that no more coupling with transducers was possible, no cell transformation occurred<sup>191</sup>.

This work suggested that the constitutive coupling of the Met mutants to downstream partners is necessary to promote cell transformation.

The activation of Wt Met by HGF requires the sequential phosphorylation of the two major tyrosines, 1234 and 1235, in the kinase domain. An intriguing result obtained by Chiara *et al* was that tyrosine 1234 was not phosphorylated in the Met mutants tested, showing a decrease in the kinase activation threshold<sup>189</sup>.

### 6.3.2. Downstream signalling

Several studies aimed to identify the signalling partners of the oncogenic Met forms<sup>174,188,192</sup>.

The MAPK pathway seems to be involved, as an increased level of MAPK phosphorylation was found in NIH3T3 cells expressing the mutated receptor compared to cells expressing the Wt Met<sup>174</sup>. However, a different cell model, derived from NIH3T3 cells expressing the M1268T mutation and able to grow in suspension, did not display a constitutive MAPK phosphorylation<sup>193</sup>.

Unlike for TPR-Met, the binding of Grb2 appears unnecessary to promote transformation by the Met forms with activating mutations<sup>188</sup>. However,

Grb2, as well as the p85 subunit of PI3-K, and Gab1 were found to be bound constitutively to Met mutants<sup>191</sup>.

The tumorigenic potential of M1268T, one of the most studied mutants, appears to be driven by c-Src. This protein phosphorylates Paxillin and Focal Adhesion Kinase (FAK), two proteins important for cytoskeleton rearrangements<sup>193</sup>, and such changes often are associated with transformation.

Changes in substrate specificity have also been reported for the M1268T Met mutation<sup>186,191</sup>. In fact, the mutation changes the sequence into a sequence characteristic of cytosolic tyrosine kinases, thus allowing the binding of c-Abl tyrosine kinase substrates.

The identification of partners or mechanisms of these different oncogenic Met mutants is impossible to generalise about since they might vary between each mutation<sup>190,192</sup>.

These differences in signalling translate into changes or variations in biological functions, such as proliferation versus apoptosis protection and the stimulation of invasion<sup>192</sup>. Thus, the M1268T and D1248H Met mutations would signal more through the Ras signalling pathway, leading to important transforming potential as seen in the focus formation assay, whereas the Y1248C Met mutant would interact more readily with PI3-K, thus protecting cells against apoptosis.

## 7. RTK mutations and cancer

As for Met, other RTKs present mutations that have been shown to contribute to the growth and metastasis of human cancers<sup>194,195</sup>. Some of these mutations confer drug resistance or, in an opposite fashion, greater sensitivity to inhibitors in expressing cells (see **Discussion-Part I**).

### *EGFR*

In 2004, somatic mutations were identified in the EGFR in 10% of patients with Non-Small Cell Lung Cancer (NSCLC)<sup>196</sup>. The hotspots of mutations have been found to be located in the tyrosine kinase domain. They correspond to point mutations, small in frame deletions or insertions.

### *Kit and Ret*

Among the RTK family, Met, Kit and Ret present a highly conserved tyrosine kinase region. Mutations identified in one of them led to the discovery of the same mutation, at the corresponding amino-acid position, in the others. Indeed, the two Met mutations (M1268T and D1246N), affecting conserved residues, were found previously in tumorigenic forms of the Ret and Kit receptors respectively<sup>172,173</sup>. The Ret M918T mutation was identified in multiple endocrine neoplasia type 2B and this mutation has been shown to be responsible for most of the cases of this tumour<sup>173</sup>. The Kit D816Y/V has been found in human mastocytosis<sup>172,197</sup>. As noted for Met and EGFR mutations, the Kit D814Y mutant and Ret R918T mutant, are highly phosphorylated<sup>198,199</sup>. In both of them, a change in substrate specificity was also observed<sup>199,200</sup>.

### *FLT-3*

The RTK Fms-Like Tyrosine kinase 3 (FLT-3), has been found mutated in the juxtamembrane<sup>201</sup> in a large proportion of acute myeloid leukaemias<sup>203</sup>

### *FGFR3*

Mutation of the Fibroblast Growth Factor 3 (FGFR3) in the kinase domain<sup>202</sup> was reported in a variety of skeletal disorders<sup>204</sup>.

All these mutations are “gain of function” events, increasing the activation of the receptors, leading to an increased activity of their downstream pathways.

Since the initiation of my project, few recently published studies have revealed trafficking perturbations of such mutants, leading to an impaired down-regulation, or to an incorrect maturation, which both could play a substantial role in the gain of function of these mutations (though this has not yet been reported for Met mutations).

## ***7.1 Mutations and trafficking modifications***

### ***7.1.1. Impaired down-regulation: EGFR***

Two of the EGFR mutations found in NSCLC, L858R and L816Q, were shown to lead to modifications in EGFR trafficking. The mutants escape ligand-induced down-regulation and are associated constitutively with chaperone protein HSP90 and the ubiquitin ligase c-Cbl<sup>205</sup>. By treating the cell with an HSP90 inhibitor, this degradation was restored suggesting that HSP90 maintains the stability of EGFR in an active conformation.

Another mutant, EGFRvIII, which lacks a part of the extra-cellular domain, presents defects in internalisation and degradation<sup>206</sup>. The impaired down-regulation was attributed to an inefficient ubiquitination due to the hypophosphorylation of the Y<sup>1045</sup> c-Cbl binding site, and thus an altered association with c-Cbl<sup>206</sup>. Although c-Cbl was shown still to bind to the EGFR mutant via Grb2, this was inefficient in terms of leading to proper ubiquitination. However, although these EGFR mutants can still be internalised they are not sorted correctly as they recycle back to the plasma membrane<sup>206,207</sup>.

#### 7.1.2. Incorrect maturation leading to intracellular accumulation

##### *Kit: accumulation in the Golgi*

An immature form of a Kit mutant, the D814V was found localised in the Golgi, from where it is able to signal, and this was sufficient to promote tumorigenesis, both *in vitro* and *in vivo*<sup>208</sup>. The same mutant had no transforming properties when localised in the Endoplasmic Reticulum (ER)<sup>208</sup>.

##### *Ret, FLT-3 and FGFR3: accumulation in the ER*

Following inefficient maturation, precursor forms of Ret, FLT-3 and FGFR3 mutants were detected in the ER where they induced downstream signalling<sup>209, 202,201</sup>. This was for example reported for the FLT-3 ITD mutant, which, as a consequence, had a reduced expression at the cell surface. Its artificial targeting to different cellular localisations was found to mediate differential signalling, leading to differences in cell growth<sup>210</sup>.

There are some possible explanations as to why these RTK mutants are improperly targeted to the plasma membrane. Their high state of phosphorylation seems to be one of the reasons since overexpression of protein tyrosine phosphatases or kinase inactivation restored maturation and surface localisation of the FGFR3 and FLT-3 mutants<sup>201,202,211</sup>. Glycosylation of RTKs seems also to be involved in their defect of trafficking to the cell surface. Thus, the FLT-3 mutant, when modified in order to eliminate the majority of its glycosylation sites, was addressed normally to the plasma membrane<sup>210</sup>.

So far, no study aiming at investigating the trafficking and the subcellular localisation of Met mutants located in the kinase domain has been conducted and thus I undertook to perform such an evaluation.

## **8. Targeting Met in Cancer**

As described above, Met was shown to be oncogenic through different processes that, ultimately, lead to quantitative and/or qualitative modifications of its signalling<sup>154,212</sup> while deregulated Met signalling was found to be implicated in a wide range of cancer types<sup>15,154</sup>. Met can impact on all the different steps of tumour progression, from initial tumour development to the underpinning of cancer spread; the process termed metastasis<sup>213</sup>. Furthermore, Met recently was reported to contribute to tumour resistance to treatments targeted toward other RTKs, such as EGFR inhibitors gefitinib<sup>214</sup> or erlotinib<sup>215</sup> in lung cancers and the anti-EGFR monoclonal antibody trastuzumab (herceptin) in breast cancers<sup>216</sup>.

Based on all of these observations, it is not surprising that Met recently became a target of choice for the development of new anti-cancer treatments<sup>217</sup>. The interest of the pharmaceutical companies in the possibilities of using Met as a therapeutic target is growing very rapidly. Before 2003 no small molecules specifically targeting Met were available. Nowadays, many have been tested in preclinical studies and currently some already are in clinical trials (phase I, II and/or III)<sup>218,219</sup>.

### **8.1. Main approaches (Fig. 9)**

Three main strategies have been developed to hamper Met activation: 1) antagonism of ligand/receptor interaction, 2) inhibition of the tyrosine kinase catalytic activity and 3) interference with the recruitment of downstream signalling molecules.

#### 8.1.1. Antagonism of ligand/receptor interaction

To prevent interaction between Met and its ligand, several types of molecules have been engineered, including competitors and neutralising or blocking monoclonal antibodies (**Table 2**).

- Competitors

The competitors developed either are antagonists or decoys of either Met or HGF.

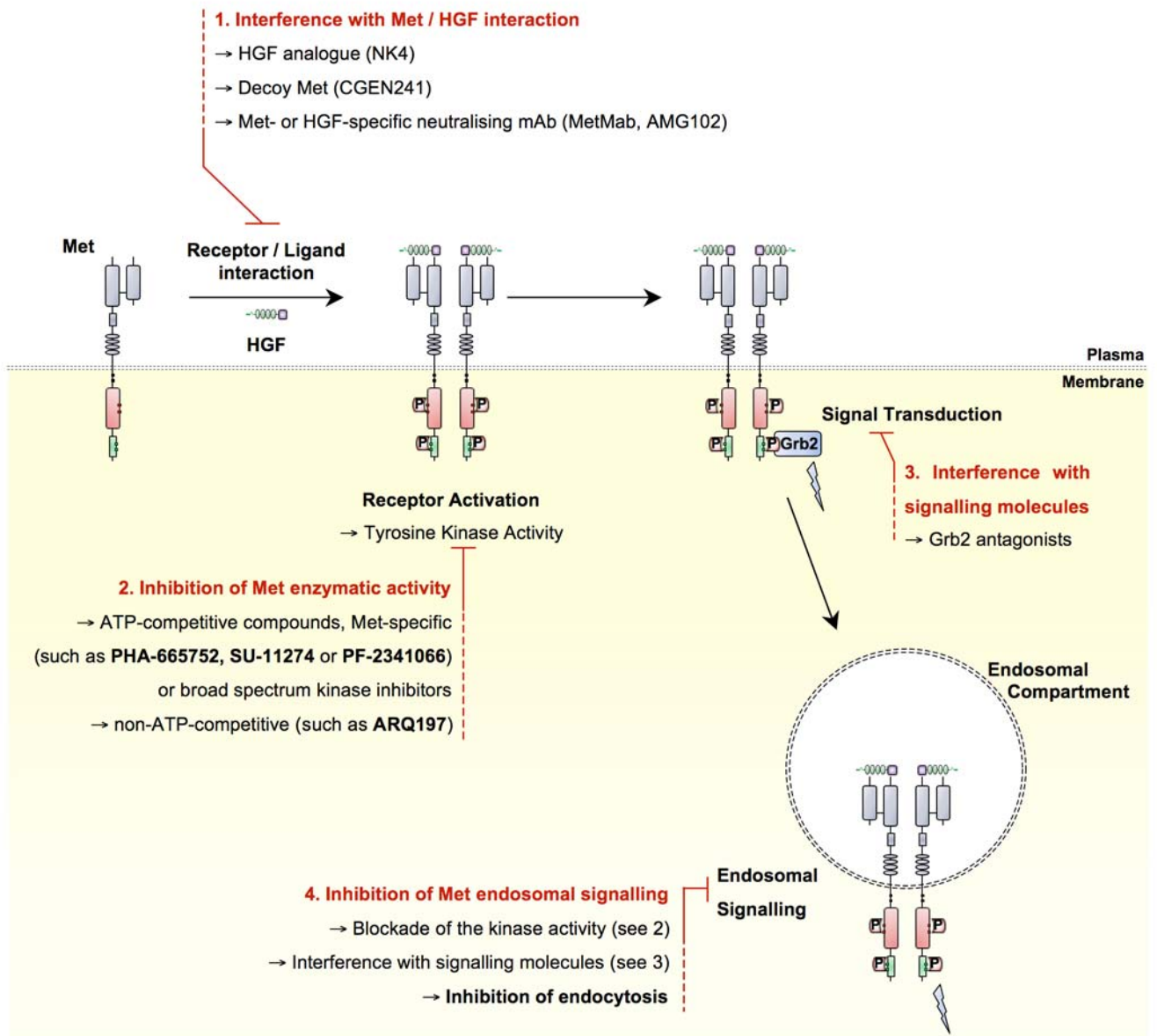


Figure 9. Different drugs, different strategies to inhibit Met-dependent signalling

### *HGF competitors*

Among the HGF antagonists generated, the molecule NK4 is the most studied and one of the more promising for modulating Met signalling. NK4 is a molecular analogue of HGF. It corresponds to a truncated form of HGF consisting of only the entire  $\alpha$  chain. NK4 binds to Met but does not induce its activation. In diverse murine tumour models, NK4 efficiently blocked tumour growth (by 60%)<sup>220</sup> as well as tumour dissemination<sup>221</sup> and the development of lung metastases<sup>222</sup>. Interestingly, independently from its HGF antagonist action, NK4 also has displayed anti-angiogenic properties<sup>220</sup> and these might enhance any HGF inhibiting therapeutic activity.

### *Met competitors*

A Met competitor, or “decoy Met”, has shown good results in several preclinical experiments<sup>223</sup>. Decoy Met corresponds to the whole of the Met extracellular region, thus it is devoid of any enzymatic activity since this is located in the intracellular domain. The decoy Met can interact with both HGF and Met to prevent ligand binding and receptor dimerisation respectively. Introduced by lentiviral technology, the decoy Met inhibited both tumour growth and metastasis without any substantial side effects<sup>223</sup>. Moreover, when combined with radiotherapy, decoy Met induced substantial tumour regression in established growths<sup>223</sup>. It is interesting to note that the same experiments, conducted in parallel with NK4<sup>223</sup>, gave similar results but with a better efficacy, in terms of tumour growth and metastasis inhibition, with the decoy Met.

- Neutralising and blocking antibodies

In parallel approaches, both neutralising and blocking monoclonal antibodies against HGF or Met have been developed.

#### *HGF antibodies*

Amgen has developed several fully human monoclonal antibodies (IgG2) against HGF<sup>224</sup>. Among them, AMG102 demonstrated good anti-tumour activity against HGF/Met dependent human tumour xenografts and, moreover, was shown to enhance the activity of conventional chemotherapeutic agents<sup>225</sup>. AMG102 currently is being evaluated in Phase II trials against advanced glioblastomas and renal cell carcinomas and a forthcoming clinical trial will assess its efficacy in association with an anti-EGFR antibody, panitumumab, against metastatic colorectal cancers (<http://www.clinicaltrials.gov>).

#### *Met antibodies*

The first generated anti-Met antibodies were inefficient at inhibiting Met activity because they had intrinsic agonist activity and thus induced Met dimerisation and activation<sup>14,226</sup>.

Then, Genentech developed the OA-5D5 (MetMab) reagent, a “one armed” anti-Met antibody that was highly efficient in preventing HGF binding. Thus, OA-5D5 is able to inhibit HGF dependent phosphorylation of Met in *in vitro* assays and to block glioma growth in an orthotopic *in vivo* model<sup>227</sup>.

Class	Compound		Mechanism of action			Inhibition of Met activation			Phase of development	Ref
	Name	Company	Targets	Mode	HGF-dependent	HGF-independent	Mutant			
HGF analogue	NK4	Kringle	Met	Compete with HGF	Yes	No	No <sup>1</sup>	Preclinical studies	220-223	
Decoy Met	CGEN241	Compugen	HGF & Met	Neutralisation (HGF) impair dimerisation (Met)	Yes	Yes	Yes (M1268T)	Preclinical studies	223	
Neutralising mAb	AMG102	Amgen	Human HGF	Neutralisation	Yes	No	No <sup>1</sup>	Phase II (SCLC, CRC, prostate, glioma, RCC, gastric adenocarcinoma)	225	
	MetMab (OA-5D5)	Genentech	Human Met	Monovalent antibody Met antagonist	Yes	No	No <sup>1</sup>	Phase II (NSCLC)	227, 228	
	SCH900105/AV-299	Shering/Aveo	Human HGF	Humanised antibody neutralisation	Yes	No	No <sup>1</sup>	Phase I (various tumours)	245	
	Tak-701	Millenium	Human HGF	Humanised antibody neutralisation	Yes	No	No <sup>1</sup>	Phase I (advanced solid tumours)	245	

<sup>1</sup>Results expected but no data published

**Table 2: HGF / Met inhibitors other than kinase inhibitors**

In addition, promising results have been obtained in preclinical studies with protocols that combined OA-5D5 with anti-VEGF antibodies and/or with EGFR inhibitors, with the best anti-tumour activity being obtained when the triple combination was utilised<sup>228</sup>. OA-5D5 at this time is in Phase I evaluation in combination with an anti-VEGFR antibody (bevacizumab) in patients with advanced or metastatic solid tumours (<http://www.clinicaltrials.gov>).

#### 8.1.2. Inhibition of the tyrosine kinase catalytic activity

Another approach that has been considered consists of the direct inhibition of the kinase activity of the receptor using small molecule inhibitors. This first was attempted with broad spectrum inhibitors but gradually inhibitors with a higher specificity for Met have been developed and tested (**Table 3**).

- ATP competitive molecules

Early work in the 90's started with the K252a compound (Cephalon) a staurosporine analogue<sup>229</sup>. Even if this Tyrosine Kinase Inhibitor (TKI) was not Met specific, it was found to be very efficient in the inhibition of the Wt form of the receptor following interaction with HGF, and even more potent at inhibiting the constitutive enzymatic activity of the M1268T Met mutant<sup>230</sup>. These promising results, associated with the accumulation of data linking Met and cancer, have encouraged the pharmaceutical industry to develop Met-specific TKIs.

Compound		Mechanism of action			Inhibition of Met activation			Phase of development	Ref
Name	Company	Target(s)	Mode	IC50 wt Met	HGF-dependent	HGF-independent	Mutant		
K252A	Fermentek	RTK	ATP competitive	No data <sup>1</sup>	Yes	Yes	Yes, M1268T	Preclinical studies	229, 230
				500 nM <sup>2</sup>					
SU-11274	Pfizer	Met	ATP competitive	10-20 nM <sup>1</sup>	Yes	Yes	Yes, M1268T No, Y1248C	Preclinical studies	231, 261
				1-1.5 μM <sup>2</sup>					
PHA-665752	Pfizer	Met	ATP competitive	9 nM <sup>1</sup>	Yes	Yes	No data	Preclinical studies	164, 182, 233, 262
				25-42 nM <sup>2</sup>					
PF-2341066	Pfizer	Met, ALK	ATP competitive	No data <sup>1</sup>	Yes	Yes	Yes, M1268T +++ Yes, Y1248C +/-	Phase I (various tumours) Phase II (ALCL) Phase III (NSCLC with ALK alterations)	166, 238, 239
				8.5-15 nM <sup>2</sup>					
PF-4217903	Pfizer	Met	ATP competitive	No data <sup>1</sup>	Yes	Yes	Yes, M1268T No, Y1248C	Phase I (various tumour types)	241
				4.8-16.9 nM <sup>2</sup>					
JNJ-38877605	Johnson	Met	ATP competitive	4 nM <sup>1</sup>	Yes	Yes	No data	Phase I (various solid tumours)	14, 245
				50 nM <sup>2</sup>					
EMD1214063	Merck Serono	Met	ATP competitive	No data <sup>1</sup>	Yes	Yes	No data	Phase I (various tumours)	242
				No data <sup>2</sup>					
AMG208	Amgen	Met	ATP competitive	9 nM <sup>1</sup>	Yes	Yes	No data	Phase I (various tumours)	14, 243
				No data <sup>2</sup>					
ARQ197	ArQule	Met	Non-ATP competitive	50 nM <sup>1</sup>	Yes	Yes	No data	Phase I (cirrhotic HCC) Phase II (MIT tumour, NSCLC, pancreatic)	14, 244
				100 nM <sup>2</sup>					

<sup>1</sup>In vitro kinase assay, <sup>2</sup>Cell-based assay

**Table 3: Met-specific kinase inhibitors**

### *Development of SU-11274 and PHA-665752*

In 2003, 2 molecules specifically targeting Met, both defined by an indolin-2-core structure were designed. SU-11274 was developed by Sugen, now Pfizer<sup>231,232</sup> and then PHA-665752 was produced by Pfizer<sup>233</sup> (**Fig. 10**). These molecules share the indolinone motif substituted at the position-5 of the indolinone core with 3-chlorobenzylsulphonide groups for SU-11274 or with 3,5-dimethylpyrrole groups for PHA-665752<sup>14</sup> (**Fig. 10**). SU-11274 and PHA-665752, are both competitive ATP inhibitors that exhibit activity against Met, with an  $I_{c50}$ , obtained in *in vitro* kinase assays, of 20nM<sup>231</sup> and 9nM<sup>233</sup>, respectively. They both exhibited 50-fold selectivity for Met as compared with the majority of other tested kinases, with the exception of VEGFR for SU-11274 and RON for PHA-665752. Met and Ron belong to the same RTK family and show a high percentage of homology in their intracellular region<sup>4</sup>. This might be the reason why PHA-665752 can inhibit either Met or Ron activity. Interestingly in cellular assays, PHA-665752 displayed at least a 10-fold greater potency than SU-11274 (**Table 3**).

### *Preclinical studies with SU-11274 and PHA-665752*

Some important preclinical studies have been performed using these drugs, thus allowing evaluation of the advantages and the limits of the actions of these two compounds.

Both drugs exhibited encouraging results against different cancer cell models *in vitro*. Indeed, both molecules inhibited Met phosphorylation efficiently, affecting, as a consequence, all the downstream signalling events. Although evaluation of SU-11274 has been limited to very few *in*

*in vivo* studies it has been shown to induce significant cytorreduction in tumours developed from lung cancer cell xenografts<sup>215</sup>. In several studies PHA-665752 was shown to reduce, very efficiently, and even to stop completely, the growth of several cancer cell lines<sup>182,234,235</sup>. PHA-665752 seemed particularly effective against xenografts where the injected cells were harbouring a Met amplification<sup>164</sup>.

Interestingly, PHA-665752 has been shown to be effective not only in HGF-dependent tumours but also in HGF-independent tumour models such as a gastric carcinoma xenograft model, in which Met is activated constitutively<sup>233,236</sup>.

Such promising results, combined with the success being obtained in the clinic with imatinib (a multitargeted TKI from Novartis) in the treatment of chronic myeloid leukaemia<sup>237</sup>, prompted pharmaceutical companies to develop Met specific drugs that could be used in human cancers. Unfortunately neither SU-11274 nor PHA-665752 are water-soluble which tends to limit their possible use.

#### *Development of PF-2341066*

In 2007, based on the co-crystal structure of PHA-665752 and the Met kinase domain, Pfizer designed the compound PF-2341066. This new, orally available 2-amino-3-benzyloxy-5-arylpyridine compound (**Fig. 10**) is a highly selective and potent ATP-competitive inhibitor of Met. It exhibited more than 100-fold selectivity for the Met enzyme compared with other evaluated kinases. Thus it is much more selective than the two other previously developed drugs, SU-11274 and PHA-665752<sup>238</sup>.

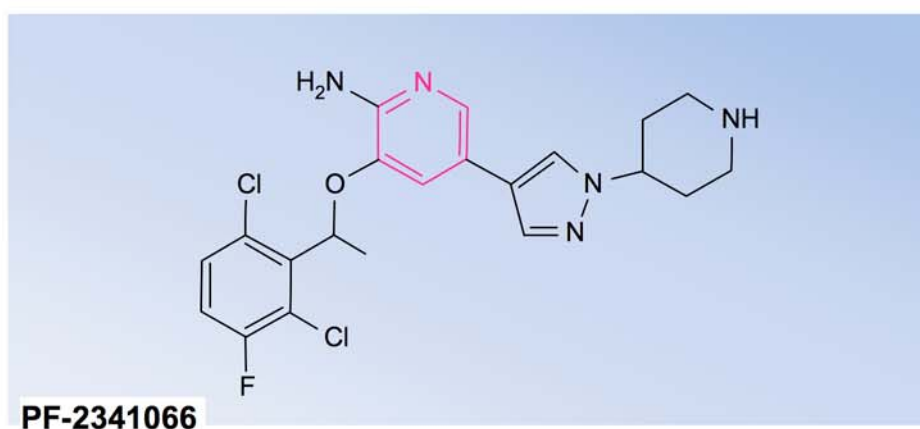
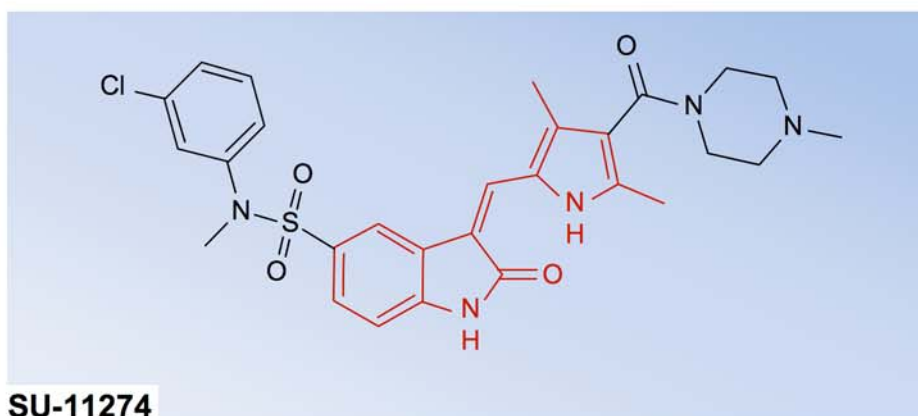
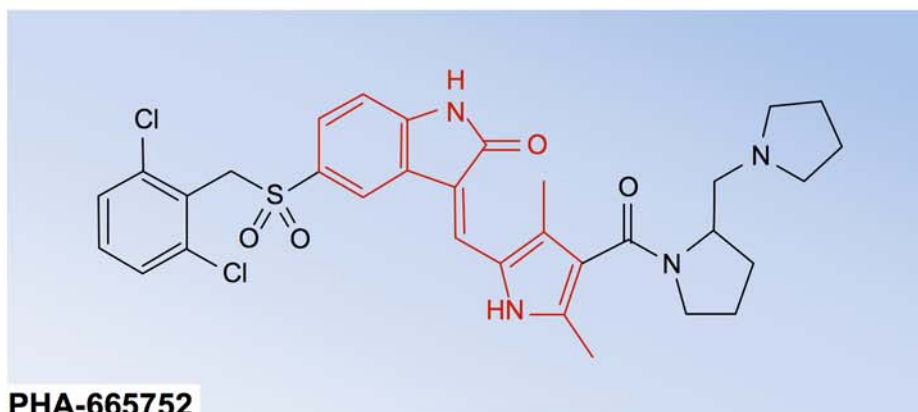


**Figure 10. Structures of three small-molecule Met inhibitors**

PHA-665752 and SU-11274 share a common pyrrole indolin-2-one core (in red). The PF-2341066 has a pyridine-based structure (in pink). This orally available compound has been developed by Pfizer to compensate for the poor pharmaceutical properties and oral bioavailability of the two other drugs.

*Adapted from  
Zhou HY et al, Cancer Res, 2007  
Comoglio PM et al, Nat. Drug. Disc, 2008  
Wang X et al, Mol. Cancer Ther., 2009*

In cellular assays, with an  $IC_{50}$  of 11nM, PF-2341066 has demonstrated a better potency against Met activity as compared with PHA-665752 (**Table 3**). It is important to note however that PF-2341066 is also a potent inhibitor of the Anaplastic Lymphoma Kinase (ALK)<sup>239</sup>, expressed only in neural, endothelial and perivascular endothelial cells in the brain.

#### *Preclinical studies with PF-2341066*

In different tumour models, whether HGF-dependent or not, PF-2341066 inhibited tumour growth very efficiently<sup>240</sup> or even totally (100% inhibition)<sup>238</sup>. Interestingly, PF-2341066 was shown also to have anti-angiogenic properties<sup>166,238</sup>.

#### *Clinical studies with PF-2341066*

A Phase I study with healthy volunteers has just been completed with PF-2341066 and several Phase I/II trials are now recruiting patients with advanced cancers (the origin is not provided) or with non-small cell lung cancers for evaluation. In addition, a Phase III study will start shortly but only against cancers with ALK identified alterations (<http://www.clinicaltrials.gov>).

#### *Development of PF-4217903*

Then, Pfizer developed a second more potent, and more selective, orally available small molecule inhibitor that targets Met, termed PF-4217903. In preclinical studies, this triazolopyrazine compound has been described to be exquisitely selective for Met, even more so than PF-2341066. Indeed,

it was determined to be more than 1000-fold selective for Met as compared to a panel of more than 200 kinases<sup>241</sup>. PF-4217903 was, until now, being evaluated in a Phase I trials but, for an unknown reason, this trial has just been suspended in mid-February 2010 (<http://www.clinicaltrials.gov>).

#### *Other specific Met TKIs in clinical studies*

Three other different companies also have developed selective ATP-competitive compounds, which can be administered *per os* (**Table 3**). These currently are in Phase I trials and are JNJ-38877605 from Johnson and Johnson, EMD1214063 from Merck-Serono<sup>242</sup> and AMG208 from Amgen<sup>14,243</sup>. Except for the latter one, which was shown to inhibit Met-mediated signalling and functions both *in vitro* and *in vivo*<sup>243</sup>, there are no original publications available on these compounds.

- Non-ATP competitive molecules

Another class of Met tyrosine kinase inhibitor, a non-ATP-competitive agent, ARQ197, also showing high selectivity for Met<sup>244</sup>, is at this time being evaluated in Phase I and II trials against various tumours<sup>14,245</sup>.

#### 8.1.3. Interference with the recruitment of downstream signalling molecules

A third strategy is emerging to block Met-dependent signalling. It relies on the prevention of the association of the receptor with its downstream partners. The adaptor Grb2 binds directly to Met and, through the

recruitment of a large panel of effectors, is thought to be accountable for the major part of the biological effects of the receptor<sup>27</sup>. Recently, compounds capable of penetrating the cells and binding to Grb2 with high affinity have been engineered<sup>246</sup>. These Grb2 antagonists efficiently blocked Grb2-dependent signalling *in vitro* and a prototype of this family of compounds was shown to block metastasis in murine model quite efficiently<sup>247</sup>. This type of molecule could, in the near future, be introduced into the clinic but it is not Met specific and because Grb2 is implicated in the signalling cascades of many types of receptors, some of which could well be beneficial, they have the potential to generate a lot of undesirable side effects. Preclinical studies and *in vivo* evaluations will have to be rigorous to rule out such possibilities.

## **8.2. Limitations**

### 8.2.1. Ligand stimulated only

Competitors and antibodies, with the exception of the decoy Met which by interfering with the Met dimerisation also inhibits HGF-independent Met activation, work by blocking the HGF / Met interaction.

Therefore, these inhibitors likely will be efficient only against tumour cells in which Met activation is dependent on ligand binding<sup>227</sup>. This may represent a major potential limitation to the success of any such of these approaches since a proportion of Met-driven cancers express a constitutively activated Met that does not need interaction with HGF in order to be activated<sup>136</sup>.

### 8.2.2. Resistance due to mutations

TKIs, by having the potential to block both HGF-dependent and HGF-independent Met signalling, may offer the most comprehensive approach to achieving Met inhibition. However TKIs against other RTKs have been used in the clinic and, unfortunately, many of the treated patients either exhibit inherited resistance or develop resistance to these drugs<sup>248,249</sup>. RTK mutations may account for this resistance and it seems plausible that Met specific TKIs are likely to face similar resistance mechanisms .

- RTK mutations and drug resistance

Activating mutations leading to primary resistance to TKI treatment have been identified in several RTKs. In lung cancer, mutations reported in exon 20 of EGFR or HER2 have been shown to confer resistance to gefitinib and erlotinib inhibition<sup>250,251</sup>. Thus, even if these insertion mutations represent a small percentage (5%) of all the known EGFR mutations<sup>248</sup>, they are, at least in part, responsible for the failure of these TKI treatments against lung cancers. The Kit D816V/Y mutation, corresponding to the Met activating mutation D1246N, also has been implicated in resistance to imatinib treatment in mast cell diseases<sup>197,252</sup>, indicating the likelihood that certain Met mutations will have significant impact upon the sensitivity of expressing cells to various inhibitors.

In contrast to these mutations which confer resistance, mutations which render expressing cells highly sensitive to the drugs, called “sensitive mutations”, have been identified and have been shown to improve overall treatment response to TKIs<sup>253,254</sup>. However, patients harbouring these

sensitive mutations also eventually become resistant to the treatment regime<sup>237,255,256</sup>. One of the most frequent reasons for this acquired resistance is due to the development of a second mutation in the same RTK<sup>255,256</sup>. Indeed, in 50% of patients with non-small cell lung cancers bearing a sensitive mutation in EGFR, who develop resistance to EGFR-targeting TKIs, the mutation T790M has been reported to occur<sup>255,257</sup>. The same corresponding mutation within the homologous codon of the Kit receptor has been identified in gastrointestinal stromal tumours (GIST), where this T610I Kit mutation was associated with acquired resistance to imatinib treatment<sup>258</sup>.

- Met mutations and drug resistance

Resistance, either primary or acquired after TKI treatment, is therefore likely to be a major problem in single-agent therapy and it seems most likely that similar problems will occur with Met TKIs<sup>259</sup>. For example, Met mutations and/or RTK pathway redundancies may cause inherited resistance to Met TKIs<sup>260,261</sup>. Indeed, even if SU-11274 and PHA-665752 were found to be very efficient against cells expressing the oncogenic, and constitutively active TPR-Met<sup>231,262</sup>, which is a product of a genetic rearrangement, other Met mutants identified in human cancers, particularly in HPRC, have displayed differential inhibition sensitivities to SU-11274<sup>261</sup> and to PF-2341066<sup>239</sup>. For example the highly activated M1268T Met mutant was reported to be sensitive, while other mutations also located in the tyrosine kinase domain (L1213V and Y1248H) were resistant, to inhibition<sup>239,261</sup>. However, not all the mutations identified in cancers have

yet been tested (D1246N for example) and so far, no studies using PHA-665752 have been conducted on cells bearing Met mutations found in HPRC.

Among the five highly specific Met TKIs currently being tested in clinical trials, only the two designed by Pfizer, (PF-2341066 and PF-4217903), have previously been evaluated in preclinical studies against cells expressing different Met mutants. Moreover, as for SU-11274, the two TKIs from Pfizer were only evaluated on a restricted panel of Met mutants<sup>238,241</sup> and it seems possible that certain patients might be treated with a drug which will be totally inefficient if they bear tumours which have Met mutations not previously assessed for TKI sensitivity.

## AIM OF THE PROJECT

Diverse Met mutations have been identified in hereditary papillary renal carcinoma (HPRC) as well as in other carcinomas. Although they are distributed throughout the gene, there is a preferential hot spot within the region encoding for the kinase domain. Met mutations are present at a low frequency in most cancer types except in PRC in which 13% of tumour samples harbouring activating Met mutations have been recorded<sup>167</sup>. My thesis has focused on three mutations located in the kinase domain: D1246N(g), M1268T(s) and Y1248C(g).

These mutations were shown to induce constitutive Met phosphorylation and malignant transformation of NIH3T3 cells<sup>263</sup> (**Table 1**). Interestingly, mice bearing these different mutations exhibit unique tumour profiles, some of which are metastatic<sup>263-265</sup>. While D1246N<sup>mu/mu</sup> and Y1248C<sup>mu/+</sup> animals developed a high frequency of sarcomas, M1268T<sup>mu/+</sup> mice were characterised by an abnormal frequency of carcinomas but did not develop any sarcomas. These differences in tumour profiles suggested that the activating mutations affect more than just phosphorylation levels of Met. It was proposed that structural changes induced by the mutations could differentially alter the ability of Met to recruit accessory proteins into an active signalling complex, leading to possible distinct signalling pathways<sup>263</sup>.

Understanding the mechanisms of these mutations in cell transformation is essential to the identification and development of successful therapeutics.

Although Met has now been identified as a target of choice to block the growth of several cancers, and although several drugs have already been generated to block its activity, many barriers still need to be removed in order to optimise Met-targeted anti-tumour therapies. For example, preclinical and clinical studies using RTK specific inhibitors for cancer treatment have demonstrated the problem of innate or acquired resistance. RTK mutations have been shown to account for a substantial part of this drug resistance. Moreover, it is impossible to predict the efficacy of a drug on a particular Met mutant based on the data obtained on another one. Therefore, in the first part of my thesis, I compared the sensitivity of Met mutants D1246N and M1268T to Met-specific TKIs, *in vitro* and *in vivo*.

In a second part, I concentrated my efforts on the identification of the mechanisms by which these mutants confer a transforming capacity to the cells. Keeping in mind that the activating mutations may affect more than just phosphorylation levels of Met, and since the endocytic trafficking of RTKs has emerged to critically modulate their signalling, I hypothesised that where the mutants signal in the cell might affect signalling and cellular outcome. I therefore investigated whether the endocytic trafficking of these mutated receptors could play a predominant role in their transforming ability.

## MATERIALS AND METHODS

### 1. Cell culture

Mouse fibroblast NIH3T3 cells, stably transfected with a construct encoding for Wt murine Met or for a mutated form of the receptor, were kindly provided by Prof. Vande Woude<sup>156</sup>. The three mutants, M1268T (s), D1246N (g) and Y1248C (g), are labelled according to their amino acid location change, and germ-line (g) vs. somatic (s) status. Cells were cultured at 37°C, 8% CO<sub>2</sub> in complete medium (DMEM, PAA) supplemented with 10% Donor Calf Serum (DCS, Gibco) and were subcultured twice a week.

Cells were seeded in 35- or 100-mm plates for biochemical experiments, or on coverslips for immunocytochemistry. When starvation was required, cells were plated 48 h before the experiment. 24 h after plating or after starvation, cells were stimulated with 50 ng/mL of recombinant human HGF (R&D) for the indicated period of time. When indicated, cells were preincubated with the appropriate drugs for 30 min in complete medium and were then stimulated with HGF. When HGF stimulation was not required, drug treatments were done for 90 min unless otherwise specified. Drugs were maintained within complete medium until the end of the experiment.

## **2. Reagents**

### **2.1. Antibodies for immunofluorescence**

Anti-EEA1 (rabbit IgG) and anti-mouse Met antibodies (B2, mouse IgG<sub>1</sub>) were used at a dilution of 1/100 and were purchased from Santa Cruz Technologies. Anti-GST (1/250, rabbit IgG), anti-PiP3 (1/200, mouse IgM) and anti-mouse Met (1/100, goat IgG) were bought from Abcam, Echelon and R&D or Sigma respectively. Antibodies specific for Rab11 (1/100, mouse IgG<sub>1</sub>), pan phosphotyrosine (1/100, 4G10, mouse IgG<sub>2b</sub>) and Rac1 (1/250, mouse IgG<sub>2b</sub>) were purchased from Upstate.

Alexa-488 labelled donkey anti-goat or anti-mouse IgG (1/500, Molecular Probes), Cy3-coupled donkey anti-rabbit or anti-mouse IgG (1/1000, Jackson ImmunoResearch) and Cy5-coupled donkey anti-rabbit or anti-mouse (1/1000, Jackson ImmunoResearch) were used as secondary antibodies.

### **2.2. Antibodies for Western Blotting**

Anti-phosphorylated ERK (1/1000, rabbit IgG), anti-phosphorylated Met (Y<sup>1234</sup>-Y<sup>1235</sup>, 1/1000, rabbit IgG) and anti-PARP (1/1000, rabbit IgG) antibodies were purchased from Cell Signalling. Antibodies specific for Grb2 (1/1000, rabbit IgG), HSC-70 (1/2000, mouse IgG<sub>2a</sub>) and Met (B2, 1/200, mouse IgG<sub>1</sub>) were bought from Santa Cruz Technologies. The antibody specific for the phosphorylated Y<sup>1349</sup> of Met was generated by Drs Kermorgant & Parker in collaboration with the CR-UK Antibody Service from the London Research Institute, or purchased from Cell Signalling (1/1000, rabbit IgG). Mouse IgG<sub>1</sub> specific for clathrin heavy

chain (CHC), and HSP90 were provided by BD and used at a dilution of 1/1000. HSP 90 beta (1/1000, mouse IgG<sub>1</sub>) and ubiquitin (1/1000, FK2, mouse IgG<sub>1</sub>) were purchased from BIOMOL International. Finally, antibodies recognising HSP90 alpha (1/1000, mouse IgG<sub>1</sub>), Rac1 (1/1000, mouse IgG<sub>1</sub>), tubulin (1/2000, mouse IgG<sub>1</sub>) were purchased from Abcam, Cytoskeleton and Sigma respectively.

HRP-coupled anti-mouse and anti-rabbit IgG secondary antibodies were purchased from Amersham and used at a dilution of 1/1000 except for detection of mouse anti-HSC-70 and tubulin where they were used at 1/2000.

### ***2.3. Antibodies for Flow cytometry***

The following antibodies were used for flow cytometry analysis: anti-heavy chain of clathrin (1/100, mouse IgG<sub>1</sub>) was purchased from BD and anti-mouse Met (1/50, goat IgG) from R&D.

Alexa-488 labelled donkey anti-goat IgG (1/250, Molecular Probes), PE-conjugated donkey anti-rat IgG (1/1250, Jackson ImmunoResearch) and APC-coupled donkey anti-mouse IgG (1/250, Jackson ImmunoResearch) were used as secondary reagents.

### ***2.4. Growth factors, inhibitors and drugs***

HGF was used at 50 ng/mL, unless otherwise specified. Alexa-546-labelled Phalloidin and Cy3-coupled transferrin were used at a final dilution of 1/250 and 1/500 respectively, and were purchased from Molecular Probes. Cycloheximide (50 ug/mL) and dynasore (80 μM) were

bought from Sigma. Rac1 inhibitor (NSC23766, 100  $\mu$ M) and SU-11274 (2  $\mu$ M) were purchased from Calbiochem. PHA-665752 (100 nM) and PF-2341066 (200 nM) were kindly provided by Dr. Christensen (Pfizer, La Jolla).

## 2.5. Plasmids

The plasmid pEGFP-dynamin2-K44A was a gift from Prof. De Camilli (Yale University). The plasmids pEF-Grb2 myc, pEF-Grb2 89A myc (SH2 mutant) and pEF-Grb2 49L/203R myc (SH3 double mutant) were given by Prof. Downward (Cancer Research UK, London Research Institute). The plasmid pcDNA-Ub-His was a gift from Dr. Basu (Institute of Cancer).

## 2.6. RNAi, short hairpin RNA

siRNA or shRNA were used to knock-down the expression of different targets as indicated in the table below.

Target	Type	N°	Sequence	Supplier
CHC	shRNA	1	CCGGGCGAACATCAATAGATGCTTACTCG AGTAAGCATCTATTGATGTTTCGCTTTTTG	Sigma
		siRNA	1	
	2	UAGAGGAGCUUAUCAACUA		
Rac1	siRNA	1	GGACGAAGCTTGATCTTAG	Dharmacon (pool)
		2	AGACGGAGCTGTTGGTAAA	
		3	GATCGGTGCTGTCAAATAC	

		4	GCAAAGTGGTATCCTGAAG	
Grb2	siRNA	1	UGAAUGAGCUGGUAGAUUA	Dharmacon
		2	CAACAUCCGUGUCCAGGAA	
Hsp90 $\alpha$	siRNA	1	CAUCAACACUUUCUAUUCA	Dharmacon (si Genome Smart Pool)
		2	GAAACAUUCGCAGUUCAUA	
		3	UGACUGAGCCUAUUGACGA	
		4	GAUAUGAGAGCCUGACGGA	
Hsp90 $\beta$	siRNA	1	GAGCUUAAACUAACGAUUGG	Dharmacon (si Genome Smart Pool)
		2	GGAAUUAUCCUGAGUAU	
		3	GAACCAAUGGGUCGUGGAA	
		4	CAUCGGACGCUCUGGAUAA	

### 3. Cell Transfection

NIH3T3 cells were transfected using a liposome-based strategy (Lipofectamine<sup>TM</sup> 2000 combined with the Plus reagent<sup>TM</sup>, both from Invitrogen). However, when a high percentage of transfection was required (for functional assays) or when this approach was not suitable for the cells, the Amaxa<sup>®</sup> Nucleofector<sup>®</sup> technology was used. This electroporation-based strategy was also used for siRNA transfections.

#### **3.1. Transfection using Lipofectamine<sup>TM</sup> 2000 and Plus reagent<sup>TM</sup>**

NIH3T3 cells were plated in 24-well plates in order to reach 60 to 70% confluency by 24 h later; the time of transfection. For each transfection

sample, 0.4  $\mu\text{g}$  of DNA was diluted with 25  $\mu\text{L}$  of Opti-MEM<sup>®</sup> (Invitrogen) and 4  $\mu\text{L}$  of Plus<sup>™</sup> reagent to enhance transfection efficiency. This mix was incubated at room temperature for 15 min. In parallel, 1  $\mu\text{L}$  of Lipofectamine 2000<sup>™</sup> was diluted in 25  $\mu\text{L}$  of Opti-MEM<sup>®</sup>. The pre-complexed DNA and diluted Lipofectamine 2000<sup>™</sup> were then combined incubated for 15 min and added to the cells. 3 h later, the transfection mixture was removed and replaced with complete medium.

### ***3.3. Transfection with Amaxa<sup>®</sup> Nucleofector<sup>®</sup> technology***

Transfection of NIH3T3 cells with Amaxa<sup>®</sup> Nucleofector<sup>®</sup> technology was performed following the manufacturer's instructions (Lonza). The kit and program of nucleofection used were "R" and "U30" respectively. Cells transfected with DNA were harvested the following day and cells transfected with siRNA were harvested 3 days later.

When NIH3T3 cells were transfected with the pEGFP-dynamin2-K44A, the transfection efficiency obtained was low, less than 50% of the cells were expressing the dynamin2-K44A-GFP. Before using these cells for functional assays, a pure population of cells expressing the dynamin2-K44A-GFP was required. Therefore, a sorting procedure was performed 48h after nucleofection based on GFP expression on a high speed MoFlo cell sorter (Beckman Coulter, Fort Collins CO). Then the cells were plated, and used the following day for the Transwell chemotactic migration assays.

### **3.4. Lentiviral transduction**

To generate stable long-term gene silencing in NIH3T3 cells, the MISSION™ TRC shRNA Lentiviral Particles kit from Sigma was used. As a selection through puromycin was required, a titration was performed to determine the minimum concentration of puromycin (here 2 µg/mL) that caused complete NIH3T3 cell death after 3-5 days. Then, 3000 cells were plated in each well of a flat-bottom 96-well plate, to ensure that they were no more than 70% confluent upon transduction. The following day, the medium was changed and lentiviral particles were added at a multiplicity of infection of 15. At day 3, the viral particles were removed and, one day later, the medium was replaced with fresh medium containing puromycin. Medium was replaced every 2 days until the positive identification of resistant cells. Western blot experiments were then performed to evaluate the knock-down efficiency.

## **4. Western Blotting**

### **4.1. Cell lysis**

Cells were grown to 70% confluence and, after the required treatment/stimulation, washed with Phosphate Buffered Saline (PBS, CR-UK Media Services) and incubated for 10 min with RIPA lysis buffer (Upstate) supplemented with 1 mM sodium orthovanadate (Sigma), 1 mM sodium fluoride (Sigma) and with a 1/100 dilution of protease inhibitor cocktail (Calbiochem). Cells were harvested and centrifuged at 13000g for 10 min at 4°C. The protein concentration of the supernatant was

determined using the Bio-Rad D<sub>c</sub> Protein Assay Kit according to manufacturer's instructions (Bio-Rad Laboratories).

#### **4.2. Western blot analysis**

For each sample, an equal amount of total cellular proteins (10-50 µg, depending on experiments) was diluted in sample buffer (Invitrogen) and resolved by sodium dodecyl sulphate-polyacrylamide gel electrophoresis (SDS-PAGE). Samples were loaded onto precast gels (4-12% Bis-Tris Gel, Invitrogen), under reducing conditions and run at 150 V for 90 min. After transfer of the proteins to Hybond nitrocellulose membranes (Schleider & Schuell), the non-specific binding sites were blocked with Tris Buffer Saline (TBS, CR-UK Media Services), 3% BSA, 0.1% Tween (Sigma) for 30 min, and incubated overnight at 4°C with the appropriate primary antibody, diluted in TBS, 3% BSA and 0.1% Tween. Blots were washed three times with TBS 0.1% Tween and incubated for an hour at room temperature with appropriate HRP-conjugated secondary antibody. Membranes were then washed three times with TBS 0.1% Tween and incubated with ECL reagents (Amersham Biosciences) for 1 min. Chemiluminescence was detected by exposure to chemiluminescence film (Amersham Biosciences). Quantifications were done by densitometry analysis.

#### **4.3. Densitometry**

Densitometry was performed using Image J software. Band densities were normalised to HSC-70 and/or tubulin levels (detected on the same

membrane), to obtain a semi-quantitative measurements of the total amount of protein, or were normalised to total protein levels for semi-quantitative measurement of protein phosphorylation status.

## **5. Immunoprecipitation**

### **5.1. Standard protocol**

$2.5 \times 10^6$  cells were plated on 15 cm plates. The next day, cells were lysed with 900  $\mu$ L of lysis buffer (25mM HEPES at pH=7.4, 100 mM NaCl, 5 mM  $MgCl_2$ , 1 mM EGTA, 10% glycerol, 1.25% CHAPS) (Sigma), protease inhibitor cocktail I and phosphatase inhibitor cocktail II (Calbiochem). Lysates were then centrifuged at 12000g for 10 min, and the soluble fraction subjected to immunoprecipitation with 5  $\mu$ g of appropriate antibody and 70  $\mu$ L of agarose-coupled anti-mouse or anti-rabbit IgG antibodies (Invitrogen). After overnight incubation at 4°C, beads were washed 3 times with lysis buffer. The bound fraction was then solubilised in 30  $\mu$ L of sample buffer (4X). For each experiment, immunoprecipitations with beads only and an isotype-matched control IgG were performed as negative controls.

Both (co-)immunoprecipitated protein/s and a fraction of the total lysate were subjected to SDS-PAGE and Western-blot analysis.

### **5.2. Protein A Sepharose-antibody coupling**

The IgG heavy and light chains of antibodies used for immunoprecipitation protocols could be detected in Western blot assay and correspond to 2 bands with a size of 50 and 25 kDa respectively. The protein Grb2 has a

size of 24 kDa, the same as the IgG light chain. Thus its detection in Western blot after (co-)immunoprecipitation is impossible as it will be confounded with the IgG light chain. To resolve this issue, anti-Grb2 and anti-Met (B2) antibodies were then covalently coupled to Protein-A Sepharose<sup>®</sup> (Invitrogen).

The concentration of salts from the coupling/washing buffer was adapted to the isotype of the antibody. For rabbit IgG and mouse IgG<sub>2a</sub>, 0.2 M sodium borate (pH 9.0) was used while mouse IgG<sub>1</sub> required a buffer with a higher concentration of salts: 3 M NaCl, 50 mM sodium borate, pH 9.0. Protein-A Sepharose<sup>®</sup> beads were washed with the appropriate buffer and incubated for 1 h at room temperature with the required antibody at a final concentration of 1 µg per µL of beads (10 µg of antibody were used for each immunoprecipitation). The beads were then washed 4 times and finally were resuspended in the appropriate buffer containing 20 mM of cross-linker (dimethylpimelimidate (DMP)). After 30 min of incubation on a rotator at room temperature, the reaction was stopped by washing the beads twice with 0.2 M ethanolamine (pH 8.0). To remove any antibody that was non-covalently bound, DMP-coupled protein-A Sepharose<sup>®</sup> beads were washed with 0.1M glycine (pH 3.0). Eventually the beads were washed twice and stored at 4°C in a required volume of PBS (20 µL = 10 µg of antibody).

## **6. Ubiquitination assay**

The level of Met ubiquitination was quantified by 2 different methods.

### **6.1. Boiling SDS-lysis method**

This technique was performed as described<sup>266</sup>.  $2.5 \times 10^6$  cells were plated on 15 cm plates. The next day, cells were lysed in boiling lysis buffer (2% SDS, 1 mM EDTA, 50 mM NaF, protease and phosphatase inhibitor cocktail preheated at 110°C). The lysates were incubated for 10 min at 110°C before being cooled down and diluted 4 times in dilution buffer (2.5% Triton X-100, 12.5 mM Tris pH 7.5, 187.5 mM NaCl, protease and phosphatase inhibitor cocktails). The lysates were then subjected to Met immunoprecipitation. Western blots for Met and ubiquitin were performed on the immunoprecipitates and on a fraction of the total lysates.

### **6.2 Nickel-NTA-agarose purification**

This method was performed as described<sup>267</sup>.  $10^6$  cells were transfected with a construct encoding a His-tagged form of ubiquitin using the Amaxa<sup>®</sup> Nucleofector<sup>®</sup> technology. The level of transfection was checked the next day by immunofluorescence with an anti-His antibody prior to performing the assay. Transfected cells were lysed in denaturing lysis buffer (6 M guanidinium-HCl / 0.1 M Na<sub>2</sub>HPO<sub>4</sub> / NaH<sub>2</sub>PO<sub>4</sub>, pH 8 / 10 mM imidazole). The lysates were sonicated 2 times for 15 seconds, then mixed with 50 µL of Nickel-NTA-Agarose (Qiagen) for 3 h at room temperature. The beads were washed twice in lysis buffer then twice in lysis buffer diluted with the following dilution buffer, 25 mM with Tris-HCl (pH 6.8)/ 20 mM imidazole

and finally twice only with the dilution buffer. Purified proteins were eluted by boiling the beads in SDS-PAGE sample buffer (4X). Western blots for Met and ubiquitin were performed on the His-ubiquitin purified complex and on a fraction of total lysates. To have a better separation between the different forms of ubiquitinated Met, samples were loaded onto precast gels, 3-8% Tris-Acetate Gels (Invitrogen), that provide better separation than 4-12% Bis-Tris gels, of large molecular weight proteins.

## **7. Immunofluorescence**

Cells were plated in 24-well plates ( $3 \cdot 10^5$  per well) onto acetic acid washed and poly-L-Lysine coated glass coverslips (0.01%, Sigma) or onto Poly-L-Lysine precoated coverslips from BD (BD BioCoat™ Poly-L-Lysine). After appropriate treatments, cells were fixed for 10 min in PBS containing 4% paraformaldehyde (Sigma) and washed once in PBS before treatment with 50mM ammonium chloride. Cells were then blocked and permeabilised in PBS containing 3% bovine serum albumin (BSA, Sigma) and 0.1% Triton X-100 (Sigma), and incubated with indicated primary antibodies diluted in PBS containing 3% BSA for 30 min. After 3 washes in PBS, cells were incubated for 30 min with the secondary antibody in PBS with 3% BSA, then washed twice in PBS and once in distilled water and mounted with DAPI antifade medium (Invitrogen).

When the anti-PIP3 antibody was used, PBS was replaced by TBS and the permeabilisation step was done with 0.5% saponin (Sigma).

### **7.1. Confocal microscopy analysis**

Confocal microscopy was performed using a confocal laser-scanning microscope (LSM510, Carl Zeiss Inc.) equipped with a 63x/1.4 Plan-Apochromat oil immersion objective. Alexa-488 was excited with the 488-nm line of an argon laser, Cy3, Alexa-546 and Alexa-555 were excited with a 543-nm HeNe laser and Cy5 was excited with a 633-nm HeNe laser. Each image represents a single section of 0.7  $\mu\text{m}$  of thickness. Scale bar: 10  $\mu\text{M}$ .

### **7.2. Transferrin uptake**

Cells were incubated for 20 min with Cy3-coupled Transferrin (20  $\mu\text{g}/\text{mL}$ , Molecular Probes) in complete medium.

### **7.3. Labelling of HGF with Alexa-555**

25  $\mu\text{g}$  HGF were labelled using Alexa Fluor® 555 Microscale Protein Labelling Kit according to the manufacturer's instructions (Molecular Probes).

### **7.4. HGF-Alexa-555 uptake**

Cells were incubated for the indicated time with HGF-Alexa-555 (50  $\text{ng}/\text{mL}$ ) in complete medium.

### **7.5. Colocalisation measurements and statistical analysis**

Picture fields were chosen randomly based on DAPI staining. Colocalisations were determined using the colocalisation platform from the MetaMorph

software and were expressed as percentage of Met or HGF within the indicated compartments. Seven pictures for each cell type were taken per experiment. The counting of cells with disorganised actin, or Rac1 at sites of membrane protrusion, were performed on at least 100 cells in each experiment. Data sets from 3 independent experiments were analysed for significance using Student's t test.  $p < 0.05$  was considered statistically significant.

## **8. Biochemical quantification of Met distribution**

### ***Biotinylation surface removal***

A modified version of the method described by Gampel et al.<sup>268</sup> was established to measure the relative proportion of Met at the cell surface and in intracellular pools. All steps were performed at 4°C to prevent the occurrence of any trafficking events. Cells were washed twice in ice-cold PBS and incubated for 10 min with rocking with PBS containing 0.15mg/mL NHS-SS-biotin (Pierce), a water-soluble membrane-impermeant biotinylation reagent. The excess of reagent was quenched by washing once with a specific buffer (25 mM Tris, pH8; 137 mM NaCl; 5 mM KCl; 2.3 mM CaCl<sub>2</sub>; 0.5 mM MgCl<sub>2</sub>; and 1 mM Na<sub>2</sub>HPO<sub>4</sub>) and three times with ice-cold PBS. Cells were then solubilised in RIPA lysis buffer (Upstate) and the lysates were centrifuged at 13000 g for 10 min. A fraction of the supernatant, corresponding to the total amount of Met in the cell, was collected. Streptavidin-agarose beads (Upstate) were added to the remaining supernatant (100 µL packed beads per 500 µL lysate) and left to tumble on a rotating wheel at 4°C for two hours. Beads were collected by centrifugation (7000 g, 1 min) and supernatant was collected;

this fraction constitutes the internal pool of Met. The beads were then washed 3 times in ice-cold lysis buffer and proteins were extracted from the beads by heating at 95°C with SDS-PAGE sample buffer (Invitrogen); this represents the surface pool of Met. Equivalent volumes were resolved by SDS-PAGE and analysed by Western blotting with an anti-Met antibody.

## **9. Met internalisation and recycling assay**

### ***9.1. Biochemical quantification of Met internalisation: Biotinylation internalisation assay***

To measure Met internalisation, cells were transferred on ice and washed twice with ice-cold PBS. The cell surface was labelled at 4°C with 0.2 mg/mL NHS-SS-biotin in PBS for 45 min. Labelled cells were then washed twice in ice-cold PBS and transferred immediately in prewarmed (37°C) cell culture medium, with or without HGF (50 ng/mL), to allow internalisation. At indicated time-points, the medium was aspirated off and the dishes were rapidly transferred on ice and washed twice with ice-cold PBS. Biotin was removed from proteins remaining at the cell surface by reduction with Sodium 2-mercaptoethanesulphonate (MesNa, Pierce). Briefly, a solution of 180 mM of MesNa in 50 mM Tris, 100 mM NaCl was adjusted to pH 8.6 and added to the cells. Reduction was allowed to proceed for 15 min on ice at 4°C with gentle rocking. MesNa was quenched by addition of 180mM Iodoacetamide (IAA, Sigma) for 10 min. Cells were then lysed and scraped. Lysates were passed 3 times through a 27-gauge needle and clarified by centrifugation (13000 g, 10 min). The

following steps are similar to those described in the previous biochemical quantification. Streptavidin-agarose beads (Upstate), diluted in lysis buffer, were added to the pellet and left to tumble on a rotating wheel at 4°C for two hours. Beads were then collected by centrifugation (7000g, 1min, 4°C), washed 3 times in lysis buffer at 4°C, dissociated from the proteins by heating at 95°C in SDS-PAGE sample buffer and analysed by Western blotting with an anti Met antibody. Densitometries were carried out.

In each internalisation, or recycling, assay, two controls were performed: i) to measure the total amount of Met at the cell surface, biotinylated cells were lysed without biotin reduction; ii) to verify the efficiency of biotin removal from the cell surface, biotin reduction and MesNa quenching were performed on cells that remained on ice (time 0) throughout the experiment to avoid any internalisation.

The percentage of internalised Met was calculated as follow:

Internalised Met = [(Met level after incubation at 37°C) – (Met level at time 0)] / (total surface Met) x 100.

## ***9.2. Biotinylation recycling assay***

To measure the proportion of internalised Met (see 9.1) that recycles back, the biotin present at the cell surface after the first incubation at 37°C was removed by reduction with MesNa (see above), and the internalised fraction was chased from the cells by placing them a second time at 37°C for 15 min. Cells were then returned to ice and biotin was removed from recycled proteins by a second step of reduction. Unreacted MesNa was quenched with IAA for 10 min and cells were lysed and processed as for

measurements of receptor internalisation.

Equivalent volumes were analysed in a Met Western blot and densitometries performed. The percentage of recycled Met was calculated from the following formula: recycled receptor =  $100 - [(Met \text{ level after } 15 \text{ min of re-incubation at } 37^{\circ}\text{C}) - (Met \text{ level at time } 0) / (Met \text{ level after first incubation at } 37^{\circ}\text{C}) - (Met \text{ level at time } 0) \times 100]$ .

## **10. Biochemical quantification of Met degradation**

### ***10.1. Total Met degradation***

Cells were pre-treated with cycloheximide (50 µg/mL, Sigma) for 10 min before HGF stimulation in order to block protein synthesis, thus allowing me to follow the degradation of the mature Met form only. After stimulation with HGF for the indicated time point, the cells were washed in PBS and lysed. Protein concentrations were measured (Bio-Rad Protein Assay) and equivalent quantities of protein were resolved by SDS-PAGE and analysed by Western blotting with an anti Met antibody and with an anti HSC-70.

### ***10.2. Biotinylation degradation assay***

Cells were washed in PBS and incubated with 0.2 mg/mL biotin in PBS for 45 min with rocking. Labelled cells were washed twice in ice-cold PBS and transferred immediately to prewarmed cell culture medium at 37°C, with or without HGF (50ng/mL) to allow internalisation. At indicated time-points, the medium was aspirated off and the dishes were rapidly transferred onto ice and washed with ice-cold PBS. Cells were lysed and scraped. Lysates

were passed 3 times through a 27-gauge needle and clarified by centrifugation at 13000 g for 10 min. Protein concentrations were measured, equivalent quantities of protein were resolved by SDS-PAGE and analysed by Western blotting with an anti Met antibody.

### **11. Rac1 activation assay**

Levels of Rac1-GTP (activated Rac1) were measured using the Rac1 activation assay Biochem Kit™ (Cytoskeleton). This assay is based on the fact that many Rho family effectors, such as PAK (p21 activated kinase), have a specific region that interacts specifically with activated Rac1 (or Cdc42); so interacting specifically with Rac1 bound to GTP. The region of PAK is called CRIB (Cdc42/Rac Interactive Binding region) or PBD (p21 Binding Domain). Thanks to this feature and to its fusion with GST, the PAK-PBD protein supplied in the kit allows the pull-down of Rac1-GTP (or Cdc42-GTP) with glutathione affinity beads.

$2.5 \times 10^6$  cells were plated in 15cm plates. The following day, culture dishes were washed once with ice-cold PBS and cells were lysed with 1mL of lysis buffer supplemented with protease inhibitors (both provided in the kit). From now, all the steps were performed at 4°C. The lysate was clarified by centrifugation, a small fraction being kept for total protein and total Rac1 quantification. The remaining lysate was snap frozen in liquid nitrogen. 500 µg of total proteins were then mixed with 20 µg of PAK-PBD beads and incubated on a rotator for 1 h at 4°C. After centrifugation, the PAK-PBD beads were washed once with a buffer provided in the kit and

the pellet resuspended in 20  $\mu$ L of sample buffer (4X). The quantity of activated Rac1 was analysed by Western blotting with anti-Rac1 antibody. In each assay, two controls were performed: i) a positive control of the pull-down in which a saturating amount of GTP $\gamma$ S was added to the cell lysate. This GTP $\gamma$ S, which is non-hydrolysable, interacts with Rac1, thus allowing GTP-bound Rac1 pull-down with the PAK-PBD beads. ii) a negative control in which GDP will be added to the cell lysate that will be loaded with Rac1 leading to no Rac1 pull-down.

## **12. Cell morphology assay**

Cells were seeded in 6-well plates in complete medium and grown for 24 hours in order to reach 60% confluence. Then, cells were treated with DMSO or 0.2  $\mu$ M of PF-2341066, or 0.1  $\mu$ M of PHA-665752, or 2  $\mu$ M of SU-11274. After 16 hours of incubation, changes in morphology were observed by microscopy and random pictures were taken.

## **13. Transwell chemotactic migration assay**

24 hours before the assay, NIH3T3 cells were serum deprived with E4 supplemented with 1% DCS.

The underside of the Transwell (Corning, 8  $\mu$ m pore size) was coated with fibronectin (Sigma) for 30 min at room temperature. The excess of fibronectin was removed and the inserts left for 1 hour to dry. Cells were then split, washed in serum free medium and resuspended in serum free medium supplemented with 0.1% BSA. The concentration was adjusted to  $10^5$  cells per mL, and 200  $\mu$ L of this suspension ( $2 \times 10^4$  cells) was

disposed into the upper part of the well in the presence of indicated drugs or DMSO. To create a gradient of chemoattractants, the lower part of the well was filled in with 600  $\mu$ L of cell culture medium (E4 + 10% DSC).

After 90 min of culture (37°C, 8% CO<sub>2</sub>), the medium was removed and the cells that did not go through the membrane were removed using a cotton bud. The inserts were fixed in 4% paraformaldehyde for 10 min and washed in PBS. Cell nuclei were then stained with Haematoxylin (Sigma) for 5 min. The membranes were cut and mounted with aqueous medium (Aquatex, VWR).

To quantify the number of cells that migrated (*i.e.* the cells present on the underside of the membrane at the end of the assay), 10 fields per porous membrane were chosen randomly and counted (x20 lens, Zeiss Axiophot microscope). When at least 3 independent experiments were done, data sets were analysed for significance using Student's t test.

#### **14. Survival assay (protection against anoikis)**

Cells were grown up to 70% confluence, washed with PBS and trypsinised. They were then washed in serum free medium and counted.  $5 \times 10^5$  cells were resuspended in 1 mL of serum free medium, in the presence of drugs or DMSO, and incubated in a 15mL tube (Polypropylene, Falcon) at 37°C. After 24 h, 400  $\mu$ L of cell suspension was taken and half of it was analysed by flow cytometry (FACSCALIBUR, BD) after staining with a live/dead discriminator reagent (Propidium Iodide (PI) or TOPRO<sup>®</sup>-3 (Invitrogen). The percentage of dead cells was determined by numbering those which had lost plasma membrane integrity and could

incorporate PI or TOPRO<sup>®</sup>-3. The other half of the cell suspension, was centrifuged, the cells were lysed and analysed by Western blotting with indicated antibodies. Data sets from 3 independent experiments were analysed for significance using Student's t test.

### **15. Soft Agar Assay**

500 cells in single cell suspension were mixed, on ice, in 5mL of medium with 0.3% agarose. After 20 min, 1 mL of medium with 10% serum was added and cells incubated at 37°C. Medium was changed every other day. Treatment started at day 5, with medium plus DMSO or dynasore (80 µM) changed daily. At day 9, the whole wells were pictured on a Zeiss, Stemi SV11 microscope and the total number of colonies counted. The total area of the colonies was determined with Image J software.

### **16. *In vivo* tumorigenicity assays**

4-6 week-old-female athymic nude mice (CD1 Nu/Nu, Charles River UK) were used, in accord with United Kingdom Coordination Committee on Cancer Research guidelines and Home Office regulations.

#### **16.1. Tumour growth assay**

For the tumour growth assay,  $5 \times 10^5$  cells were inoculated subcutaneously in the flank region of nude mice. The tumours were measured (width and length) with a caliper. Tumour volumes were calculated by using the formula:  $\text{length} \times \text{width}^2 \times (\pi/6)$ . In some experiments, the entire skin surface over the tumours (when they reached

a volume of around 50 mm<sup>3</sup>) or where cells have been injected, was painted everyday with indicated reagents. When tumours reached the critical size of 1 cm in length in any directions, mice were killed humanely and tumours were resected, snap-frozed or fixed in formal saline. Protein lysates were generated from frozen samples and analysed by Western blotting. Fixed samples were paraffin embedded. Sections of 4 µM were processed for immunofluorescence.

### **16.2. Lung colonisation assay**

For the experimental “metastasis” assay, cells expressing the indicated Met protein were resuspended in PBS at 5x10<sup>6</sup> /mL and 100 µL (5x10<sup>5</sup> cells) were injected into the tail vein of the mice. 10 days later mice were killed and the lungs were removed, weighed and fixed in formal saline. The same area of each lung was cut and paraffin embedded. Sections of 4 µM were processed and haematoxylin/eosin staining was performed before analysis on a Zeiss Axiophot microscope.

### **17. Statistical analysis**

Two-tailed Student's t test was performed, unpaired between the different cells, paired between different conditions for a given cell. Quantitative data of the indicated number of independent experiments are expressed as means ± SEM.

## **RESULTS - PART I**

### **Small Molecule Inhibitors Differentially Affect Distinct Oncogenic Met Mutants**

Since Wt and oncogenic forms of Met have been shown to play an important role in tumour progression and metastatic spread of many cancers<sup>15</sup>, a number of pharmaceutical companies have engineered small-molecule inhibitors that target this receptor. Although these drugs have been reported to be specific for Met, a major question mark remains concerning their relative efficiencies against various tumorigenic forms of the receptor. Different mutations potentially can impact in different ways on the conformation, expression, stability, level of activation or subcellular localisation of a receptor, rendering each mutant differentially sensitive to a given drug. Therefore, results obtained with a particular molecule on a certain mutant would not necessarily predict results likely to be obtained on other mutants. Thus it seems important to me that each drug/mutant combination should be tested independently. Such an approach could allow the optimisation of anti-cancer therapies by matching a given mutation to what is likely to be its most efficient treatment.

Here, I have studied and compared the sensitivity of two Met mutants, D1246N and M1268T, previously identified in human papillary renal carcinoma, to three pharmacological inhibitors, SU-11274, PHA-665752 and PF-2341066, the latest of which currently is being tested in several Phase I clinical trials.

## **1. D1246N and M1268T Met mutants are highly phosphorylated and highly tumorigenic**

I used NIH3T3 cells (expressing very low levels of endogenous Met) stably transfected with Wt Met or with a specific mutant containing one of the following amino-acid changes: D1246N, M1268T or Y1248C. Mutants M1268T and Y1248C were expressed at levels comparable to the Wt while D1246N expression was elevated slightly (1.6 fold) (**Fig. 1A**). In the absence of exogenous HGF, tyrosines 1234-1235 in the kinase domain, and 1349 in the docking site, were highly phosphorylated in the D1246N and M1268T Met mutants relative to the Wt. These results were consistent with what was previously detected for total Met phosphorylation by co-immunoprecipitation studies<sup>156</sup>, where D1246N and M1268T mutants had been shown to be the more highly phosphorylated<sup>156</sup>. The phosphorylation of the Y1248C Met mutant was also increased in relation to the Wt Met but not significantly. Normalisation on Met expression clearly excluded that these results were due to higher expression levels (**Fig. 1B and 1D**). The NIH3T3 fibroblasts used produce low amounts of HGF<sup>156</sup> so that, under basal conditions, the three mutants clearly were phosphorylated spontaneously to a greater degree than Wt Met. Exogenous HGF significantly enhanced phosphorylation both of the Wt and of the mutants (**Fig. 1B-D**).

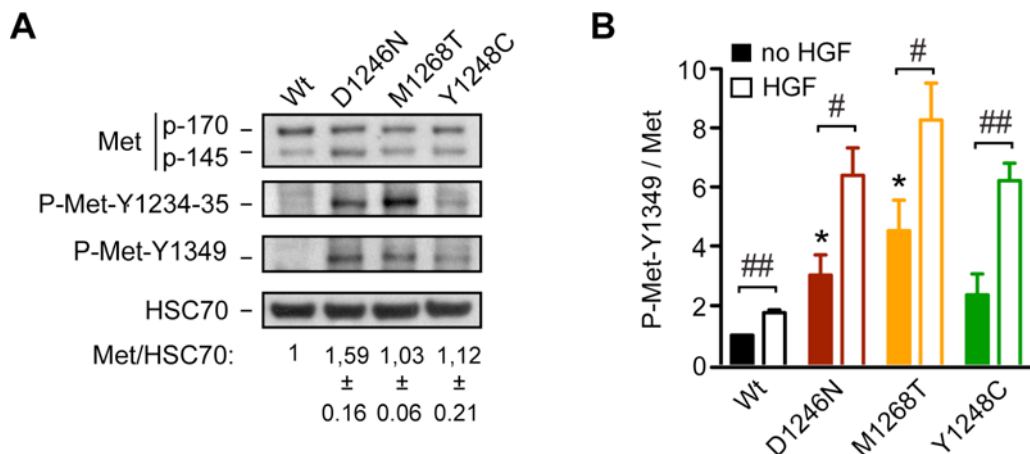


**Fig.1. D1246N and M1268T Met mutants are highly phosphorylated and highly tumorigenic**

**(A)** Western blots for Met, phosphorylated Met (Y1234-35 and Y1349) and HSC-70 were performed on cells expressing Wt, D1246N, M1268T or Y1248C Met forms. Numbers represent fold increase of Met p-145 / HSC-70 ratios (between mutants and the Wt) obtained from six independent experiments.

**(B)** The graph shows phosphorylated Met-Y1349 / Met ratios identified by densitometries from Western blots (not shown) in the indicated cells non stimulated (no HGF) or stimulated with HGF (HGF) for 15 min. Data are represented in arbitrary units (from three independent experiments).

#, \* $p < 0.05$ , ##  $p < 0.01$ .

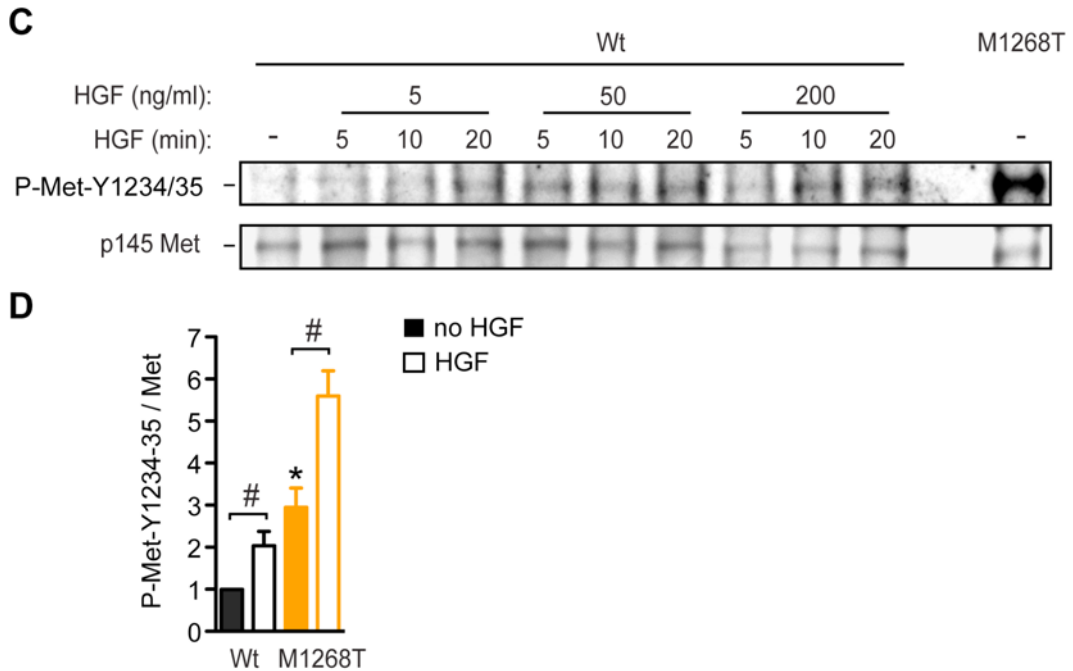


**Fig.1. D1246N and M1268T Met mutants are highly phosphorylated and highly tumorigenic**

**(C)** Western blots for Met and phosphorylated Met (Y1234-35) were performed on cells expressing Wt and M1268T Met forms. Cells were stimulated, or not, with HGF at 5, 50 and 200 ng/mL for 5, 10 and 20 min.

**(D)** The graph represents phosphorylated Met-Y1234-35/Met ratios quantified by densitometries from Western blots (not shown) in the indicated cells non stimulated (no HGF) stimulated with HGF (50 ng/mL). Data are represented in arbitrary units (from three independent experiments).

#, \* $p < 0.05$ .

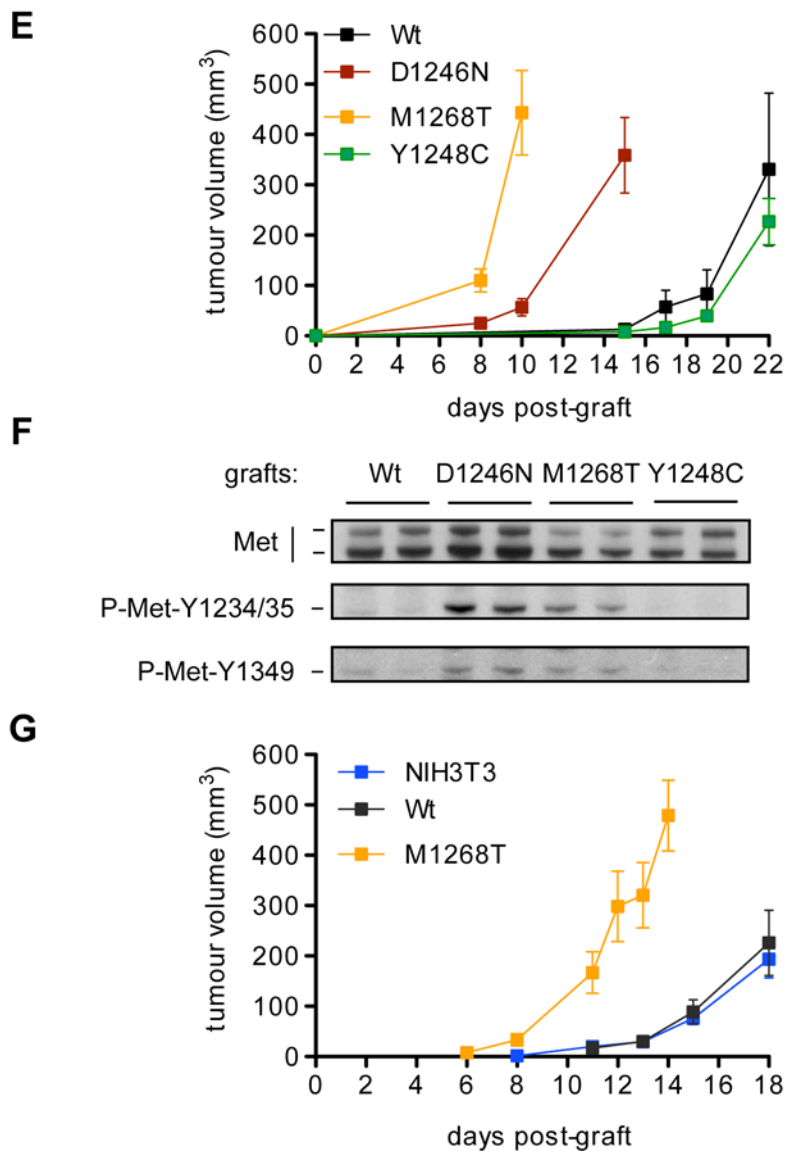


**Fig.1. D1246N and M1268T Met mutants are highly phosphorylated and highly tumorigenic**

**(E)** Wt, D1246N, M1268T and Y1248C Met expressing cells (500,000 / 100 $\mu$ l) were injected subcutaneously into nude mice (five per group). The graph plots tumour volumes (width<sup>2</sup> x length x ( $\pi$  /6) against time post-injection.

**(F)** Western blots of lysates from resected tumour tissues for phosphorylated Met (Y1234-35 and Y1349), Met and HSC-70.

**(G)** NIH3T3 cells, Wt and M1268T Met expressing cells were injected subcutaneously into nude mice (five per group). The graph plots tumour volumes (width<sup>2</sup> x length x ( $\pi$  /6) against time post-injection.

I acknowledge Prof. Ian Hart for injecting the cells and for training me for all the *in vivo* experiments.

To analyse the functional consequences of the hyperactivated status of the mutants, I tested their tumorigenicity *in vivo* by grafting each cell type subcutaneously into nude mice. While M1268T and D1246N Met mutants formed palpable tumours one week post-graft, Wt and Y1248C Met expressing cells generated detectable tumours around 17 days post-graft (**Fig. 1E**). Non-transfected NIH3T3 cells developed tumours at a rate similar to that of Wt and Y1248C expressing cells (**Fig. 1G**). All animals were killed when tumours reached a volume of 400-500 mm<sup>3</sup> (days 10-15 for M1268T and D1246N; day 22 for Y1248C and Wt). D1246N and M1268T mutants remained highly phosphorylated in tumour tissue (**Fig. 1F**). Taken together, these results established a strong correlation between the level of Met phosphorylation and tumorigenic potential.

## **2. The three Met inhibitors tested inhibit the basal activation of the M1268T mutant efficiently but have little or no effect on D1246N**

In agreement with the literature<sup>156</sup>, my data showed that the three studied Met mutants are highly phosphorylated, and therefore highly activated, under basal conditions. There were, however, some differences among the three mutants in the levels of phosphorylation. Thus M1268T and D1246N were the most phosphorylated while Y1248C was the least phosphorylated. Interestingly, we also observed that only the M1268T and D1246N mutants were highly tumorigenic *in vivo*. Cells expressing either of these two forms of the receptor therefore were considered to constitute an ideal model with which to study the transforming mechanisms of Met activity and to analyse the relative potency of several Met-specific

Tyrosine Kinase Inhibitors (TKI). We tested three different compounds: PHA-665752<sup>233</sup>, SU-11274<sup>231</sup> and PF-2341066<sup>238</sup>; the latter being the only one among the three, to be administered *per os*. These three drugs act by blocking ATP-binding to the kinase domain of Met, thereby inhibiting, as a consequence, its catalytic activity.

Previously the efficiency of these three drugs in inhibiting Met activation has been tested in different cellular models. SU-11274 exhibited less potency than the two other TKIs, PHA-665752 and PF-2341066. It required a minimum concentration of 2  $\mu\text{M}$  of SU-11274 to inhibit Met phosphorylation in a Western blot experiment<sup>231,261</sup> as compared with the 0.1  $\mu\text{M}$  and 0.01  $\mu\text{M}$  concentrations for PHA-665752<sup>233,262</sup> and PF-2341066<sup>166,240</sup> respectively. These previously reported data helped me, in my cell system, initially to establish the range of concentrations likely to be required to evaluate, in dose response assays, the potency of these three different TKIs.

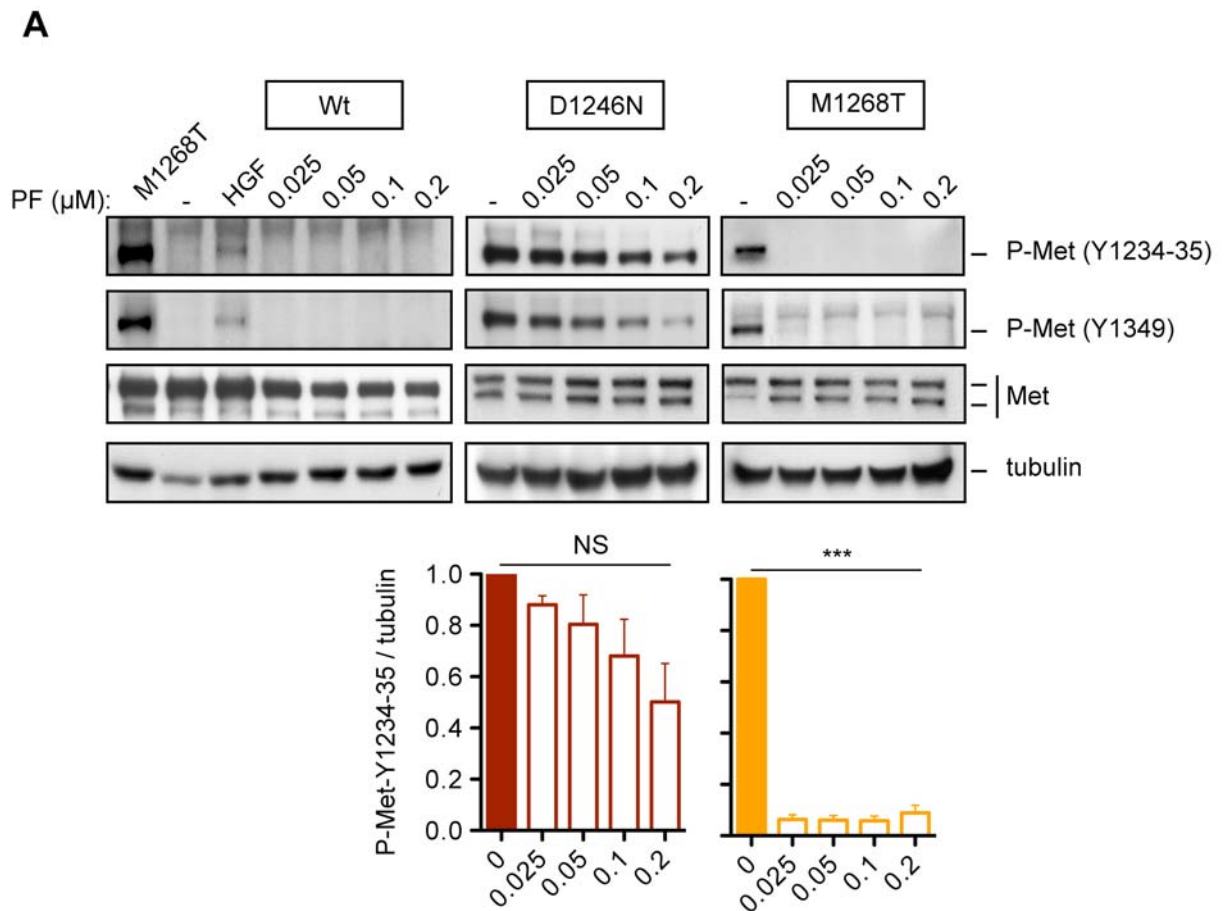
First, consistent with the literature, I observed that PF-2341066 blocked the induced HGF Wt Met phosphorylation efficiently<sup>240</sup>.

Second, in cells expressing the M1268T mutant, the basal level of phosphorylation of the tyrosines 1234-35 and 1349, located within the kinase domain and the docking site of the receptor respectively, was diminished strongly by all the TKIs tested (**Fig. 2A-C**). Among the three drugs, PHA-665752 and PF-2341066 seemed to be the more powerful, given that a concentration of 0.025  $\mu\text{M}$  was shown to affect the phosphorylation of the receptor on these tyrosines significantly and that a concentration of 0.1-0.2  $\mu\text{M}$  fully blocked their activity ( $p < 0.01$ ,  $p < 0.001$ )

**(Fig. 2A-B).** In contrast, SU-11274 was at least 10 times less efficient as a significant degree of inhibition was only observed at concentrations equal to or greater than 1  $\mu$ M ( $p < 0.01$ ) **(Fig 2C).**

Third, SU-11274 and PHA-665752 had no impact on the phosphorylation status of the D1246N mutant, even at high concentrations (5  $\mu$ M) **(Fig. 2B-C).** PF-2341066 decreased phosphorylation levels at concentrations above 0.1  $\mu$ M. These reductions did not achieve significance levels.

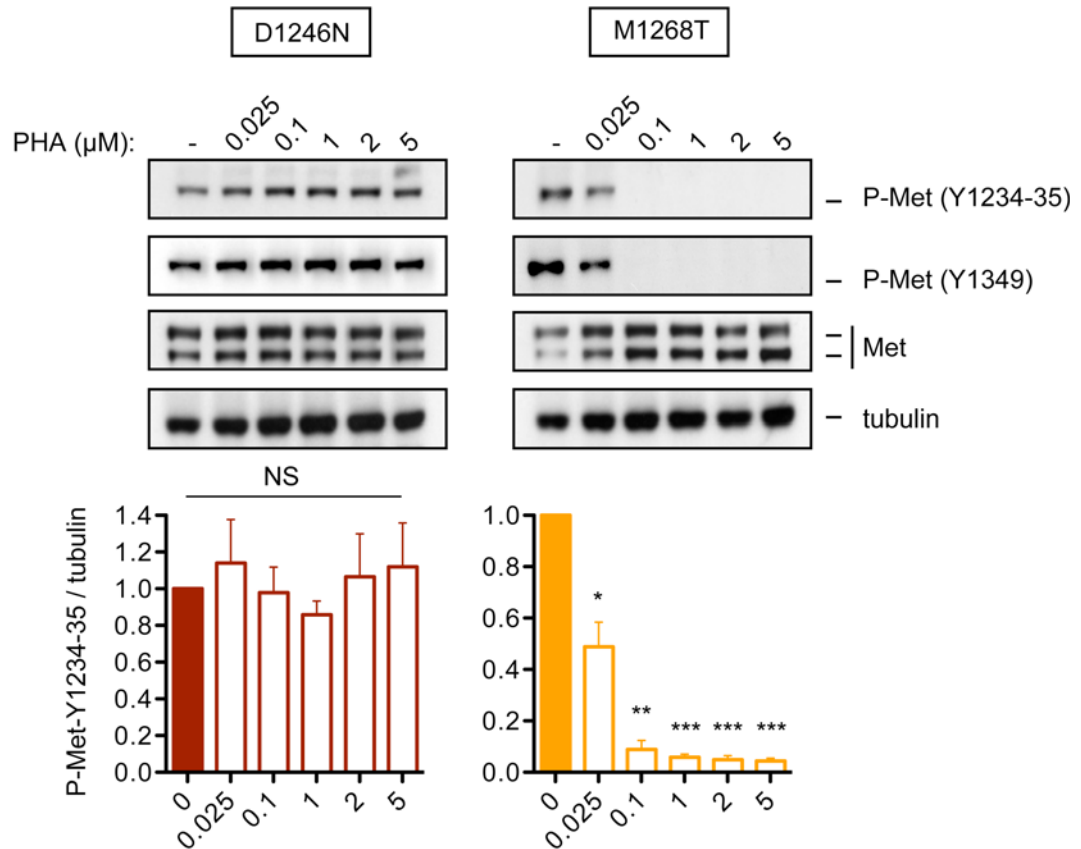
This dose/response assay thus allowed me to demonstrate that the M1268T Met mutant was highly sensitive to the drugs while the D1246N mutant appeared resistant or, at least, very poorly sensitive. Thanks to this approach I also determined, for the different inhibitors, the optimal concentrations to use in the rest of the study: these were determined to be 0.1  $\mu$ M, 2  $\mu$ M and 0.2  $\mu$ M for PHA-665752, SU-11274 and PF-2341066 respectively.



**Fig.2. The three Met inhibitors tested inhibit the basal activation of the M1268T mutant efficiently but have little or no effect on D1246N.**

**(A)** Western blots for Met, phosphorylated Met (Y1234-35), (Y1349) and tubulin were performed on Wt ± HGF (15 min, 50 ng/ml), D1246N and M1268T Met expressing cells treated with DMSO (-) or with increasing concentrations (0.025, 0.05, 0.1 and 0.2 μM) of PF-2341066 (PF). The graphs represent phosphorylated Met (Y1234-35) / tubulin ratios obtained by densitometric analysis from three independent experiments.

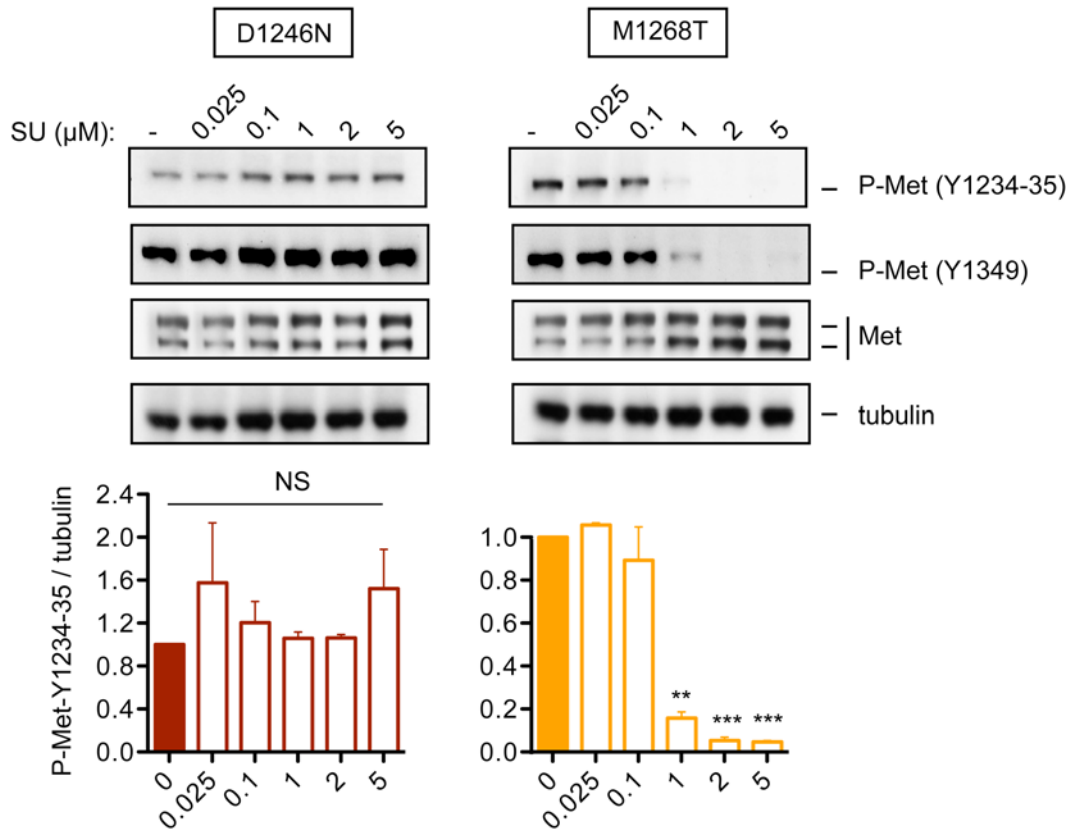
\*p<0.01, \*\*p<0.01, \*\*\*p<0.001.

**B**

**Fig.2. The three Met inhibitors tested inhibit the basal activation of the M1268T mutant efficiently but have little or no effect on D1246N.**

**(B)** Western blots for Met, phosphorylated Met (Y1234-35), (Y1349) and tubulin were performed on D1246N and M1268T Met expressing cells treated with DMSO (-) or with increasing concentrations (0.025, 0.01, 1, 2 and 5  $\mu$ M) with PHA-665752 (PHA). The graphs represent phosphorylated Met (Y1234-35) / tubulin ratios obtained by densitometric analysis from three independent experiments.

\*p<0.01, \*\*p<0.01, \*\*\*p<0.001.

**C**

**Fig.2. The three Met inhibitors tested inhibit the basal activation of the M1268T mutant efficiently but have little or no effect on D1246N.**

**(C)** Western blots for Met, phosphorylated Met (Y1234-35), (Y1349) and tubulin were performed on D1246N and M1268T Met expressing cells treated with DMSO (-) or with increasing concentrations (0.025, 0.01, 1, 2 and 5  $\mu$ M) of SU-11274 (SU). The graphs represent phosphorylated Met (Y1234-35) / tubulin ratios obtained by densitometric analysis from three independent experiments.

\* $p < 0.01$ , \*\* $p < 0.01$ , \*\*\* $p < 0.001$ .

### **3. The three Met inhibitors revert transformed morphology, migration and survival of cells expressing the M1268T Met mutant, but not the D1246N Met mutant**

Met mutants conferred upon the expressing cells a high transforming potential<sup>156,174</sup> which translated into evident morphological changes. This observation was confirmed in our system. NIH3T3 cells expressing Wt Met were flattened, with tight interactions, while cells expressing D1246N or M1268T mutants were loosely adherent, rounded in shape and exhibited a less differentiated shape (**Fig. 3A**). To further characterise the effect of the drugs on the different mutants, I next studied if exposure of the cells to Met-specific TKIs could affect this transformed morphology. After 16h of treatment, cells expressing the M1268T Met mutant reverted their phenotype and acquired a more flattened morphology, closer to that of the cells expressing Wt Met. In contrast, the shape of the cells expressing the D1246N Met mutant or the Wt form of the receptor appeared almost completely unchanged by these inhibitors (**Fig. 3A**). These results confirmed that the M1268T Met mutant was sensitive to the drugs whereas the D1246N mutant was resistant and, together with the data on the inhibition of the phosphorylation, suggested strongly that the transformed morphology of cells expressing the M1268T Met mutant was due to the constitutive activation of the receptor.

It previously has been shown that expression of Met mutants in Madin-Darby canine kidney cells strongly increased their motility<sup>174</sup>. To test the impact of the different mutants on the migratory properties of the NIH3T3 cells, we set-up a Transwell migration assay. Cells, previously cultured in

1% serum, were plated in serum-free medium into the upper part of the well in the presence of the indicated drugs or the DMSO diluent as a control. To create a gradient of chemoattractants, the lower part of the well was filled in with cell culture medium containing 10% serum supplemented, or not, with HGF. After 2 h of incubation, only very few Wt Met expressing cells had migrated through the membrane under basal conditions. HGF significantly increased the number of cells found on the lower side of the membrane, demonstrating the ability of Met to promote cell migration ( $p < 0.05$ ). Moreover, cells expressing the M1268T or D1246N mutants had a significant higher migratory potential than the Wt cells ( $p < 0.05$ ) (**Fig. 3B**). As expected, when the cells were treated with the PHA-665752 or PF-2341066, the migration of the M1268T cells was inhibited significantly ( $p < 0.05$ ). Conversely, the migration of the cells expressing the D1246N mutant was not prevented significantly even though PF-2341066 at the same dose reduced D1246N phosphorylation slightly; a reduction that did not achieve significance (see **Fig. 2A**) (**Fig. 3C**). These results confirmed that the high migratory potential of the M1268T expressing cells was due to Met activity and that the D1246N mutant was resistant to these drugs. Interestingly, PHA-665752 seemed a more potent inhibitor than PF-2341066 in this assay. Indeed, the percentage of inhibition of migration of the M1268T expressing cells obtained with PHA-665752 was greater (76%) than that achieved with PF-2341066 (52%) ( $p < 0.05$ ).

As an increase in survival capacity could be another factor in favour of cell transformation and resultant tumorigenesis, I next analysed whether these

cells also exhibited an advantage in terms of survival. I first tested this hypothesis by evaluating the capacity of cells expressing each of the Met forms to survive the phenomenon known as anoikis; i.e. the induction of apoptosis by loss of adherence to a substrate. Cells were cultured in serum free medium and were maintained in non-adherent conditions for a period of 16 h. Both of the cell lines expressing the Met mutants exhibited an increase in survival (from 22% to 33%) relative to survival of Wt Met cells ( $p < 0.05$ ) (**Fig. 3D**). This protection from anoikis could be due to a decreased apoptosis since the cleaved PARP enzyme (Poly(ADP-ribose) Polymerase), used as a marker of cells undergoing apoptosis, was detected in higher proportions in Wt Met than in D1246N and M1268T Met expressing cells (**Fig. 3E**).

The Met inhibitor PHA-665752 dramatically reduced the increase in survival associated with the expression of the M1268T mutant by 85% ( $p < 0.001$ ), thus establishing a direct link between cell survival and Met activation. In contrast, PHA-665752 did not affect the survival potential of cells expressing the D1246N Met mutant, confirming the resistance of this mutant to these drugs. Moreover, correlating with the results already obtained and presented in **Fig. 2**, the level of phosphorylation of the M1268T Met mutant at the end of the survival assay was decreased considerably when cells were treated with PHA-665752 whereas this drug did not modify phosphorylation of the mutant D1246N (**Fig. 3F**).

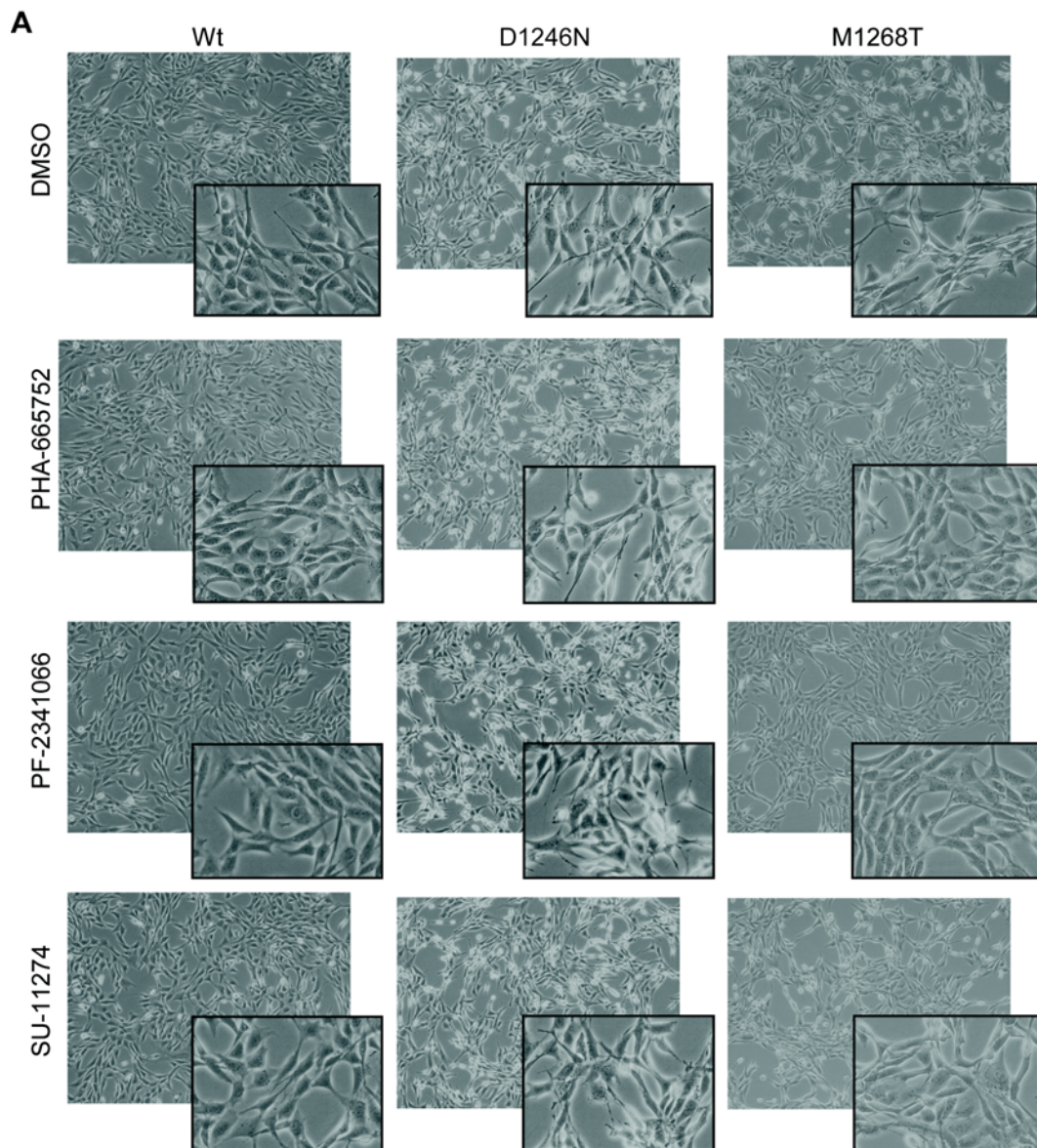


**Fig.3. The three Met inhibitors revert transformed morphology, migration and survival of cells expressing the M1268T Met mutant, but not the D1246N Met mutant**

**(A)** Wt, D1246N and M1268T Met expressing cells were treated overnight (16 h) with DMSO, or with one of the TKIs: 0.1  $\mu$ M PHA-665752, 2  $\mu$ M SU-11274, 0.2  $\mu$ M PF-2341066 and morphological changes were observed with an inverted microscope.

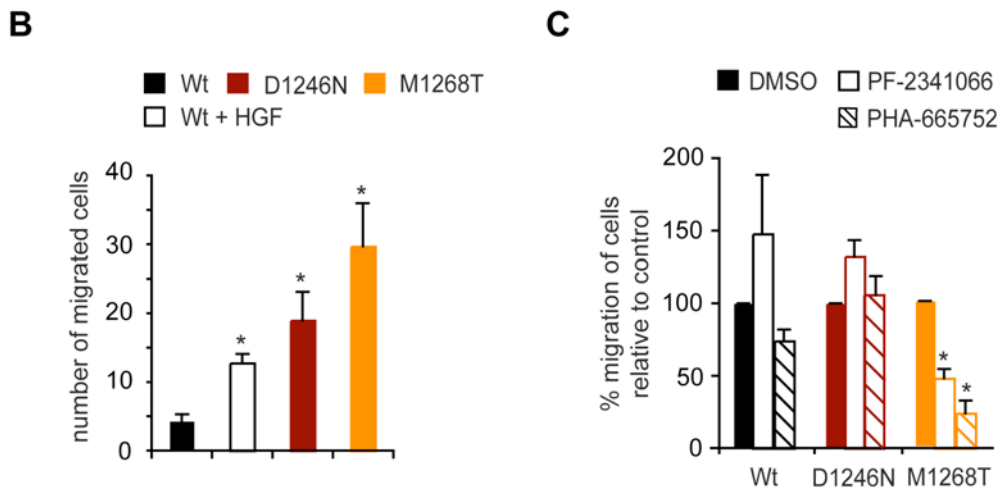


**Fig.3. The three Met inhibitors revert transformed morphology, migration and survival of cells expressing the M1268T Met mutant, but not the D1246N Met mutant**

**(B)** The graph represents the average number of Wt, D1246N and M1268T Met expressing cells that have migrated through Transwells over 2 hours of incubation with, as a chemoattractant, 10% serum (DCS) or HGF (50 ng/mL) from at least three independent experiments.

**(C)** The graph represents the percentage of Wt, D1246N and M1268T Met expressing cells that have migrated through Transwells (serum gradient) when treated with DMSO or 0.1  $\mu$ M PHA-665752, or 0.2  $\mu$ M PF-2341066 from three independent experiments.

\* $p < 0.01$ , \*\* $p < 0.001$ .

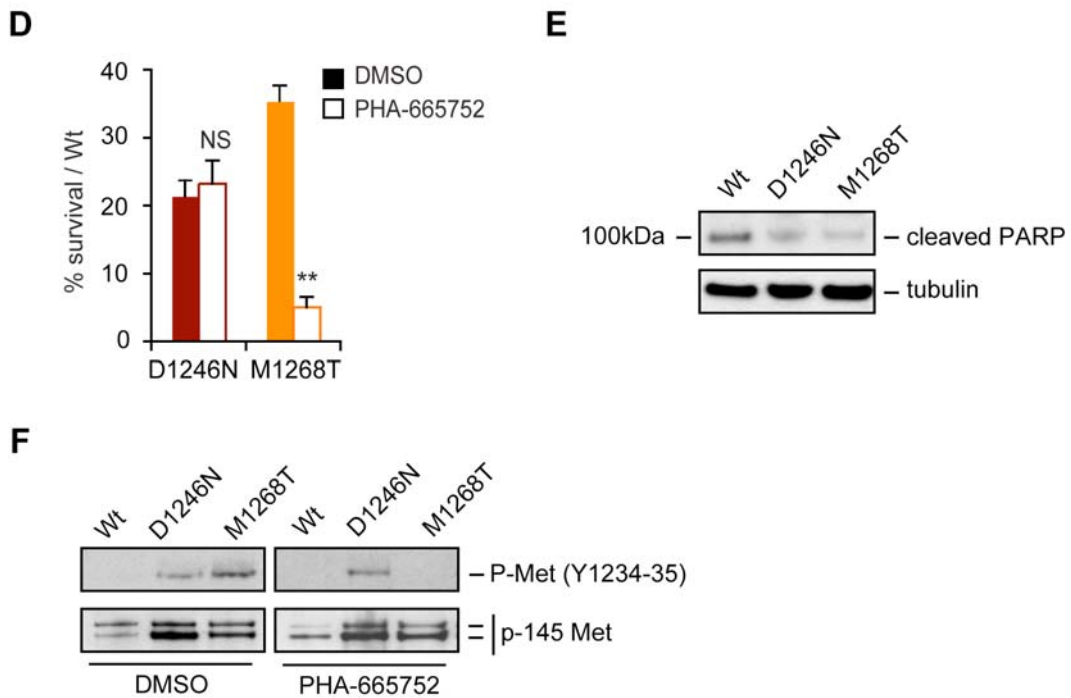


**Fig.3. The three Met inhibitors revert transformed morphology, migration and survival of cells expressing the M1268T Met mutant, but not the D1246N Met mutant**

**(D)** Wt, D1246N and M1268T Met expressing cells were incubated in suspension for 16 hours in serum-free medium supplemented with DMSO or with 0.1 $\mu$ M PHA-665752. Cells were stained with Propidium Iodide. The graph represents the % of increase in survival of mutant expressing cells versus Wt expressing cells in control condition (DMSO) or PHA-665752 treatment from three independent experiments.

**(E-F)** Cell aliquots from experiments (D) were lysed and analysed by Western blotting, with anti-cleaved PARP and an anti-tubulin **(E)** or with an anti-phosphorylated-Met (Y1234-35) and an anti-Met **(F)**.

\*p<0.01, \*\*p<0.001.

#### **4. Topical application of PHA-665752 and PF-2341066 inhibited tumour growth of cells expressing the M1268T Met mutant, but not the D1246N Met mutant**

Inhibiting the activity of the M1268T mutant cells with Met-specific TKIs decreased cell migration and survival but had no effect on the D1246N mutant. The next question I chose to address was then to investigate the influence of the TKIs on *in vivo* tumour growth driven by these mutants.

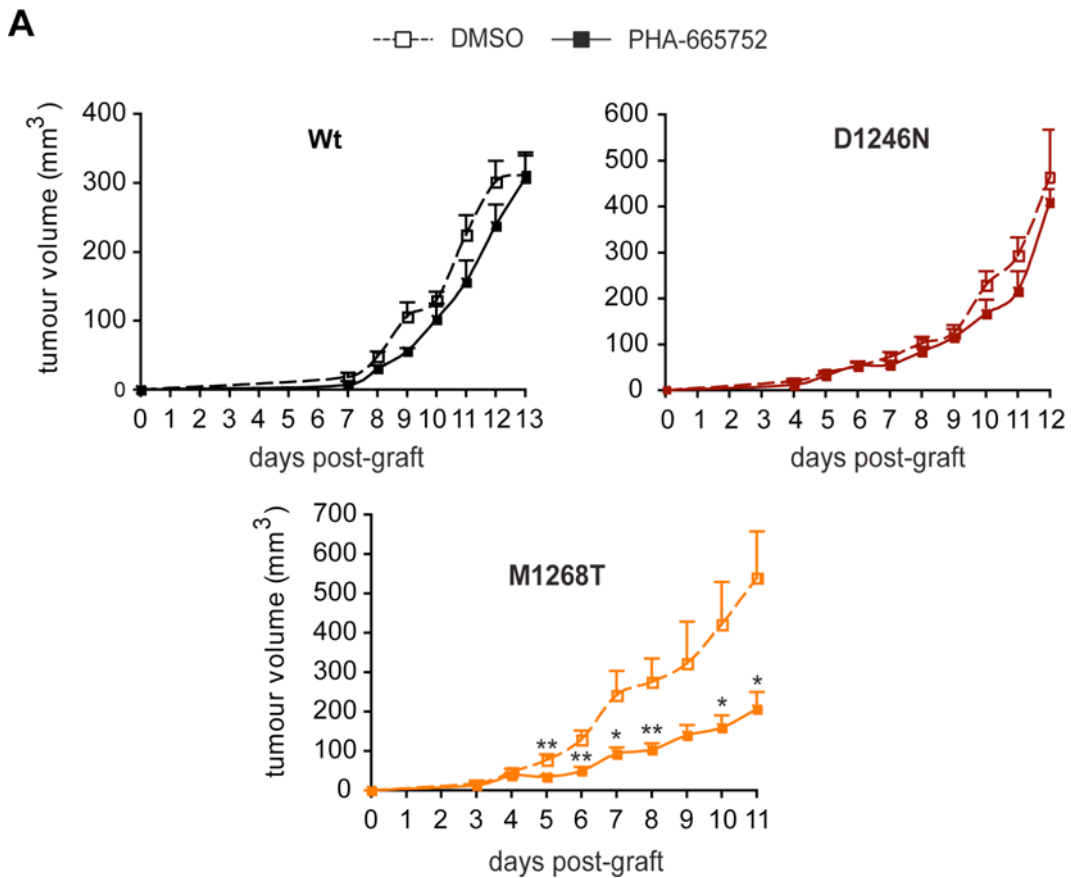
Cells expressing the Wt, or one of the two mutated forms of Met were grafted subcutaneously into *nude* mice (as described in **Fig. 1E**). When the volume of the tumours reached a size comprised of between 30 and 50mm<sup>3</sup>, daily treatment with the indicated drug was initiated. PHA-665752 was not water-soluble and, as a consequence, could not be administered orally. Treatment by daily injection of the drug into the tail vein<sup>233</sup> or into the tumour<sup>236</sup> had been reported previously where the treatment had some success against tumour growth. However, I was concerned that daily injection of DMSO, the solvent used, might be harmful so I thought about another approach. As DMSO increases the penetration of substances through the skin, and as PHA-665752 is DMSO-soluble, I decided to apply a solution of these TKIs by painting them daily over the skin surface above the growing tumours.

The skin remained healthy after several days of treatment, showing that the DMSO by itself was not irritant or toxic. Strikingly, from day 5 post-graft, the topical application of PHA-665752 rapidly induced a slow down in tumour growth in those grafts derived from M1268T mutant expressing cells. This led at the end of the assay, to a reduction of tumour size by

60% versus the size of the control DMSO treated tumours ( $p < 0.05$ ) (**Fig. 4A**). Conversely, no significant change in tumour size was observed in similarly treated mice grafted with Wt Met expressing cells; again demonstrating that the growth of these tumours was not dependent on Met activity. Interestingly, and consistent with our *in vitro* data, PHA-665752 had no effect on tumours derived from implanted D1246N Met mutant-expressing cells (**Fig. 4A**).

A comparable set of data was obtained when PF-2341066, also soluble in DMSO, was applied topically. Indeed this drug inhibited the growth of the M1268T tumour but had no effect on tumours derived from Wt Met or D1246N Met mutant-expressing cells. As observed in the migration assay, PF-2341066 also appeared to be somewhat less effective than PHA-665752 in this model (**Fig. 4B**). While PHA-665752 slowed down tumour development after its first application PF-2341066 seemed to require several days of treatment to have a significant effect. Moreover, the percentage of tumour growth inhibition at the end of the experiment was slightly greater with PHA-665752 (62%) than it was with PF-2341066 (57%) although this difference was not significant.

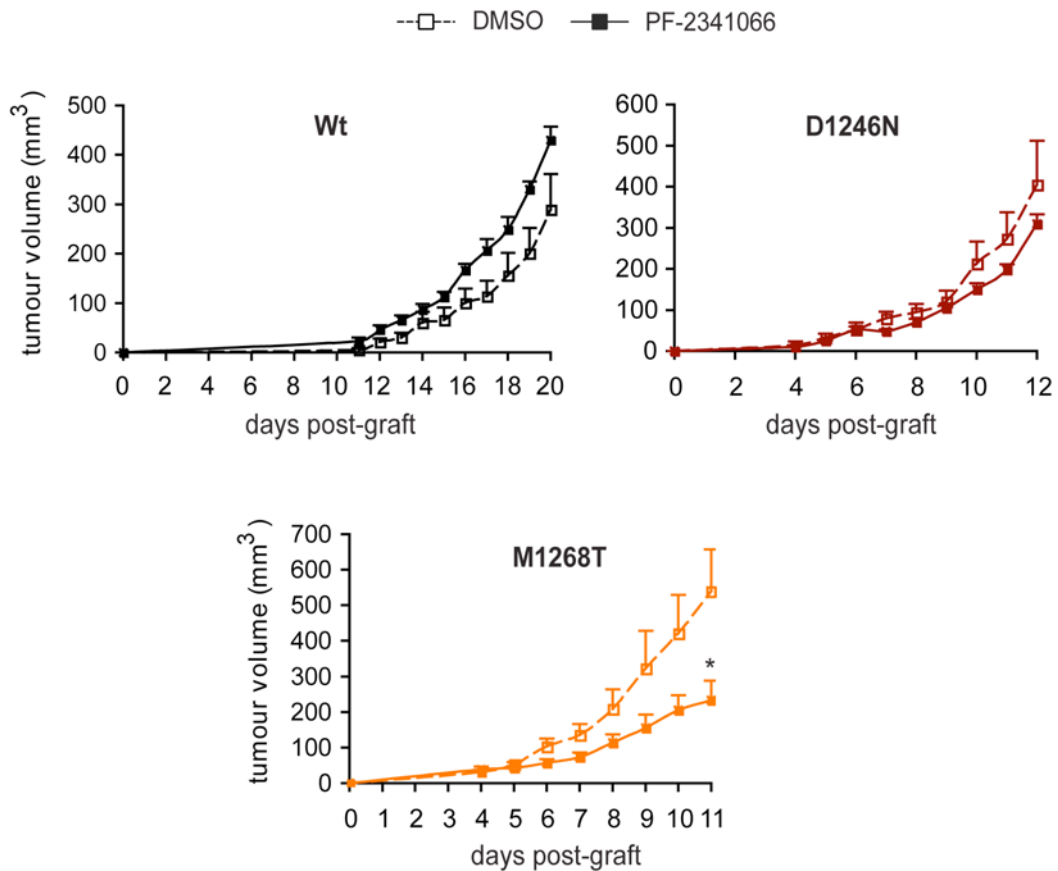
This method of application appeared to have worked because the TKIs could penetrate into the tumours where they inhibited Met M1268T activation, and as a consequence slowed down the tumour expansion.



**Fig.4. Topical application of PHA-665752 and PF-2341066 inhibited tumour growth of cells expressing the M1268T Met mutant, but not the D1246N Met mutant**

**(A)** Wt, D1246N and M1268T Met expressing cells were injected subcutaneously into nude mice. The graph plots tumour volumes against time post-injection. When tumours had reached 30-50 mm<sup>3</sup>, DMSO or PHA-665752 (0.1 μM) was applied topically over the surface of the tumour mass each day (from two independent experiments, except for experiment with Wt cells done one time).

\*p<0.05, \*\*p<0.01.

**B**

**Fig.4. Topical application of PHA-665752 and PF-2341066 inhibited tumour growth of cells expressing the M1268T Met mutant, but not the D1246N Met mutant**

**(B)** D1246N and M1268T Met expressing cells were injected subcutaneously into nude mice. The graphs plot tumour volumes against time post-injection. When tumours had reached 30-50 mm<sup>3</sup>, DMSO or PF-2341066 (0.2 μM) were applied topically over the surface of the tumour mass each day (5 mice per group).

\*p<0.05, \*\*p<0.01.

## **5. Oral administration of PF-2341066 inhibited growth of M1268T Met mutant tumours but not of D1246N Met mutant expressing cells**

In the clinic such tumour painting might seem attractive but it would have to be restricted to some types of tumours, such as melanoma in which Met recently has been identified as a new therapeutic target<sup>234</sup>, with treatment restricted to those which are located superficially. These are not likely to be numerous. Therefore, the most practical way to administer a drug is likely to be *per os*. PF-2341066 is water-soluble and designed for this purpose. In order to test the efficiency of this drug using this classic route of administration, a tumour growth assay was conducted. Thus PF-2341066 was given daily by oral gavage at a dose of 50 mg/kg; a dose reported to be efficient in several tumour models in which tumour growth was dependent on Met activation<sup>238</sup>. As expected, tumour cells expressing the D1246N Met mutant were resistant to PF-2341066 treatment whereas tumours derived from the M1268T expressing cells were highly sensitive (**Fig. 5**).

Taken together, these data suggest that the three Met-specific TKIs tested in this study can inhibit Met mutant M1268T-dependent tumour growth. However the D1246N Met mutant was resistant to the treatment. These observations suggested that, although distinct activating mutations occurring in the kinase domain can lead to similar cell behaviour (here M1268T and D1246N both modify cell morphology, increase migration and survival similarly), such mutations confer upon the receptor different sensitivities to different drugs. My results underline the importance of

developing new “types” of Met-specific drugs, especially when resistance occurs.

My data also reinforce the importance of screening patients for the specific mutations driving their cancers in order that the most efficient treatment can be used, rather than applying a general inhibitor to a range of mutations.

Finally, I have demonstrated here that TKIs administered topically are able to penetrate through the skin and agents delivered in this fashion slowed down subcutaneous tumour growth efficiently.

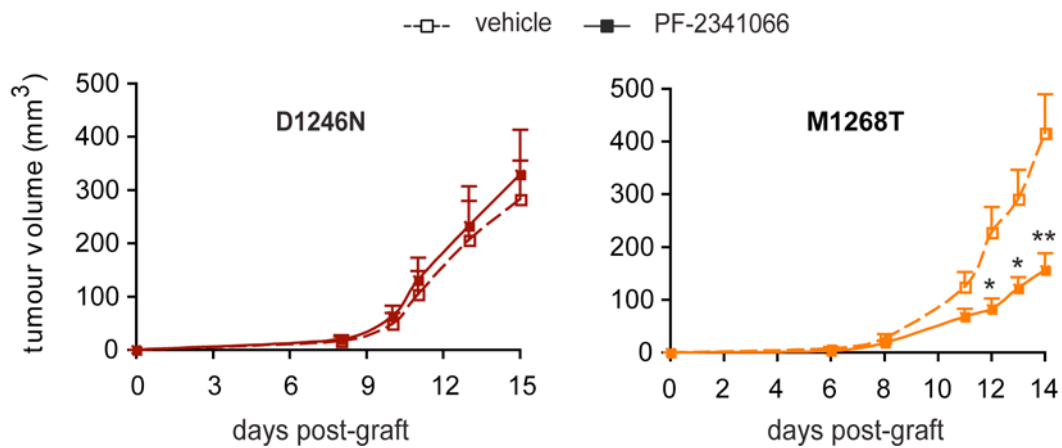


**Fig.5. Oral administration of PF-2341066 inhibited growth of M1268T Met mutant tumours but not of D1246N Met mutant expressing cells**

D1246N and M1268T Met expressing cells were injected subcutaneously into nude mice. The graph plots tumour volumes against time post-injection. Mice bearing tumours of 30-50 mm<sup>3</sup> received vehicle alone or PF-2341066 (50 mg/kg) administered daily by oral gavage (from two independent experiments).

\*p<0.05, \*\*p<0.01.

## DISCUSSION - PART I

In the first part of the present study, I have reported that two Met forms, mutated in the kinase domain with both leading to high Met phosphorylation, constitute an ideal model with which to study Met-driven tumorigenesis. Our data confirm Met plays a role in cell transformation and tumorigenesis and underline the possibilities that the use of Met-specific TKIs may represent a valuable strategy for cancer therapy. However, I also have been able to show that one of the mutants is resistant to various TKIs used, emphasising the importance of developing new TKIs or new “types” of drugs that are Met specific. In addition, I have demonstrated that topical application is a novel and potentially advantageous way, of administering drug. This at least is true for preclinical studies and it may be that such a screening system could be a useful way of evaluating efficacy against a broad range of Met mutations. Finally then another interesting aspect of my work is that I have identified and characterised a Met-driven tumorigenesis model that could be used to test the efficiency of any drugs on any Met mutant.

### **Activation of Met mutants**

I showed that, in absence of the ligand, the Met mutants D1246N and M1268T are highly activated as compared to Wt Met and that HGF enhances their activation. These results are in accordance with the literature<sup>156,174</sup>. Thanks to the recent availability of antibodies specifically recognising the different Met phosphorylated tyrosines, I was able to

dissect out the Met mutants' phosphorylation status, more precisely than previously reported in different studies relying on Met immunoprecipitation and blotting with a pan anti-phosphotyrosine antibody. I notably showed that D1246N and M1268T Met mutants are both significantly more phosphorylated on tyrosines located within the kinase domain and the docking site than is Wt Met. The NIH3T3 cells used in my studies produce a low amount of HGF<sup>156</sup>, which suggests that the Met phosphorylations that I have detected are constitutive. Consistent with this, Jeffers et al previously excluded the existence of an autocrine activation loop using a chimeric Met receptor composed of the extra-cellular domain of the Nerve Growth Factor (NGF) fused to the mutated intracellular domain of Met. By expressing this chimera in NIH3T3 cells (which do not secrete any NGF), they showed that the cells were highly tumorigenic *in vitro* and *in vivo*, more than those expressing a chimera made with the intracellular domain from the Wt form of the receptor<sup>174</sup>. This demonstrated that the transforming potential of Met mutants is due to the intrinsic properties of the mutated receptors.

### **No requirement for HGF binding for alteration of various cell functions**

Although it has been claimed that the transformation mediated by Met mutants is ligand-dependent<sup>190,269</sup>, most studies agree on there being a ligand independency for this characteristic<sup>156,174,191</sup>. We found in our model that, in the absence of exogenous HGF, cells expressing the Met mutants exhibited a transformed morphology, with a dedifferentiated shape,

exhibited a higher migratory capacity and had an enhanced survival potential compared with cells expressing Wt Met. Consistent with our data, the introduction of the M1268T and D1246N mutations in RON, another member of the Met subfamily, confers on the mutated receptor a transforming potential. Notably it became highly phosphorylated and highly tumorigenic *in vitro* in the absence of its ligand, the Macrophage Stimulating Protein (MSP), thus confirming that the ligand is not necessary for cell transformation<sup>270,271</sup>. An unresolved question is whether Met mutations alone can promote tumorigenesis *in vivo* in “HGF free” conditions. Our lab may investigate this in the future. Murine HGF cannot stimulate Human Met<sup>219,224,272</sup>. Thus, human cells expressing a Human Met (either Wt or mutated) could be grafted subcutaneously into immunoincompetent mice. In such a situation the murine HGF secreted by the tumoral environment would not be able to influence tumour development. We would then be able to determine the role played by activated Met mutants alone in tumorigenesis without the confounding influence of concurrent HGF stimulation.

**Different mutants, different TKIs, and the importance of characterising the sensitivity of each mutation: typing cancer patients to optimise therapies**

According to the literature, aberrant activation of Met, through activating mutations, can positively influence tumorigenesis. More generally, primary or secondary mutations in RTK frequently constitute a key event in cancer

progression and are one of the most important causes of failure in tumour responses to TKI<sup>237,248</sup>.

### ***Distinct Met mutations sensitivity to the same TKIs***

We have evaluated the sensitivity of two oncogenic Met mutations, D1246N and M1268T, to three specific Met inhibitors, PHA-665752, SU-11274 and PF-2341066. These two mutations were first identified in PRC<sup>168</sup> but the M1268T mutation was also detected in Head and Neck Squamous Cell Carcinomas<sup>176</sup> and in Childhood Hepatocellular Carcinomas<sup>175</sup>. We found that the M1268T Met mutant is sensitive to all three of the compounds tested. PF-2341066 was previously described as being efficient in inhibiting the activity of the M1268T Met mutant<sup>238</sup>. However, this conclusion was drawn based only on *in vitro* kinase assays on a recombinant or immunoprecipitated Met in a test tube and no data on the potency of PHA-665752 have been described. Moreover, I have established that the D1246N mutant is resistant to three of the TKIs that we tested and this had never been reported before.

Interestingly, these mutations both are activating mutations located in the kinase domain of the receptor though their location within this region is different. While M1268T is located in the P+1 loop, the D1246N mutation affects the activation loop (A loop)<sup>186</sup>. This suggests that the efficiency of TKIs could depend on the location of the mutation within the kinase domain. This hypothesis is reinforced by a study demonstrating that distinct single-points mutations within the kinase domain lead to different conformational changes of the receptor<sup>167,186</sup>. Indeed, analyses of these

structures showed that the D1246N mutation contributes to the stabilisation of the active conformation of the enzyme while the M1268T mutation favours its active form by destabilising the inhibitory position of the A loop<sup>186</sup>. These structural modifications could affect differentially the accessibility of the drug to Met, thus explaining the difference in the sensitivity of the different mutants. In accord with this hypothesis, the three TKIs tested in our study, all of which are ATP-competitive molecules, should bind to Met in a similar manner. This similarity in mode of action could explain why none of them is efficient against the D1246N mutation and why all of them affect the M1268T mutant. Interestingly, the analogous D1246N mutation in the Kit receptor, D816Y/V, confers resistance to the TKI, imatinib<sup>252</sup>. This suggests that the same mutation at the corresponding-amino-acid position in other RTKs may predict TKI sensitivity or resistance. Had I had more time available I might have tested this possibility using a larger panel of cell lines.

This variability, in terms of sensitivity to a given drug of the different Met mutants and the resistance to Met TKIs that could be encountered in tumours harbouring Met mutations, leads to at least three important conclusions. First, new compounds have to be developed to overcome the different mechanisms of resistance. Second, all the drugs should be tested systematically both *in vitro* and *in vivo* against all the different mutants identified in human cancer prior to entrance into any clinical trial. Third, patients should be screened before starting any treatment in order to match a certain mutation to its most effective inhibitor (when ever possible). This systematic approach would help to avoid sub-optimal

clinical trials in which patients are treated with a drug which is inefficient against the mutated receptors expressed by their autochthonous tumour cells.

### ***Drug dose efficiency***

#### Difference in sensitivity to TKIs between Wt and mutated Met

I have tested, for the first time, the ability of both PHA-665752 and PF-2341066 to inhibit *in vivo* tumorigenesis of cells expressing these two mutations.

I showed that a dose of 50mg/kg of PF-2341066, administered *per os*, induced a significant reduction of 60% ( $P < 0.05$ ) in the size of tumours derived from M1268T-expressing cells as compared to diluent controls. In previous studies, this dose resulted in a total blockade of Met dependent tumour growth<sup>238</sup>, and 50% of inhibition was obtained with a dose of only 12.5 mg/kg<sup>240</sup>. Models used in these studies were different from ours. They used cell systems in which Met is not mutated, for example the UM-22B HNSCC cell line<sup>240</sup> or cells with constitutively activated, although not mutated, Met. For instance, GTL-16 gastric carcinoma cells express constitutively activated Met as a consequence of Met amplification<sup>238</sup>. U87MG glioblastoma cells are also expressing the activated form since Met in these cells is activated *via* an autocrine secretion of HGF<sup>238</sup>.

The origin of the discrepancy in the efficiency of the drugs between these different models is difficult to explain. It might simply be due to the fact that the mutated receptor is more difficult to inhibit than the activated Met, due to conformational changes for example. Nevertheless, these observations

highlight the importance of testing the potency of each TKI against all the different Met mutants, and determining the efficiency of these drugs in *in vivo* models and not only in *in vitro* assays.

#### Balance between drug potency and drug selectivity

In our *in vivo* experiment of topical application, where the two molecules were given *via* the same route and with the same solvation vehicle, PHA-665752 seemed more potent in its activity than PF-2341066, even though the dose used for PF-2341066 was higher (0.2  $\mu$ M versus 0.1  $\mu$ M) and its published IC<sub>50</sub>, evaluated on Wt Met, smaller (4 nM versus 9 nM)<sup>233,239</sup>. Thus, although PF-2341006 was reported to be more Met specific than PHA-665752<sup>239</sup>, it seems less potent to inhibit M1268T Met mutant activity in our model.

A similar observation has been made about PF-2341066 and PF-4217903 in the literature<sup>241</sup>; PF-4217903 is highly Met selective and is even more specific than PF-2341066. However, although these two compounds present the same potency against Wt Met, they display differences in their ability to inhibit the activity of diverse Met mutations. In fact, PF-4217903 seems less potent and less able to hamper Met mutations as compared to the activity of PF-2341066.

Together these results suggest that increasing the selectivity of the TKI might decrease its potency to inhibit activating mutations. If this is the case, then it may imply that a balance between selectivity and potency against mutations has to be taken into account for the generation of new TKIs<sup>241</sup>.

## **Met specific TKIs and angiogenesis**

We have demonstrated that the three TKIs tested abolish the constitutive phosphorylation of the M1268T Met mutant efficiently. This correlates with a decrease in cell survival, which probably accounts for most of the reduction in tumour growth observed in our *in vivo* model under TKI administration. However, a direct effect of the drugs on Met expressed by tumour cells does not exclude an indirect action on the local environment of the tumour, most notably the possibility that the inhibitors are working through an effect on angiogenesis.

The HGF/Met axis promotes angiogenesis by modulating different processes. HGF can, for example, directly promote the migration and proliferation of endothelial cells<sup>147,273</sup>. HGF can also act indirectly, by promoting VEGF production by both endothelial and tumour cells<sup>274,275</sup>. The involvement of Met in the vascularisation process was reported also in different studies in which blocking Met activity with an HGF neutralising antibody<sup>220</sup>, decoy Met<sup>223</sup> or specific inhibitors, such as PHA-665752 or PF-2341066, were found to inhibit angiogenesis<sup>166,236</sup> predominately by affecting endothelial cell migration and tubulogenesis<sup>238</sup>. Moreover, in an *in vivo* matrigel xenograft tumour model, PHA-665752 and PF-2341066 treatments resulted in a dramatic reduction in the number of intra-tumoral cells expressing CD31, a specific marker of endothelial cells. In this system, PHA-665752 treatment decreased the production of VEGF while increasing the production of the angiogenesis inhibitor Thrombospondin-1<sup>236</sup>.

All of these data, associated with the presence of an important network of blood vessels infiltrating the tumour in our model (data not shown) suggest that the anti-tumour effect of PHA-665752 and PF-2341066 could result, in part, from their action on angiogenesis. Should such an activity be a possible explanation for our *in vivo* results, we can at least exclude a major role for a direct inhibition of Met in endothelial cells. For example, if Met-dependent signalling in endothelial cells was necessary for tumour growth, the drug treatments used should also affect the growth of the tumour in mice grafted with the D1246N mutant-expressing cells. We obtained good inhibitions *in vitro*, where the tumour cells are cultured alone, suggesting that the prime activity was against these transformed cells.

PHA-665752 and PF-2341066 nevertheless could block angiogenesis indirectly, by inhibiting Met-dependent VEGF production by tumour cells. It would be interesting to evaluate the contributions of angiogenesis in our tumour model and to determine if PHA-665752 or PF-2341066 treatments have an impact on the formation of new blood vessels by, for example, inhibiting the production of pro-angiogenic factors, or by enhancing the secretion of anti-angiogenic molecules. In line with the different ongoing clinical trials, it also would be of interest to compare the impact on tumour growth of blocking only Met or of neutralising both Met and the VEGFR. XL880, a new compound from Exelixis (**Table 4**), currently is being tested in clinical trials (Phase I and II) and is capable of antagonising the two receptors<sup>218</sup> such that it would be a very good reagent with which to address this question in my model system .

Compound		Mechanism of action			Inhibition of Met activation			Phase of development	Ref
Name	Company	Targets	Mode	IC50 wt Met	HGF-dependent	HGF-independent	Mutant		
BMS-777606	Bristol-Myers Squibb	Met, Ron, Axl, Tyro-3, Mer	ATP competitive	3.9 nM <sup>1</sup> 100 nM <sup>2</sup>	Yes	Yes	No data	Phase I (various tumours)	245
XL880 GSK1363089	Exelixis/GSK	Met, VEGFR2, Tie2, RON, c-Kit, PDGFR	ATP competitive	0.4 nM <sup>1</sup> 21-23 nM <sup>2</sup>	Yes	Yes	Yes, D1246N, M1268T, Y1248C	Phase I (various tumours) Phase II (papillary renal, gastric, head & neck)	284
XL184	Exelixis	Met, VEGFR2, Ret, c-Kit, Flt3, Tie2	ATP competitive	No data <sup>1</sup> No data <sup>2</sup>	Yes	Yes	Yes, D1246N, M1268T, Y1248C (preliminary data)	Phase I (various tumours) Phase II (glioblastoma, NSCLC) Phase III (medullary thyroid)	245
MP470	SuperGen	Met, c-Kit, Flt3, PDGFR, AXL	ATP competitive	No data <sup>1</sup> No data <sup>2</sup>	Yes	Yes	No data	Phase I (various tumours)	14, 245
MGCD265	MethylGene	Met, VEGFR1-3, Tie2, Ron, c-Kit, Flt3	ATP competitive	No data <sup>1</sup> nM range <sup>2</sup>	Yes	Yes	No data	Phase I (various tumours)	245
MK-2461	Merck	Met, VEGFR2, Flt1, 3, 4, FGFR1-3	ATP competitive	No data <sup>1</sup> No data <sup>2</sup>	Yes	Yes	No data	Phase I completed (various tumours)	245

<sup>1</sup>In vitro kinase assay, <sup>2</sup>cell-based assay

Table 4: Broad spectrum kinase inhibitors

## **New perspectives**

### ***TKIs with a new binding mode***

To overcome the mechanisms of resistance, the design of new compounds with different binding modes is necessary and such an approach could bring major clinical benefits. Amgen already have started to engineer such a novel generation of Met small-molecule inhibitors<sup>276,277</sup>. In a recent study, Bellon et al compared the binding mode of AM7 (Amgen), a new orally bioavailable Met-specific TKI, to SU-11274. When they superimposed the crystal structure of the two compounds interacting with the unphosphorylated form of the receptor, they observed only a partial overlap. Although the two molecules bind to the kinase linker, they occupy totally different areas of the kinase domain<sup>276</sup>. Interestingly, these differences in binding modes are translated into efficiency of inhibition. The new compound is effective against the D1246N mutant that we found resistant to the three different TKIs we tested. Interestingly this new Met specific inhibitor could inhibit tumour growth in both HGF-dependent and HGF- independent xenograft models<sup>276</sup>.

### ***Multitargeting drugs***

In addition to the appearance of secondary mutation(s), the activation of another oncogene upon specific RTK inhibition, “oncogene switching”, could be the reason for observed acquired resistance<sup>278,279</sup> including that to Met TKI<sup>256</sup>. In addition, recent evidence has indicated that cooperations between the different receptors are common in RTK-driven malignancies<sup>280</sup>.

Thus, in order to overcome drug resistance, in parallel with the pursuit of improving the specificity of the inhibitors, the clinical evaluation of specific molecules able to target several RTKs recently has begun (this approach is via combined therapies or via the use of broad spectrum TKIs).

Trials (Phase I, II, III) with six broad spectrum TKIs (including inhibitions of Met, Ron, VEGFR1-3, Ret, Kit, Tie-2, PGFR and FLT-3) are ongoing **(Table 4)**.

TKIs that target both Met and VEGFR have emerged as a promising approach in term of combinations that notably inhibit tumour angiogenesis; a phenomenon known to contribute to and to be necessary, for cancer progression. Attempts to block tumour angiogenesis with VEGFR2 inhibitors have led to disappointing results<sup>281</sup>. One of the explanations for these failures could be that the Met/HGF axis can also promote angiogenesis and seems to act synergistically with the VEGFR2<sup>273</sup>. Therefore inhibiting Met and VEGFR in combination is a promising option to prevent angiogenesis and, in consequence, to slow down tumour progression by preventing the supply of oxygen and nutrients to the developing cancer<sup>282</sup>. The compound XL880 (Exelixis), targeting more specifically both Met and VEGFR2, currently is being tested in the clinic<sup>283,284</sup>.

### ***HSP90 inhibitors***

A recent study reported an indirect way to inhibit Met-driven tumours<sup>285</sup>. Because Met is a client for the Heat Shock Protein 90 (HSP90), it has been proposed that interfering with the activity of this chaperone molecule

could induce the degradation of Met. Based on this hypothesis, the authors established a protocol inducing a durable inhibition of Met and downstream signals of Met using an HSP90 inhibitor, 17-AAG (17-allylamino-17-demethoxygeldanamycin)<sup>285</sup>. This approach is a highly attractive theoretical option as the inhibition induced on downstream effectors with SU-11274 was not durable<sup>285</sup>. Indeed, upon SU-11274 treatment, even if Met phosphorylation was still blocked efficiently, downstream pathways of Met became reactivated. In contrast, this reactivation was completely prevented with 17-AAG<sup>285</sup>. These results suggested that this type of inhibitor should be tested in Met driven tumours.

### ***A new way for drug administration***

Based on the cell migration assay, PHA-665752 seemed to have greater inhibitor activity than PF-2341066 on cells expressing the M1268T Met mutant. In order to compare side-by-side the efficiency of these two drugs in an *in vivo* tumour growth assay, because PHA-665752 is not water soluble and cannot be administrated *per os*, we developed an alternative strategy to deliver the two compounds. Drugs were first diluted in DMSO and then applied topically, with a paintbrush, onto the skin over the tumour. Fairly soon after PHA-665752 applications, I observed a significant slow down in growth rate that was evident when the vehicle was applied alone.

This experiment demonstrated that these types of drugs can be delivered by topical application. This approach may be quite interesting as an assay

in preclinical studies and even possibly in the clinic for some tumours as it limits the whole body toxicity consequent to systemic application. Drug concentrations could be reduced using this approach. For example, PF-2341066, used at 50 mg/kg for a mouse of 20 g, required 1mg of compound. In contrast 100  $\mu$ l of PF-2341066 at 200 nM for topical application required only 9 $\mu$ g. Even though this method of delivery probably would be restricted to very specific types of cancers, most likely located in superficial areas of the body such as melanomas in which Met recently has been implicated as a major driver<sup>234</sup> and probably would be restricted to palliative rather than curative intent, it seems to me that there might be indications for evaluating this approach. Certainly however in preclinical graft systems, still the basis of most drug evaluations, such a route of delivery could be built into a screening approach.

### ***Preventing endosomal signalling***

An emerging concept recently reported in the literature could generate new avenues for anti-cancer drug development. It has been proposed that signalling events are regulated according to time but also to space<sup>115,116</sup>. This means, for example, that many receptors continue to signal after internalisation, this activity modulating qualitatively and/or quantitatively the signals delivered initially from the plasma membrane<sup>111</sup>. These observations imply that endocytosis should not anymore be considered as only a way of desensitisation and drugs that disturb signal localisation, like the ones, which disturb signal intensity, potentially could become new therapeutic agents (see **Fig. 9 in Introduction**). This particularly could be

true for Met, which requires endocytosis for full activation and optimal downstream signalling<sup>70,71,132</sup>.

In conclusion, the cell model I have used, NIH3T3 cells stably transfected with Met mutants in the kinase domain, is an ideal model with which to study Met dependent tumorigenesis. In addition to being a suitable model to evaluate the potency of different TKIs against Met mutations, it also could be used to elucidate the mechanisms of oncogenic Met which lead to cell transformation. The following part of my study has focused on this aspect. More precisely it has focused on the relevance of RTK endosomal signalling in cell transformation and examined whether the topical application, over the skin of the tumours, of agents which inhibit endocytosis, could represent a useful method for blocking tumour development.

## RESULTS - PART II

### A Direct Role For Met Endocytosis In Tumorigenesis

We showed (see Results -Part-I), that Met mutants are strongly activated under basal conditions and only the D1246N and M1268T Met mutants are highly tumorigenic *in vivo*. Indeed, tumours derived from cells expressing the Y1248C Met mutant, even if it was slightly more activated than the Wt Met, developed similarly to the Wt tumour derived cells. As recently reported in the literature, “spatio-temporal signalling” could modulate cellular responses<sup>41,132</sup> and Met was shown to require endocytosis for full activation and downstream signalling<sup>70,71</sup>. We therefore investigated whether the D1246N and M1268T Met mutants’ endocytic trafficking could play a role in their transforming abilities.

#### 1. The active D1246N and M1268T Met mutants accumulate in intracellular compartments

We first analysed Met localisation by immunofluorescence. In basal conditions, while Wt and mutated Met all were expressed at the plasma membrane (**Fig. 1A**), an intracellular punctate localisation of Met was observed in around 60% of the cells expressing D1246N and M1268T, whereas this pattern of distribution occurred in around only 35% of the cells expressing the Wt and the Y1248C Met ( $p < 0.05$  and  $p < 0.01$ ) (**Fig. 1A, B**). Thus, the mutants D1246N and M1268T were localised both at the plasma membrane (as unstimulated Wt) and inside the cell (as HGF

stimulated Wt). Colocalisation with phospho-tyrosine suggested that the D1246N and M1268T mutants were activated in these intracellular pools as well as at the plasma membrane. In contrast, phospho-tyrosine staining was weak in cells expressing the Y1248C and Wt Met (**Fig. 1A**). The Met specific TKI PHA-665752 totally abolished the phospho-tyrosine staining of the M1268T mutant expressing cells, confirming the phospho-tyrosine staining resulted from Met activity (**Fig. 1C**).

These data were confirmed using a biochemical “biotin surface removal assay”<sup>268</sup> allowing separation of cell surface from intracellular proteins. The different fractions (total, intracellular [= unbound] and surface [= bound]) were analysed by Western blot for Met and phosphorylated Met. Around 50% of the D1246N and M1268T mutants were in the intracellular fraction, where they were activated, as compared to 15% of Wt Met (**Fig. 1D, E**).

Thus a significant proportion of the D1246N and M1268T Met mutants are present in intracellular compartments, in a high-activated state, without HGF stimulation.

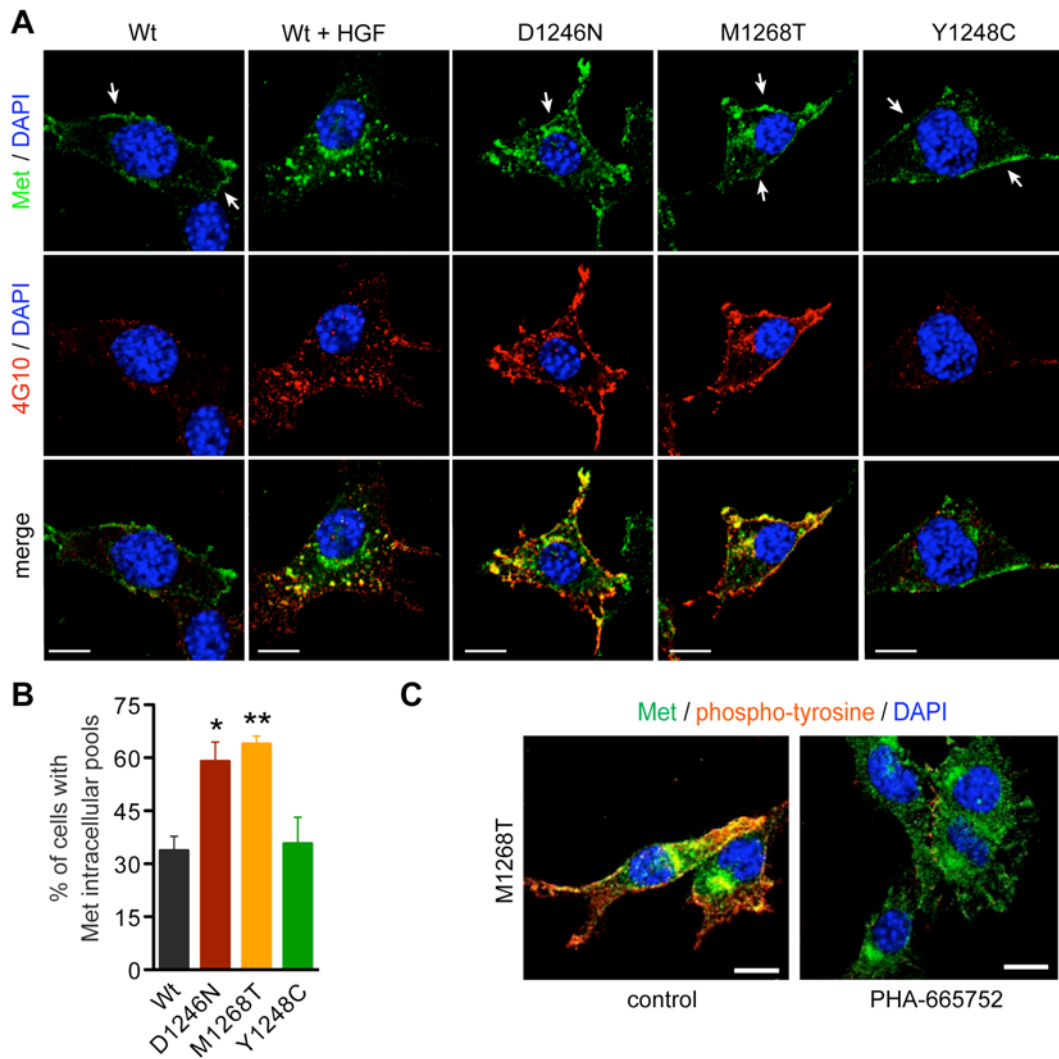


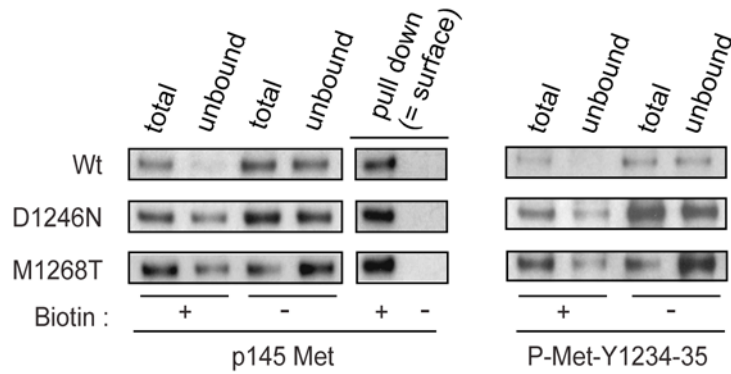
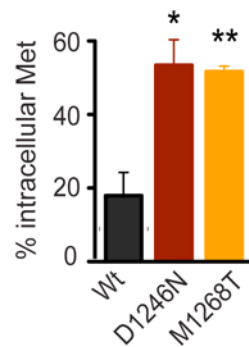
**Fig.1. The active D1246N and M1268T Met mutants accumulate in intracellular compartments.**

**(A)** Representative confocal sections of Wt ( $\pm$  HGF for 15 min), D1246N, M1268T and Y1248C Met expressing NIH3T3 cells stained for Met (green), phospho-tyrosine clone 4G10 (red) and DAPI (blue). Arrows show Met at the plasma membrane.

**(B)** Percentage (%) of indicated cells with observable Met intracellular pools obtained from three independent experiments.

**(C)** Representative confocal sections of M1268T Met expressing cells treated or not with PHA-665752 (PHA) for 90 min and then stained for Met (green) and phospho-tyrosine clone 4G10 (red) and DAPI (blue).

Scale bar: 10  $\mu$ M. \* $p < 0.05$ , \*\* $p < 0.01$ .

**D****E**

**Fig.1. The active D1246N and M1268T Met mutants accumulate in intracellular compartments.**

**(D)** Proportion of intracellular pools versus total cellular Met as determined from a biotin surface removal assay (see Materials and Methods). The indicated cells were surface-biotinylated and the surface protein fraction removed by streptavidin pull down. The total sample before pull down (Total), the supernatant corresponding to the intracellular fraction (Unbound) and the surface fractions (Bound) were analysed by Western blot for Met and phosphorylated Met (Y1234-35).

**(E)** Quantitation of **(D)**. The graph represents the percentage of intracellular Met calculated as a ratio to the total form and is the mean of three independent experiments.

\* $p < 0.05$ , \*\* $p < 0.01$ .

## 2. The D1246N and M1268T Met mutants shuttle between the plasma membrane and endosomes

We investigated whether the D1246N and M1268T Met mutants displayed modification in their trafficking compared to the Wt Met both under basal conditions and after stimulation with HGF. First, following incubation of cells with coupled-Cyanin3-transferrin (Cy3-transferrin), the D1246N and M1268T Met mutants, were found in transferrin positive vesicles to a greater extent (30% and 19% respectively) than non-stimulated Wt Met (8.6%) ( $p < 0.05$ ) (**Fig. 2A**). Next, after different times of cell incubation at 37°C, the rate of surface biotinylated Met internalisation was measured by streptavidin-agarose pull-down followed by Met Western blot (**Fig. 2B** top panel). After fifteen minutes of incubation, around 20% of the M1268T Met mutant had internalised (**Fig. 2B** top panel); a level similar to that of the Wt Met stimulated with HGF (**Fig. 2C**) while 10% of non-stimulated Wt Met had internalised ( $p < 0.05$ ) (**Fig. 2B** bottom panel). After five minutes of incubation, 14% of the D1246N Met mutant had internalised whereas only 3% of the Wt Met had internalised (**Fig. 2D**). These internalised Met molecules were phosphorylated (data not shown). Cy3-transferrin uptake was similar in all cells (**Fig. 2E**). Finally, the D1246N and M1268T mutants colocalised with EEA1 positive endosomes such as was seen with HGF-stimulated Wt Met (**Fig. 2F**). A significantly higher colocalisation between EEA1 (Early Endosome Antigen 1) and the D1246N (23%) (data not shown) and M1268T (19%) Met mutants was detected than it was for the Met Wt (9%) ( $p < 0.05$ ) (**Fig. 2F**). Taken together, these results indicated

that the activated D1246N and M1268T mutants internalise and are recruited to the EEA1 positive early endosome under basal conditions.

Met mutant colocalisation with transferrin (**Fig. 2A**) as well as localisation on endosomes and at the plasma membrane, unlike HGF-stimulated Wt visualised only on endosomes (**Fig. 1A, 2A, F, G and I**), suggested that some internalised Met mutants might recycle back to the plasma membrane. This indeed was the case as found by co-staining for the small GTPase Rab11. D1246N (data not shown) and M1268T Met colocalisation with Rab11 was 26% and 37.5% respectively as compared to 15% for Wt Met (**Fig. 2I**). In a biotin recycling assay, where the pool of biotinylated protein that had internalised (after 15 minutes of incubation at 37°C) was allowed to recycle back during cell re-incubation at 37°C post-internalisation (here 15 minutes), the proportion of the internalised M1268T Met mutant was reduced strongly compared with the Wt Met (**Fig. 2J**) indicating that it had recycled back. Potential degradation was excluded (**see Fig. 4B**).

Together, these data demonstrate that a proportion of the D1246N and M1268T Met mutants undergo a shuttling between the plasma membrane and the endosomes. These studies were conducted in the presence of cycloheximide, thus possible endosomal location of a neo-synthesised Met precursor or a mature form of Met in the endosomal secretory pathway were excluded as major alternative mechanisms.

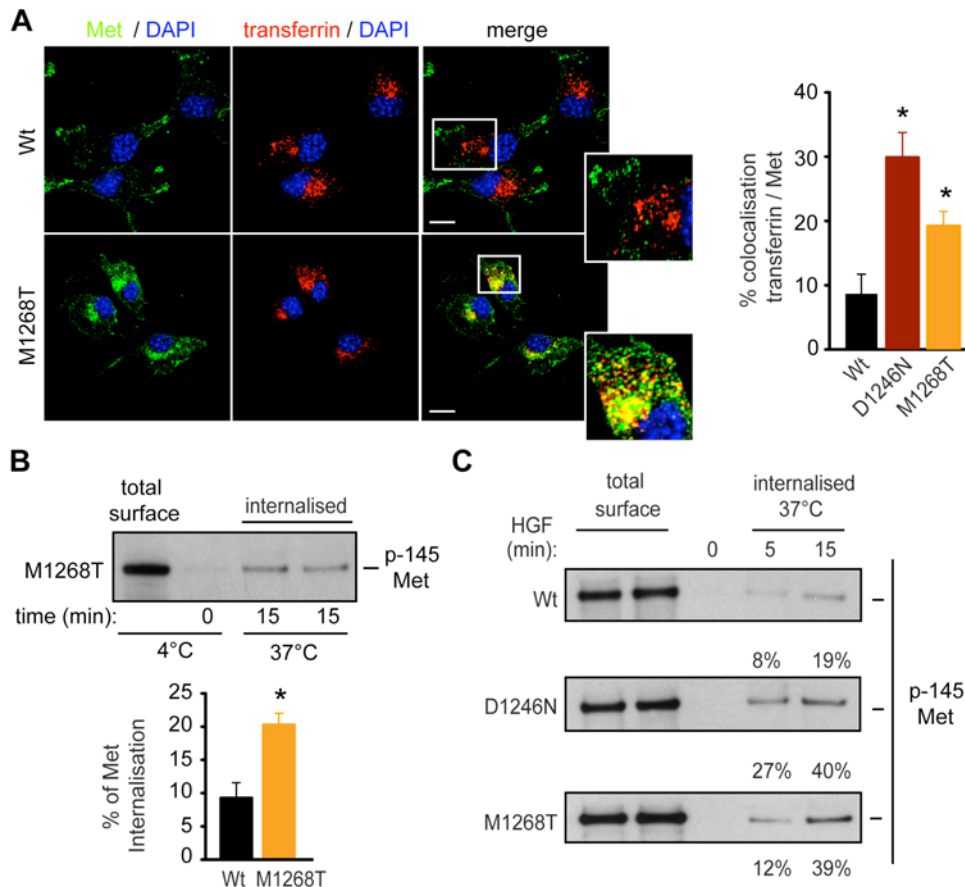


**Fig.2. The D1246N and M1268T Met mutants shuttle between the plasma membrane and endosomes**

**(A)** Confocal sections of Wt and M1268T Met expressing cells stained for Met (green), transferrin (red) and DAPI (blue). Indicated cells, pre-treated with cycloheximide for 4 hours (50 µg/ml), were incubated with Cy3-transferrin for 30 min before fixation. The graph represents the percentage of colocalisation in three independent experiments. Scale bar: 10 µM.

**(B-C)** Biotin internalisation assay. Surface biotinylated Wt and M1268T Met expressing cells were incubated for 15 min at 37°C **(B)** or for 5 and 15 min with HGF **(C)**. The biotin was cleaved and the remaining biotinylated Met (internalised) detected by Western blotting for Met (see Materials and Methods). **(B, bottom panel)** The graph is the quantitation of basal Met internalisation for Wt and M1268T from four independent experiments.

\*p<0.05.

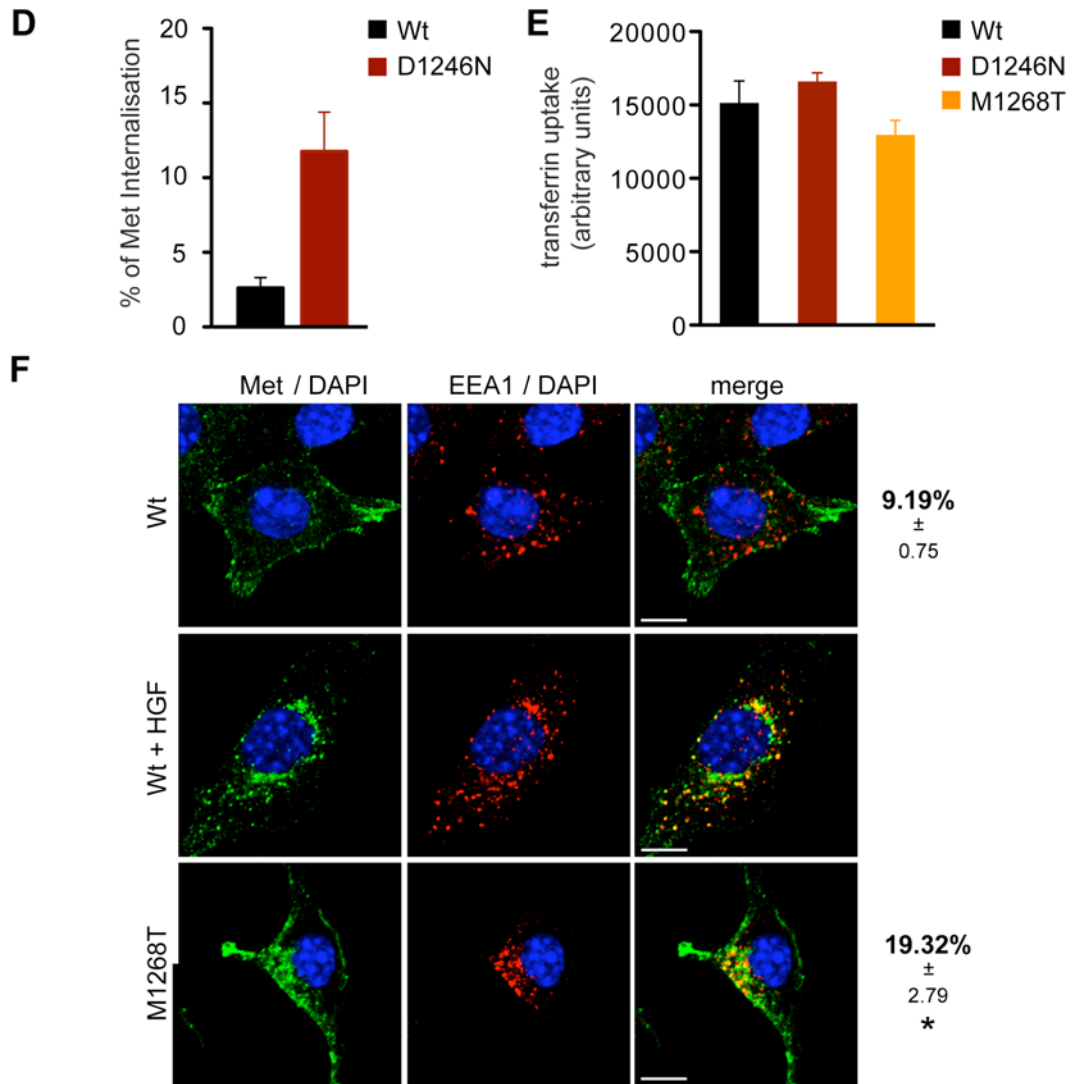


**Fig.2. The D1246N and M1268T Met mutants shuttle between the plasma membrane and endosomes**

**(D)** The graph represents the quantitation of Met internalisation for Wt and D1246N from two independent biotin internalisation assays. Surface biotinylated Wt and D1246N Met expressing cells were incubated for 15 min at 37°C.

**(E)** The graph represents the rate of Cy-3 transferrin uptake in the indicated cells, expressed in arbitrary units in 3 independent experiments.

**(F)** Confocal sections of Wt and M1268T Met expressing cells pre-treated with cycloheximide for 4 hours, stimulated or not with HGF and then stained for Met (green), EEA1 (red) and DAPI (blue). Numbers are the percentage of colocalisation obtained from three independent experiments. Scale bar: 10 μM.

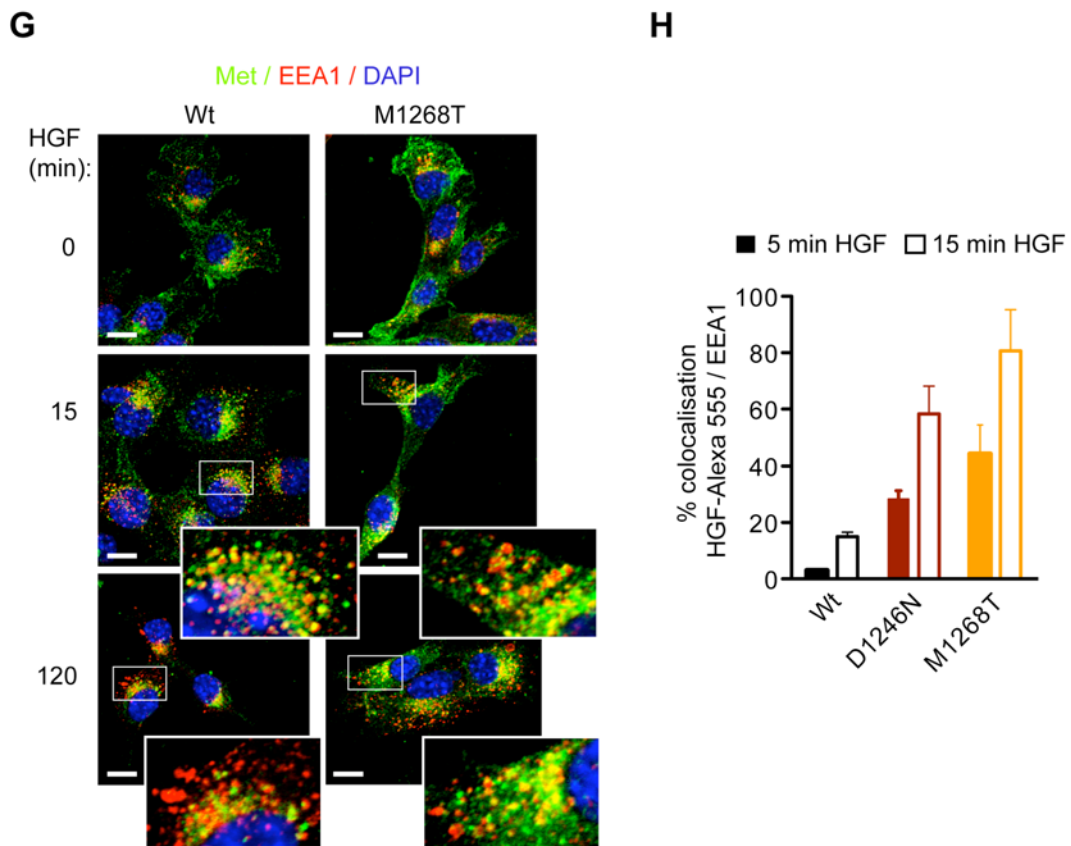


**Fig.2. The D1246N and M1268T Met mutants shuttle between the plasma membrane and endosomes**

**(G)** Confocal sections of Wt and M1268T expressing cells, stimulated with HGF for 0, 15 and 120 min and stained for Met (green), EEA1 (red) and DAPI (blue). Colocalisations appear in yellow. Scale bar: 10  $\mu$ M.

**(H)** Wt, D1246N and M1268T Met expressing cells were stimulated with HGF-Alexa-555 for, 0, 5 and 15 min then stained for EEA1 (image not shown). The graph represents the percentage of colocalisation between EEA1 and HGF-Alexa 555 at 5 and 15 min, determined using Metamorph software, from two independent experiments.

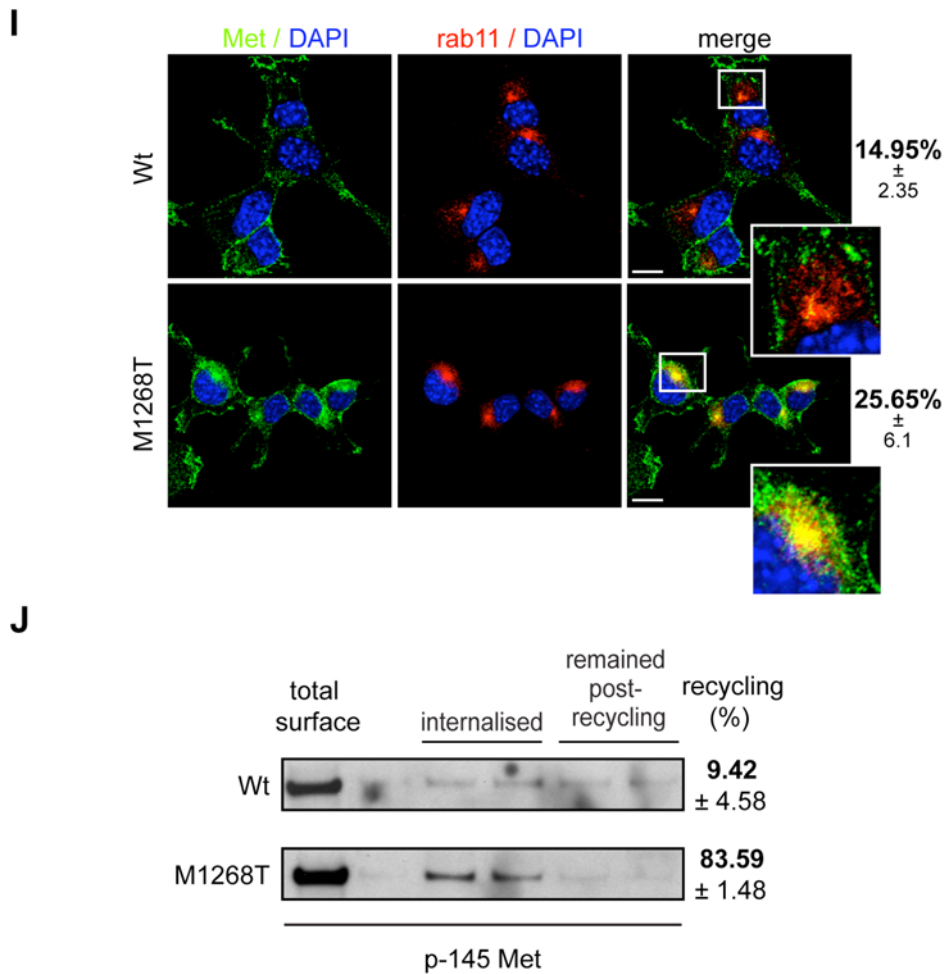


**Fig.2. The D1246N and M1268T Met mutants shuttle between the plasma membrane and endosomes**

**(I)** Confocal sections of indicated cells stained for Met (green), Rab11 (red) and DAPI (blue). Numbers represent the percentage of colocalisation from two independent experiments. Scale bar: 10  $\mu$ M.

**(J)** In the indicated cells, the level of internalised Met recycling was measured with a recycling biotinylation assay over a 30 min time course (15 min internalisation, 15min recycling) (see Materials and Methods). Numbers indicate the percentage of internalised Met that has recycled back to the plasma membrane, from one experiment.

### **3. Endocytosis of the D1246N and M1268T Met mutants is clathrin, dynamin and Grb2 dependent but independent of high activation status**

Investigation into the internalisation of the Met mutants was then performed using the following endocytic blockers: a dominant negative of dynamin (dynamin 2 K44A-GFP), the dynamin pharmacological inhibitors dynasore<sup>286</sup> and dynole 34-2<sup>287</sup> and Clathrin Heavy Chain (CHC) transient and stable knock down by RNAi and shRNA (**Fig. 3B**). All blockers inhibited HGF-Alexa 555 cellular uptake in all cells (**Fig. 3C-G**) and therefore, Met endocytosis<sup>71</sup> (**Fig. 3J**). Secondly all blockers inhibited the constitutive internalisation of the M1268T Met mutant. This is illustrated in **Fig. 3A** showing the blocking of the M1268T Met mutant internalisation by dynasore as measured by the biotinylation internalisation assay; **Fig. 3D and 3I** show the increase of the M1268T Met mutant at the plasma membrane and its decrease in intracellular pools in cells knocked down for CHC. These results confirmed that the intracellular accumulation of the Met mutants results from an increased endocytosis, which is dynamin- and clathrin-dependent.

It recently was reported that adaptor protein Grb-2-mediated interactions regulate clathrin-dependent endocytosis of Wt Met simulated by HGF<sup>122</sup>. Additionally, previous studies had reported a constitutive association of the D1246N and M1268T mutants with the adaptor Grb2<sup>191,193</sup>. We hypothesised therefore that Grb2 could be responsible for the enhanced endocytosis of the D1246N and M1268T Met mutants. Knocking down Grb2 (**Fig. 3K**) significantly reduced, by three fold, the constitutive

endocytosis of the M1268T Met mutant ( $P < 0.05$ ) (**Fig. 3L**). Co-immunoprecipitation studies confirmed that the M1268T Met mutant was associated constitutively with Grb2 (**Fig. 3M and 3N**). Thus Met mutants' clathrin endocytosis is mediated by the adaptor Grb2.

To investigate whether the Met mutants' constitutive endocytosis was the results of their increased level of activation, the rate of internalisation of the M1268T Met mutant was measured by biotin internalisation assay in cells treated with DMSO or PHA-665752. Surprisingly, reducing activation (assessed by phosphorylated Met Western blot) did not modify the level of endocytosis of the M1268 Met mutant, which remained at 20% (**Fig. 3O**).

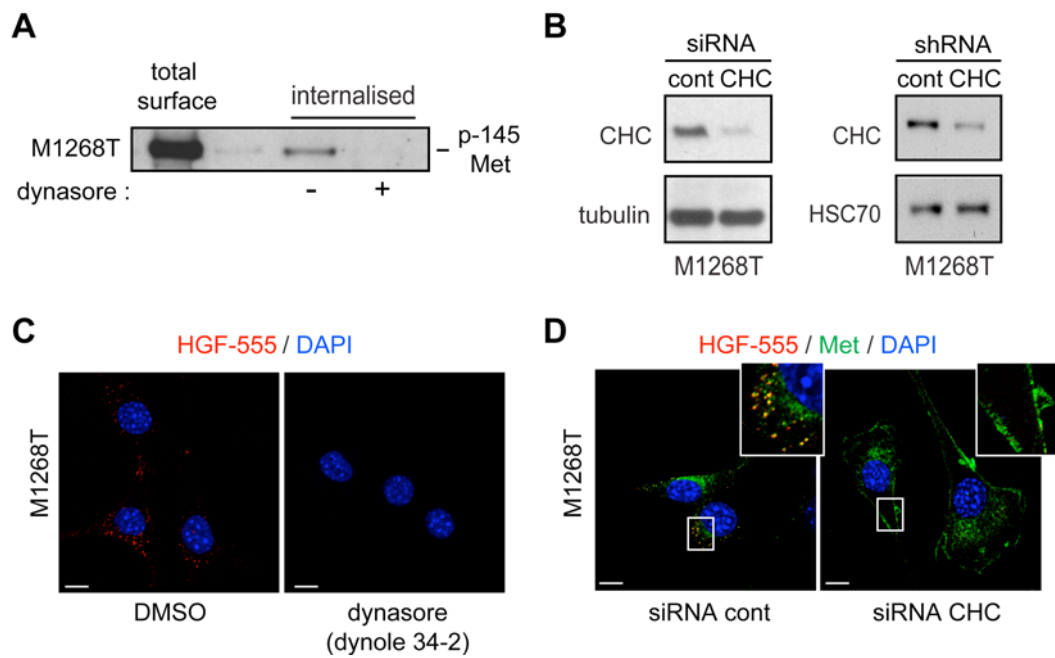


**Fig.3. Endocytosis of the D1246N and M1268T Met mutants is clathrin, dynamin and Grb2 dependent but independent of high activation status**

**(A)** Biotin internalisation assay (as in **Fig. 2B**) with M1268T Met expressing cells pre-treated with DMSO (-) or dynasore (+) (80  $\mu$ M) for 30 min.

**(B)** M1268T Met expressing cells were transfected with control or Clathrin Heavy Chain (CHC) siRNA or transduced with a control shRNA or CHC shRNA. CHC and tubulin or HSC70 Western blots are shown.

**(C-D)** Confocal section of M1268T Met expressing cells incubated with HGF-Alexa-555 (red) for 15 min then stained for Met (green) and DAPI (blue). **(C)** Cells were treated with DMSO, dynasore or dynole 34-2 prior to HGF stimulation. Pictures of DMSO and dynasore treated cells are shown. Dynole 34-2 gave the same results as dynasore (picture not shown). **(D)** Confocal section of M1268T Met expressing cells transfected for 3 days with control or CHC siRNA, incubated with HGF-Alexa-555 (red) for 15 min. Scale bar: 10  $\mu$ M.

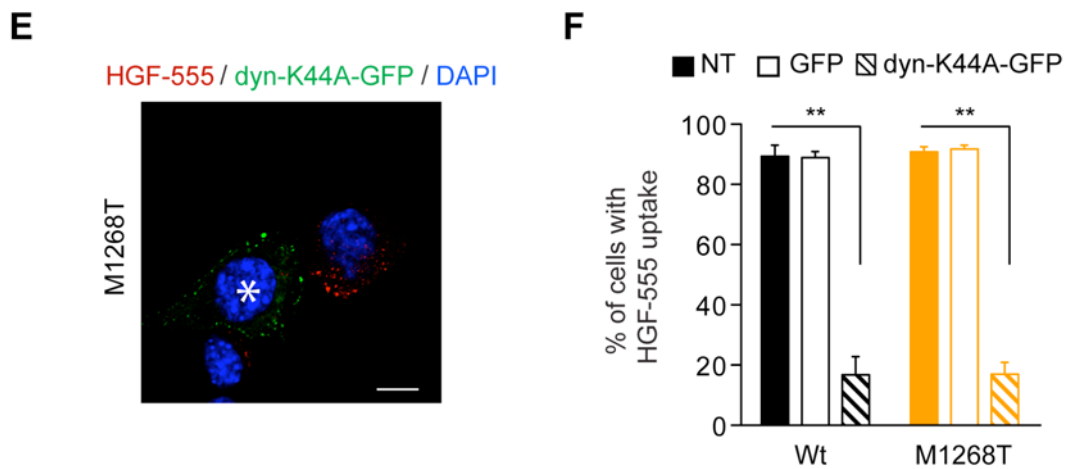


**Fig.3. Endocytosis of the D1246N and M1268T Met mutants is clathrin, dynamin and Grb2 dependent but independent of high activation status**

**(E)** Confocal section of M1268T Met expressing cells transfected for 24 hours with dynamin 2 K44-GFP (dyn-K44A-GFP), incubated with HGF-Alexa-555 (red) for 15 min.

**(F)** The graph represents the percentage of uptake of HGF-Alexa-555 in non transfected cells (NT), transfected with a GFP vector (GFP) or with a dynamin 2 K44-GFP (dyn-K44A-GFP) from three independent experiments. Scale bar: 10  $\mu$ M.

\* $p < 0.05$ , \*\* $p < 0.01$ .

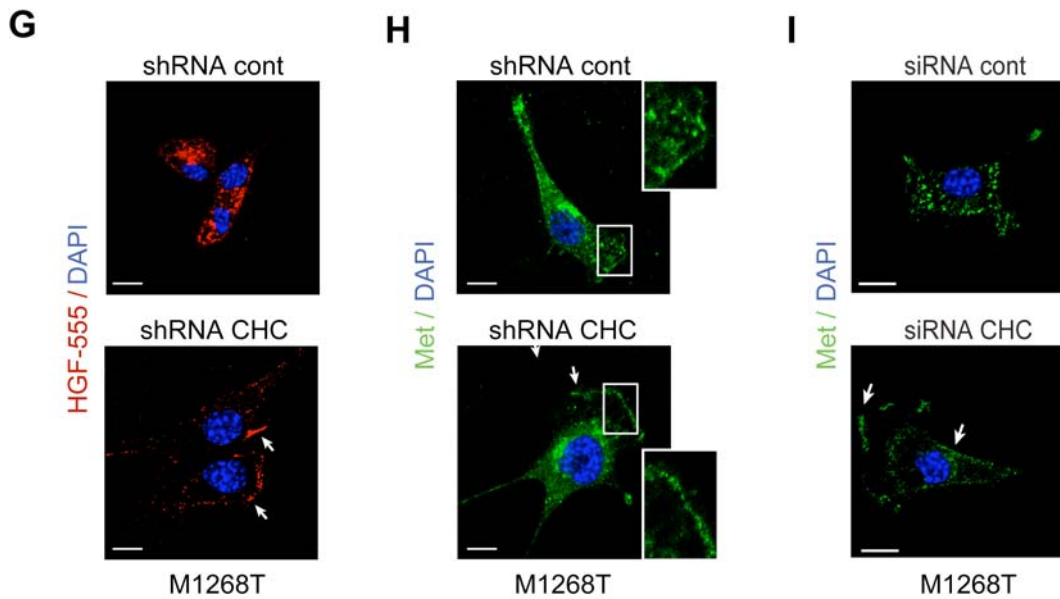


**Fig.3. Endocytosis of the D1246N and M1268T Met mutants is clathrin, dynamin and Grb2 dependent but independent of high activation status**

**(G-H)** M1268T Met expressing cells were transduced with control or CHC shRNAs. **(G)** Confocal sections of cells incubated with HGF-Alexa-555 (red) for 15 min. **(H)** Confocal sections of cells stained for Met (green) and DAPI (blue).

**(I)** Representative confocal sections of M1268T Met expressing cells transduced with control or CHC RNAs, stained for Met (green) and DAPI (blue). Scale bar: 10  $\mu$ M.

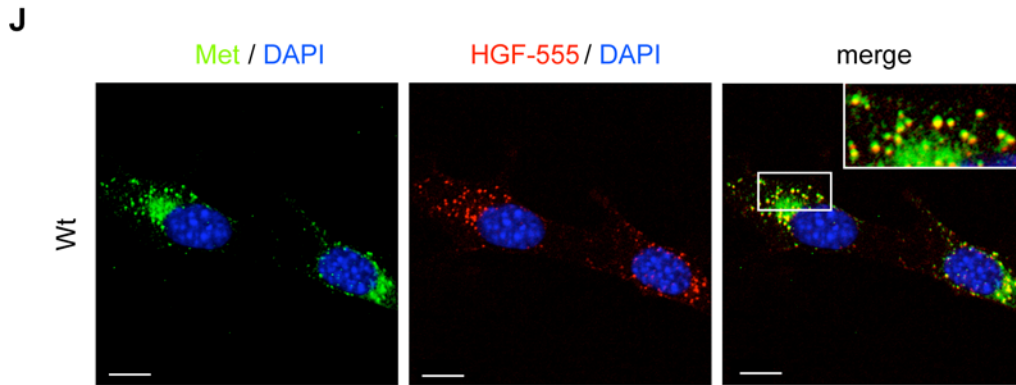


**Fig.3. Endocytosis of the D1246N and M1268T Met mutants is clathrin, dynamin and Grb2 dependent but independent of high activation status**

**(J)** Confocal sections of Wt Met expressing cells incubated with HGF-Alexa-555 for 15 min (red) stained for Met (green) and DAPI (blue). Scale bar: 10  $\mu$ M.

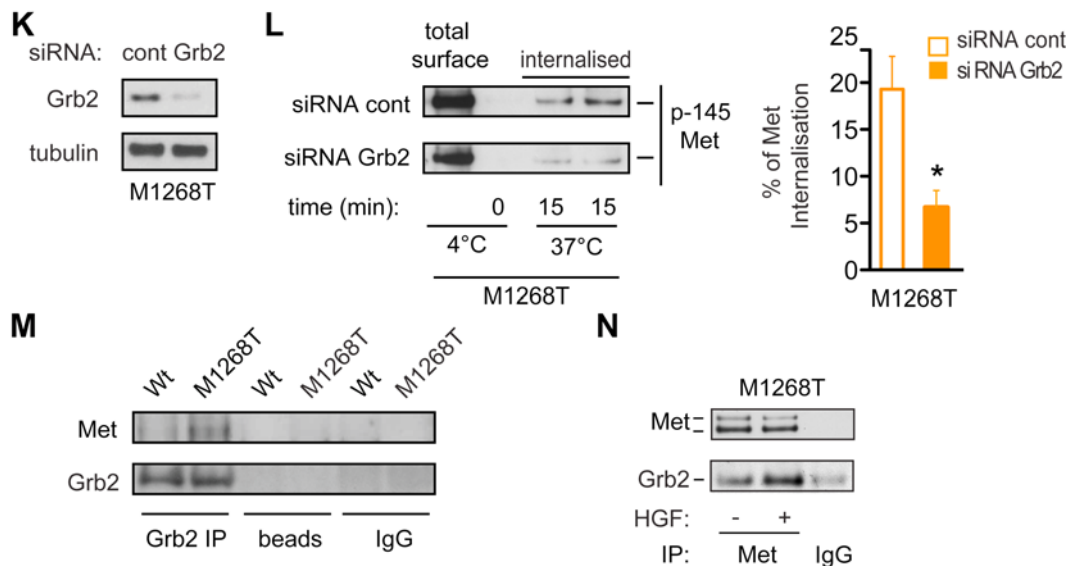


**Fig.3. Endocytosis of the D1246N and M1268T Met mutants is clathrin, dynamin and Grb2 dependent but independent of high activation status**

\*p<0.05

**(K-L)** M1268T Met expressing cells were transfected with control or Grb2 RNAs. Grb2 and tubulin Western blot are shown. **(L)** Biotin internalisation assay as in **(Fig. 2B)**. The graph represents the quantitation of Met internalisation obtained from three experiments.

**(M)** Grb2 immunoprecipitation (IP) from cells expressing Wt and M1268T Met expressing cells. Met and Grb2 Western blots are shown.

**(N)** Met immunoprecipitation (IP) from M1268T Met expressing cells. Met and Grb2 Western blots are shown.

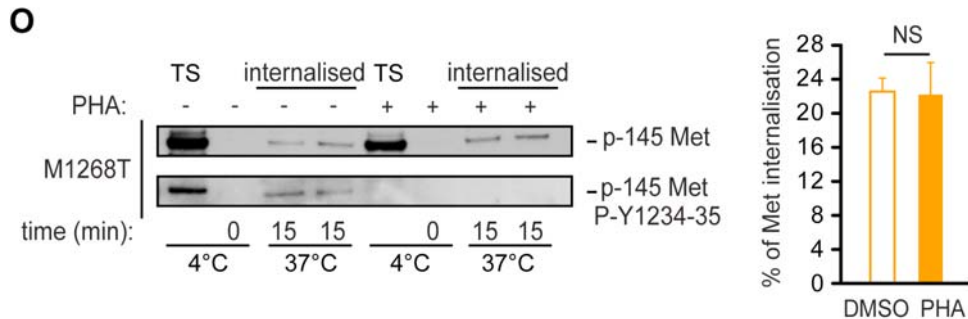


**Fig.3. Endocytosis of the D1246N and M1268T Met mutants is clathrin, dynamin and Grb2 dependent but independent of high activation status**

NS: non significant.

**(O)** Biotin Internalisation Assay. M1268T Met expressing cells were pretreated for 45 min (+), or not (-), with PHA-665752 (PHA), surface biotinylated and then incubated at 37°C for 15 min with (+) or without (-) PHA. The biotin was then cleaved, and the remaining biotinylated Met was analysed by Western blotting with an anti-Met or with an anti-phosphorylated Met (Y1234-35) antibody. The graph represents the percentage of Met internalisation from three independent experiments.

#### **4. The D1246N and M1268T Met Mutants present an impaired degradation due to HSP90 activity**

The recycling of the internalised M1268T Met mutant prompted us to analyse whether its degradation behaviour was modified. The expression levels of Wt Met and M1268T Met mutant initially present at the cell surface were analysed over time using a “biotin degradation assay”. The M1268T mutant degraded less than the Wt (**Fig. 4A**), indicating that its increased constitutive internalisation does not lead to an increased degradation but rather to a delay, consistent with its recycling back to the cell surface. As HGF stimulation normally induces a substantial degradation of endogenous Wt Met<sup>119</sup>, we speculated that differences in degradation rates between the Met forms would be more pronounced following HGF stimulation. First, Met protein levels were analysed by Western blot in lysates from cells pre-treated with cycloheximide allowing us to follow stability of the mature form of Met. Endogenous Met, in HeLa cells, is progressively degraded with only 20% of the initial Met expression after 8 hours of HGF stimulation<sup>119</sup>. We reproduced these results with Wt Met (**Fig. 4B**) indicating that our Wt Met behaves like endogenous Met in another cell system. In marked contrast, degradation of the D1246N and M1268T mutants was reduced dramatically, with a level of Met expression non significantly different between 0 and 8 hours of HGF stimulation. The Y1248C Met mutant had a degradation level statistically similar to that of the Wt Met (**Fig. 4B**). Analysis of HGF stimulated degradation of plasma membrane biotinylated Met revealed that, after 8 hours of HGF

stimulation, a substantial quantity of the M1268T Met mutant still was observed whereas Wt Met was undetectable (**Fig. 4C**).

These results indicate that the Met D1246N and M1268T Met mutants present an impaired degradation, thus contributing to their endosomal accumulation. Indeed, the M1268T mutant remained in EEA1 positive endosomes even after 120 minutes of HGF stimulation (**Fig. 2G**).

The defect in degradation does not result from an impaired endocytosis upon HGF stimulation (**Fig. 2C, G and H**) or from a defect in ubiquitination (**Fig. 4D-F**). In fact, if anything an increased ubiquitination level of the mutant over Wt Met was observed.

The molecular chaperone heat-shock protein 90 (HSP90) plays a key role in ensuring the correct conformation, stability, and activity of many oncogenic client proteins. Thus recent studies have reported that inhibiting HSP90 activity triggers the degradation of oncogenic RTKs, such as mutated RON<sup>288</sup>, mutated EGFR<sup>205,289</sup> and mutated Kit<sup>290</sup>. We hypothesised therefore that HSP90 activity might protect the Met mutants against degradation. Inhibiting HSP90 activity with the pharmacological compound 17-AAG (17-(Allylamino)-17 demethoxygeldana-mycin), or knocking down HSP90 isoforms  $\alpha$  and  $\beta$  (**Fig. 4G**), restored the Met mutant degradation to a similar level to that of Wt Met (**Fig. 4H**). Consistent with these results, co-immunoprecipitation studies detected HSP90 association with the M1268T mutant (**Fig. 4I**). These results indicate that the defect in degradation of Met mutants is not a consequence of defective ubiquitination but rather is dependent on HSP90 activity.

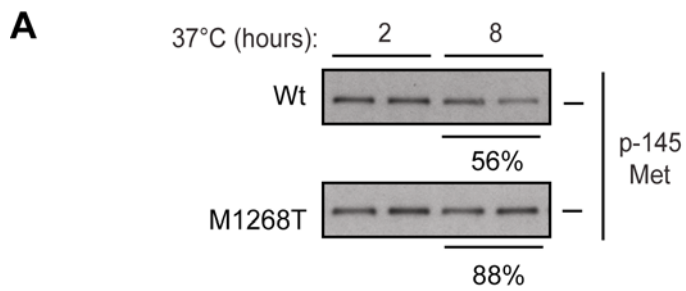


**Fig.4. The D1246N and M1268T Met Mutants present an impaired degradation due to HSP90 activity**

**(A)** Biotinylation degradation assay. Wt and M1268T Met expressing cells were surface biotinylated and then incubated at 37°C. At the indicated times, cells were lysed and the remaining biotinylated Met, after streptavidin pull-down, was analysed by Western blotting with an anti-Met antibody.

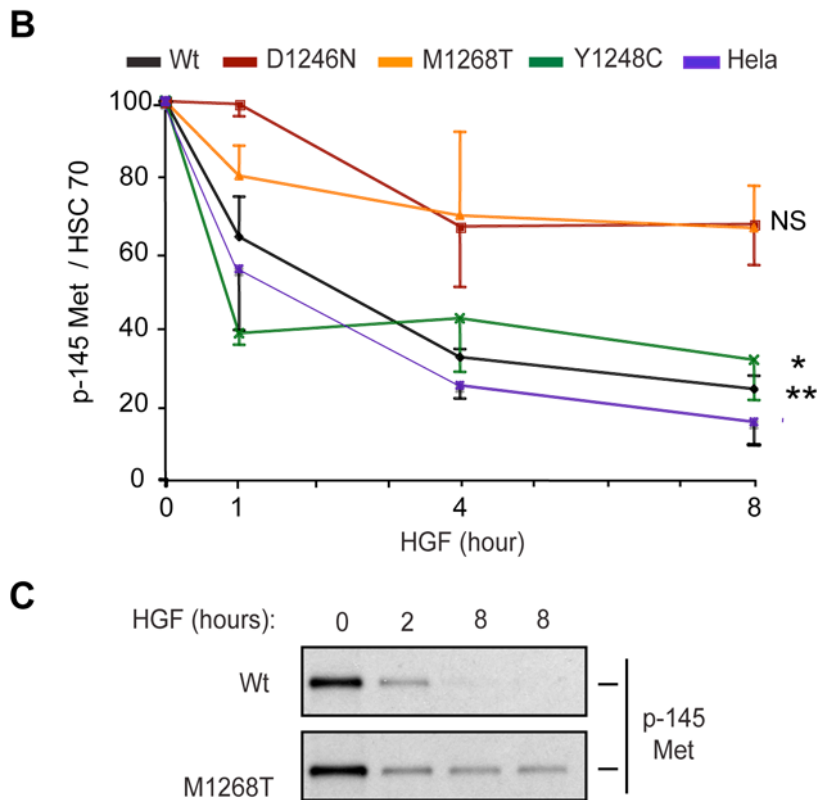


**Fig.4. The D1246N and M1268T Met Mutants present an impaired degradation due to HSP90 activity**

**(B)** Met / HSC-70 ratios obtained by densitometric analyses of Western blots from three independent experiments and plotted as the percentage of the initial content. Wt, D1246N, M1268T and Y1248C Met expressing cells and HeLa cells were pre-treated with cycloheximide (50  $\mu$ g/ml) for 15 min and stimulated with HGF for the indicated times.

**(C)** Biotin degradation assay. Indicated cells were surface biotinylated and incubated with HGF. At the indicated times, cells were lysed and the remaining biotinylated Met, after streptavidin pull-down, was analysed by Western blotting for Met.

\* $p < 0.05$ , \*\* $p < 0.01$ , NS: non significant, compared to  $t=0$ .

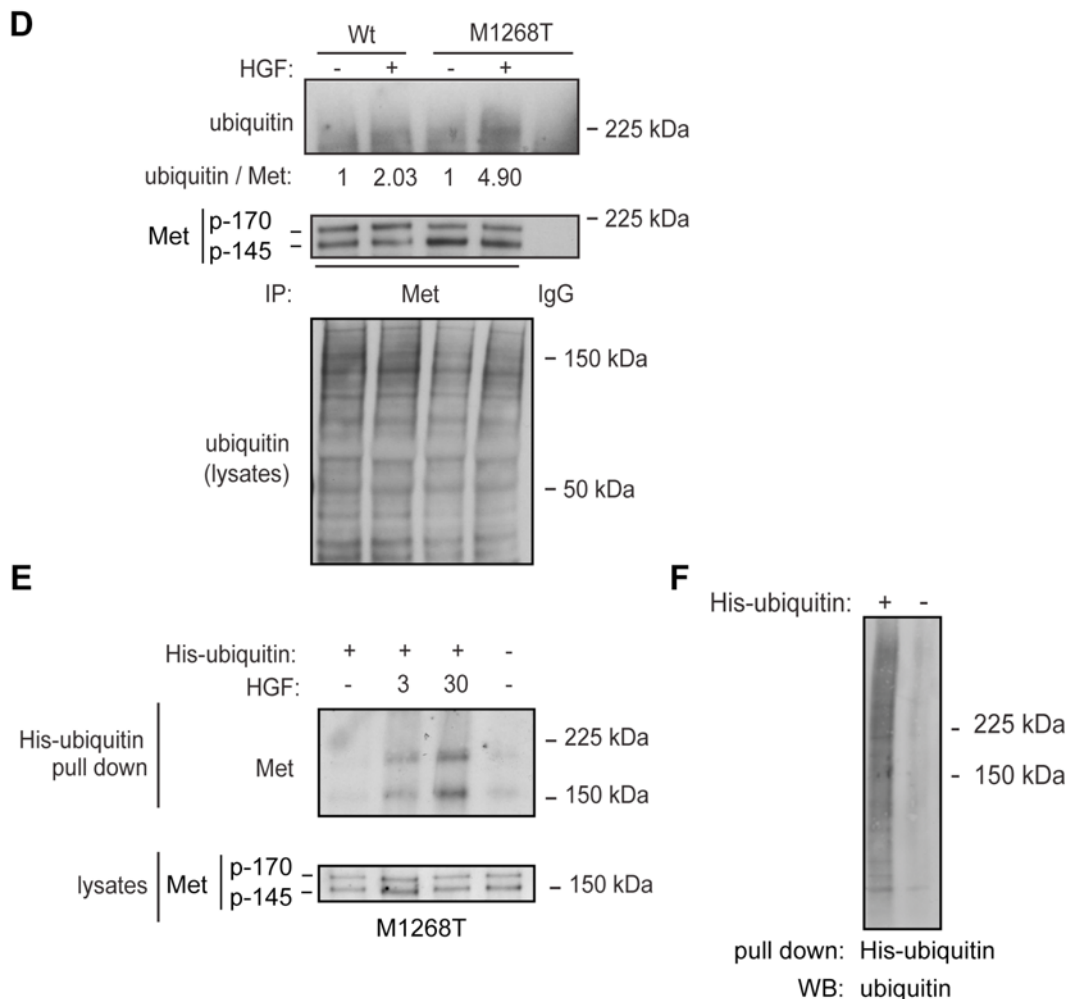


**Fig.4. The D1246N and M1268T Met Mutants present an impaired degradation due to HSP90 activity**

**(D)** The indicated cells were stimulated, or not, with HGF for 5 min, then lysed in SDS-boiling lysis buffer and subjected to Met immunoprecipitation (IP). Ubiquitin (upper panel) and Met (middle panel) Western blots from the immunoprecipitates and an Ubiquitin Western blot from the lysates (lower panel) are shown. The numbers represent the fold increase in Met ubiquitination upon HGF stimulation over no stimulation (Met ubiquitination was calculated as the ratio of the intensity of ubiquitin co-IP over the intensity of Met IP, obtained by densitometry).

**(E-F)** M1268T Met expressing cells were transfected with His-tagged Ubiquitin (+) or with empty vector (-), stimulated with HGF for 0, 3 and 30 min and subjected to His pull-down with Nickel-NTA-Agarose beads. Western blot for Met from pull downs and from total lysate are shown. **(F)** Western blot for ubiquitin from lysates is shown.

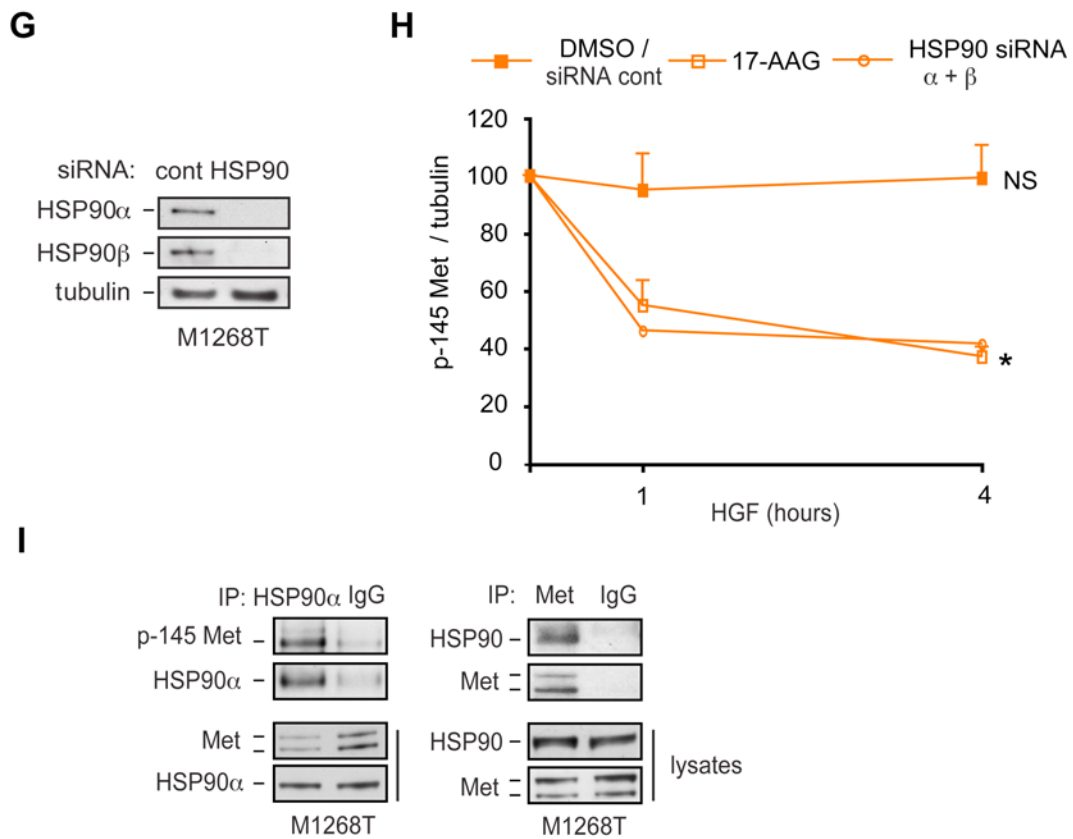


**Fig.4. The D1246N and M1268T Met Mutants present an impaired degradation due to HSP90 activity**

**(G)** Western blots for HSP90  $\alpha$ ,  $\beta$  and tubulin from M1268T Met expressing cells transfected with control or HSP90  $\alpha$  and  $\beta$  RNAs.

**(H)** Met / HSC-70 ratios obtained by densitometric analysis of Western blots and plotted as the percentage of the initial content. M1268T Met expressing cells treated with DMSO or 17-AAG (100 nM) or subjected to HSP90  $\alpha$  and  $\beta$  siRNA were pre-treated with cycloheximide (50  $\mu$ g/ml) and stimulated with HGF for the indicated times (three independent experiment were done with 17-AAG and one with HSP90 RNAi, each experiment was done in triplicate).

**(I)** Lysates from M1268T Met expressing cells were subjected to HSP90 alpha IP (left panel) or Met IP (right panel). Met, HSP90  $\alpha$  and pan HSP90 Western blot from IP or from total lysates are shown.

\* $p < 0.05$ , NS: non significant.

## **5. The D1246N and M1268T Met mutants require the endocytosis machinery to stimulate cell migration**

Endosomal accumulation of the active D1246N and M1268T Met mutants could be responsible for cellular outcomes. According to the change in morphology, such as reduced adhesion and rounded shape, described in **Results-Part I, Fig. 3A**, staining for paxillin revealed that the number of focal adhesions was reduced significantly in cells expressing the D1246N and M1268T Met mutants (**Fig. 5A**). The organisation of F-actin (visualised by phalloidin-Cy3 staining) was perturbed dramatically under basal conditions in cells expressing the D1246N and M1268T Met mutants (**Fig. 5C**), similarly to Wt cells upon HGF treatment (**Fig. 5D**). 60 to 78% of the D1246N and M1268T mutant expressing cells presented a disorganised actin pattern with no detectable stress fibres, while only 10 to 25% of the Wt and Y1248C mutant expressing cells presented a similar phenotype (**Fig. 5B**). In the M1268T mutant expressing cells, PHA-665752 significantly restored paxillin patches (**Fig. 5A**) and stress fibres (**Fig. 5B**), thus leading to a decrease in cells with actin disorganisation (**Fig. 5C**), confirming these phenotypes are due to Met activity. The D1246N mutant expressing cells did not respond to this treatment (**Fig. 5B, C**), consistent with no reduction of Met phosphorylation (**Results-Part I, Fig. 2B**).

Interestingly, decreasing Met mutant accumulation on endosomes, using endocytic blockers such as dynasore, expression of dynamin 2 K44A-GFP and CHC stable knock down (**Fig. 5E-H**) or impairing Grb2 function through knock-down or through expression of mutants in SH2 or SH3 domains (**Fig. 5I-J**) or inhibiting HS90 activity with 17AAG (**Fig. 5K**) led to

restoration of the stress fibres in cells expressing the D1246N and M1268T mutants.

Together, these results indicate that Met activation, increased internalisation and a defect in degradation, participated in the loss of actin stress fibres and that blocking endocytosis could overcome the resistance to inhibition by Met specific TKI (PHA-665752) of the D1246N mutant.

Decreased focal contacts, together with disorganised actin, likely participate in the high motility of the cells expressing the D1246N and M1268T mutants (**Fig. 5L** and see **Results-Part I, Fig. 3B**).

After 2 hours of incubation, at least three fold more D1246N and M1268T mutant expressing cells had migrated through the pores than had Wt cells or Y1248C mutant expressing cells (**Fig. 5L and 5M**). HGF stimulation further increased the migration of the D1246N and M1268T Met mutant expressing cells (**Fig. 5N**). Interestingly, all endocytic blockers (dynamamin 2 K44A-GFP, dynasore, CHC RNAi and shRNA) significantly reduced the increased migratory capacity of the D1246N and M1268T mutant expressing cells (**Fig. 5L, O**). The same blockers (PHA-665752, dynamamin2 K44A-GFP, CHC RNAi) did not reduce the migration of Wt or Y1248C cells (**Fig. 5L and 5P**). Interestingly, Grb2 knock down and HSP90 inhibition by 17AAG also reduced the migration of the M1268T and D1246N mutant expressing cells (**Fig. 5O and 5Q, R**). Clearly the D1246N and M1268T Met mutants regulate cell migration both through activation and accumulation on endosomes; and thus blocking endocytosis, unlike PHA-665752 (**Results-Part I, Fig. 3C**), efficiently blocked the migration of the D1246N Met mutant expressing cells.

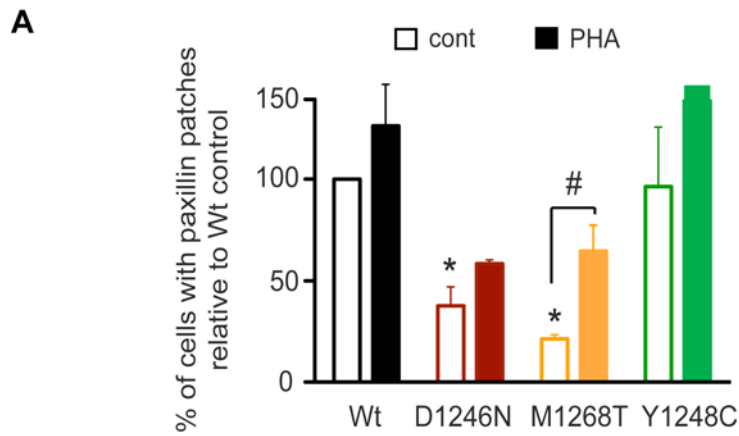


**Fig.5. The D1246N and M1268T Met mutants require the endocytosis machinery to stimulate cell migration**

**(A)** The graph represents the number of indicated cells showing marked patches of paxillin, determined on confocal pictures (not shown), counted in indicated cells treated with DMSO or PHA-665752 (PHA) for 30 min and presented as percentages from three independent experiments.

#, \*  $p < 0.05$ , \*\*  $p < 0.01$ , \*\*\*  $p < 0.001$ .

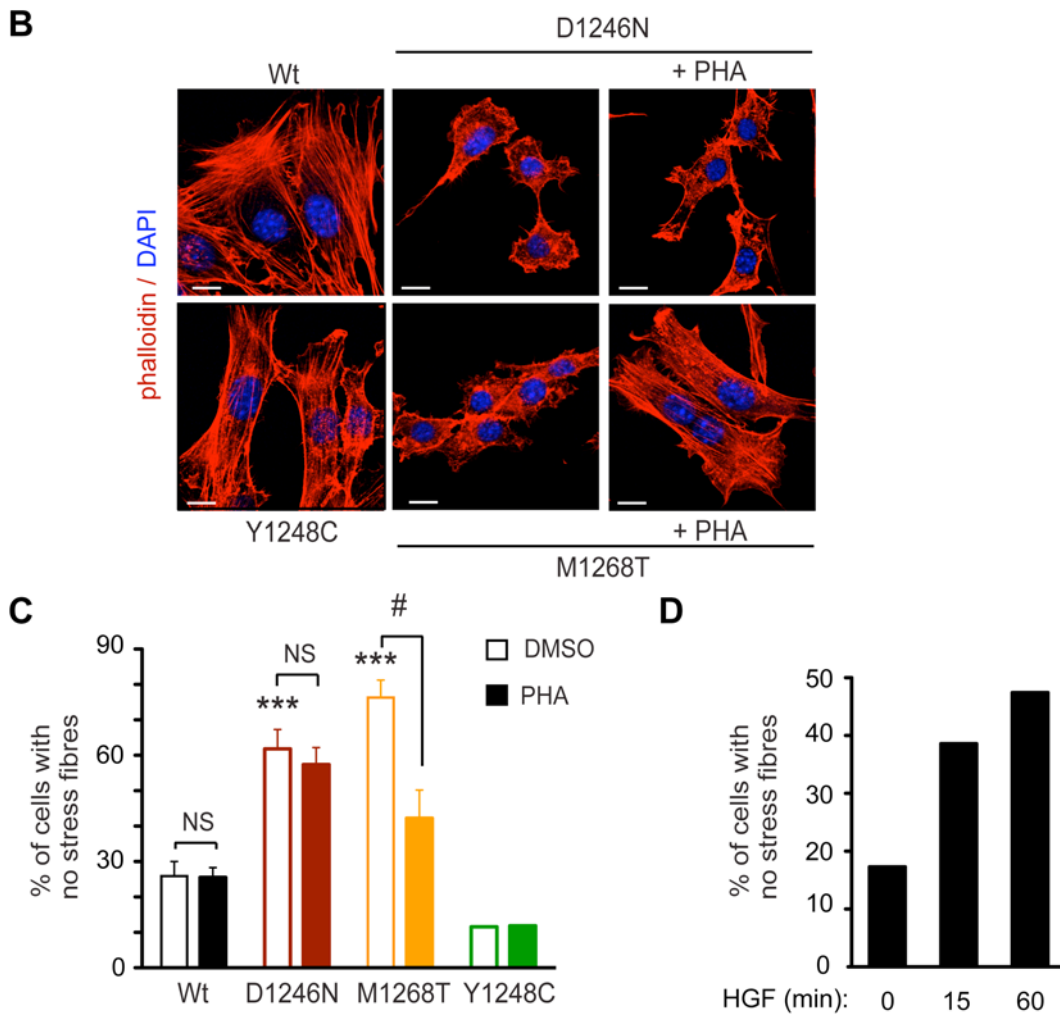


**Fig.5. The D1246N and M1268T Met mutants require the endocytosis machinery to stimulate cell migration**

**(B-D)** Indicated cells were stained with Cy3-phalloidin (red) and DAPI (blue). **(B-C)** Cells were treated with DMSO or PHA for 90 mins. **(B)** Representative Confocal sections. **(C)** The graph represents the percentage of cells with no stress fibres obtained from three independent experiments. **(D)** The graph represents the percentage of Wt Met expressing cells with no stress fibres upon HGF stimulation for 15 and 60 min. One experiment was performed. Scale bar: 10  $\mu$ M.

#, \*  $p < 0.05$ , \*\*  $p < 0.01$ , \*\*\*  $p < 0.001$ .

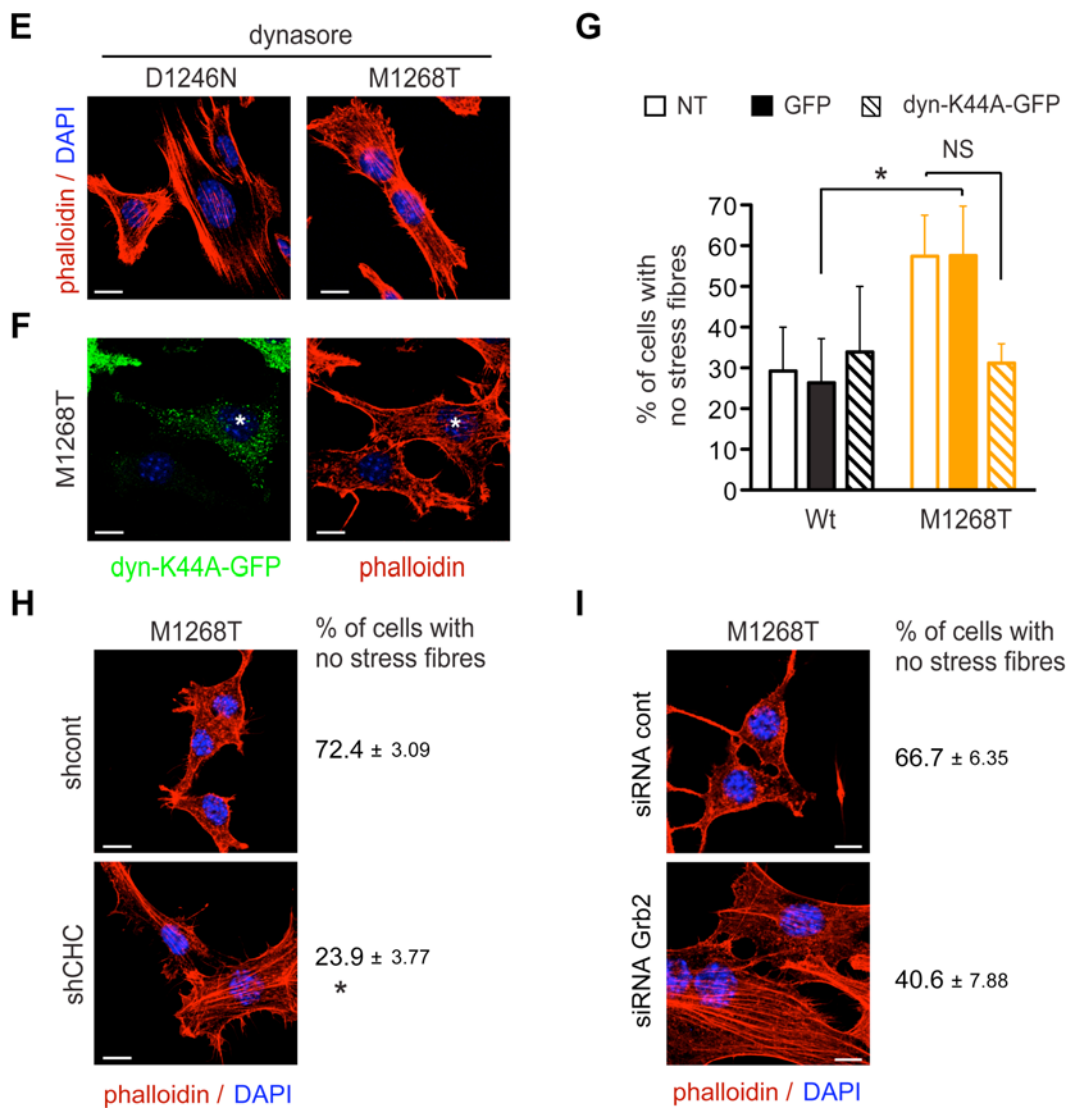


**Fig.5. The D1246N and M1268T Met mutants require the endocytosis machinery to stimulate cell migration**

(E-I) Indicated cells were stained with Cy3-phalloidin (red) and DAPI (blue). (E) Confocal sections of cells treated with dynasore for 90 mins. (F-G) Indicated cells were transfected, or not (NT), for 24 hours with GFP or GFP- dynamin 2 K44A dominant-negative mutant. (F) Representative confocal section. \* = transfected cell. (G) The graph represents the percentage of cells with no stress fibres in treatment groups as indicated from three independent experiments. (H-I) Confocal sections of M1268T Met expressing cells transduced with control or CHC shRNA (H) or transfected with control or Grb2 siRNA (I). Scale bar: 10  $\mu$ M.

\*  $p < 0.05$ , NS: non significant.

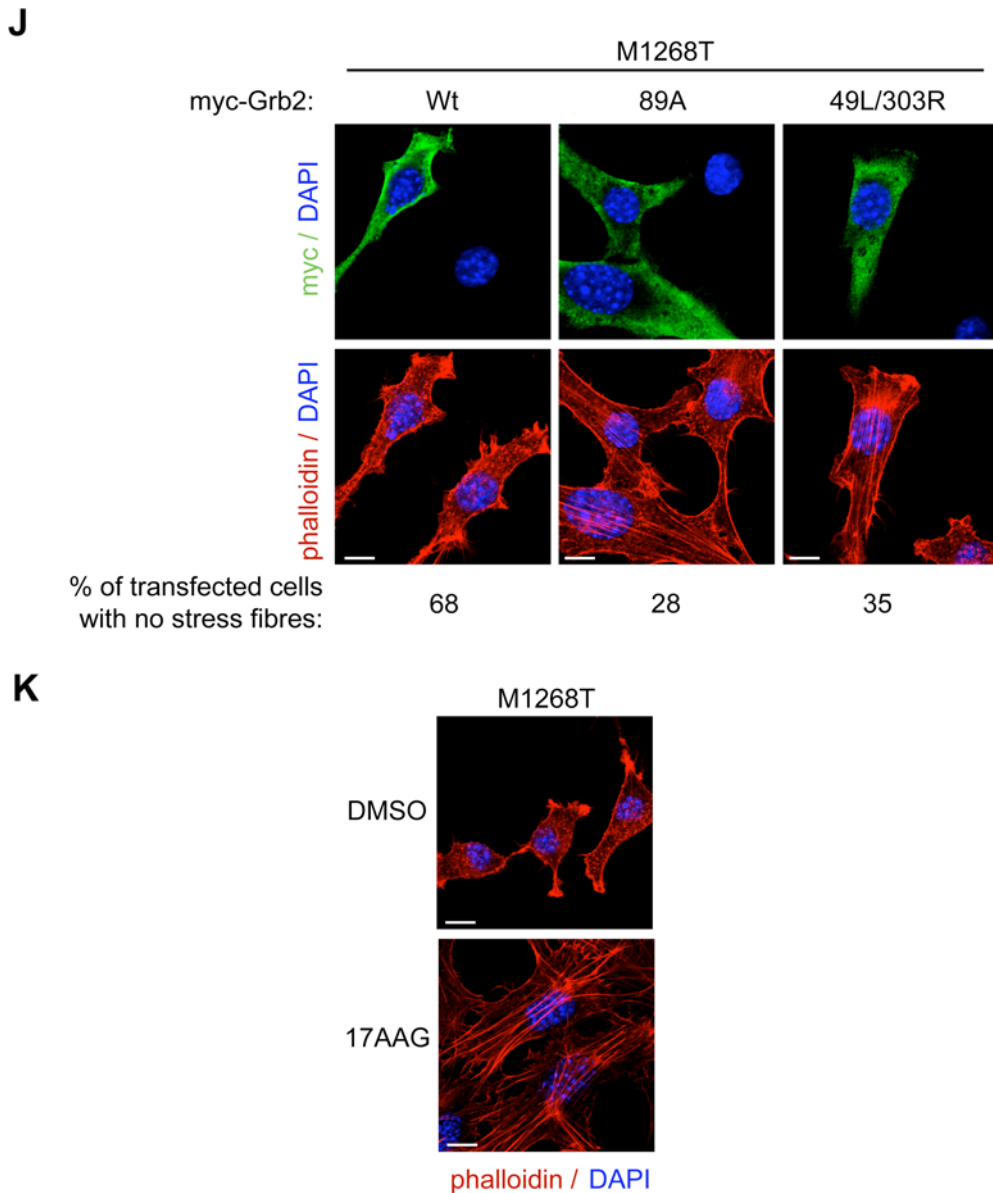


**Fig.5. The D1246N and M1268T Met mutants require the endocytosis machinery to stimulate cell migration**

**(J-K)** Indicated cells were stained with Cy3-phalloidin (red) and DAPI (blue). **(J)** Confocal sections of cells transfected with myc-tagged Grb2 constructs (Wt, dominant negative mutants 89A and 49L/303R). **(K)** Confocal sections of M1268T Met expressing cells treated with DMSO or 17-AAG (100 nM). Scale bar: 10  $\mu$ M.

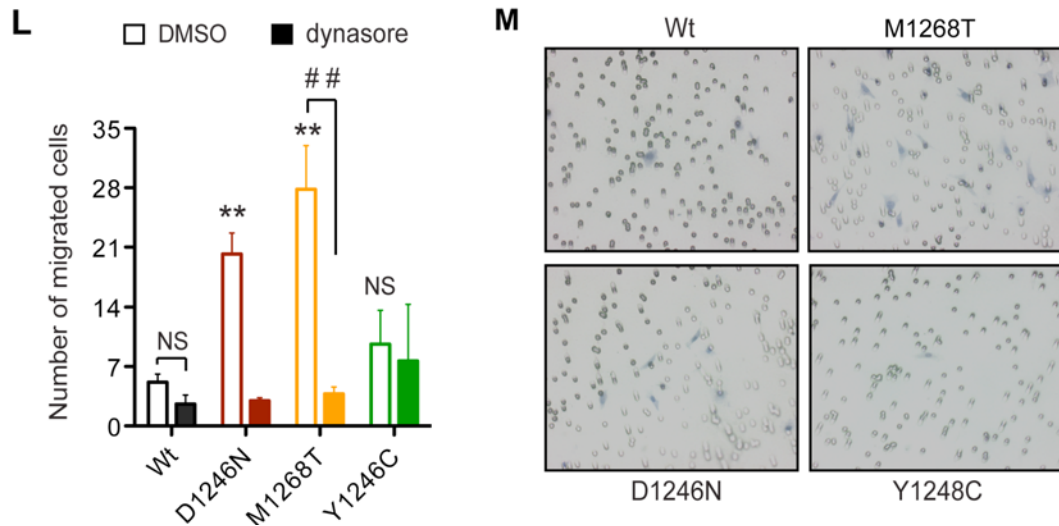


**Fig.5. The D1246N and M1268T Met mutants require the endocytosis machinery to stimulate cell migration**

**(L)** Mean numbers of the indicated cells that have migrated through Transwell pores over 2 hours of incubation in the presence of DMSO or dynasore, obtained from three independent experiments performed in triplicate or from two independent experiments performed in triplicate for dynasore treatments on D1246N and Y1248C expressing cells.

**(M)** Representative field of migratory cells that went through the membrane after the Transwell assay.

#, \*  $p < 0.05$ , ##, \*\*  $p < 0.01$ .

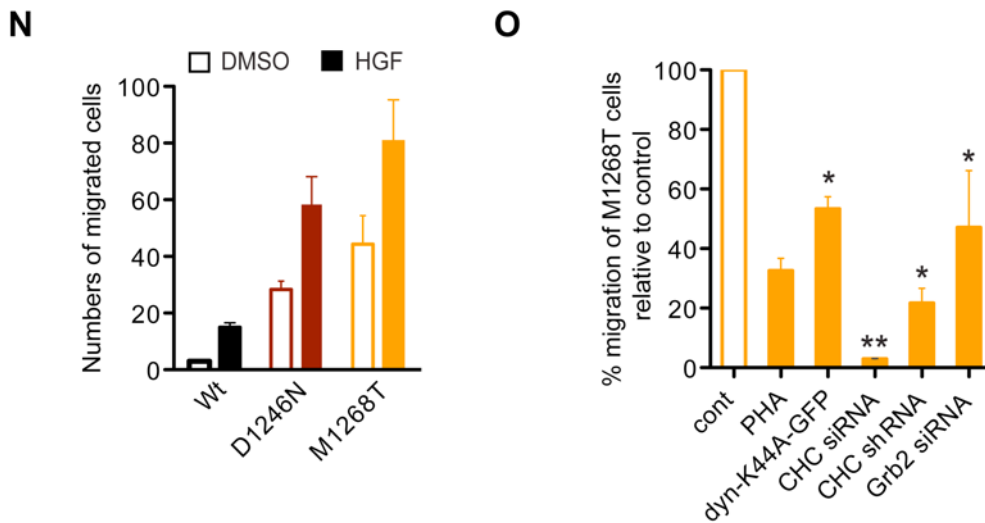


**Fig.5. The D1246N and M1268T Met mutants require the endocytosis machinery to stimulate cell migration**

**(N)** Mean numbers of the indicated cells that went through the membrane over 2 hours of incubation  $\pm$  HGF gradient. One experiment done in triplicate.

**(O)** The graph represents the percentage of M1268T Met expressing cells that have migrated through Transwell pores when treated with PHA-665752 (PHA) (from two independent experiments), transfected with dynamin 2 K44A-GFP, CHC siRNA (from three independent experiments) or Grb2 siRNA (from three independent experiments) or transduced with shRNA CHC (from two independent experiments). Data are normalised to appropriate controls (DMSO, GFP, siRNA control and shRNA control respectively). All experiments were performed in triplicate.

\*  $p < 0.05$ , \*\*  $p < 0.01$ .

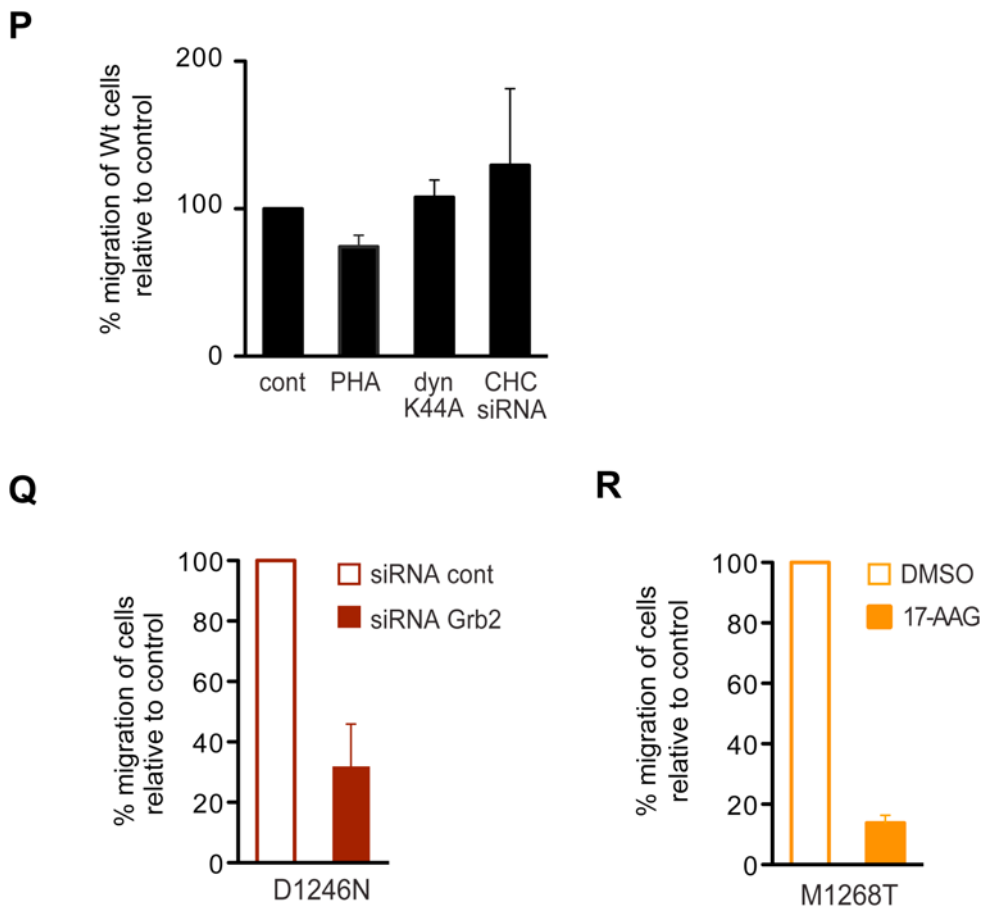


**Fig.5. The D1246N and M1268T Met mutants require the endocytosis machinery to stimulate cell migration**

**(P)** The graph represents the percentage of Wt Met expressing cells that have migrated through Transwell pores when treated with PHA-665752 (PHA), transfected with dynamin-K44A-GFP dominant negative mutant or with CHC siRNA over appropriate controls (DMSO, GFP vector and siRNA control respectively). Three experiments were performed in triplicate except experiments with PHA, which were done twice in triplicate.

**(Q-R)** The graph represents the percentage of D1246N Met expressing cells transfected with Grb2 RNAI. **(Q)** or M1268T Met expressing cells treated with DMSO or 17-AAG **(R)** that have migrated through Transwell pores. One experiment was performed in triplicate.

## **6. The D1246N and M1268T Met Mutants induce Rac1 activation, which is dependent on endocytosis**

Since Rac1 has been shown to induce actin stress fibre loss<sup>47</sup> we investigated this pathway. Rac1 activation was detected in D1246N and M1268T mutant expressing cells using GST pull-down assays (**Fig. 6A**). Inhibition by both a Rac inhibitor and Rac1 RNAi mediated knock down led to a restoration of stress fibres and thus to a significant reduction in the percentage of cells with disorganised actin (**Fig. 6B and 6C**) as well as an inhibition of cell migration (**Fig. 6D**) in D1246N and M1268T expressing cells but not Y1248C or Wt cells (**Fig. 6B and 6E**). Rac1 was knocked down efficiently (**Fig. 6F**).

These results indicate that the D1246N and M1268T mutants trigger actin remodelling as well as cell migration through activating Rac1.

Interestingly, Rac1 activation appeared to be endocytosis dependent in M1268T expressing cells since it was undetectable upon CHC knock down (**Fig. 6G**) suggesting the D1246N and M1268T mutants require endocytosis to activate Rac1.

In Wt and Y1248C expressing cells Rac1 staining was diffuse whereas in cells expressing D1246N and M1268T Met, Rac1 was observed at membrane protrusions (**Fig. 6H, I**), resembling HGF-stimulated Wt cells (**Fig. 6J**), and in punctate cytoplasmic structures, partially colocalising with EEA1 (**Fig. 6H**). When treated with PHA-665752 (**Fig. 6I, H**) or the recycling inhibitor primaquine (data not shown), the percentage of M1268T expressing cells displaying Rac1 staining at membrane protrusions was reduced down to that of Wt expressing cells. These results suggested

further that D1246N and M1268T Met mutants could lead to Rac1 activation on endosomes with subsequent recycling back to the plasma membrane, as recently described in HeLa cells stimulated by HGF stimulation or transfected by Rab5<sup>108</sup>. Consistent with this hypothesis, expression of dynamin 2 K44A-GFP decreased Rac1 localisation to endosomes and membrane protrusions significantly (**Fig. 6K**), reducing this to a level similar to that exhibited by Wt expressing cells (data not shown). Taken together, these results strongly suggest that the D1246N and M1268T mutants require endocytosis to activate Rac1.

Pharmacological inhibition of PI3-K by LY294002 (LY) reduced Rac1 localisation significantly in the membrane protrusions in M1268T cells (**Fig. 6L**) but not in Wt Met expressing cells (**Fig. 6M**), suggesting that, Met mutants activate Rac1 through PI3-K activation, which previously has been shown to promote Rac activation through the generation of the second messenger PIP3, which can in turn elicit activation of some GEFs<sup>62</sup>. PIP3 staining was detected in the D1246N and M1268T expressing cells only, where it was located in punctate cytoplasmic structures partially colocalising with Met (**Fig. 6N**). These data suggested a possible stimulation of PI3-K by Met on the endosome leading to local generation of PIP3. LY and PHA-665752 treatment abolished PIP3 staining in the M1268T mutant expressing cells, confirming the specificity of the staining and that generation of PIP3 is dependent on Met activity in these cells (data not shown). Following LY treatment stress fibres were restored (**Fig. 6O**) and cell migration impaired (**Fig. 6P**) in the M1268T cells but not in the Wt cells (**Fig. 6Q**).

Together these results indicate that the D1246N and M1268T Met mutants activate PI3-K, which is responsible for endocytosis dependent Rac1 activation, causing loss of stress fibres and enhanced cell migration. In addition, they strongly suggest that Rac1 is activated on endosomes.

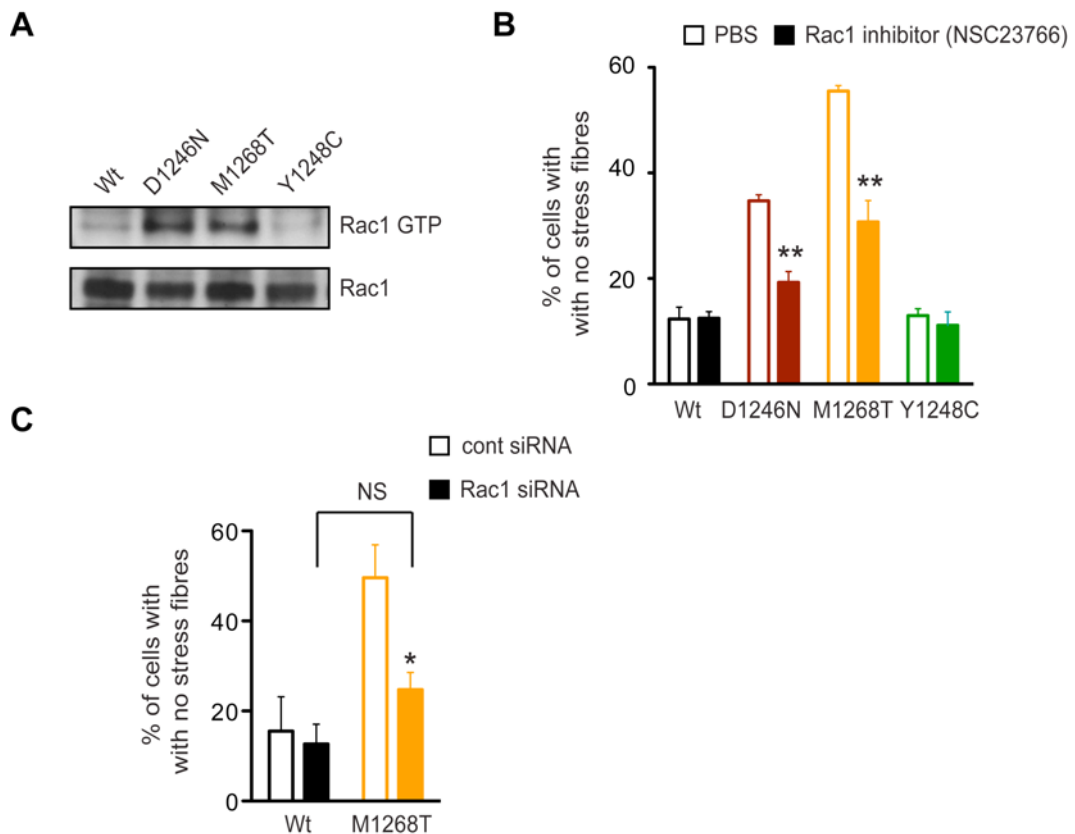


**Fig.6. The D1246N and M1268T Met mutants induce Rac1 activation, which is dependent on endocytosis**

**(A)** Levels of Rac1-GTP measured by GST-CRIB pull down and of total Rac1 in (see Materials and Methods) in the indicated cells.

**(B)** The graph presents the percentage, from three independent experiments, of indicated cells with no stress fibres after treatment for 60 min with PBS or with a Rac inhibitor (NSC23766).

**(C)** The graph represents the percentage, from three independent experiments, of indicated cells with disorganised actin when the indicated cells were transfected with control or Rac1 siRNA.

\*  $p < 0.05$ , \*\*  $p < 0.01$ .

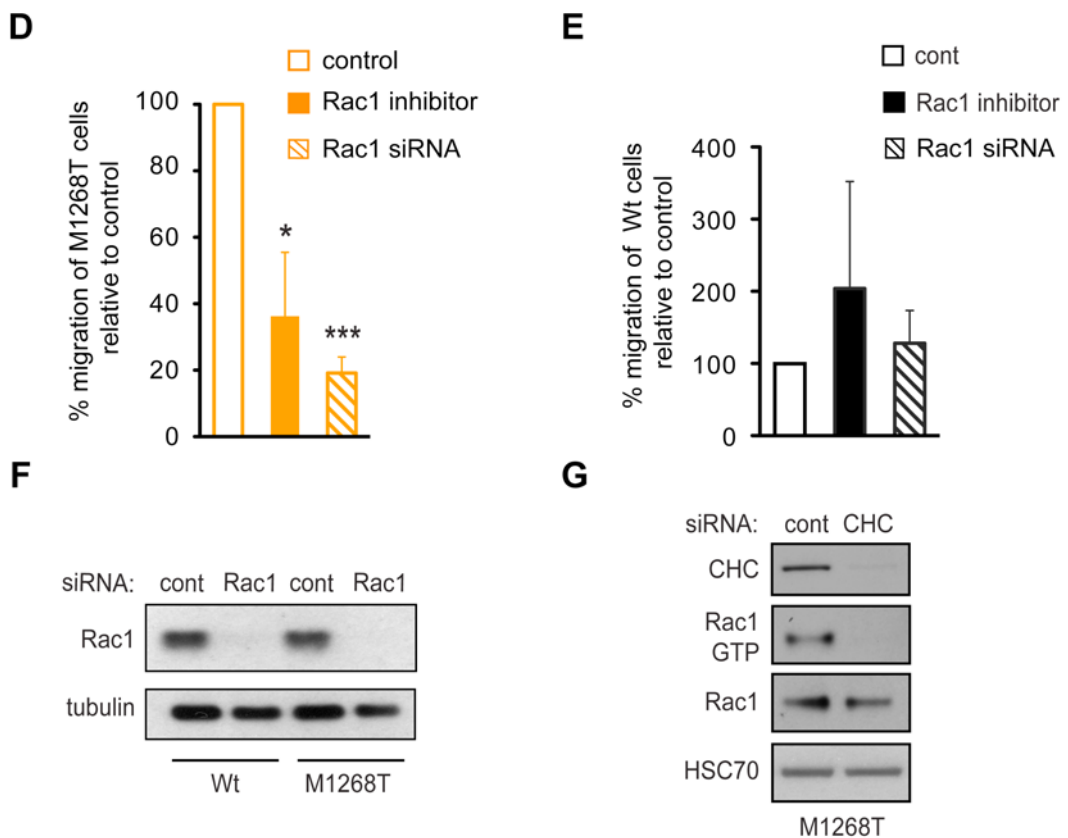


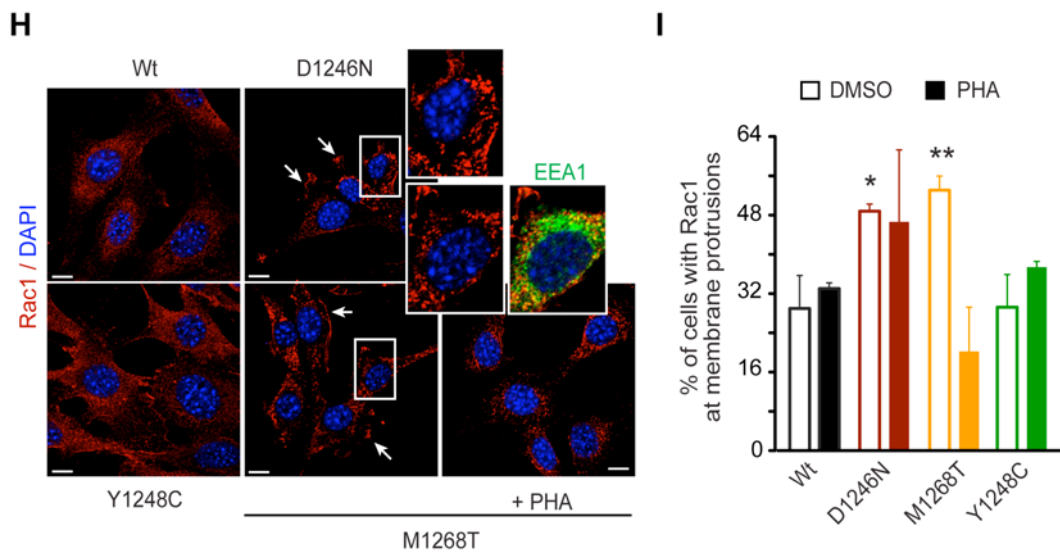
**Fig.6. The D1246N and M1268T Met mutants induce Rac1 activation, which is dependent on endocytosis**

(D-E) The graphs represent the percentage of M1268T Met expressing cells from three independent experiments (D) or Wt Met expressing cells from two independent experiments (E) that have migrated through Transwells when treated with the Rac inhibitor (NSC23766) or transfected with Rac1 siRNA, over the appropriate controls (PBS and control siRNA, respectively).

(F) Western blots for Rac1 and tubulin from indicated transfected cells with control or Rac1 RNAs.

(G) Levels of CHC, Rac1-GTP, total Rac1 and HSC70 in M1268T Met expressing cells transfected with control or CHC siRNA.

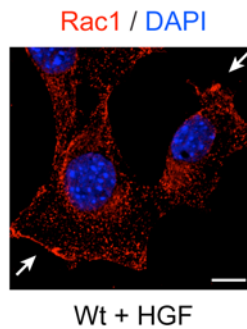
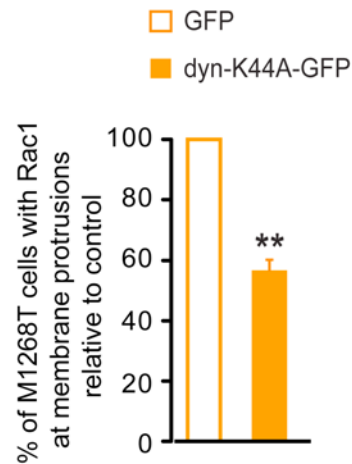
\*  $p < 0.05$ , \*\*  $p < 0.01$ , \*\*\*  $p < 0.001$ .



**Fig.6. The D1246N and M1268T Met mutants induce Rac1 activation, which is dependent on endocytosis**

**(H-I)** Indicated cells were treated with DMSO or PHA-665752 (PHA) for 60 min and stained for Rac1 (red), EEA1 (green) and DAPI (blue). **(H)** Confocal sections. **(I)** The graph represents the percentage of indicated cells with marked Rac1 staining present at membrane protrusions from three independent experiments, except for Y1248C Met expressing cells done 2 times. Scale bar: 10  $\mu$ M.

\*  $p < 0.05$ , \*\*  $p < 0.01$ .

**J****K**

**Fig.6. The D1246N and M1268T Met mutants induce Rac1 activation, which is dependent on endocytosis**

**(J)** Confocal sections of Wt Met expressing cells after 30 min of HGF stimulation, stained for Rac1 (red) and DAPI (blue). Arrows indicates membrane protrusions. Scale bar: 10  $\mu$ M.

**(K)** The graph represents the percentage of M1268T Met expressing cells, transfected with GFP vector (GFP) or with dynamin 2-K44A-GFP (dyn-K44A-GFP), with Rac1 at membrane protrusions, from three independent experiments.

\*  $p < 0.05$ , \*\*  $p < 0.01$ .

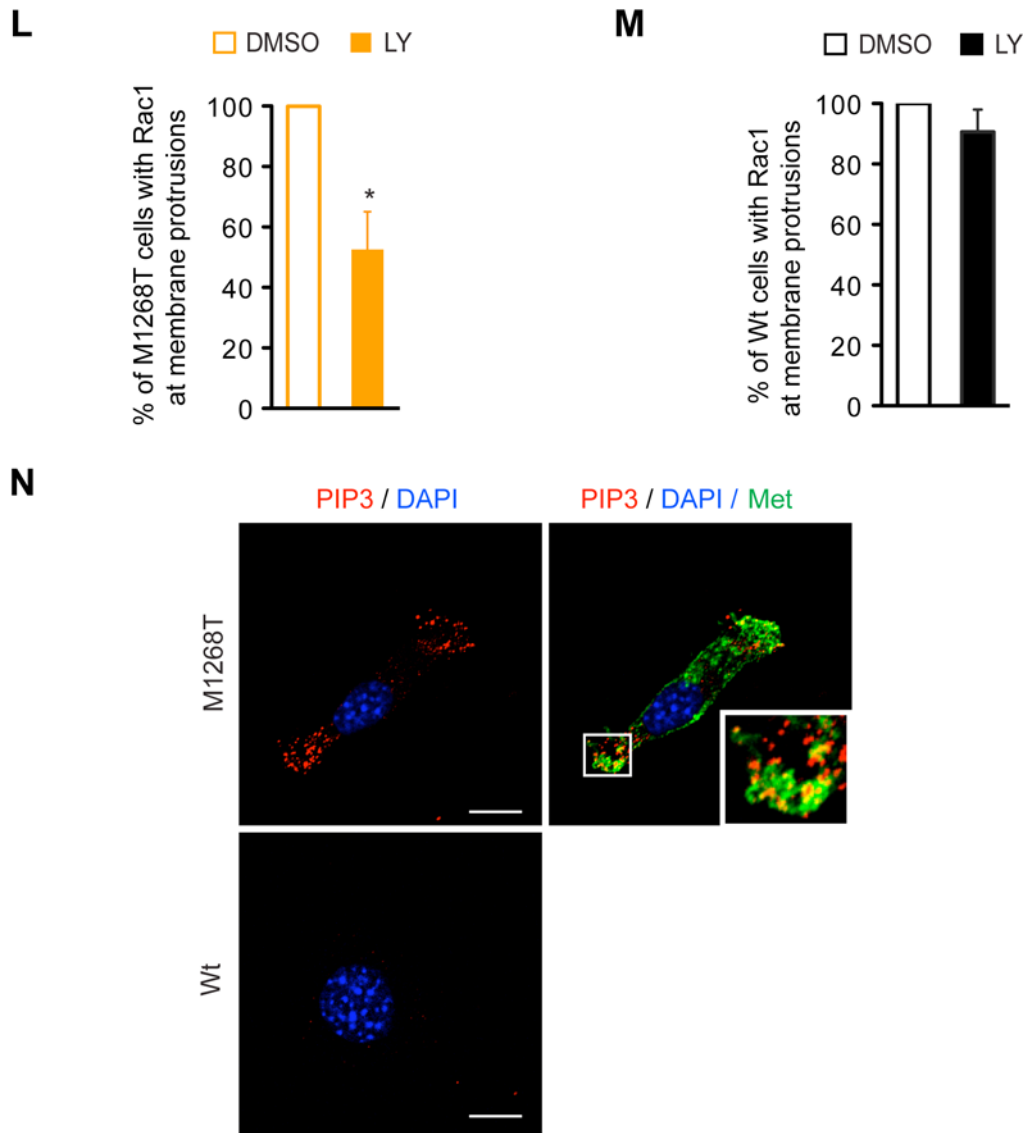


**Fig.6. The D1246N and M1268T Met mutants induce Rac1 activation, which is dependent on endocytosis**

**(L-M)** The graph represents the percentage of cells with Rac1 at membrane protrusions when M1268T **(L)** or Wt Met expressing cells **(M)** were treated for 60 min with DMSO or LY-294002 (LY). Data obtained from three and two independent experiments with M1268T and Wt Met expressing cells respectively.

**(N)** Confocal sections of indicated cells stained for PIP3 (red), Met (green) and DAPI (blue). Scale bar: 10  $\mu$ M.

\*  $p < 0.05$ .

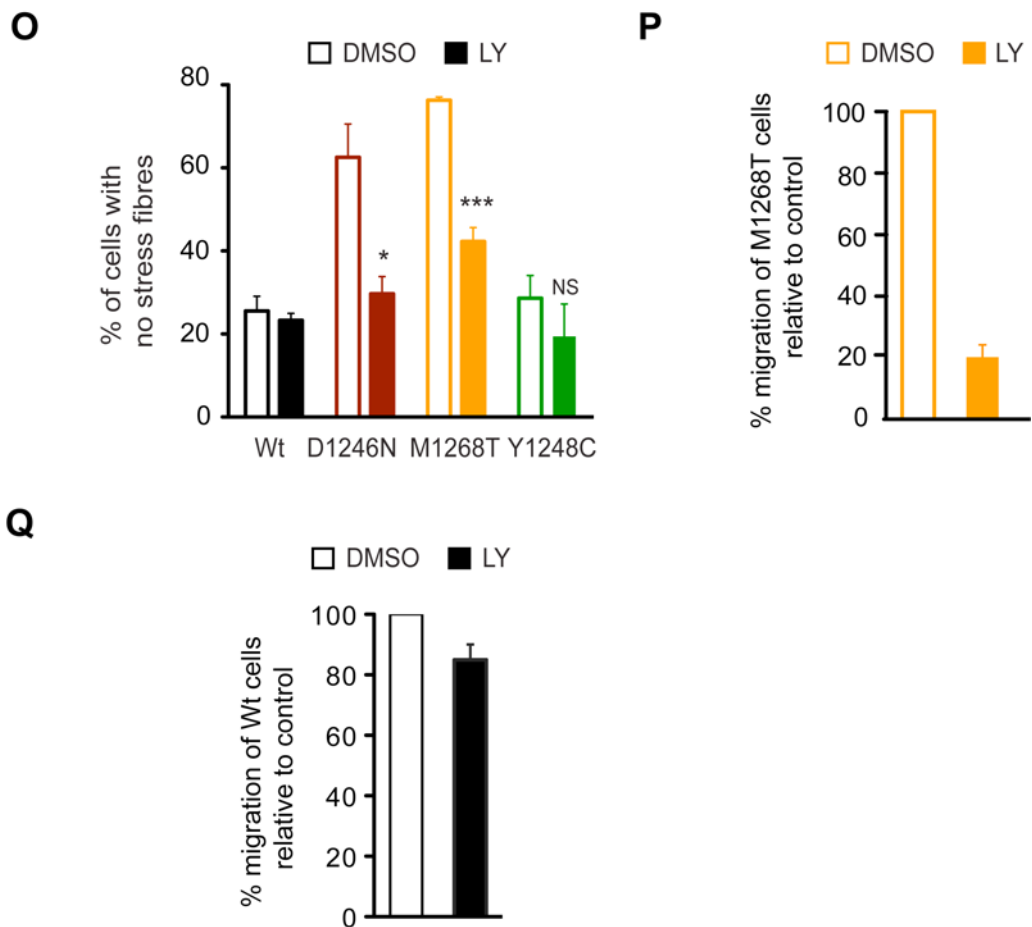


**Fig.6. The D1246N and M1268T Met mutants induce Rac1 activation, which is dependent on endocytosis**

**(O)** The graph represents the percentage of indicated cells with disorganised actin when treated with DMSO or LY-294002 for 90 min from three independent experiments.

**(P-Q)** The graph represents the percentage of the M1268T Met expressing cells **(P)** or Wt Met expressing cells **(Q)** that have migrated through Transwell pores when treated with LY-294002.

\*  $p < 0.05$ , \*\*  $p < 0.01$ , \*\*\*  $p < 0.001$ .

## **7. Blocking endocytosis reduces tumour transformation, stimulated by the D1246N and M1268T Met Mutants, both *in vitro* and *in vivo***

To assess growth in anchorage independent conditions, as a measure of cell transformation, the various lines were embedded and grown in three-dimensional soft agar gels to measure their colony formation. After 9 days of culture, colony number (**Fig. 7A**) and area (**Fig. 7B**) were increased significantly in the D1246N and M1268T mutant expressing cells versus Wt and Y1248C expressing cells. Interestingly, dynasore treatment from day five reduced the colony area of the D1246N and M1268T mutant expressing cells significantly (**Fig. 7B**) while stable CHC knock down (**Fig. 7C**) almost prevented the growth of the M1268T mutant expressing cells, indicating that endosomal signalling contributes to their transformed phenotype.

To investigate the requirement of endocytosis for *in vivo* tumorigenesis driven by Met mutants, dynasore, or control DMSO diluents, were applied topically (by paint-brush) to animals on the skin surface over tumours once they had achieved 50 mm<sup>3</sup> size (**Fig. 7D**) or on the day following cell injection (**Fig. 7E**). Tumour volumes were measured daily. Strikingly, the tumour growth slowed dramatically and significantly in grafts derived from D1246N and M1268T mutant expressing cells treated with dynasore versus DMSO. Thus, tumour sizes were approximately 50% after 5 days of treatment with dynasore relative to controls (**Fig. 7D**). Significant inhibition of M1268T tumour growth also was obtained with the novel dynamin inhibitor dynole 34.2 (**Fig. 7F**). Moreover, stable clathrin (CHC)

knock down, by lentivirus technology, also led to a significant reduction of tumour size by 50%, indicating that non-specific effects outside of endocytosis inhibition were not involved (**Fig. 7G**). Importantly, no significant change in tumour growth was observed in grafts of Wt and Y1248C expressing cells (**Fig. 7D-F**), indicating that the growth of these tumours, which is unrelated to Met activity, is unrelated to endocytosis.

Importantly, dynasore led to the same inhibition of M1268T tumour growth as the Met TKI PHA-665752 while the D1246N tumours were resistant to PHA-665752 (as already demonstrated in **Results-Part I, Fig. 4A**) but sensitive to dynasore. Thus, blocking endocytosis overcomes the resistance of D1246N to TKI in *in vivo* tumorigenesis.

Interestingly, the HSP90 inhibitor 17AAG also inhibited M1268T tumour growth by 50% (**Fig. 7H**); a result consistent with the restoration of Met mutant degradation (**Fig. 4H**).

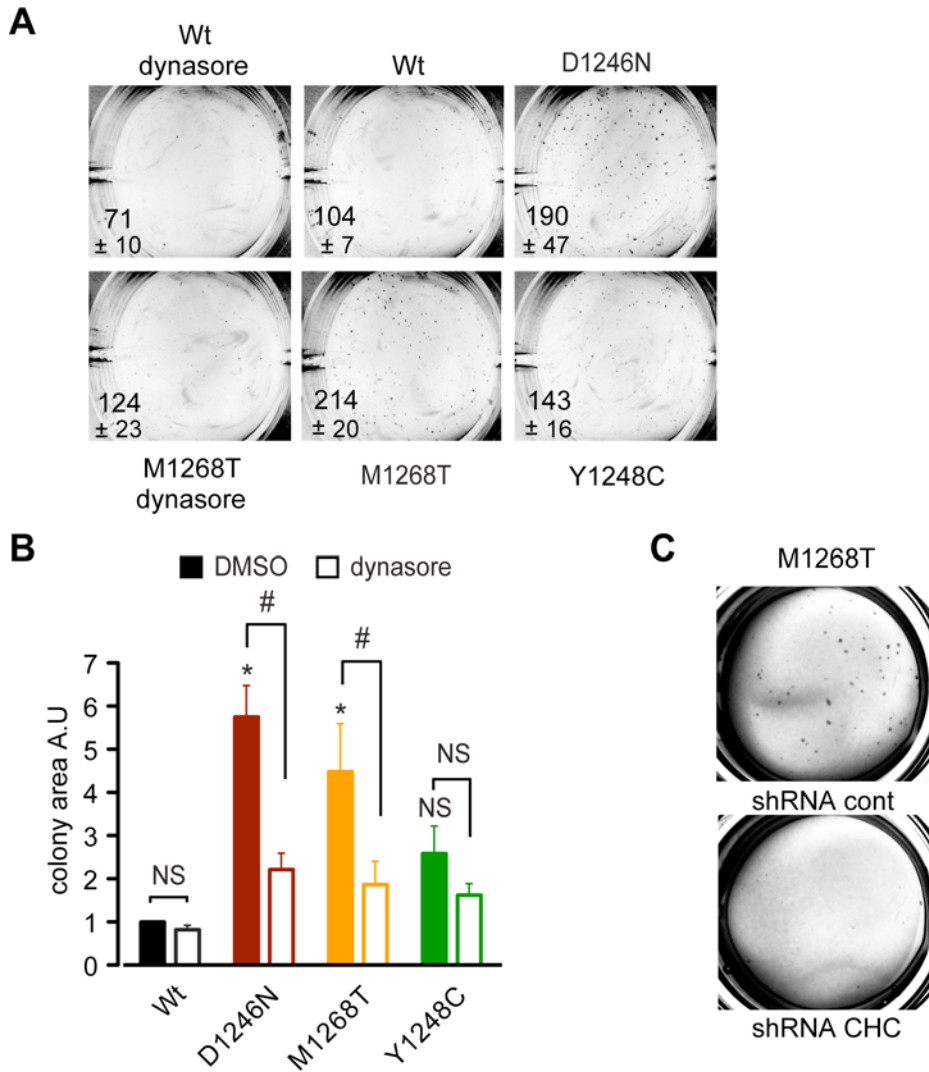
Finally, the M1268T mutant cells knocked down for CHC displayed a drastic reduction in lung colonisation capacity following injection in the tail vein of nude mice as compared to the cells knocked down with control shRNA (**Fig. 7I-J**). Lungs from mice grafted with cells expressing the M1268T shRNA control displayed a significant increase in size and weight compared with the lungs from mice grafted with cells expressing the M1268T shRNA CHC cells (**Fig. 7I**). Haematoxylin / eosin staining on paraffin sections of the tumours showed that the lungs of mice grafted with M1268T shRNA control expressing cells were infiltrated with tumour cells and almost no healthy area could be observed. Conversely, lungs from

mice grafted with M1268T control shRNA or Wt Met expressing cells, looked similar with no or few tumour infiltrated cells (**Fig. 7J**).

This result indicates that Met mutant endocytosis promotes experimental metastasis, consistent with its role on the actin cytoskeleton and in cell migration (**Fig. 5**).

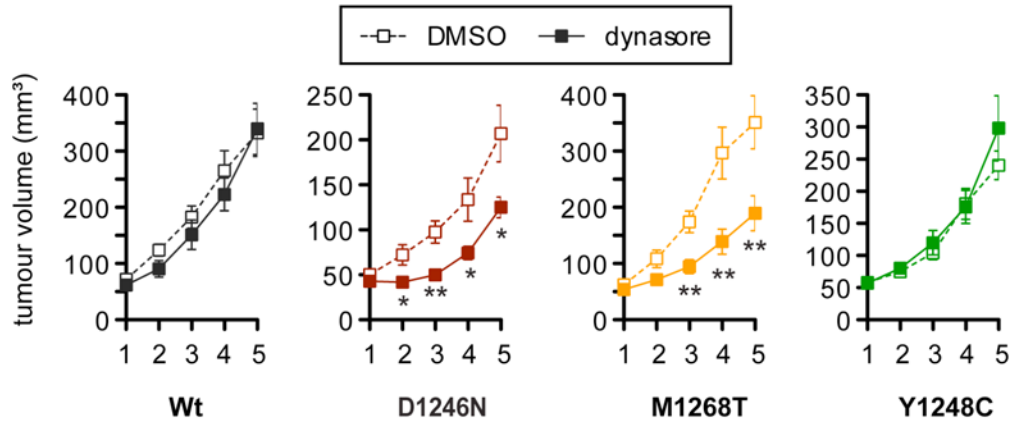
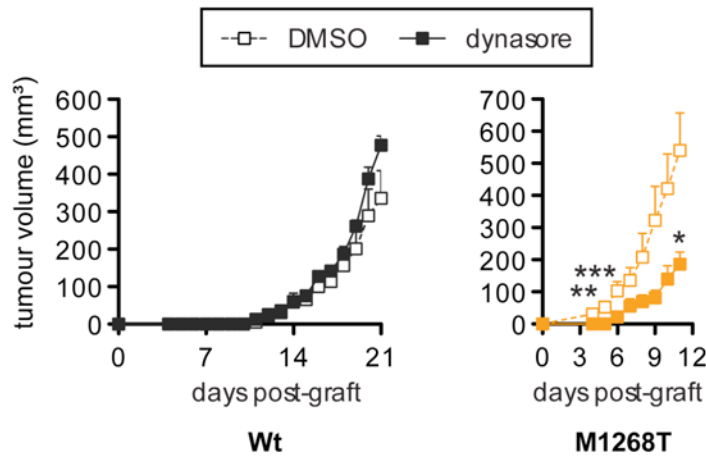
The localisation of Met was analysed by performing immunofluorescence on fixed DMSO- or dynasore- treated tumours (from **Fig. 7D**). Wt and Y1248C Met were expressed at the plasma membrane in a high proportion of cells within tumors while D1246N and M1268T Met were expressed in EEA1 positive endosomes rather than at the plasma membrane (**Fig. 7K**). Dynasore increased D1246N (data not shown) and M1268T mutants (**Fig. 7K**) at the plasma membrane. We conclude that activated D1246N and M1268T Met mutants are tumorigenic *in vivo* due to their enhanced endosomal trafficking, leading to their accumulation and signalling on endosomes (**Fig. 8**, model). Interestingly, dynasore did not reduce the level of phosphorylation of the different Met forms (or indeed the level of expression) in the tumours (**Fig. 7L**). Consistent with this, *in vitro* CHC or Grb2 knock down also did not reduce the level of the M1268T Met phosphorylation (**Fig. 7M-N**). Moreover, tumours derived from cells stably knocked down for CHC did not present any change in Met phosphorylation level as compared to control cells (**Fig. 7O**).

All together, these data strongly suggest that the high tumorigenicity of the D1246N and M1268T mutants is linked directly to their enhanced endosomal trafficking. These results suggest that it is localisation, rather than activation *per se*, which determines transformation capacity.



**Fig.7. Blocking endocytosis reduces tumour transformation, stimulated by the D1246N and M1268T Met mutants, both *in vitro* and *in vivo*.**

**(A-C)** Indicated cells were cultured in soft agar. **(A-B)** After day 5, DMSO or dynasore were added daily to the medium. **(A)** Pictures at day 9. Numbers are the mean total number of colonies per plate obtained from three independent experiments. **(B)** Average colony areas obtained from three independent experiments. A.U: Arbitrary Units **(C)** M1268T Met expressing cells transduced with control or CHC shRNA. Pictures at day 9. \* or #  $p < 0.05$ .

**D****E**

**Fig.7. Blocking endocytosis reduces tumour transformation, stimulated by the D1246N and M1268T Met mutants, both *in vitro* and *in vivo*.**

(D-E) The indicated cells (500,000) were injected subcutaneously into nude mice (minimum 5 mice per group). The graphs represent the tumour growth curves of the different cell lines over treatment time. When tumours had reached around 50 mm<sup>3</sup> (D) or the day after the graft (E), DMSO or dynasore (80 μM) were applied topically over the surface of the tumour mass each day for five days (from two independent experiments for D and one for E).

\* or # p<0.05, \*\*p<0.01, \*\*\*p<0.001.

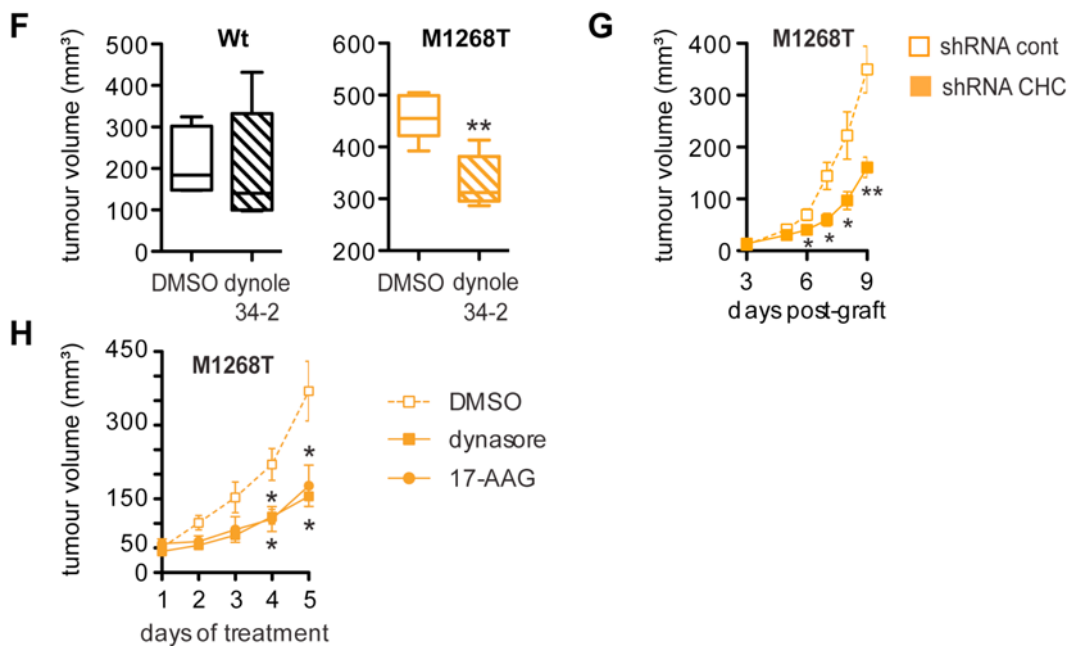


**Fig.7. Blocking endocytosis reduces tumour transformation, stimulated by the D1246N and M1268T Met mutants, both *in vitro* and *in vivo*.**

**(F)** The indicated cells were injected subcutaneously into nude mice (minimum 5 mice per group). When tumours had reached around 50 mm<sup>3</sup> DMSO or dynole 34-2 (30 μM) were applied topically over the surface of the tumour mass each day for five days. The results are represented as box and whisker plots, a histogram like method for displaying upper and lower quartiles and maximum and minimum values in addition to median. They represent the tumour volume after 7 days of treatment.

**(G)** M1268T Met expressing cells transduced with control or CHC shRNAs were injected subcutaneously into nude mice (minimum 5 mice per group). The graphs represent the tumour growth curves of the different cell lines over treatment time.

**(H)** M1268T Met expressing cells were injected subcutaneously into nude mice (minimum 5 mice per group). The graphs represent the tumour growth curves of the different cell lines over treatment time. When tumours had reached around 50 mm<sup>3</sup>, DMSO or 17-AAG (100 μM) were applied topically over the surface of the tumour mass each day for 5 days.

\* or # p<0.05, \*\*p<0.01.

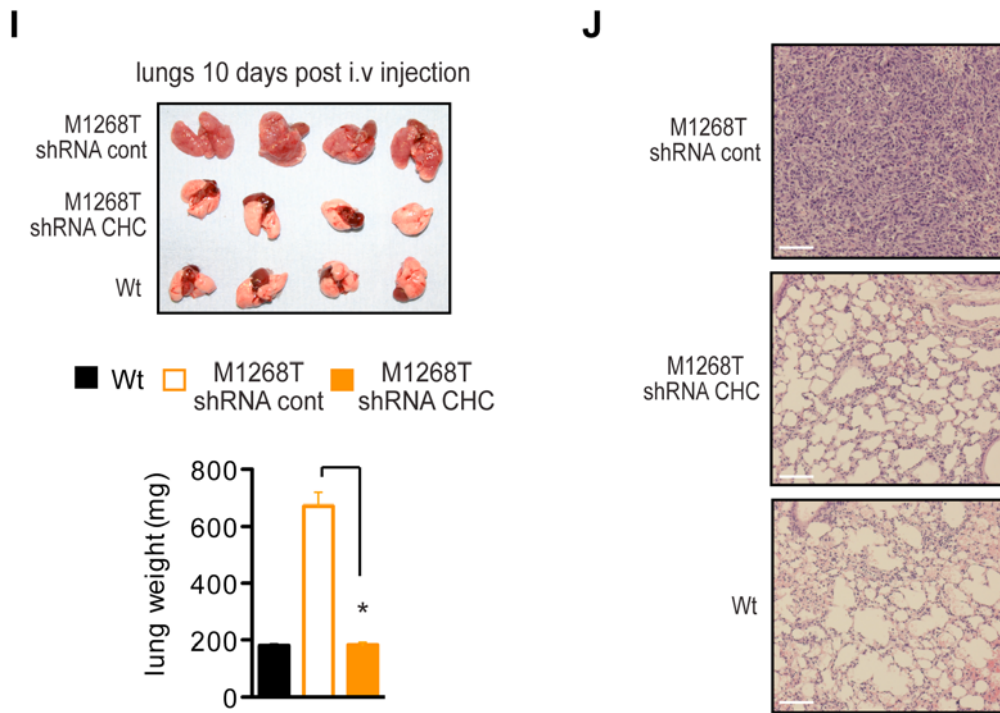


**Fig.7. Blocking endocytosis reduces tumour transformation, stimulated by the D1246N and M1268T Met mutants, both *in vitro* and *in vivo*.**

**(I-J)** M1268T Met expressing cells (500,000) transduced with control or CHC shRNA were injected intravenously and, after 10 days, lungs were photographed and weighed **(I)**. Haematoxylin/eosin staining of the paraffin embedded lung sections from the mice grafted with the indicated cells **(J)**.

Scale bar: 100  $\mu$ M. \* $p < 0.05$ .

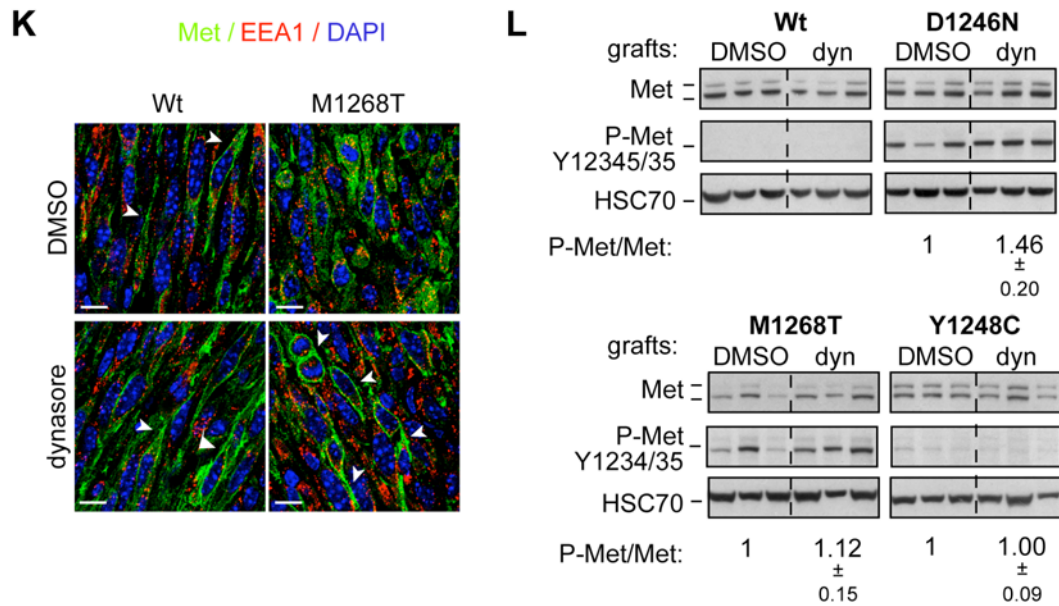


**Fig.7. Blocking endocytosis reduces tumour transformation, stimulated by the D1246N and M1268T Met mutants, both *in vitro* and *in vivo*.**

**(K)** Confocal sections of tumour sections from Wt and M1268T Met expressing cells (from **D**) stained for c-Met (green), EEA1 (red) and DAPI (blue). Arrows show plasma membrane Met.

**(L)** Western blots for phosphorylated Met (Y1234-35), total Met and HSC-70 performed on tumour samples from three different mice for each condition from **D**. The numbers are the fold increases of the phosphorylated Met (P-Met / Met) for dynasore treatment versus DMSO. Scale bar: 10  $\mu$ M.

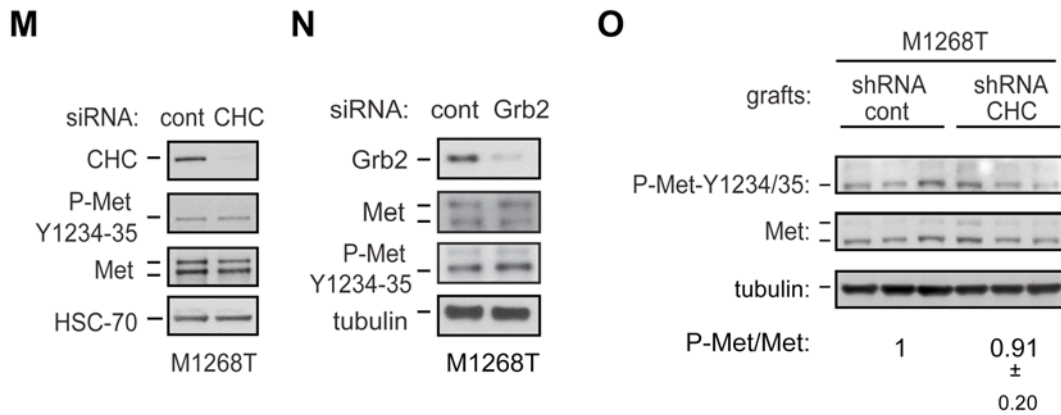


**Fig.7. Blocking endocytosis reduces tumour transformation, stimulated by the D1246N and M1268T Met mutants, both *in vitro* and *in vivo*.**

**(M-N)** M1268T Met expressing cells were transfected with control, CHC or Grb2 siRNA. Western blots for CHC **(M)**, Grb2 **(N)**, phosphorylated Met (Y1234-25), Met and tubulin are shown.

**(O)** Western blots for phosphorylated Met (Y1234-35), total Met and tubulin were performed on tumour samples from three different mice for each condition from **G**. The numbers are the fold increases of phosphorylated Met (Y1234-35) for shRNA control versus shRNA CHC cells.

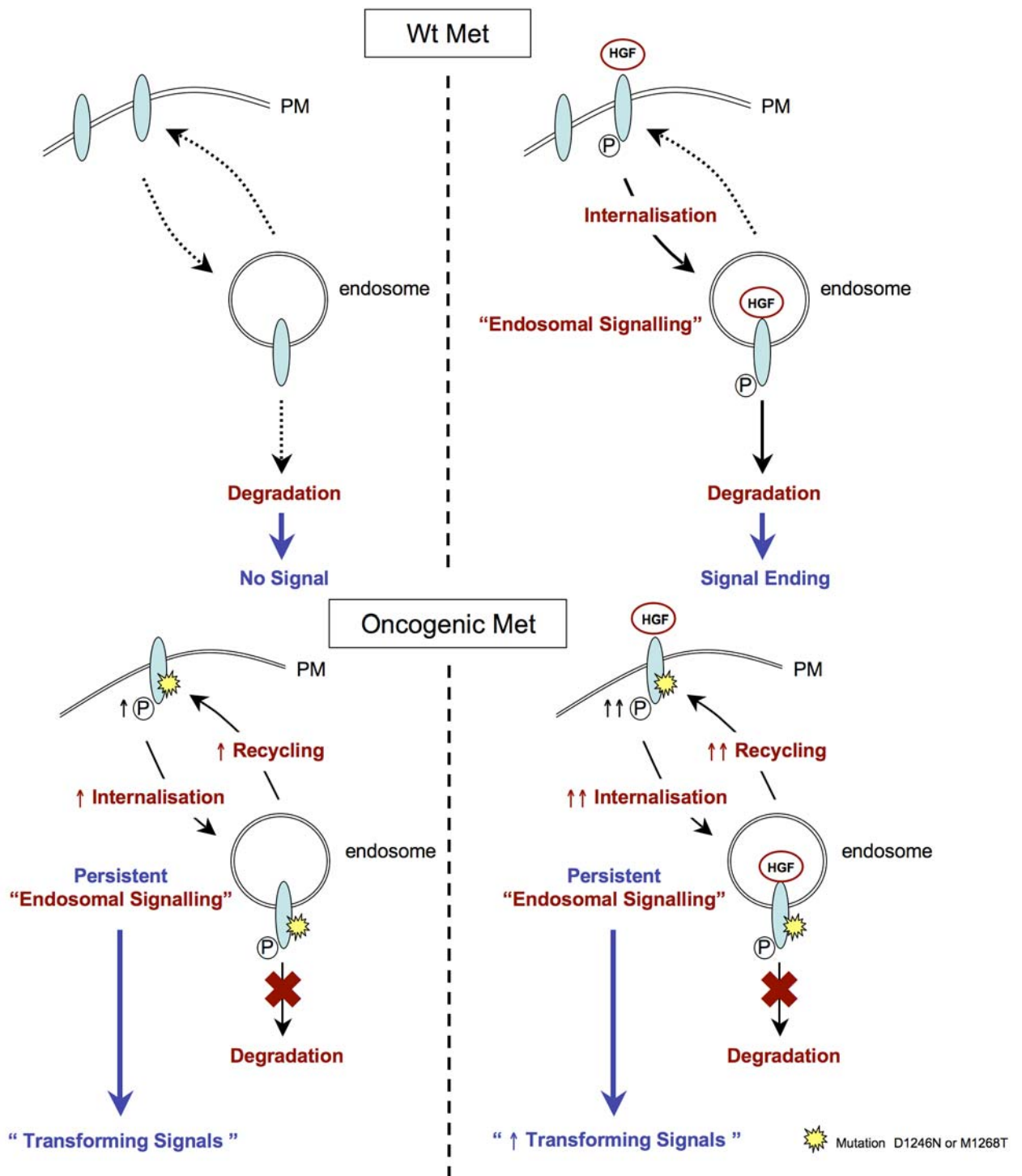


**Fig. 8. Signalling model of the Wt Met and of the D1246N and M1268T oncogenic Met mutants**

PM, plasma membrane. Signal specificity (generated through endosomal signalling) and signal persistence (due to the mutants' constitutive activation, shuttling between plasma membrane and endosomes and impaired degradation) constitute the "transforming signals".

## DISCUSSION - PART II

I have reported here that two Met activating mutations, found in human cancer, displayed constitutive endocytosis and recycling, coupled to an impaired down-regulation. These modifications in trafficking had important consequences for associated biological functions. Indeed, specific blocking of endocytosis resulted in the significant reduction of various parameters of *in vitro* transformation and in a striking slow down in tumour progression and experimental lung metastasis in immunoincompetent mice. Thus, in this study, I demonstrate a direct link between endocytosis and tumorigenicity.

### **Enhanced intracellular localisation of the M1268T and D1246N Met mutants**

#### ***Intracellular and plasma membrane localisation***

I reported that, in addition to their plasma membrane location, the activated mature forms of the D1246N and M1268T Met mutants are localised in an intracellular pool corresponding to endosomes. In unstimulated cells, RTKs are not found commonly on endosomes. An exception to this general statement however, is VEGFR which has been detected in an endosomal pool corresponding to what has been thought to be acting as a storage compartment<sup>268</sup>. Because Wt Met is located predominantly at the plasma membrane, I conclude that this internal location of the two mutants is due to the mutation itself.

Several mutated RTKs have been reported to accumulate, in their immature state, in intracellular compartments which are distinct from endosomes. Thus, immature Kit mutants accumulate in the Golgi<sup>208</sup> while immature Ret, FLT-3 and FGFR3 mutants accumulate in the endoplasmic reticulum (ER)<sup>201,209,211</sup>. These mutants present with a defect in sorting and, thus their mature forms are not expressed, or are expressed at very low levels, at the plasma membrane.

All the Met forms which I have examined are well expressed at the plasma membrane, as I demonstrated by immunofluorescence and biochemical analysis. From these data I conclude that the Met mutants are matured correctly and can be addressed to the plasma membrane. My results indicate that, for Met mutants, it is only the mature form (p-145), which is phosphorylated, confirming further that the observed intracellular accumulation of the activated Met mutants corresponds to correctly processed Met forms that accumulate intracellularly on endosomes.

When I started my thesis, no mutated RTKs had been reported in their mature form on endosomal compartments. However, a new study at the end of my thesis, in November 2009, reported that this indeed is the case for three constitutively activated EGFR mutants identified in NSCLC; EGFR  $\Delta$ 746-750,  $\Delta$ 747-749/A750P and L858R/T90M<sup>291</sup>. Although these EGFR mutants were investigated previously in several studies, none of them had investigated their subcellular localisation<sup>205,292</sup>.

The endosomal localisation of D1246N and M1268T Met mutants suggested that they could induce important modifications in receptor

trafficking. Consistent with this hypothesis, I have shown that these two distinct Met mutants displayed a constitutive endocytosis / recycling behaviour and a reduced degradation, which could account for their transforming activity.

### ***Increased endocytosis***

Using immunofluorescence and biochemical assays, I have demonstrated that the accumulation of the two oncogenic Met mutants on endosomes results from their significantly enhanced rate of basal internalisation as compared to Wt Met.

I further demonstrated that the constitutive endocytosis of the two Met mutants is dynamin- and clathrin- dependent, as previously reported for Wt Met<sup>71,119</sup>. This indicates that endocytosis of the Met oncogenic mutants probably is controlled by the same pathways as are involved in the endocytosis of Wt Met.

Consistent with the emerging role of the adaptor Grb2 in clathrin-dependent endocytosis of RTKs<sup>111,122</sup>, and its previously described constitutive association with the M1268T mutant<sup>191,193</sup> (that I reproduced in our system), I found that Grb2 is required for internalisation of the Met mutants.

The adaptor and ubiquitin ligase c-Cbl directly and indirectly interacts with Wt Met<sup>121,122</sup>. The indirect interaction between Wt Met and c-Cbl has been reported to occur through Grb2 and was shown to be required for HGF-dependent Wt Met internalisation<sup>122</sup>. In addition, the ubiquitin ligase activity of c-Cbl would appear to be essential to mediate HGF-dependent

Met internalisation<sup>122</sup>. Thus, one possibility would be that c-Cbl constitutively interacts with the activated Met mutants indirectly via Grb2 to promote their internalisation.

Importantly, I reported that Met M1268T internalises to the same extent when its activity is inhibited (or at least strongly reduced) by a Met specific TKI. Accordingly, previous studies have shown that an EGFR kinase dead (K721A) is able to internalise<sup>293,294</sup> and that if EGFR kinase activity is partially inhibited, ubiquitination of the receptor can mediate its internalisation<sup>80</sup>. Dimerisation has also been proposed to be required for RTK internalisation over activation status<sup>294</sup>. As a potential residual phosphorylation of Met may remain following TKI treatment, generation of mutations in the kinase domain of the Met mutants would determine for sure whether or not the mutants require activation for their internalisation. Nevertheless, our results with the TKI demonstrate that the increased endocytosis rate of the mutants is not simply a consequence of their increased activation state.

### ***Decreased degradation***

I demonstrated that, although the rate at which mutants D1246N and M1268T undergo internalisation is increased, their basal degradation is no higher than that of the Wt Met; in fact, if anything, their degradation is somewhat delayed. Furthermore, upon HGF treatment, these two mutants, in striking contrast with Wt and Y1248C Met, were unable to undergo efficient degradation. This impaired degradation was not due to an

impaired internalisation since, upon HGF treatment, Met mutants displayed enhanced endocytosis.

There is growing evidence that impaired RTK downregulation is associated with human cancer<sup>295,296</sup>. Interestingly, defective degradation recently was reported to occur with several EGFR forms mutated in the extracellular domain (the EGFRvIII mutant)<sup>206,207</sup> or in the kinase domain (L858R, L858R/T790M and L861R)<sup>205,292</sup>; however to our knowledge, no association with increased endocytosis has been described for such mutants. Furthermore, the defective degradation of some of these EGFR mutants was associated with a reduced, or an impaired, endocytosis combined with a lack of effective ubiquitination<sup>207,292</sup>. Absence or reduced coupling with c-Cbl<sup>207,292</sup>, or a defect in its ubiquitin ligase activity<sup>205</sup>, were proposed as possible mechanisms to explain this absence in ubiquitination.

Met degradation defects associated with a normal internalisation process have been reported previously. Because c-Cbl binds to Met on a phosphorylated tyrosine at the position 1003, the Met mutant Y1003F was generated and this, therefore, was unable to be ubiquitinated. While this mutant failed to degrade, it could be internalised with similar kinetics to those of the Wt Met<sup>124</sup>. Y1003 is located in the juxtamembrane domain, where a naturally occurring mutation was identified in lung cancer, leading to the generation of a deleted form of Met lacking the juxtamembrane domain<sup>185</sup>. This Met deletion mutant also was targeted inefficiently for degradation, but no investigation was done on its internalisation. Similarly,

the oncogenic mutant TPR-Met<sup>123</sup>, which also lacks the tyrosine 1003, displayed inefficient degradation.

Our data indicate that the mechanisms leading to the defects in degradation of the D1246N and M1268T mutants are different from a simple defect in ubiquitination. In fact, if anything an increased ubiquitination level of the mutant M1268T over Wt Met was observed upon HGF stimulation. This might suggest a possible defect in de-ubiquitination of the Met mutants.

Deubiquitination is operated by endosomal DeUBiquitinating enzymes (DUBs). To date, it is unknown which DUB, among 79 members, affect(s) Met degradation. Recently, 12 DUBs have been identified and characterised to be involved in the HGF dependent scattering response but they had no influence on Met expression levels<sup>297</sup>. Two DUBs, UBPY (UB-specific Protease Y) and AMSH (Associated Molecule with the SH3 domain of STAM), both de-ubiquitinate the EGFR on endosomes but, depending on the studies, have been reported to promote<sup>298,299</sup> or prevent<sup>300,85,86</sup> EGFR degradation.

In fact, while ubiquitination promotes the sorting of cargos towards degradative compartments, a step of deubiquitination is required for their enclosure into the multivesicular body, a step considered necessary for the degradation<sup>298</sup>. In addition, in order to be delivered into internal vesicles of the MVBs, RTKs interact on endosomes with the protein Hrs that, in turn, recruits the ESCRT complex. Hrs binds only ubiquitinated RTKs. Thus, as suggested by McCullough et al<sup>86</sup>, it seems logical that

when DUBs act on RTKs before their interaction with Hrs, RTKs cannot be targeted to the degradation pathway anymore.

Thus, deubiquitination is a complex process that can lead to opposite fates for the cargo depending on when and where the deubiquitinating enzymes act along the trafficking route.

In the studies reporting that AMSH prevent EGFR degradation, its role in promoting EGFR recycling was also observed<sup>85,86</sup>. AMSH may, for example, be implicated in the high recycling rates that the Met mutants D1246N and M1268T display.

Interestingly, I showed that the degradation of D1246N and M1268T Met mutants can be restored through inhibiting HSP90 activity. Because I found the M1268T mutant was complexed with HSP90, as previously described for constitutively activated EGFR mutants (L858R and L861Q)<sup>205</sup>, it is reasonable to propose that HSP90 inhibits Met mutant degradation directly rather than acting on a related protein. However, further studies would be needed to determine this. Moreover cell transformation and *in vivo* tumorigenesis induced by D1246N and M1268T Met mutants, are reduced significantly upon 17-AAG treatment. This suggests that such therapeutic approaches could be exploited to inhibit cancers driven by such oncogenic Met mutants.

## **Endosomal signalling: Specificity of pathways and of cellular outcome**

Since Met recruits almost all its downstream partners through only 2 tyrosines (Y1349 and Y1356) in a unique docking site<sup>27,301</sup>, the basis of signalling selectivity has remained elusive. Endosomal signalling of Met, by spatially and temporally restricting signalling, may contribute to pathway specificity<sup>71,116,132</sup>.

I identified Rac1 as the major regulatory molecule in the endosomal pathway which is responsible for the reduction in actin stress fibres and increased cell migration stimulated by the two transforming D1246N and M1268T Met mutants. In these cells, Rac1 activation requires intact clathrin- and dynamin-mediated endocytosis as well as PI-3K activity; findings consistent with recent data published on HeLa cells<sup>108</sup>. In this latter study, Palamidessi et al reported that HGF dependent Rac1 activation occurs on endosomes<sup>108</sup>. Then Rac1 was targeted to the plasma membrane and induced the formation of actin-based migratory protrusions, including peripheral and circular ruffles. In my cell model, although circular ruffles were not observed, major actin remodelling occurred including peripheral ruffles and loss of stress fibres. As was observed by Palamidessi et al, I see in my model that endocytosis is required for Rac1 activation. I suggest that Rac1 endosomal activation may occur on endosomes through the recruitment of a GEF to the D1246N and M1268T Met mutants. In this study of Palamidessi and colleagues, the GEF Tiam1 was observed on endosomes<sup>108</sup>. Further

experiments are required to identify which GEF activates Rac1 in my model.

I also show that, in addition to Met activity, Rac1 activation and further translocation to the plasma membrane requires PI3-K activity. PIP3 staining was observed only in cells expressing D1246N and M1268T Met mutants. The cytoplasmic punctate localisation of PIP3 suggests a possible activation of PI3-K by Met mutants on the endosome leading to this local production of PIP3. PIP3 could, in turn, activate the GEF leading to an increase in Rac1 GTP loading. Once activated on endosomes, Rac1-GTP would be targeted at the plasma membrane, eventually to induce actin reorganisation and promote cell motility. Thus, although further investigations are required to fully dissect out the mechanisms, I suggest that the D1246N and M1268T Met mutant generate the whole signalling cascade necessary to Rac1 recruitment and activation on endosomes.

### **Endocytosis and cancer**

Since I started work on my thesis, there has been an increasing recognition of a mode of compartmental signalling of RTKs, the “endosomal signalling”<sup>66,111,302</sup>, which corresponds to the signalling of mature forms of RTKs on endosomes, post-internalisation from the plasma membrane.

While initially, considered solely as being the way whereby RTK desensitisation was achieved, endocytosis recently has emerged as an important mechanism to also influence the signalling of the RTKs

positively. Signalling from a variety of receptors can be sustained, amplified or specifically generated along the endocytic pathway<sup>70,71,90,108,110,111,116,132</sup>. Interestingly, these pathways (ERK, STAT3, Rac) are known to play a role in tumour progression. Moreover, endocytosis very recently has emerged as an important regulator of cell functions such as cell cycle, cell polarity, mitosis and migration<sup>66</sup>. All these functions need to be tightly regulated and loss of their control is a major determinant in the development of cancers. Therefore, as proposed in two recent reviews<sup>112,303</sup>, the idea currently is emerging that deregulation of endocytic trafficking may be involved in cancer progression

Indeed, some endocytic proteins have been found to display a modification in their expression in human cancers<sup>303,304</sup>. Thus, the clathrin-associated protein HIP1 (Huntingtin Interacting Protein 1) was reported to be overexpressed in a wide variety of carcinomas, including prostate and colon cancers<sup>305</sup>. Moreover, experimentally overexpressed HIP1 transformed, both *in vitro* and *in vivo*, NIH3T3 cells on the one hand, and induces *in vitro* overexpression of several RTKs, including EGFR, and increases their trafficking, on the other hand<sup>306</sup>. These results suggested a role for increased RTK trafficking in cell transformation.

The endocytic protein NUMB, that interacts with Eps15 and AP2 on endosomes<sup>307</sup>, was found to be underexpressed in breast cancers<sup>308</sup>. A recent study demonstrated that NUMB, through inhibiting the E3 ubiquitin ligase of p53, led to the stability of this latter protein and therefore to the maintenance of its tumour suppressor activity<sup>308</sup>. However, the precise

role of the endocytosis process in this control of p53 function remains to be fully established<sup>112</sup>.

A recent study reported that a mutant p53, through gain of function, drives cell invasion by promoting the enhancement of the integrin  $\alpha 5\beta 1$  and EGFR recycling. This increased recycling was dependent on Rab-Coupling Proteins, and resulted in a constitutive activation of the EGFR<sup>309</sup>. Thus, all these studies report on some molecular modifications in the cell (change of expression of endocytic regulators, p53 mutation), which impinge on trafficking of RTKs. However modification of RTK endocytic trafficking on its own has not, until now, been reported though oncogenic RTKs usually were shown to find ways to escape degradation<sup>207,292</sup>. Thus, in the present work, I provide the first evidence of a direct link between RTK endocytosis and cancer development.

**Constitutive endocytosis / recycling and defects in degradation: signal specificity and persistence lead to transformation**

I propose that, at least in our model, continuous endocytosis associated with an impaired degradation contributes to the maintenance of the activated receptor on endosomes and therefore to the persistence of endosomal signals. Thus, signal specificity (generated through endosomal signalling) and signal persistence together may constitute the “transforming signals”.

I have shown that the M1268T mutant recycles back to the plasma membrane post-endocytosis. The enhanced endocytosis / recycling of the

transforming mutants, associated with their impaired degradation, suggests they undergo a persistent shuttling between the plasma membrane and the endosomes.

Such shuttling of ligand-stimulated RTK, as well as the integrins, recently has been described as regulating spatial restriction of signalling necessary for directed migration<sup>109,310</sup>.

Recent studies on RTKs, such as EGFR<sup>87</sup> and TGF- $\beta$  receptor<sup>97</sup>, suggest that degradation is associated with endocytosis but poor recycling, while enhanced signalling rather is associated with endocytosis but high recycling. Accordingly, upon ligand binding, Wt Met gets endocytosed, signals on endosomes and gets progressively degraded but is recycled poorly, allowing signal termination. In contrast the signal is maintained for the oncogenic Met mutants, which display an increased recycling and a poor level of degradation (see **Results-part II, Fig. 8**).

I suggest that the generation of “transforming signals” by D1246N and M1268T Met mutants may require a substantial amount of recycling in addition to endocytosis. Hence, in the implanted subcutaneous tumours, the endocytic blocker dynasore, which strongly increased Met at the plasma membrane, did not totally deplete Met from endosomes (**Fig. 7K**) but it did reduce tumour size by two-fold relative to the control (**Fig. 7D**). While the cellular uptake of dynasore might be less than optimal, because of our novel route of topical application, these results suggest that dynamic shuttling between plasma membrane and endosome plays an important role in tumorigenesis, rather than the outcome being dependent on simple endosomal localisation only.

## **Signalling on the Endosome Positively influences Tumorigenesis**

RTKs are known to be oncogenic through their increased level of activation due to overexpression, autocrine signalling or activating mutations<sup>2,311</sup>. Generally, the global intensity of activation in the cell or tissue is the only parameter which has been taken into account, with little attention paid to the precise localisation of the signals.

Interestingly however, recent studies, cited above, have reported the signalling of mutated activated RTKs, in an immature form, from intracellular compartments of the secretory pathway, such as the Golgi for Kit D814V<sup>208</sup> and the endoplasmic reticulum for Ret R918T<sup>209</sup>, mutated FGFR3<sup>202,211</sup> and FLT3-ITD<sup>201,210</sup>.

These mislocalised receptors generate different signals, in intensity, duration or nature, than they do when localised solely at the plasma membrane<sup>210</sup>. Kit D814V when localised in the Golgi was shown to enhance Stat3 and Stat5 activation as compared to plasma membrane location<sup>208</sup>. FLT3-ITD activated Stat5 preferentially when localised in the ER and only initiated ERK1/2 activation when it was located at the cell surface<sup>210</sup>. Moreover, intracellular localisation of Kit D814V, (Golgi or cytoplasm), was shown to promote fatal myeloproliferative disease in mice while the plasma membrane localisation of this mutant was not associated with this pathology<sup>208</sup>.

Thus, these studies favour the general concept of ‘compartmental signalling’ where receptor signalling can be altered by the localisation of the trafficking molecule.

In the present study, I have shown that another mode of compartmental signalling of RTKs, the “endosomal signalling”, which corresponds to the signalling of mature forms of RTKs on endosomes, plays a role in cell transformation *in vitro* and *in vivo*.

Thus, it is shown here that D1246N and M1268T Met mutants display an increased endocytosis / recycling, leading to persistent signalling from the endosome and to cell transformation *in vitro* and *in vivo*.

Construction of 3-dimensional models of Wt and mutated catalytic domains suggested that the mutations either prevent Met from adopting an inhibitory conformation or stabilise it in an active form<sup>186</sup>. Uncoupling signal transducers from Met mutants, through mutation of the two major docking tyrosines, abrogates cell transformation and inhibits invasive growth<sup>191</sup>. Thus it has been assumed that the D1246N and M1268T mutants are oncogenic simply because they are highly activated. A major finding in our study is that Met activation alone is not sufficient to confer oncogenicity but that there is an additional spatial requirement for the generation of transforming signals. Met mutants are oncogenic not only because they are activated but also because they signal on endosomes. Indeed upon endocytosis inhibition, the D1246N and M1268T Met mutants remain activated but are not oncogenic.

Based on our data, the current model of tumorigenesis stimulated by oncogenic RTK might need to be refined to also take into account the potential contribution of endosomal signalling to the process.

## **Interfering with Endocytic Trafficking or Endosomal Signalling as an Anti-Tumour Strategy?**

I have shown that inhibition of the transforming capacity of the D1246N and M1268T Met mutants can be achieved through endocytosis inhibition. Most strikingly *in vivo* tumour growth and/or experimental metastasis dependent on these Met mutants is reduced significantly by topical administration of pharmacological blockers of endocytosis or by stable clathrin knock down. These studies represent proof of principle that, at least in our model, endocytosis plays a role in tumour transformation.

Met is a promising target for cancer therapy, as evidenced by its association with resistance of non-small cell lung and breast cancer to gefitinib and trastuzumab (or herceptin), which target EGFR and HER2<sup>214,216</sup> and by increasing efforts to design Met inhibitors in the pharmaceutical industry<sup>312</sup>. Although it is not yet well established as to whether Met mutations occur widely in human cancer, they contribute strongly to improving our understanding of how oncogenic Met is transforming and therefore point to how to intervene in the tumorigenesis pathway.

Of high interest, this novel inhibition method appears to overcome the resistance of one mutant to a Met specific TKI, *in vitro* and *in vivo*. Therefore, the phosphorylation of the D1246N Met mutant, the phenotypic modifications it induces, such as actin disorganisation, Rac1 localisation at membrane protrusions or increased cell migration, as well as tumour growth, were not modified by the Met specific TKI. However these

behavioural traits were significantly impaired by inhibition of endocytosis (**Fig. 5, 6 and 7**).

Thus, my study is consistent with the possibility that oncologists could exploit novel strategies to inhibit Met dependent tumorigenesis based on interference with Met localisation or, more specifically, by designing “endosome-specific targeting” strategies as recently suggested<sup>85</sup> (see **Fig. 9 in Introduction**). Since Met also is involved in several non tumorigenic functions and is responsible for homeostasis maintenance, modifying its localisation or inhibiting the endosomal signalling, but not its global activity, could lead to an inhibition of the “transforming signals” generated on endosomes while maintaining the non-transforming signals.

More generally, for some RTKs / cancers, interfering with the endocytic pathway or the endosomal signals may overcome the currently elevated tumour resistance to RTK specific TKIs or antibodies.

I have established a direct link between endocytosis and cancer. These results, representing proof of principle, suggest that new anti-tumour strategies might be based on manipulating endosomal signalling.

## CONCLUDING REMARKS

Since its discovery in 1984<sup>6</sup>, and its identification as a member of the RTK family in 1986<sup>9</sup>, scientific interest in Met has not stopped growing. This interest has increased rapidly over the years, particularly since the deregulation of Met activity has been established to play a crucial role in cancer development<sup>15,265</sup>. Thus Met recently has emerged as a target of choice for cancer therapy by cancer researchers and pharmaceutical companies<sup>14,169,218,245</sup>.

The discovery of Met activating mutations in human cancers<sup>167,168,175</sup> contributed to establishing the link between Met and cancer and underlined the importance of understanding the signalling mechanisms of the different mutationally activated forms of Met for the development of successful cancer therapeutics. Importantly, as for other mutated RTKs, as an issue which will need to be addressed, the potential problem of drug resistance of mutated Met has been raised<sup>261</sup>.

When I started my thesis in 2006, although it had been demonstrated that several RTKs<sup>89,92,94,95</sup>, including Met<sup>70,132</sup>, could signal from endosomal compartments, the concept of “endosomal signalling” was only just emerging.

Four years later, the interest in the field has increased significantly and more studies have shown that endocytosis is not a desensitisation mechanism only. Endosomes have been proposed to play the role of essential platforms in signal transduction<sup>66,85,111</sup> rather than just as

“vehicles” for the receptors. Endocytosis now has been proposed to control cellular functions such as cell cycle, cytokinesis, polarity and migration<sup>66,304</sup>.

Since it controls pathways and functions involved in cancer, endocytosis recently was proposed to possibly play a role in cancer development and progression<sup>112,303,304</sup>. However so far, clear evidence for this possibility was lacking. The main aim of my project was to test this hypothesis, using Met oncogenic mutations as a model. Thus, my subject area was in a fast growing and competitive field.

I first demonstrated that one of the Met mutants I analysed is resistant to three Met-specific TKIs *in vitro* and *in vivo*. This underlined the importance of knowing patient genetic alterations in order to make decisions on treatment and the importance of developing new TKIs or new “types” of Met specific drugs.

Then, I showed that two activated Met mutants, unlike Met Wt, were constitutively internalised and recycled back to the plasma membrane. I further demonstrated that endocytosis is required for the Met mutants’ dependent ability to affect *in vivo* tumorigenesis and experimental metastasis. Thus, I have demonstrated for the first time, a direct link between RTK endocytosis and cancer.

We, in our laboratory, propose that it is the permanent shuttling between the plasma membrane and endosomes, associated to a defect in

degradation, that leads to the persistent generation of specific signals, “the transforming signals”, leading to cell transformation.

Interestingly, while blocking Met mutant endocytosis inhibited tumour growth, it did not reduce their activation state, suggesting that signal location rather than activation which dictated cellular outcomes. Moreover, the mutant I have shown to be resistant to the Met specific TKIs in the first part of my thesis, was sensitive to endocytosis inhibition. Thus, this novel way of inhibition may overcome resistance to TKIs in some cases.

These results open the way for the consideration of new potential therapies, aimed at preventing endosomal signalling as a means of targeting against Met-driven cancers and this potentially could be applied to other RTKs.

## REFERENCES

1. Schlessinger, J. Cell signaling by receptor tyrosine kinases. *Cell* **103**, 211-225 (2000).
2. Blume-Jensen, P. & Hunter, T. Oncogenic kinase signalling. *Nature* **411**, 355-365 (2001).
3. Longati, P., Comoglio, P.M. & Bardelli, A. Receptor tyrosine kinases as therapeutic targets: the model of the MET oncogene. *Curr Drug Targets* **2**, 41-55 (2001).
4. Ronsin, C., Muscatelli, F., Mattei, M.G. & Breathnach, R. A novel putative receptor protein tyrosine kinase of the met family. *Oncogene* **8**, 1195-1202 (1993).
5. Comoglio, P.M. & Boccaccio, C. The HGF receptor family: unconventional signal transducers for invasive cell growth. *Genes Cells* **1**, 347-354 (1996).
6. Cooper, C.S., *et al.* Molecular cloning of a new transforming gene from a chemically transformed human cell line. *Nature* **311**, 29-33 (1984).
7. Dean, M., *et al.* The human met oncogene is related to the tyrosine kinase oncogenes. *Nature* **318**, 385-388 (1985).
8. Park, M., *et al.* Mechanism of met oncogene activation. *Cell* **45**, 895-904 (1986).
9. Park, M., *et al.* The met oncogene: a new member of the tyrosine kinase family and a marker for cystic fibrosis. *Cold Spring Harb Symp Quant Biol* **51 Pt 2**, 967-975 (1986).
10. Liu, Y. The human hepatocyte growth factor receptor gene: complete structural organization and promoter characterization. *Gene* **215**, 159-169 (1998).
11. Park, M., *et al.* Sequence of MET protooncogene cDNA has features characteristic of the tyrosine kinase family of growth-factor receptors. *Proc Natl Acad Sci U S A* **84**, 6379-6383 (1987).

12. Rodrigues, G.A., Naujokas, M.A. & Park, M. Alternative splicing generates isoforms of the met receptor tyrosine kinase which undergo differential processing. *Mol Cell Biol* **11**, 2962-2970 (1991).
13. Lee, C.C. & Yamada, K.M. Identification of a novel type of alternative splicing of a tyrosine kinase receptor. Juxtamembrane deletion of the c-met protein kinase C serine phosphorylation regulatory site. *J Biol Chem* **269**, 19457-19461 (1994).
14. Comoglio, P.M., Giordano, S. & Trusolino, L. Drug development of MET inhibitors: targeting oncogene addiction and expedience. *Nat Rev Drug Discov* **7**, 504-516 (2008).
15. Birchmeier, C., Birchmeier, W., Gherardi, E. & Vande Woude, G.F. Met, metastasis, motility and more. *Nat Rev Mol Cell Biol* **4**, 915-925 (2003).
16. Stoker, M., Gherardi, E., Perryman, M. & Gray, J. Scatter factor is a fibroblast-derived modulator of epithelial cell mobility. *Nature* **327**, 239-242 (1987).
17. Nakamura, T., Nawa, K., Ichihara, A., Kaise, N. & Nishino, T. Purification and subunit structure of hepatocyte growth factor from rat platelets. *FEBS Lett* **224**, 311-316 (1987).
18. Nakamura, T., *et al.* Molecular cloning and expression of human hepatocyte growth factor. *Nature* **342**, 440-443 (1989).
19. Gherardi, E. & Stoker, M. Hepatocytes and scatter factor. *Nature* **346**, 228 (1990).
20. Bottaro, D.P., *et al.* Identification of the hepatocyte growth factor receptor as the c-met proto-oncogene product. *Science* **251**, 802-804 (1991).
21. Naldini, L., *et al.* Scatter factor and hepatocyte growth factor are indistinguishable ligands for the MET receptor. *Embo J* **10**, 2867-2878 (1991).
22. Naldini, L., *et al.* Hepatocyte growth factor (HGF) stimulates the tyrosine kinase activity of the receptor encoded by the proto-oncogene c-MET. *Oncogene* **6**, 501-504 (1991).

23. Naldini, L., *et al.* Extracellular proteolytic cleavage by urokinase is required for activation of hepatocyte growth factor/scatter factor. *Embo J* **11**, 4825-4833 (1992).
24. Naldini, L., *et al.* Biological activation of pro-HGF (hepatocyte growth factor) by urokinase is controlled by a stoichiometric reaction. *J Biol Chem* **270**, 603-611 (1995).
25. Basilico, C., Arnesano, A., Galluzzo, M., Comoglio, P.M. & Michieli, P. A high affinity hepatocyte growth factor-binding site in the immunoglobulin-like region of Met. *J Biol Chem* **283**, 21267-21277 (2008).
26. Gherardi, E., *et al.* Structural basis of hepatocyte growth factor/scatter factor and MET signalling. *Proc Natl Acad Sci U S A* **103**, 4046-4051 (2006).
27. Ponzetto, C., *et al.* A multifunctional docking site mediates signaling and transformation by the hepatocyte growth factor/scatter factor receptor family. *Cell* **77**, 261-271 (1994).
28. Gandino, L., Longati, P., Medico, E., Prat, M. & Comoglio, P.M. Phosphorylation of serine 985 negatively regulates the hepatocyte growth factor receptor kinase. *J Biol Chem* **269**, 1815-1820 (1994).
29. Hashigasako, A., Machide, M., Nakamura, T., Matsumoto, K. & Nakamura, T. Bi-directional regulation of Ser-985 phosphorylation of c-met via protein kinase C and protein phosphatase 2A involves c-Met activation and cellular responsiveness to hepatocyte growth factor. *J Biol Chem* **279**, 26445-26452 (2004).
30. Downward, J., Waterfield, M.D. & Parker, P.J. Autophosphorylation and protein kinase C phosphorylation of the epidermal growth factor receptor. Effect on tyrosine kinase activity and ligand binding affinity. *J Biol Chem* **260**, 14538-14546 (1985).
31. Schaeper, U., *et al.* Coupling of Gab1 to c-Met, Grb2, and Shp2 mediates biological responses. *J Cell Biol* **149**, 1419-1432 (2000).
32. Weidner, K.M., Sachs, M. & Birchmeier, W. The Met receptor tyrosine kinase transduces motility, proliferation, and morphogenic signals of scatter factor/hepatocyte growth factor in epithelial cells. *J Cell Biol* **121**, 145-154 (1993).

33. Nguyen, L., *et al.* Association of the multisubstrate docking protein Gab1 with the hepatocyte growth factor receptor requires a functional Grb2 binding site involving tyrosine 1356. *J Biol Chem* **272**, 20811-20819 (1997).
34. Bardelli, A., Longati, P., Gramaglia, D., Stella, M.C. & Comoglio, P.M. Gab1 coupling to the HGF/Met receptor multifunctional docking site requires binding of Grb2 and correlates with the transforming potential. *Oncogene* **15**, 3103-3111 (1997).
35. Ponzetto, C., *et al.* Specific uncoupling of GRB2 from the Met receptor. Differential effects on transformation and motility. *J Biol Chem* **271**, 14119-14123 (1996).
36. Forman-Kay, J.D. & Pawson, T. Diversity in protein recognition by PTB domains. *Curr Opin Struct Biol* **9**, 690-695 (1999).
37. Rosario, M. & Birchmeier, W. How to make tubes: signaling by the Met receptor tyrosine kinase. *Trends Cell Biol* **13**, 328-335 (2003).
38. Boccaccio, C., *et al.* Induction of epithelial tubules by growth factor HGF depends on the STAT pathway. *Nature* **391**, 285-288 (1998).
39. Graziani, A., Gramaglia, D., dalla Zonca, P. & Comoglio, P.M. Hepatocyte growth factor/scatter factor stimulates the Ras-guanine nucleotide exchanger. *J Biol Chem* **268**, 9165-9168 (1993).
40. Rodriguez-Viciana, P., *et al.* Role of phosphoinositide 3-OH kinase in cell transformation and control of the actin cytoskeleton by Ras. *Cell* **89**, 457-467 (1997).
41. Schenck, A., *et al.* The endosomal protein Appl1 mediates Akt substrate specificity and cell survival in vertebrate development. *Cell* **133**, 486-497 (2008).
42. Ishibe, S., Joly, D., Liu, Z.X. & Cantley, L.G. Paxillin serves as an ERK-regulated scaffold for coordinating FAK and Rac activation in epithelial morphogenesis. *Mol Cell* **16**, 257-267 (2004).
43. Stoker, M. & Perryman, M. An epithelial scatter factor released by embryo fibroblasts. *J Cell Sci* **77**, 209-223 (1985).
44. Ridley, A.J., Comoglio, P.M. & Hall, A. Regulation of scatter factor/hepatocyte growth factor responses by Ras, Rac, and Rho in MDCK cells. *Mol Cell Biol* **15**, 1110-1122 (1995).

45. Royal, I., Lamarche-Vane, N., Lamorte, L., Kaibuchi, K. & Park, M. Activation of cdc42, rac, PAK, and rho-kinase in response to hepatocyte growth factor differentially regulates epithelial cell colony spreading and dissociation. *Mol Biol Cell* **11**, 1709-1725 (2000).
46. Wherlock, M. & Mellor, H. The Rho GTPase family: a Racs to Wrchs story. *J Cell Sci* **115**, 239-240 (2002).
47. Heasman, S.J. & Ridley, A.J. Mammalian Rho GTPases: new insights into their functions from in vivo studies. *Nat Rev Mol Cell Biol* **9**, 690-701 (2008).
48. Vega, F.M. & Ridley, A.J. Rho GTPases in cancer cell biology. *FEBS Lett* **582**, 2093-2101 (2008).
49. Schmidt, A. & Hall, A. Guanine nucleotide exchange factors for Rho GTPases: turning on the switch. *Genes Dev* **16**, 1587-1609 (2002).
50. Scheffzek, K., Ahmadian, M.R. & Wittinghofer, A. GTPase-activating proteins: helping hands to complement an active site. *Trends Biochem Sci* **23**, 257-262 (1998).
51. Olofsson, B. Rho guanine dissociation inhibitors: pivotal molecules in cellular signalling. *Cell Signal* **11**, 545-554 (1999).
52. Jaffe, A.B. & Hall, A. Rho GTPases: biochemistry and biology. *Annu Rev Cell Dev Biol* **21**, 247-269 (2005).
53. Hall, A. Rho GTPases and the actin cytoskeleton. *Science* **279**, 509-514 (1998).
54. Ridley, A.J. Rho GTPases and actin dynamics in membrane protrusions and vesicle trafficking. *Trends Cell Biol* **16**, 522-529 (2006).
55. Ellis, S. & Mellor, H. Regulation of endocytic traffic by rho family GTPases. *Trends Cell Biol* **10**, 85-88 (2000).
56. Ridley, A.J. Rho GTPases and cell migration. *J Cell Sci* **114**, 2713-2722 (2001).
57. Ridley, A.J., Paterson, H.F., Johnston, C.L., Diekmann, D. & Hall, A. The small GTP-binding protein rac regulates growth factor-induced membrane ruffling. *Cell* **70**, 401-410 (1992).

58. Etienne-Manneville, S. & Hall, A. Rho GTPases in cell biology. *Nature* **420**, 629-635 (2002).
59. Ridley, A.J., *et al.* Cell migration: integrating signals from front to back. *Science* **302**, 1704-1709 (2003).
60. Ridley, A.J. & Hall, A. The small GTP-binding protein rho regulates the assembly of focal adhesions and actin stress fibers in response to growth factors. *Cell* **70**, 389-399 (1992).
61. Nobes, C.D. & Hall, A. Rho, rac, and cdc42 GTPases regulate the assembly of multimolecular focal complexes associated with actin stress fibers, lamellipodia, and filopodia. *Cell* **81**, 53-62 (1995).
62. Schiller, M.R. Coupling receptor tyrosine kinases to Rho GTPases--GEFs what's the link. *Cell Signal* **18**, 1834-1843 (2006).
63. Welch, H.C., *et al.* P-Rex1, a PtdIns(3,4,5)P<sub>3</sub>- and Gbetagamma-regulated guanine-nucleotide exchange factor for Rac. *Cell* **108**, 809-821 (2002).
64. Kraynov, V.S., *et al.* Localized Rac activation dynamics visualized in living cells. *Science* **290**, 333-337 (2000).
65. Myers, K.R. & Casanova, J.E. Regulation of actin cytoskeleton dynamics by Arf-family GTPases. *Trends Cell Biol* **18**, 184-192 (2008).
66. Gould, G.W. & Lippincott-Schwartz, J. New roles for endosomes: from vesicular carriers to multi-purpose platforms. *Nat Rev Mol Cell Biol* **10**, 287-292 (2009).
67. Xiao, G.H., *et al.* Anti-apoptotic signaling by hepatocyte growth factor/Met via the phosphatidylinositol 3-kinase/Akt and mitogen-activated protein kinase pathways. *Proc Natl Acad Sci U S A* **98**, 247-252 (2001).
68. Maulik, G., *et al.* Activated c-Met signals through PI3K with dramatic effects on cytoskeletal functions in small cell lung cancer. *J Cell Mol Med* **6**, 539-553 (2002).
69. Potempa, S. & Ridley, A.J. Activation of both MAP kinase and phosphatidylinositide 3-kinase by Ras is required for hepatocyte growth factor/scatter factor-induced adherens junction disassembly. *Mol Biol Cell* **9**, 2185-2200 (1998).

70. Kermorgant, S., Zicha, D. & Parker, P.J. PKC controls HGF-dependent c-Met traffic, signalling and cell migration. *Embo J* **23**, 3721-3734 (2004).
71. Kermorgant, S. & Parker, P.J. Receptor trafficking controls weak signal delivery: a strategy used by c-Met for STAT3 nuclear accumulation. *J Cell Biol* **182**, 855-863 (2008).
72. Lai, W.H., *et al.* Ligand-mediated internalization, recycling, and downregulation of the epidermal growth factor receptor in vivo. *J Cell Biol* **109**, 2741-2749 (1989).
73. Wiley, H.S. & Burke, P.M. Regulation of receptor tyrosine kinase signaling by endocytic trafficking. *Traffic* **2**, 12-18 (2001).
74. Conner, S.D. & Schmid, S.L. Regulated portals of entry into the cell. *Nature* **422**, 37-44 (2003).
75. Mosesson, Y., *et al.* Endocytosis of receptor tyrosine kinases is driven by monoubiquitylation, not polyubiquitylation. *J Biol Chem* **278**, 21323-21326 (2003).
76. Thien, C.B. & Langdon, W.Y. Cbl: many adaptations to regulate protein tyrosine kinases. *Nat Rev Mol Cell Biol* **2**, 294-307 (2001).
77. Maldonado-Baez, L. & Wendland, B. Endocytic adaptors: recruiters, coordinators and regulators. *Trends Cell Biol* **16**, 505-513 (2006).
78. Soubeyran, P., Kowanetz, K., Szymkiewicz, I., Langdon, W.Y. & Dikic, I. Cbl-CIN85-endophilin complex mediates ligand-induced downregulation of EGF receptors. *Nature* **416**, 183-187 (2002).
79. Mukhopadhyay, D. & Riezman, H. Proteasome-independent functions of ubiquitin in endocytosis and signaling. *Science* **315**, 201-205 (2007).
80. Huang, F., Goh, L.K. & Sorkin, A. EGF receptor ubiquitination is not necessary for its internalization. *Proc Natl Acad Sci U S A* **104**, 16904-16909 (2007).
81. Grovdal, L.M., Stang, E., Sorkin, A. & Madshus, I.H. Direct interaction of Cbl with pTyr 1045 of the EGF receptor (EGFR) is required to sort the EGFR to lysosomes for degradation. *Exp Cell Res* **300**, 388-395 (2004).

82. Blatner, N.R., *et al.* The molecular basis of the differential subcellular localization of FYVE domains. *J Biol Chem* **279**, 53818-53827 (2004).
83. Maxfield, F.R. & McGraw, T.E. Endocytic recycling. *Nat Rev Mol Cell Biol* **5**, 121-132 (2004).
84. Hurley, J.H. & Emr, S.D. The ESCRT complexes: structure and mechanism of a membrane-trafficking network. *Annu Rev Biophys Biomol Struct* **35**, 277-298 (2006).
85. Murphy, J.E., Padilla, B.E., Hasdemir, B., Cottrell, G.S. & Bunnett, N.W. Endosomes: a legitimate platform for the signaling train. *Proc Natl Acad Sci U S A* **106**, 17615-17622 (2009).
86. McCullough, J., Clague, M.J. & Urbe, S. AMSH is an endosome-associated ubiquitin isopeptidase. *J Cell Biol* **166**, 487-492 (2004).
87. Sigismund, S., *et al.* Clathrin-mediated internalization is essential for sustained EGFR signaling but dispensable for degradation. *Dev Cell* **15**, 209-219 (2008).
88. Di Guglielmo, G.M., Baass, P.C., Ou, W.J., Posner, B.I. & Bergeron, J.J. Compartmentalization of SHC, GRB2 and mSOS, and hyperphosphorylation of Raf-1 by EGF but not insulin in liver parenchyma. *Embo J* **13**, 4269-4277 (1994).
89. Grimes, M.L., *et al.* Endocytosis of activated TrkA: evidence that nerve growth factor induces formation of signaling endosomes. *J Neurosci* **16**, 7950-7964 (1996).
90. Miaczynska, M., Pelkmans, L. & Zerial, M. Not just a sink: endosomes in control of signal transduction. *Curr Opin Cell Biol* **16**, 400-406 (2004).
91. McPherson, P.S., Kay, B.K. & Hussain, N.K. Signaling on the endocytic pathway. *Traffic* **2**, 375-384 (2001).
92. Sorkin, A., McClure, M., Huang, F. & Carter, R. Interaction of EGF receptor and grb2 in living cells visualized by fluorescence resonance energy transfer (FRET) microscopy. *Curr Biol* **10**, 1395-1398 (2000).
93. Wang, Y., Pennock, S., Chen, X. & Wang, Z. Internalization of inactive EGF receptor into endosomes and the subsequent

- activation of endosome-associated EGF receptors. Epidermal growth factor. *Sci STKE* **2002**, PL17 (2002).
94. Wang, Y., Pennock, S., Chen, X. & Wang, Z. Endosomal signaling of epidermal growth factor receptor stimulates signal transduction pathways leading to cell survival. *Mol Cell Biol* **22**, 7279-7290 (2002).
  95. Wang, Y., Pennock, S.D., Chen, X., Kazlauskas, A. & Wang, Z. Platelet-derived growth factor receptor-mediated signal transduction from endosomes. *J Biol Chem* **279**, 8038-8046 (2004).
  96. Tsukazaki, T., Chiang, T.A., Davison, A.F., Attisano, L. & Wrana, J.L. SARA, a FYVE domain protein that recruits Smad2 to the TGFbeta receptor. *Cell* **95**, 779-791 (1998).
  97. Di Guglielmo, G.M., Le Roy, C., Goodfellow, A.F. & Wrana, J.L. Distinct endocytic pathways regulate TGF-beta receptor signalling and turnover. *Nat Cell Biol* **5**, 410-421 (2003).
  98. Vieira, A.V., Lamaze, C. & Schmid, S.L. Control of EGF receptor signaling by clathrin-mediated endocytosis. *Science* **274**, 2086-2089 (1996).
  99. Ceresa, B.P., Kao, A.W., Santeler, S.R. & Pessin, J.E. Inhibition of clathrin-mediated endocytosis selectively attenuates specific insulin receptor signal transduction pathways. *Mol Cell Biol* **18**, 3862-3870 (1998).
  100. Haugh, J.M., Huang, A.C., Wiley, H.S., Wells, A. & Lauffenburger, D.A. Internalized epidermal growth factor receptors participate in the activation of p21(ras) in fibroblasts. *J Biol Chem* **274**, 34350-34360 (1999).
  101. McKay, M.M. & Morrison, D.K. Integrating signals from RTKs to ERK/MAPK. *Oncogene* **26**, 3113-3121 (2007).
  102. Wunderlich, W., *et al.* A novel 14-kilodalton protein interacts with the mitogen-activated protein kinase scaffold mp1 on a late endosomal/lysosomal compartment. *J Cell Biol* **152**, 765-776 (2001).

103. Teis, D., Wunderlich, W. & Huber, L.A. Localization of the MP1-MAPK scaffold complex to endosomes is mediated by p14 and required for signal transduction. *Dev Cell* **3**, 803-814 (2002).
104. Nada, S., *et al.* The novel lipid raft adaptor p18 controls endosome dynamics by anchoring the MEK-ERK pathway to late endosomes. *EMBO J* **28**, 477-489 (2009).
105. Miaczynska, M., *et al.* APPL proteins link Rab5 to nuclear signal transduction via an endosomal compartment. *Cell* **116**, 445-456 (2004).
106. Lin, D.C., *et al.* APPL1 associates with TrkA and GIPC1 and is required for nerve growth factor-mediated signal transduction. *Mol Cell Biol* **26**, 8928-8941 (2006).
107. Watson, F.L., *et al.* Neurotrophins use the Erk5 pathway to mediate a retrograde survival response. *Nat Neurosci* **4**, 981-988 (2001).
108. Palamidessi, A., *et al.* Endocytic trafficking of Rac is required for the spatial restriction of signaling in cell migration. *Cell* **134**, 135-147 (2008).
109. Jekely, G., Sung, H.H., Luque, C.M. & Rorth, P. Regulators of endocytosis maintain localized receptor tyrosine kinase signaling in guided migration. *Dev Cell* **9**, 197-207 (2005).
110. Teis, D., *et al.* p14-MP1-MEK1 signaling regulates endosomal traffic and cellular proliferation during tissue homeostasis. *J Cell Biol* **175**, 861-868 (2006).
111. Sorkin, A. & von Zastrow, M. Endocytosis and signalling: intertwining molecular networks. *Nat Rev Mol Cell Biol* **10**, 609-622 (2009).
112. Scita, G. & Di Fiore, P.P. The endocytic matrix. *Nature* **463**, 464-473.
113. Zoncu, R., *et al.* A phosphoinositide switch controls the maturation and signaling properties of APPL endosomes. *Cell* **136**, 1110-1121 (2009).
114. Pasternak, S.H., *et al.* Presenilin-1, nicastrin, amyloid precursor protein, and gamma-secretase activity are co-localized in the lysosomal membrane. *J Biol Chem* **278**, 26687-26694 (2003).

115. Kholodenko, B.N. Cell-signalling dynamics in time and space. *Nat Rev Mol Cell Biol* **7**, 165-176 (2006).
116. von Zastrow, M. & Sorkin, A. Signaling on the endocytic pathway. *Curr Opin Cell Biol* **19**, 436-445 (2007).
117. Taub, N., Teis, D., Ebner, H.L., Hess, M.W. & Huber, L.A. Late endosomal traffic of the epidermal growth factor receptor ensures spatial and temporal fidelity of mitogen-activated protein kinase signaling. *Mol Biol Cell* **18**, 4698-4710 (2007).
118. Hammond, D.E., Urbe, S., Vande Woude, G.F. & Clague, M.J. Down-regulation of MET, the receptor for hepatocyte growth factor. *Oncogene* **20**, 2761-2770 (2001).
119. Kermorgant, S., Zicha, D. & Parker, P.J. Protein kinase C controls microtubule-based traffic but not proteasomal degradation of c-Met. *J Biol Chem* **278**, 28921-28929 (2003).
120. Li, N., Xiang, G.S., Dokainish, H., Ireton, K. & Elferink, L.A. The Listeria protein internalin B mimics hepatocyte growth factor-induced receptor trafficking. *Traffic* **6**, 459-473 (2005).
121. Petrelli, A., *et al.* The endophilin-CIN85-Cbl complex mediates ligand-dependent downregulation of c-Met. *Nature* **416**, 187-190 (2002).
122. Li, N., Lorinczi, M., Ireton, K. & Elferink, L.A. Specific Grb2-mediated interactions regulate clathrin-dependent endocytosis of the cMet-tyrosine kinase. *J Biol Chem* **282**, 16764-16775 (2007).
123. Peschard, P., *et al.* Mutation of the c-Cbl TKB domain binding site on the Met receptor tyrosine kinase converts it into a transforming protein. *Mol Cell* **8**, 995-1004 (2001).
124. Abella, J.V., *et al.* Met/Hepatocyte growth factor receptor ubiquitination suppresses transformation and is required for Hrs phosphorylation. *Mol Cell Biol* **25**, 9632-9645 (2005).
125. Carter, S., Urbe, S. & Clague, M.J. The met receptor degradation pathway: requirement for Lys48-linked polyubiquitin independent of proteasome activity. *J Biol Chem* **279**, 52835-52839 (2004).

126. Jeffers, M., Taylor, G.A., Weidner, K.M., Omura, S. & Vande Woude, G.F. Degradation of the Met tyrosine kinase receptor by the ubiquitin-proteasome pathway. *Mol Cell Biol* **17**, 799-808 (1997).
127. Longva, K.E., *et al.* Ubiquitination and proteasomal activity is required for transport of the EGF receptor to inner membranes of multivesicular bodies. *J Cell Biol* **156**, 843-854 (2002).
128. Shattuck, D.L., *et al.* LRIG1 is a novel negative regulator of the Met receptor and opposes Met and Her2 synergy. *Mol Cell Biol* **27**, 1934-1946 (2007).
129. Webb, C.P., *et al.* The geldanamycins are potent inhibitors of the hepatocyte growth factor/scatter factor-met-urokinase plasminogen activator-plasmin proteolytic network. *Cancer Res* **60**, 342-349 (2000).
130. Koga, F., Tsutsumi, S. & Neckers, L.M. Low dose geldanamycin inhibits hepatocyte growth factor and hypoxia-stimulated invasion of cancer cells. *Cell Cycle* **6**, 1393-1402 (2007).
131. Maulik, G., *et al.* Modulation of the c-Met/hepatocyte growth factor pathway in small cell lung cancer. *Clin Cancer Res* **8**, 620-627 (2002).
132. Kermorgant, S. & Parker, P.J. c-Met signalling: spatio-temporal decisions. *Cell Cycle* **4**, 352-355 (2005).
133. McShane, M.P. & Zerial, M. Survival of the weakest: signaling aided by endosomes. *J Cell Biol* **182**, 823-825 (2008).
134. Rosse, C., *et al.* PKC and the control of localized signal dynamics. *Nat Rev Mol Cell Biol* **11**, 103-112.
135. Ma, P.C., Maulik, G., Christensen, J. & Salgia, R. c-Met: structure, functions and potential for therapeutic inhibition. *Cancer Metastasis Rev* **22**, 309-325 (2003).
136. Trusolino, L. & Comoglio, P.M. Scatter-factor and semaphorin receptors: cell signalling for invasive growth. *Nat Rev Cancer* **2**, 289-300 (2002).
137. Gentile, A. & Comoglio, P.M. Invasive growth: a genetic program. *Int J Dev Biol* **48**, 451-456 (2004).

138. Bladt, F., Riethmacher, D., Isenmann, S., Aguzzi, A. & Birchmeier, C. Essential role for the c-met receptor in the migration of myogenic precursor cells into the limb bud. *Nature* **376**, 768-771 (1995).
139. Uehara, Y., *et al.* Placental defect and embryonic lethality in mice lacking hepatocyte growth factor/scatter factor. *Nature* **373**, 702-705 (1995).
140. Schmidt, C., *et al.* Scatter factor/hepatocyte growth factor is essential for liver development. *Nature* **373**, 699-702 (1995).
141. Birchmeier, C. & Gherardi, E. Developmental roles of HGF/SF and its receptor, the c-Met tyrosine kinase. *Trends Cell Biol* **8**, 404-410 (1998).
142. Ebens, A., *et al.* Hepatocyte growth factor/scatter factor is an axonal chemoattractant and a neurotrophic factor for spinal motor neurons. *Neuron* **17**, 1157-1172 (1996).
143. Kermorgant, S., *et al.* Developmental expression and functionality of hepatocyte growth factor and c-Met in human fetal digestive tissues. *Gastroenterology* **112**, 1635-1647 (1997).
144. Michalopoulos, G.K. & DeFrances, M.C. Liver regeneration. *Science* **276**, 60-66 (1997).
145. Nakamura, T., *et al.* Myocardial protection from ischemia/reperfusion injury by endogenous and exogenous HGF. *J Clin Invest* **106**, 1511-1519 (2000).
146. Chmielowiec, J., *et al.* c-Met is essential for wound healing in the skin. *J Cell Biol* **177**, 151-162 (2007).
147. Bussolino, F., *et al.* Hepatocyte growth factor is a potent angiogenic factor which stimulates endothelial cell motility and growth. *J Cell Biol* **119**, 629-641 (1992).
148. Rosen, E.M. & Goldberg, I.D. Regulation of angiogenesis by scatter factor. *Exs* **79**, 193-208 (1997).
149. Soman, N.R., Correa, P., Ruiz, B.A. & Wogan, G.N. The TPR-MET oncogenic rearrangement is present and expressed in human gastric carcinoma and precursor lesions. *Proc Natl Acad Sci U S A* **88**, 4892-4896 (1991).

150. Iyer, A., *et al.* Structure, tissue-specific expression, and transforming activity of the mouse met protooncogene. *Cell Growth Differ* **1**, 87-95 (1990).
151. Rong, S., Segal, S., Anver, M., Resau, J.H. & Vande Woude, G.F. Invasiveness and metastasis of NIH 3T3 cells induced by Met-hepatocyte growth factor/scatter factor autocrine stimulation. *Proc Natl Acad Sci U S A* **91**, 4731-4735 (1994).
152. Kermorgant, S., Aparicio, T., Dessirier, V., Lewin, M.J. & Lehy, T. Hepatocyte growth factor induces colonic cancer cell invasiveness via enhanced motility and protease overproduction. Evidence for PI3 kinase and PKC involvement. *Carcinogenesis* **22**, 1035-1042 (2001).
153. Park, M., Park, H., Kim, W.H., Cho, H. & Lee, J.H. Presence of autocrine hepatocyte growth factor-Met signaling and its role in proliferation and migration of SNU-484 gastric cancer cell line. *Exp Mol Med* **37**, 213-219 (2005).
154. Danilkovitch-Miagkova, A. & Zbar, B. Dysregulation of Met receptor tyrosine kinase activity in invasive tumors. *J Clin Invest* **109**, 863-867 (2002).
155. Giordano, S., *et al.* The c-met/HGF receptor in human tumours. *Eur J Cancer Prev* **1 Suppl 3**, 45-49 (1992).
156. Jeffers, M., *et al.* Activating mutations for the met tyrosine kinase receptor in human cancer. *Proc Natl Acad Sci U S A* **94**, 11445-11450 (1997).
157. Wang, R., Kobayashi, R. & Bishop, J.M. Cellular adherence elicits ligand-independent activation of the Met cell-surface receptor. *Proc Natl Acad Sci U S A* **93**, 8425-8430 (1996).
158. Lai, A.Z., Abella, J.V. & Park, M. Crosstalk in Met receptor oncogenesis. *Trends Cell Biol* **19**, 542-551 (2009).
159. Edakuni, G., Sasatomi, E., Satoh, T., Tokunaga, O. & Miyazaki, K. Expression of the hepatocyte growth factor/c-Met pathway is increased at the cancer front in breast carcinoma. *Pathol Int* **51**, 172-178 (2001).

160. Ayhan, A., Ertunc, D., Tok, E.C. & Ayhan, A. Expression of the c-Met in advanced epithelial ovarian cancer and its prognostic significance. *Int J Gynecol Cancer* **15**, 618-623 (2005).
161. Kammula, U.S., *et al.* Molecular co-expression of the c-Met oncogene and hepatocyte growth factor in primary colon cancer predicts tumor stage and clinical outcome. *Cancer Lett* **248**, 219-228 (2007).
162. Kaposi-Novak, P., *et al.* Met-regulated expression signature defines a subset of human hepatocellular carcinomas with poor prognosis and aggressive phenotype. *J Clin Invest* **116**, 1582-1595 (2006).
163. Miller, C.T., *et al.* Genomic amplification of MET with boundaries within fragile site FRA7G and upregulation of MET pathways in esophageal adenocarcinoma. *Oncogene* **25**, 409-418 (2006).
164. Smolen, G.A., *et al.* Amplification of MET may identify a subset of cancers with extreme sensitivity to the selective tyrosine kinase inhibitor PHA-665752. *Proc Natl Acad Sci U S A* **103**, 2316-2321 (2006).
165. Di Renzo, M.F., Poulson, R., Olivero, M., Comoglio, P.M. & Lemoine, N.R. Expression of the Met/hepatocyte growth factor receptor in human pancreatic cancer. *Cancer Res* **55**, 1129-1138 (1995).
166. Seiwert, T.Y., *et al.* The MET receptor tyrosine kinase is a potential novel therapeutic target for head and neck squamous cell carcinoma. *Cancer Res* **69**, 3021-3031 (2009).
167. Schmidt, L., *et al.* Novel mutations of the MET proto-oncogene in papillary renal carcinomas. *Oncogene* **18**, 2343-2350 (1999).
168. Schmidt, L., *et al.* Germline and somatic mutations in the tyrosine kinase domain of the MET proto-oncogene in papillary renal carcinomas. *Nat Genet* **16**, 68-73 (1997).
169. Peruzzi, B. & Bottaro, D.P. Targeting the c-Met signaling pathway in cancer. *Clin Cancer Res* **12**, 3657-3660 (2006).
170. Yamashita, J., *et al.* Immunoreactive hepatocyte growth factor is a strong and independent predictor of recurrence and survival in human breast cancer. *Cancer Res* **54**, 1630-1633 (1994).

171. Zhuang, Z., *et al.* Trisomy 7-harboring non-random duplication of the mutant MET allele in hereditary papillary renal carcinomas. *Nat Genet* **20**, 66-69 (1998).
172. Longley, B.J., *et al.* Somatic c-KIT activating mutation in urticaria pigmentosa and aggressive mastocytosis: establishment of clonality in a human mast cell neoplasm. *Nat Genet* **12**, 312-314 (1996).
173. Carlson, K.M., *et al.* Single missense mutation in the tyrosine kinase catalytic domain of the RET protooncogene is associated with multiple endocrine neoplasia type 2B. *Proc Natl Acad Sci U S A* **91**, 1579-1583 (1994).
174. Jeffers, M., *et al.* The mutationally activated Met receptor mediates motility and metastasis. *Proc Natl Acad Sci U S A* **95**, 14417-14422 (1998).
175. Park, W.S., *et al.* Somatic mutations in the kinase domain of the Met/hepatocyte growth factor receptor gene in childhood hepatocellular carcinomas. *Cancer Res* **59**, 307-310 (1999).
176. Di Renzo, M.F., *et al.* Somatic mutations of the MET oncogene are selected during metastatic spread of human HNSC carcinomas. *Oncogene* **19**, 1547-1555 (2000).
177. Lorenzato, A., *et al.* Novel somatic mutations of the MET oncogene in human carcinoma metastases activating cell motility and invasion. *Cancer Res* **62**, 7025-7030 (2002).
178. Schmidt, L., *et al.* Two North American families with hereditary papillary renal carcinoma and identical novel mutations in the MET proto-oncogene. *Cancer Res* **58**, 1719-1722 (1998).
179. Ma, P.C., *et al.* c-MET mutational analysis in small cell lung cancer: novel juxtamembrane domain mutations regulating cytoskeletal functions. *Cancer Res* **63**, 6272-6281 (2003).
180. Lee, J.H., *et al.* A novel germ line juxtamembrane Met mutation in human gastric cancer. *Oncogene* **19**, 4947-4953 (2000).
181. Wasenius, V.M., *et al.* MET receptor tyrosine kinase sequence alterations in differentiated thyroid carcinoma. *Am J Surg Pathol* **29**, 544-549 (2005).

182. Ma, P.C., Schaefer, E., Christensen, J.G. & Salgia, R. A selective small molecule c-MET Inhibitor, PHA665752, cooperates with rapamycin. *Clin Cancer Res* **11**, 2312-2319 (2005).
183. Jagadeeswaran, R., *et al.* Functional analysis of c-Met/hepatocyte growth factor pathway in malignant pleural mesothelioma. *Cancer Res* **66**, 352-361 (2006).
184. Ma, P.C., *et al.* Functional expression and mutations of c-Met and its therapeutic inhibition with SU11274 and small interfering RNA in non-small cell lung cancer. *Cancer Res* **65**, 1479-1488 (2005).
185. Kong-Beltran, M., *et al.* Somatic mutations lead to an oncogenic deletion of met in lung cancer. *Cancer Res* **66**, 283-289 (2006).
186. Miller, M., *et al.* Structural basis of oncogenic activation caused by point mutations in the kinase domain of the MET proto-oncogene: modeling studies. *Proteins* **44**, 32-43 (2001).
187. Weidner, K.M., Sachs, M., Riethmacher, D. & Birchmeier, W. Mutation of juxtamembrane tyrosine residue 1001 suppresses loss-of-function mutations of the met receptor in epithelial cells. *Proc Natl Acad Sci U S A* **92**, 2597-2601 (1995).
188. Jeffers, M., Koochekpour, S., Fiscella, M., Sathyanarayana, B.K. & Vande Woude, G.F. Signaling requirements for oncogenic forms of the Met tyrosine kinase receptor. *Oncogene* **17**, 2691-2700 (1998).
189. Chiara, F., Michieli, P., Pugliese, L. & Comoglio, P.M. Mutations in the met oncogene unveil a "dual switch" mechanism controlling tyrosine kinase activity. *J Biol Chem* **278**, 29352-29358 (2003).
190. Maritano, D., Accornero, P., Bonifaci, N. & Ponzetto, C. Two mutations affecting conserved residues in the Met receptor operate via different mechanisms. *Oncogene* **19**, 1354-1361 (2000).
191. Bardelli, A., *et al.* Uncoupling signal transducers from oncogenic MET mutants abrogates cell transformation and inhibits invasive growth. *Proc Natl Acad Sci U S A* **95**, 14379-14383 (1998).
192. Giordano, S., *et al.* Different point mutations in the met oncogene elicit distinct biological properties. *Faseb J* **14**, 399-406 (2000).

193. Nakaigawa, N., Weirich, G., Schmidt, L. & Zbar, B. Tumorigenesis mediated by MET mutant M1268T is inhibited by dominant-negative Src. *Oncogene* **19**, 2996-3002 (2000).
194. Lengyel, E., Sawada, K. & Salgia, R. Tyrosine kinase mutations in human cancer. *Curr Mol Med* **7**, 77-84 (2007).
195. Sawada, K., *et al.* c-Met overexpression is a prognostic factor in ovarian cancer and an effective target for inhibition of peritoneal dissemination and invasion. *Cancer Res* **67**, 1670-1679 (2007).
196. Sharma, S.V., Bell, D.W., Settleman, J. & Haber, D.A. Epidermal growth factor receptor mutations in lung cancer. *Nat Rev Cancer* **7**, 169-181 (2007).
197. Pardanani, A., *et al.* Imatinib for systemic mast-cell disease. *Lancet* **362**, 535-536 (2003).
198. Piao, X. & Bernstein, A. A point mutation in the catalytic domain of c-kit induces growth factor independence, tumorigenicity, and differentiation of mast cells. *Blood* **87**, 3117-3123 (1996).
199. Santoro, M., *et al.* Activation of RET as a dominant transforming gene by germline mutations of MEN2A and MEN2B. *Science* **267**, 381-383 (1995).
200. Piao, X., Paulson, R., van der Geer, P., Pawson, T. & Bernstein, A. Oncogenic mutation in the Kit receptor tyrosine kinase alters substrate specificity and induces degradation of the protein tyrosine phosphatase SHP-1. *Proc Natl Acad Sci U S A* **93**, 14665-14669 (1996).
201. Schmidt-Arras, D.E., *et al.* Tyrosine phosphorylation regulates maturation of receptor tyrosine kinases. *Mol Cell Biol* **25**, 3690-3703 (2005).
202. Lievens, P.M., Mutinelli, C., Baynes, D. & Liboi, E. The kinase activity of fibroblast growth factor receptor 3 with activation loop mutations affects receptor trafficking and signaling. *J Biol Chem* **279**, 43254-43260 (2004).
203. Thiede, C., *et al.* Analysis of FLT3-activating mutations in 979 patients with acute myelogenous leukemia: association with FAB

- subtypes and identification of subgroups with poor prognosis. *Blood* **99**, 4326-4335 (2002).
204. Tavormina, P.L., *et al.* A novel skeletal dysplasia with developmental delay and acanthosis nigricans is caused by a Lys650Met mutation in the fibroblast growth factor receptor 3 gene. *Am J Hum Genet* **64**, 722-731 (1999).
  205. Yang, S., *et al.* Association with HSP90 inhibits Cbl-mediated down-regulation of mutant epidermal growth factor receptors. *Cancer Res* **66**, 6990-6997 (2006).
  206. Han, W., Zhang, T., Yu, H., Foulke, J.G. & Tang, C.K. Hypophosphorylation of residue Y1045 leads to defective downregulation of EGFRvIII. *Cancer Biol Ther* **5**, 1361-1368 (2006).
  207. Grandal, M.V., *et al.* EGFRvIII escapes down-regulation due to impaired internalization and sorting to lysosomes. *Carcinogenesis* **28**, 1408-1417 (2007).
  208. Xiang, Z., Kreisel, F., Cain, J., Colson, A. & Tomasson, M.H. Neoplasia driven by mutant c-KIT is mediated by intracellular, not plasma membrane, receptor signaling. *Mol Cell Biol* **27**, 267-282 (2007).
  209. Runeberg-Roos, P., Virtanen, H. & Saarma, M. RET(MEN 2B) is active in the endoplasmic reticulum before reaching the cell surface. *Oncogene* **26**, 7909-7915 (2007).
  210. Choudhary, C., *et al.* Mislocalized activation of oncogenic RTKs switches downstream signaling outcomes. *Mol Cell* **36**, 326-339 (2009).
  211. Lievens, P.M., Roncador, A. & Liboi, E. K644E/M FGFR3 mutants activate Erk1/2 from the endoplasmic reticulum through FRS2 alpha and PLC gamma-independent pathways. *J Mol Biol* **357**, 783-792 (2006).
  212. Gao, C.F. & Vande Woude, G.F. HGF/SF-Met signaling in tumor progression. *Cell Res* **15**, 49-51 (2005).
  213. Corso, S., *et al.* Silencing the MET oncogene leads to regression of experimental tumors and metastases. *Oncogene* **27**, 684-693 (2008).

214. Engelman, J.A., *et al.* MET amplification leads to gefitinib resistance in lung cancer by activating ERBB3 signaling. *Science* **316**, 1039-1043 (2007).
215. Tang, Z., *et al.* Dual MET-EGFR combinatorial inhibition against T790M-EGFR-mediated erlotinib-resistant lung cancer. *Br J Cancer* **99**, 911-922 (2008).
216. Shattuck, D.L., Miller, J.K., Carraway, K.L., 3rd & Sweeney, C. Met receptor contributes to trastuzumab resistance of Her2-overexpressing breast cancer cells. *Cancer Res* **68**, 1471-1477 (2008).
217. Corso, S., Comoglio, P.M. & Giordano, S. Cancer therapy: can the challenge be MET? *Trends Mol Med* **11**, 284-292 (2005).
218. Eder, J.P., Vande Woude, G.F., Boerner, S.A. & LoRusso, P.M. Novel therapeutic inhibitors of the c-Met signaling pathway in cancer. *Clin Cancer Res* **15**, 2207-2214 (2009).
219. Knudsen, B.S. & Vande Woude, G. Showering c-MET-dependent cancers with drugs. *Curr Opin Genet Dev* **18**, 87-96 (2008).
220. Matsumoto, K. & Nakamura, T. NK4 (HGF-antagonist/angiogenesis inhibitor) in cancer biology and therapeutics. *Cancer Sci* **94**, 321-327 (2003).
221. Tomioka, D., *et al.* Inhibition of growth, invasion, and metastasis of human pancreatic carcinoma cells by NK4 in an orthotopic mouse model. *Cancer Res* **61**, 7518-7524 (2001).
222. Kuba, K., *et al.* HGF/NK4, a four-kringle antagonist of hepatocyte growth factor, is an angiogenesis inhibitor that suppresses tumor growth and metastasis in mice. *Cancer Res* **60**, 6737-6743 (2000).
223. Michieli, P., *et al.* Targeting the tumor and its microenvironment by a dual-function decoy Met receptor. *Cancer Cell* **6**, 61-73 (2004).
224. Burgess, T., *et al.* Fully human monoclonal antibodies to hepatocyte growth factor with therapeutic potential against hepatocyte growth factor/c-Met-dependent human tumors. *Cancer Res* **66**, 1721-1729 (2006).
225. Jun, H.T., *et al.* AMG 102, a fully human anti-hepatocyte growth factor/scatter factor neutralizing antibody, enhances the efficacy of

- temozolomide or docetaxel in U-87 MG cells and xenografts. *Clin Cancer Res* **13**, 6735-6742 (2007).
226. Prat, M., Crepaldi, T., Pennacchietti, S., Bussolino, F. & Comoglio, P.M. Agonistic monoclonal antibodies against the Met receptor dissect the biological responses to HGF. *J Cell Sci* **111 ( Pt 2)**, 237-247 (1998).
227. Martens, T., *et al.* A novel one-armed anti-c-Met antibody inhibits glioblastoma growth in vivo. *Clin Cancer Res* **12**, 6144-6152 (2006).
228. Merchant, M. MetMab significantly enhances anti-tumor activity of anti-VEGF and/or erlotinib in several animal tumor models. In the *AACR-NCI-ETORC International Conference on Molecular Targets and Cancer Therapeutics*. Abstract 556 (2008).
229. Miknyoczki, S.J., Chang, H., Klein-Szanto, A., Dionne, C.A. & Ruggeri, B.A. The Trk tyrosine kinase inhibitor CEP-701 (KT-5555) exhibits significant antitumor efficacy in preclinical xenograft models of human pancreatic ductal adenocarcinoma. *Clin Cancer Res* **5**, 2205-2212 (1999).
230. Morotti, A., Mila, S., Accornero, P., Tagliabue, E. & Ponzetto, C. K252a inhibits the oncogenic properties of Met, the HGF receptor. *Oncogene* **21**, 4885-4893 (2002).
231. Sattler, M., *et al.* A novel small molecule met inhibitor induces apoptosis in cells transformed by the oncogenic TPR-MET tyrosine kinase. *Cancer Res* **63**, 5462-5469 (2003).
232. Wang, X., *et al.* Potent and selective inhibitors of the Met [hepatocyte growth factor/scatter factor (HGF/SF) receptor] tyrosine kinase block HGF/SF-induced tumor cell growth and invasion. *Mol Cancer Ther* **2**, 1085-1092 (2003).
233. Christensen, J.G., *et al.* A selective small molecule inhibitor of c-Met kinase inhibits c-Met-dependent phenotypes in vitro and exhibits cytoreductive antitumor activity in vivo. *Cancer Res* **63**, 7345-7355 (2003).
234. Puri, N., *et al.* c-Met is a potentially new therapeutic target for treatment of human melanoma. *Clin Cancer Res* **13**, 2246-2253 (2007).

235. Yang, Y., *et al.* A selective small molecule inhibitor of c-Met, PHA-665752, reverses lung premalignancy induced by mutant K-ras. *Mol Cancer Ther* **7**, 952-960 (2008).
236. Puri, N., *et al.* A selective small molecule inhibitor of c-Met, PHA665752, inhibits tumorigenicity and angiogenesis in mouse lung cancer xenografts. *Cancer Res* **67**, 3529-3534 (2007).
237. Deininger, M., Buchdunger, E. & Druker, B.J. The development of imatinib as a therapeutic agent for chronic myeloid leukemia. *Blood* **105**, 2640-2653 (2005).
238. Zou, H.Y., *et al.* An orally available small-molecule inhibitor of c-Met, PF-2341066, exhibits cytoreductive antitumor efficacy through antiproliferative and antiangiogenic mechanisms. *Cancer Res* **67**, 4408-4417 (2007).
239. Christensen, J.G., *et al.* Cytoreductive antitumor activity of PF-2341066, a novel inhibitor of anaplastic lymphoma kinase and c-Met, in experimental models of anaplastic large-cell lymphoma. *Mol Cancer Ther* **6**, 3314-3322 (2007).
240. Knowles, L.M., *et al.* HGF and c-Met participate in paracrine tumorigenic pathways in head and neck squamous cell cancer. *Clin Cancer Res* **15**, 3740-3750 (2009).
241. Timofeevski, S.L., *et al.* Enzymatic characterization of c-Met receptor tyrosine kinase oncogenic mutants and kinetic studies with aminopyridine and triazolopyrazine inhibitors. *Biochemistry* **48**, 5339-5349 (2009).
242. Walker, K. & Padhiar, M. AACR-NCI-EORTC--21st International Symposium. Molecular targets and cancer therapeutics--Part 2. *IDrugs* **13**, 10-12.
243. Zhang, Y., *et al.* Identification of a novel recepteur d'origine nantais/c-met small-molecule kinase inhibitor with antitumor activity in vivo. *Cancer Res* **68**, 6680-6687 (2008).
244. Gu, X. Inhibition of HGF/c-Met pathway by ARQ197: characterisation of pharmacodynamic markers in vitro and in vivo. *In the AACR Annual Meeting*. Abstract 1748 (2009).

245. Liu, X., Newton, R.C. & Scherle, P.A. Developing c-MET pathway inhibitors for cancer therapy: progress and challenges. *Trends Mol Med* **16**, 37-45.
246. Dharmawardana, P.G., Peruzzi, B., Giubellino, A., Burke, T.R., Jr. & Bottaro, D.P. Molecular targeting of growth factor receptor-bound 2 (Grb2) as an anti-cancer strategy. *Anticancer Drugs* **17**, 13-20 (2006).
247. Giubellino, A., *et al.* Inhibition of tumor metastasis by a growth factor receptor bound protein 2 Src homology 2 domain-binding antagonist. *Cancer Res* **67**, 6012-6016 (2007).
248. Hammerman, P.S., Janne, P.A. & Johnson, B.E. Resistance to Epidermal Growth Factor Receptor Tyrosine Kinase Inhibitors in Non-Small Cell Lung Cancer. *Clin Cancer Res* **15**, 7502-7509 (2009).
249. Shah, N.P., *et al.* Multiple BCR-ABL kinase domain mutations confer polyclonal resistance to the tyrosine kinase inhibitor imatinib (STI571) in chronic phase and blast crisis chronic myeloid leukemia. *Cancer Cell* **2**, 117-125 (2002).
250. Wang, S.E., *et al.* HER2 kinase domain mutation results in constitutive phosphorylation and activation of HER2 and EGFR and resistance to EGFR tyrosine kinase inhibitors. *Cancer Cell* **10**, 25-38 (2006).
251. Greulich, H., *et al.* Oncogenic transformation by inhibitor-sensitive and -resistant EGFR mutants. *PLoS Med* **2**, e313 (2005).
252. Gowney, J.D., *et al.* Activation mutations of human c-KIT resistant to imatinib mesylate are sensitive to the tyrosine kinase inhibitor PKC412. *Blood* **106**, 721-724 (2005).
253. Pao, W., *et al.* EGF receptor gene mutations are common in lung cancers from "never smokers" and are associated with sensitivity of tumors to gefitinib and erlotinib. *Proc Natl Acad Sci U S A* **101**, 13306-13311 (2004).
254. Heinrich, M.C., *et al.* Kinase mutations and imatinib response in patients with metastatic gastrointestinal stromal tumor. *J Clin Oncol* **21**, 4342-4349 (2003).

255. Kosaka, T., *et al.* Analysis of epidermal growth factor receptor gene mutation in patients with non-small cell lung cancer and acquired resistance to gefitinib. *Clin Cancer Res* **12**, 5764-5769 (2006).
256. Wang, C.M., *et al.* Molecular mechanisms of secondary imatinib resistance in patients with gastrointestinal stromal tumors. *J Cancer Res Clin Oncol* (2009).
257. Pao, W., *et al.* Acquired resistance of lung adenocarcinomas to gefitinib or erlotinib is associated with a second mutation in the EGFR kinase domain. *PLoS Med* **2**, e73 (2005).
258. Tamborini, E., *et al.* A new mutation in the KIT ATP pocket causes acquired resistance to imatinib in a gastrointestinal stromal tumor patient. *Gastroenterology* **127**, 294-299 (2004).
259. McDermott, U., Pusapati, R.V., Christensen, J.G., Gray, N.S. & Settleman, J. Acquired Resistance of Non-Small Cell Lung Cancer Cells to MET Kinase Inhibition Is Mediated by a Switch to Epidermal Growth Factor Receptor Dependency. *Cancer Res* **70**, 1625-1634.
260. Zimmer, Y., *et al.* Differential inhibition sensitivities of MET mutants to the small molecule inhibitor SU11274. *Cancer Lett* (2009).
261. Berthou, S., *et al.* The Met kinase inhibitor SU11274 exhibits a selective inhibition pattern toward different receptor mutated variants. *Oncogene* **23**, 5387-5393 (2004).
262. Accornero, P., *et al.* An in vivo model of Met-driven lymphoma as a tool to explore the therapeutic potential of Met inhibitors. *Clin Cancer Res* **14**, 2220-2226 (2008).
263. Graveel, C.R., London, C.A. & Vande Woude, G.F. A mouse model of activating Met mutations. *Cell Cycle* **4**, 518-520 (2005).
264. Graveel, C., *et al.* Activating Met mutations produce unique tumor profiles in mice with selective duplication of the mutant allele. *Proc Natl Acad Sci U S A* **101**, 17198-17203 (2004).
265. Graveel, C.R., *et al.* Met induces diverse mammary carcinomas in mice and is associated with human basal breast cancer. *Proc Natl Acad Sci U S A* **106**, 12909-12914 (2009).

266. Urbe, S., *et al.* The UIM domain of Hrs couples receptor sorting to vesicle formation. *J Cell Sci* **116**, 4169-4179 (2003).
267. Campanero, M.R. & Flemington, E.K. Regulation of E2F through ubiquitin-proteasome-dependent degradation: stabilization by the pRB tumor suppressor protein. *Proc Natl Acad Sci U S A* **94**, 2221-2226 (1997).
268. Gampel, A., *et al.* VEGF regulates the mobilization of VEGFR2/KDR from an intracellular endothelial storage compartment. *Blood* **108**, 2624-2631 (2006).
269. Michieli, P., *et al.* Mutant Met-mediated transformation is ligand-dependent and can be inhibited by HGF antagonists. *Oncogene* **18**, 5221-5231 (1999).
270. Santoro, M.M., *et al.* Point mutations in the tyrosine kinase domain release the oncogenic and metastatic potential of the Ron receptor. *Oncogene* **17**, 741-749 (1998).
271. Peace, B.E., Hughes, M.J., Degen, S.J. & Waltz, S.E. Point mutations and overexpression of Ron induce transformation, tumor formation, and metastasis. *Oncogene* **20**, 6142-6151 (2001).
272. Rong, S., *et al.* Met proto-oncogene product is overexpressed in tumors of p53-deficient mice and tumors of Li-Fraumeni patients. *Cancer Res* **55**, 1963-1970 (1995).
273. Ding, S., Merkulova-Rainon, T., Han, Z.C. & Tobelem, G. HGF receptor up-regulation contributes to the angiogenic phenotype of human endothelial cells and promotes angiogenesis in vitro. *Blood* **101**, 4816-4822 (2003).
274. Zhang, Y.W., Su, Y., Volpert, O.V. & Vande Woude, G.F. Hepatocyte growth factor/scatter factor mediates angiogenesis through positive VEGF and negative thrombospondin 1 regulation. *Proc Natl Acad Sci U S A* **100**, 12718-12723 (2003).
275. Saucier, C., *et al.* The Shc adaptor protein is critical for VEGF induction by Met/HGF and ErbB2 receptors and for early onset of tumor angiogenesis. *Proc Natl Acad Sci U S A* **101**, 2345-2350 (2004).

276. Bellon, S.F., *et al.* c-Met inhibitors with novel binding mode show activity against several hereditary papillary renal cell carcinoma-related mutations. *J Biol Chem* **283**, 2675-2683 (2008).
277. D'Angelo, N.D., *et al.* Design, synthesis, and biological evaluation of potent c-Met inhibitors. *J Med Chem* **51**, 5766-5779 (2008).
278. Arteaga, C.L. HER3 and mutant EGFR meet MET. *Nat Med* **13**, 675-677 (2007).
279. Jones, H.E., *et al.* Growth factor receptor interplay and resistance in cancer. *Endocr Relat Cancer* **13 Suppl 1**, S45-51 (2006).
280. Stommel, J.M., *et al.* Coactivation of receptor tyrosine kinases affects the response of tumor cells to targeted therapies. *Science* **318**, 287-290 (2007).
281. Herbst, R.S., *et al.* Phase II study of efficacy and safety of bevacizumab in combination with chemotherapy or erlotinib compared with chemotherapy alone for treatment of recurrent or refractory non small-cell lung cancer. *J Clin Oncol* **25**, 4743-4750 (2007).
282. You, W.K. & McDonald, D.M. The hepatocyte growth factor/c-Met signaling pathway as a therapeutic target to inhibit angiogenesis. *BMB Rep* **41**, 833-839 (2008).
283. Bean, J., *et al.* MET amplification occurs with or without T790M mutations in EGFR mutant lung tumors with acquired resistance to gefitinib or erlotinib. *Proc Natl Acad Sci U S A* **104**, 20932-20937 (2007).
284. Qian, F., *et al.* Inhibition of tumor cell growth, invasion, and metastasis by EXEL-2880 (XL880, GSK1363089), a novel inhibitor of HGF and VEGF receptor tyrosine kinases. *Cancer Res* **69**, 8009-8016 (2009).
285. Wang, S., Pashtan, I., Tsutsumi, S., Xu, W. & Neckers, L. Cancer cells harboring MET gene amplification activate alternative signaling pathways to escape MET inhibition but remain sensitive to Hsp90 inhibitors. *Cell Cycle* **8**, 2050-2056 (2009).

286. Kirchhausen, T., Macia, E. & Pelish, H.E. Use of dynasore, the small molecule inhibitor of dynamin, in the regulation of endocytosis. *Methods Enzymol* **438**, 77-93 (2008).
287. Hill, T.A., *et al.* Inhibition of dynamin mediated endocytosis by the dynoles--synthesis and functional activity of a family of indoles. *J Med Chem* **52**, 3762-3773 (2009).
288. Germano, S., *et al.* Geldanamycins trigger a novel Ron degradative pathway, hampering oncogenic signaling. *J Biol Chem* **281**, 21710-21719 (2006).
289. Shimamura, T., *et al.* Hsp90 inhibition suppresses mutant EGFR-T790M signaling and overcomes kinase inhibitor resistance. *Cancer Res* **68**, 5827-5838 (2008).
290. Bauer, S., Yu, L.K., Demetri, G.D. & Fletcher, J.A. Heat shock protein 90 inhibition in imatinib-resistant gastrointestinal stromal tumor. *Cancer Res* **66**, 9153-9161 (2006).
291. Chung, B.M., *et al.* Aberrant trafficking of NSCLC-associated EGFR mutants through the endocytic recycling pathway promotes interaction with Src. *BMC Cell Biol* **10**, 84 (2009).
292. Shtiegman, K., *et al.* Defective ubiquitinylation of EGFR mutants of lung cancer confers prolonged signaling. *Oncogene* **26**, 6968-6978 (2007).
293. Honegger, A.M., Schmidt, A., Ullrich, A. & Schlessinger, J. Separate endocytic pathways of kinase-defective and -active EGF receptor mutants expressed in same cells. *J Cell Biol* **110**, 1541-1548 (1990).
294. Wang, Q., Villeneuve, G. & Wang, Z. Control of epidermal growth factor receptor endocytosis by receptor dimerization, rather than receptor kinase activation. *EMBO Rep* **6**, 942-948 (2005).
295. Bache, K.G., Slagsvold, T. & Stenmark, H. Defective downregulation of receptor tyrosine kinases in cancer. *Embo J* **23**, 2707-2712 (2004).
296. Peschard, P. & Park, M. Escape from Cbl-mediated downregulation: a recurrent theme for oncogenic deregulation of receptor tyrosine kinases. *Cancer Cell* **3**, 519-523 (2003).

297. Buus, R., Faronato, M., Hammond, D.E., Urbe, S. & Clague, M.J. Deubiquitinase activities required for hepatocyte growth factor-induced scattering of epithelial cells. *Curr Biol* **19**, 1463-1466 (2009).
298. Alwan, H.A. & van Leeuwen, J.E. UBPY-mediated epidermal growth factor receptor (EGFR) de-ubiquitination promotes EGFR degradation. *J Biol Chem* **282**, 1658-1669 (2007).
299. Ma, Y.M., *et al.* Targeting of AMSH to endosomes is required for epidermal growth factor receptor degradation. *J Biol Chem* **282**, 9805-9812 (2007).
300. Mizuno, E., *et al.* Regulation of epidermal growth factor receptor down-regulation by UBPY-mediated deubiquitination at endosomes. *Mol Biol Cell* **16**, 5163-5174 (2005).
301. Comoglio, P.M. Pathway specificity for Met signalling. *Nat Cell Biol* **3**, E161-162 (2001).
302. Polo, S. & Di Fiore, P.P. Endocytosis conducts the cell signaling orchestra. *Cell* **124**, 897-900 (2006).
303. Mosesson, Y., Mills, G.B. & Yarden, Y. Derailed endocytosis: an emerging feature of cancer. *Nat Rev Cancer* **8**, 835-850 (2008).
304. Lanzetti, L. & Di Fiore, P.P. Endocytosis and cancer: an 'insider' network with dangerous liaisons. *Traffic* **9**, 2011-2021 (2008).
305. Rao, D.S., *et al.* Huntingtin-interacting protein 1 is overexpressed in prostate and colon cancer and is critical for cellular survival. *J Clin Invest* **110**, 351-360 (2002).
306. Rao, D.S., *et al.* Altered receptor trafficking in Huntingtin Interacting Protein 1-transformed cells. *Cancer Cell* **3**, 471-482 (2003).
307. Santolini, E., *et al.* Numb is an endocytic protein. *J Cell Biol* **151**, 1345-1352 (2000).
308. Colaluca, I.N., *et al.* NUMB controls p53 tumour suppressor activity. *Nature* **451**, 76-80 (2008).
309. Muller, P.A., *et al.* Mutant p53 drives invasion by promoting integrin recycling. *Cell* **139**, 1327-1341 (2009).
310. Pellinen, T. & Ivaska, J. Integrin traffic. *J Cell Sci* **119**, 3723-3731 (2006).

311. Robertson, S.C., Tynan, J. & Donoghue, D.J. RTK mutations and human syndromes: when good receptors turn bad. *Trends Genet* **16**, 368 (2000).
312. Christensen, J.G., Burrows, J. & Salgia, R. c-Met as a target for human cancer and characterization of inhibitors for therapeutic intervention. *Cancer Lett* **225**, 1-26 (2005).

## ACKNOWLEDGEMENTS

I spent four wonderful years in the Tumour Biology Department, surrounded by great and talented people that I would sincerely like to thank:

The first and most important is my supervisor Stephanie. Since the moment she chose me to do this PhD, she never stopped helping me, giving me advice and pushing me forward. She is very enthusiastic and passionate about science and together we spent many hours developing great experiments. For all these reasons, I would just like to say, "Thank you Stephanie. You are a great boss and I will never forget you".

Secondly, there is Prof. Ian Hart. I was privileged and very lucky to do experiments with him and in doing so, perhaps get to know him a bit better than other students did. I greatly enjoyed all of the moments that we spent together with the mice in the animal house. He helped me to improve my English even though it is sometimes still difficult to understand his jokes.

Then, there are all the members of my group. It was so great to work with all of you! Virgine, you were a fantastic colleague, clever, helpful and I enjoyed all of our discussions, scientific or not...and now I think that I have found a real friend. Ludo, I was very happy to meet you and to have the opportunity to know you. You are one of those rare people who is truly a kind person. I like you a lot. Rachel, you also are a precious person. You were so patient with my English. I thank you very much for your contribution to my thesis work over the last nine months. I think that maybe without you, I would not have been able to cope with the end of my

thesis. Your help was important and I hope that you will be as lucky as me with your PhD. James, it is a shame that I could not get to know you better. I am sure that you will enjoy belonging to this team as much as I did.

I would also, of course, like to thank my colleagues from the department, who created a wonderful working atmosphere, which was perfectly balanced between friendship and science. I thank all of the PhD students, but particularly Fiecke, with whom I enjoyed working long hours. Then, I could not forget Myrto - a fantastic Post-doc. You have become such a good friend to me and I sincerely hope that our friendship will continue with time. There is also Delphine whose knowledge of science is great and with whom I have spent many pleasant moments.

I am also thankful to Debbie, Katie and Stephen who have helped me lots throughout these years.

Then, my Mum... She taught me thousands of things and she developed in me the curiosity and passion required to be a good researcher. I know that even when I am far away you are always supporting me ....Thank you.

Finally, there is my husband Olivier. Without him, becoming a Doctor, would probably not have been possible. His passion and interest for science, coupled with his talent, certainly pushed me to do a PhD. I am so happy and glad to have done a PhD and to have the chance to become a doctor. Without your huge moral support and your precious help during the writing up, I could not have achieved it. You are a wonderful husband!!  
With all my love, "Thank you".

